

STRUCTURAL AND PHOSPHORYLATION STUDIES OF
CARDIAC ATP-SENSITIVE POTASSIUM CHANNELS

Thesis submitted for the degree of
Doctor of Philosophy
at the University of Leicester

by

Harprit Singh Khatkar BSc (Leicester)
Department of Medicine
University of Leicester

October 2002

UMI Number: U170816

All rights reserved

INFORMATION TO ALL USERS

The quality of this reproduction is dependent upon the quality of the copy submitted.

In the unlikely event that the author did not send a complete manuscript and there are missing pages, these will be noted. Also, if material had to be removed, a note will indicate the deletion.



UMI U170816

Published by ProQuest LLC 2013. Copyright in the Dissertation held by the Author.
Microform Edition © ProQuest LLC.

All rights reserved. This work is protected against
unauthorized copying under Title 17, United States Code.



ProQuest LLC
789 East Eisenhower Parkway
P.O. Box 1346
Ann Arbor, MI 48106-1346

Title page	(i)
Contents	(ii)
Abstract	(viii)
Acknowledgements	(ix)
Abbreviations	(x)
Chapter 1: Introduction	1
1.1. ATP-Sensitive Potassium Channel Structure	1
1.2. General ATP-Sensitive Potassium Channel Function	4
1.3. Physiological roles of K_{ATP} channels in different tissues	6
1.4. Potassium Channels	8
1.4.1. Voltage-gated potassium channels	8
1.4.2. Calcium sensitive potassium channels	11
1.4.3. Ether-a-go-go related channels	12
1.4.4. Cyclic-nucleotide gated K^+ channels	12
1.4.5. Other potassium channels	12
1.5. Cloning and Reconstitution of K_{ATP} channels	13
1.5.1. Cloning of K_{ATP} channels	13
1.5.2. Kir6.1 Subunit	14
1.5.3. SUR1 Subunit	14
1.5.4. Kir6.2/SUR1 Channel	15
1.5.5. Kir6.2/SUR2A Channel	16
1.5.6. Kir6.2/SUR2B Channel	16
1.6. Molecular assembly and intracellular interactions of K_{ATP} channels	18
1.6.1. Molecular Assembly of K_{ATP} channels	18
1.6.2. Persistent Hyperinsulinemic-Hypoglycemia of Infancy	19
1.6.3. Cytoplasmic domain interactions of Kir6.2 subunit	20
1.6.4. Assembly of heterologous Kir6.0 Channels	21
1.6.5. Coassembly between SUR subunits	22
1.7. Molecular Entities involved in K_{ATP} channel gating: ATP inhibition	23
1.8. Stimulatory and inhibitory effects of Mg nucleotides	

and putative Mg nucleotide binding site on K _{ATP} channels	25
1.8.1. MgADP and K _{ATP} channels	25
1.8.2. MgATP and K _{ATP} channels	26
1.9. Sulphonylurea receptor: site for potassium channel openers and blockers	27
1.9.1. Potassium channel openers (KCO)	27
1.9.2. Potassium channel antagonists: Sulphonylureas	28
1.10. Modulation of K _{ATP} channels by phosphatidylinositol- 4,5 biphosphate	29
1.11. Modulation of K _{ATP} channels by phosphorylation	31
1.12. Other modulators of K _{ATP} channels	35
1.12.1. Acidic pH	35
1.12.2. Regulation by G-protein-coupled receptors	36
1.13. Ischaemic Preconditioning	37
1.13.1. Ischaemic Preconditioning and Cardiac K _{ATP} channels	38
1.13.2. Involvement of PKC and other Kinases in IP	45
1.14. Aims	49
 Chapter 2: Materials and Methods	 51
2.1. Materials	51
2.2. Preparation of polyclonal antibodies	51
2.3. Expression of K _{ATP} channel subunits	52
2.3.1. Transformation of Competent cells	52
2.3.2. Purification of plasmid DNA	52
2.3.3. Spectrophotometric Analysis	53
2.3.4. Agarose gel electrophoresis	53
2.3.5. Proteinase K treated DNA and Phenol Chloroform Extraction	55
2.3.6. <i>In vitro</i> translation	55
2.4. Electrophoresis	55
2.5. Immunoprecipitation of <i>in vitro</i> translated K _{ATP} channel subunit proteins	56

2.6. Tissue culture	57
2.7. Isolation of single ventricular myocytes	58
2.8. Immunocytochemistry	58
2.9. Confocal Microscopy	59
2.10. Isolation of mitochondria fraction from rat heart	60
2.11. Determination of Protein Concentrations	61
2.12. Western blotting	63
2.13. <i>In vitro</i> phosphorylation	63
2.13.1. Phosphorylation with Protein Kinase A	63
2.13.2. Phosphorylation with Protein Kinase C	64
2.13.3. Immunoprecipitation of <i>in vitro</i> phosphorylated samples	64
2.14. <i>In vivo</i> phosphorylation	64
2.15. Two Dimensional Phosphopeptide analysis	66
2.15.1. Elution of phosphorylated polypeptides from polyacrylamide gel	66
2.15.2. Precipitation of eluted ³² P-labelled polypeptide	66
2.15.3. Oxidation of Eluted ³² P-labelled polypeptide	66
2.15.4. Proteolytic Digestion of ³² P-labelled polypeptide	67
2.15.5. First Dimension electrophoresis	67
2.15.6. Second dimension chromatography	67
2.16. Phosphoamino acid analysis	68
2.17. Site-directed Mutagenesis	71
2.17.1. Creating Oligonucleotide Primers	71
2.17.2. QuikChange™ Site-Directed Mutagenesis reaction	71
2.17.3. Mutant DNA sequencing	72
2.18. Densitometry	73
Chapter 3: Characterization of anti-Kir6.0 and SUR2	
Polyclonal Antisera	74
3.1. Production of Polyclonal Antisera to K _{ATP} Channel	
Subunit Isoforms	74
3.2. Immunoprecipitation of <i>in vitro</i> Translated Kir6.0 and SUR2	
polypeptides	74
3.3. Western blotting of <i>in vitro</i> translated Kir6.0 and SUR2	

polypeptides	79
3.4. Immunocytochemistry of HEK 293 cells stably expressing Kir6.2/SUR2A or SUR2A transiently transfected with additional K _{ATP} channel subunits	82
3.5. Summary	92
Chapter 4: Localization of Kir6.0 and SUR2 K_{ATP} Channel Subunit Isoforms in Isolated rat Cardiac Myocytes	
Myocytes	93
4.1. Localization of the Kir6.1 Subunit in Isolated Rat Cardiac Myocytes	93
4.2. Localization of the Kir6.2 Subunit in Isolated Rat Cardiac Myocytes	97
4.3. Localization of the SUR2A Subunit in Isolated Rat Cardiac Myocytes	100
4.4. Localization of the SUR2B Subunit in Isolated Rat Cardiac Myocytes	103
4.5. Western blotting of K _{ATP} channel subunits in isolated cardiac ventricular myocytes	106
4.6. Preparation of Rat Heart Mitochondria Fractions	109
4.7. K _{ATP} channel subunit distribution in subcellular fractionations of cardiac myocytes	113
4.8. Summary	119
Chapter 5: Phosphorylation of Kir6.0 and SUR2 K_{ATP} channel subunits	
channel subunits	120
5.1. <i>In vitro</i> phosphorylation of expressed Kir6.1 and Kir6.2 subunits	120
5.2. <i>In vivo</i> phosphorylation of Kir6.0 and SUR2 subunits in isolated rat cardiomyocytes	125
5.3. Dependence on adenosine concentration of <i>in vivo</i> phosphorylation of the Kir6.1 subunit in isolated rat cardiac myocytes	129

5.4. <i>In vivo</i> phosphorylation of the Kir6.1 subunit in isolated rat cardiac myocytes stimulated by 2-chloro-N ⁶ -cyclopentyladenosine (CCPA) in the presence of various kinase inhibitors	131
5.5. Mapping of sites on Kir6.1 phosphorylated by <i>in vitro</i> using 2D-phosphopeptide mapping	135
5.6. Two-dimensional phosphoamino acid analysis of <i>in vivo</i> Kir6.1 subunit phosphorylated in isolated rat cardiomyocytes by PKC	135
5.7. Mapping of a PKC phosphorylation site in Kir6.1 using Kir6.1/Kir6.2 chimaeras	138
5.7.1. Construction of Kir6.1/6.2 3' swap and Kir6.2/6.1 3' swap (123 and 213)	138
5.7.2. Construction of Kir6.2/6.1 pore swap (21P)	139
5.7.3. Construction of Kir6.2/6.1 5' swap (215)	139
5.7.4. Construction of Kir6.1/Ki6.2 Sph-EcoRV and Kir6.2/Ki6.1 Sph-EcoRV (1121 and 2212)	139
5.7.5. <i>In vitro</i> expression of the chimera clones	141
5.7.6. <i>In vitro</i> PKC-mediated phosphorylation of Kir6.0 chimaeras	143
5.8. Two-dimensional phosphoamino acid analysis of <i>in vitro</i> PKC-mediated phosphorylation of Kir6.0 chimaeras	144
5.9. <i>In vitro</i> phosphorylation of expressed point mutants of Kir6.1	147
5.9.1. <i>In vitro</i> expression of Kir6.1 mutants	148
5.9.2. PKC-mediated phosphorylation of <i>in vitro</i> expressed Kir6.1 mutants	150
5.10. Summary	153
Chapter 6: Discussion	154
6.1. Antibody Characterization	155
6.2. Localization of Kir6.0 and SUR2 subunits	157
6.2.1. Kir6.1 subunit	157
6.2.2. Kir6.2 subunit	159

6.2.3. SUR2A subunit	160
6.2.4. SUR1 subunit	161
6.2.5. SUR2B subunit	164
6.3. Future experiments regarding localization of K _{ATP} channel subunits	165
6.4. Phosphorylation of cardiac K _{ATP} channels	168
6.4.1. <i>In vitro</i> phosphorylation of expressed Kir6.0 subunits	169
6.4.2. Kir6.1 as the major target for phosphorylation in cardiac K _{ATP} channels	169
6.4.3. Protein kinase C phosphorylates Serine 379 directly in the Kir6.1 subunit in rat isolated ventricular myocytes	171
6.4.4. Possible implication of PKC-mediated phosphorylation of the MitoK _{ATP} channel Kir6.1 subunit in ischaemic preconditioning	174
6.5. Future experiments regarding phosphorylation of K _{ATP} channel subunits	178
6.6. Summary and Conclusion	179
References	181

Abstract

Both the sarcolemmal (sarcK_{ATP}) and mitochondrial K_{ATP} channel (mitoK_{ATP}) in heart have a significant role in the complex pathway of ischaemic preconditioning. These channels may be the final mediator of protection for ischaemic preconditioning, activated by phosphorylation via a complex kinase cascade including tyrosine kinase, p38- mitogen-activated protein kinase (p38MAPK) and c-Jun N-terminal Kinase (JNK), where protein kinase C (PKC) appears to be the first element. Little is known about the kinase that phosphorylates the cardiac K_{ATP} channel. The sarcK_{ATP} has been suggested to consist of Kir6.2 inward rectifier and SUR2A sulfonylurea receptor subunits, whereas the subunit composition of mitoK_{ATP} channel is unknown. To understand the different roles sarcK_{ATP} and mitoK_{ATP} channels play during cardiac protection the molecular composition of each needs to be resolved.

To establish the localization of K_{ATP} channel subunits in rat isolated cardiac ventricular myocytes, characterized polyclonal antibodies (anti-Kir6.1, Kir6.2, SUR2A and SUR2B) were utilized in immunocytochemistry experiments and Western blots on subcellular fractions isolated from rat heart. Results from immunocytochemistry and Western blots showed the presence of all four subunits in cardiac myocytes. Kir6.1 was predominantly localized in mitochondria shown by immunocytochemistry and Western blots on isolated rat heart mitochondrial fractions. Kir6.2 was localized to the sarcolemma, with some present in mitochondria. Western blots on microsomal membrane fractions further confirmed localization of Kir6.2 in sarcolemma. Immunocytochemistry results revealed SUR2A was localized to sarcolemma and mitochondria, but was not detected in Western blots on mitochondrial fraction. However, [³²P] Kir6.1 was co-immunoprecipitated by anti-SUR2A from whole myocyte extracts after stimulation of PKA and PKC. SUR2B localized to T-tubules of the myocytes. Both the SUR2 polypeptides were detected in immunoblots of microsomal membrane fractions.

In vitro phosphorylation of K_{ATP} channel inward rectifier subunits revealed Kir6.1 to be a substrate for cyclic-AMP dependent protein kinase (PKA) and PKC-mediated phosphorylation, which was also confirmed by *in vivo* phosphorylation in isolated cardiac myocytes stimulated with forskolin and adenosine, respectively. *In vivo* phosphorylation of the Kir6.1 subunit, when stimulated with A1 receptor agonist, 2-chloro-N⁶-cyclopentyladenosine (CCPA), was significantly reduced when cells were incubated with the PKC inhibitor (Chelerythrine) but was unaltered when cells were incubated with other kinase inhibitors. Phosphoamino acid analysis on *in vivo* phosphorylated Kir6.1 subunit revealed serine as the major phosphorylated amino acid residue. *In vitro* PKC-mediated phosphorylation of chimaeras between Kir6.1 and Kir6.2 revealed the location of the phosphoserine residue to be between serine³⁵⁴-serine³⁹⁷ of the Kir6.1 protein, where five potential serine phosphorylation sites are present. Out of the five potential serine phosphorylation sites, *in vitro* expressed Kir6.1 mutant S379A was not phosphorylated in the presence of PKC.

In conclusion, there is strong evidence suggesting Kir6.2/SUR2A form a typical sarcK_{ATP} channel and that SUR2A possibly partners with Kir6.1 in mitoK_{ATP} channel. The Kir6.1 subunit in native tissue was shown to be the sole target site for PKC-mediated phosphorylation on serine residue 379, suggesting the possible involvement of mitoK_{ATP} channels as one of the end mediators of protection for ischaemic preconditioning.

Acknowledgement

I would like to express my sincere thanks to my supervisor Dr. R.I. Norman for his excellent advice and encouragement throughout the project. I would like to thank Dr. D. Lodwick for guiding me through the site-directed mutagenesis experiments; Dr. D. Hudman and Dr. C. Lawrence for isolating rat ventricular myocytes; Dr D. Hudman again for operating the confocal microscope and analysing the data; Richard Rainbow for transfecting HEK 293 cells; Dr. H. Kuhlman for presenting the Kir6.0 chimaeras. I would also like to thank Dr. K. Campbell for his generosity in providing the anti-IXE11₂ antisera, and H. Patel for giving up his precious time in helping me print my thesis. A big thanks to the MRC for granting me with the research grant for this project, which otherwise would not be operational. Finally last but not least, my family, especially my wife, Rajbinder Kaur, for supporting me throughout my research.

Abbreviations

A549	human epithelial cell line
ADP	adenosine diphosphate
ACh	acetylcholine
AMP	adenosine monophosphate
ATP	adenosine triphosphate
BIM	bisindolylmaleimide
BK	maxi-calcium sensitive potassium channels
bp	base-pair
BSA	bovine serum albumin
cAMP	cyclic adenosine monophosphate
cDNA	complementary DNA
CCD	charge coupled device
CCPA	2-chloro-N⁶-cyclopentyladenosine
CGRP	calcitonin gene-related peptide
CN	sodium cyanide
DAG	diacylglycerol
DCIP	2, 6-dichlorophenol-indophenol
DNA	deoxyribonucleic acid
dNTP	deoxy-nucleotide triphosphate
DNP	dinitrophenol
dsDNA	double stranded deoxyribonucleic acid
DTT	dithiothreitol
eag	ether-a-go-go
EC₅₀	concentration at which half activation occurs
EDTA	diaminoethanetetra acetic acid
ELISA	enzyme-Linked Immunosorbent Assay
ERK1/2	extracellular signal-regulated kinases 1/2
ERR	endoplasmic reticular-retention
EGTA	ethylene glycol-bis (β-aminoethyl ether)-tetraacetic acid
E_K	potassium equilibrium potential
elk	eag-like K⁺ channel
ER	endoplasmic reticulum
FCS	foetal Calf Serum
FITC	fluorescein isothiocyanate
F_T	total fluorescence
GCK	germinal center kinase
GLK	GCK-like kinase
GST	glutathione S-transferase
5-HD	5-hydroxydecanoate
HEK 293	human embryonic kidney cells
HEPES	N-2-hydroxyethylpiperazine-N'-2-ethanesulfonic acid
HERG	human eag related gene
HITT	hamster insulin secreting tumour cell
hHGF	human hepatocyte growth factor
HPK1	hematopoietic progenitor kinase-1
HTLE-7000	Hunters thin layer electrophoresis apparatus
IgG	immunoglobulin G

I_K	potassium current
IP	ischaemic preconditioning
I_{tail}	transient current
JNK	c-Jun N-terminal kinase
K_{ATP} channels	ATP-sensitive potassium channels
KCO	potassium channel opener
K_i	concentration at which half inhibition occurs
K_{ir}	Inwardly rectifiers
K_v	voltage-gated potassium channels
MBP	maltose-binding protein
MES	2-N-morpholino-ethanesulfonic acid
ml	millilitre
mM	millimolar
mitoK_{ATP}	mitochondrial K_{ATP} channel
MAPK	mitogen-activating protein kinase
MAPKAPK-2	MAPK-activated protein kinase-2
MKK	MAPK kinase
MOPS	3-N-morpholino propane-sulfonic acid
MRNA	messenger RNA
MRP	multi drug resistance-associated protein fragment
NBF	nucleotide-binding fold
NIK	Nck-interacting kinase
nM	nanomolar
nm	nanometres
OD	optical density
PAK	p21-activated kinase
PBS	phosphate saline buffer
PCR	polymerase chain reaction
PdBu	phorbol ester
PDD	phorbol 12,13-didecanote
PKA	protein kinase A
PKC	protein kinase C
PHHI	persistent hyperinsulinemic-hypoglycemia of infancy
PIP₂	phosphatidyl inositol bisphosphate
p38MAPK	p38 mitogen-activating protein kinase
PVDF	polyvinylidene difluoride
PLC	Phospholipase C
PMA	phorbol 12, 13 myristate acetate
PNACL	protein and nucleic acid chemistry laboratory
PS	phosphatidylserine
pS	picosiemans
RNA	ribonucleic Acid
RNAi	RNA interference
RNase A	ribonuclease type A
ROA	region of interest
ROS	reactive oxygen species
sarcK_{ATP}	sarcolemma K_{ATP} channel
SDS	sodium dodecyl sulphate
siRNA	small interfering RNA
SK	small calcium sensitive potassium channels

SUR	sulfonylurea receptor
TAE	tris acetate-EDTA
αTC-6	glucagonoma-α cell line
TLC	thin-layer chromatography
TMD	transmembrane domain
TRITC	rhodamine
T-tubule	transverse tubule
UHQ	ultra high quality
μl	microlitre
μM	micromolar
VSM	vascular smooth muscle
W_A	Walker A
W_B	Walker B
$\Delta\psi$	mitochondrial transmembrane potential

Chapter 1: Introduction

Ischaemic preconditioning is a complex event where a brief period of ischaemia prevents myocardium damage from long sustained periods of ischaemia. Two ATP-sensitive potassium channels (K_{ATP} channels), sarcolemmal and mitochondrial K_{ATP} channels are expressed in cardiac myocytes (Inagaki et al., 1996; Inoue et al., 1991). Evidence suggests these channels may be end mediators of a very complex series of ischaemic preconditioning events (Yao et al., 1994; Grover et al., 1995; Armstrong et al., 1995). Another important component of these events is protein kinase C (PKC). It is believed that the ischaemic-preconditioning event involves the activation of cardiac K_{ATP} channels by PKC-mediated phosphorylation (Liang et al., 1997). Which cardiac K_{ATP} channel is the substrate for PKC-mediated phosphorylation still remains to be determined. The main aim of this study was to identify the K_{ATP} channel subunit(s) which is/are potential target site(s) for PKC phosphorylation in expressed cardiac myocytes.

1.1. ATP-Sensitive Potassium Channel Structure

K_{ATP} channels are heterooctomers (Clement et al. 1997) comprising the inward rectifier subunit, which form the pore region (Tucker et al., 1997), and a sulfonylurea receptor subunit, (SUR) which belongs to the ATP-binding cassette superfamily with two nucleotide-binding folds (Tusnady et al., 1997). Expression of functional K_{ATP} channels requires both subunit types to be present, since endoplasmic reticular-retention (ERR) signals on each subunit are masked only when both subunits are expressed together (Zerangue et al., 1999; Schwappach et al., 2000). The inward rectifier potassium channels (Kir) constitute a large family of proteins (**Table 1.1**). The Kir1.0 subfamily contains ATP-regulating potassium channels, the Kir2.0 are strong inward rectifiers and the Kir3.0 subfamily is a group of G-protein-activated channels. The Kir6 subfamily contains subunits of the K_{ATP} channels.

Kir proteins have been predicted by hydropathy analysis to have two transmembrane spanning helices, named M1 and M2, flanking a segment, H5, with a -Gly-Phe-Gly- (or -Gly-Tyr-Gly-) sequence, like that identified in other K^+ selective channels (Doupnik et al. 1995). SUR isoforms are predicted to have 11 transmembrane helices

before the first nucleotide-binding fold (NBF), and then a second region with six predicted transmembrane helices followed by NBF-2 as shown in **Figure 1.1**. This model is based on multisequence alignment, hydropathy analysis (Tusnàdy et al., 1997) and by cysteine surface labelling assays and immunocytochemistry (Conti et al., 2001). Several groups showed that 1:1 stoichiometry was sufficient to form a functional channel by demonstrating that a dimeric Kir6.2/SUR1 fusion construct was capable of forming functional channels (Clement et al., 1997; Shyng et al., 1997). Channel activity was reduced when this construct was coexpressed with Kir6.2, but was restored by supplementation with wt SUR1. More importantly, mixtures of two triple fusion K_{ATP} channels (one a weak inward rectifier (SUR1/Kir6.2-Kir6.2) and the other a strong inward rectifier (SUR1/ Kir6.2_{N160D}-Kir6.2_{N160D})) displayed intermediate rectification properties on addition of monomeric SUR1, which otherwise without SUR1 would not express suggesting four Kir6.2 subunits are required to form the K_{ATP} channel pore (Clement et al., 1997) and that a K_{ATP} channel is an octameric complex with a 4:4 stoichiometry.

Kir Family	Nomenclature	Reference
Kir1.0 subfamily	Kir1.1a	Ho et al., 1993
	Kir1.1b	Zhou et al., 1994
Kir2.0 subfamily	Kir2.1	Kubo et al., 1993
	Kir2.2	Morishige et al., 1994
	Kir2.3	Takahashi et al., 1994
Kir3.0 family	Kir3.1	Dascal et al., 1993
	Kir3.2	Lesage et al., 1994
	Kir3.3	Lesage et al., 1994
	Kir3.4	Spauschus et al., 1996
Kir4.0 family	Kir4.1	Takumi et al., 1995
Kir5.0 family	Kir5.1	Bond et al., 1994
Kir6.0 family	Kir6.1	Inagaki et al., 1995
	Kir6.2	Bond et al., 1994

Table 1.1. A classification of inward rectifier potassium channels

1.2. General ATP-Sensitive Potassium Channel Function

K_{ATP} channels are widely distributed in vertebrate tissues (Inagaki et al., 1995; Inagaki et al., 1996; Isomoto et al., 1996; Yamada et al., 1997). The types of K_{ATP} channels present in various tissues (Table 1.2) have been determined by cloning K_{ATP} channel subunits and examining electrophysiological and pharmacological properties of reconstituted channels expressed in heterologous expression systems as discussed in detail in section 1.4. K_{ATP} channels close when they bind ATP and will open again when it is released (Noma et al., 1983). The hydrolysis of ATP is not required for shutting or opening of the channel, since non-hydrolysable analogues of ATP have the same effect as ATP itself (Inagaki et al., 1995). These channels link the cellular metabolism to electrical activity of cell membranes in many types of cells. Nucleotide levels affect the activity of K_{ATP} channels, thus these channels couple metabolism to membrane conductance.

K_{ATP} Channel	Subunit	References
β -cell/neuronal	Kir6.2/SUR1	Inagaki et al. 1995
Cardiac	Kir6.2/SUR2A	Inagaki et al. 1996
Skeletal	Kir6.2/SUR2A	Inagaki et al. 1996
Smooth Muscle	Kir6.2/SUR2B Kir6.1/SUR2B	Isomoto et al. 1996 Yamada et al 1997

Table 1.2 Tissue distribution of ATP-Sensitive Potassium Channels

K_{ATP} channels contribute to the control of membrane potential towards the potassium equilibrium potential (E_K) in various cells (Inagaki et al., 1995). Patch clamp recording has established that K_{ATP} channels conduct ions in the inward direction at very negative membrane potentials and allow outward conductance at membrane potentials that are positive to the E_K (Inagaki et al., 1995). The patch clamp technique with whole-cell recording permits voltage clamp to be used to investigate ion channel activity. This allows the membrane voltage of the patched cell to be clamped at potentials that are both depolarised and hyperpolarized with respect to the equilibrium potential of the ion under investigation. At each of these voltage commands,

membrane currents are measured and plotted to produce a current-voltage relationship. The K_{ATP} channel current-voltage relationship is shown in **Figure 1.2**. The patch clamp can also be used to measure single channel conductance, which is calculated from the slope of the current-voltage curve. **Figure 1.3** shows the different patch clamp configurations.

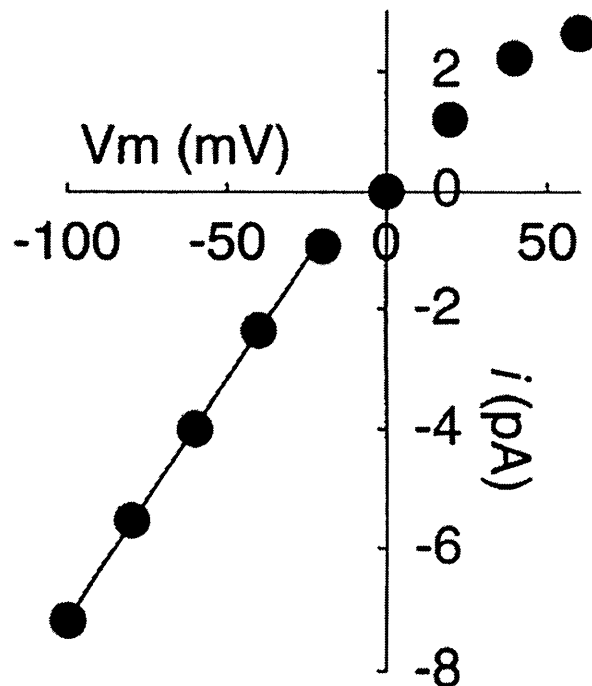


Figure 1.2 The current-voltage relationship of HEK293 cells coexpressing Kir6.2 and SUR2B subunits. The figure is taken from Isomoto et al. (1997) and describes the single-channel current-voltage relationship in cell attached for Kir6.2/SUR2B in stably transfected HEK cells. Membrane currents were obtained with an external and internal potassium concentration of 145mM, under test pulse potentials ranging between -100mV and 60mV . The current-voltage relationship of native smooth muscle K_{ATP} channel (Kir6.2/SUR2B) demonstrates weak rectification.

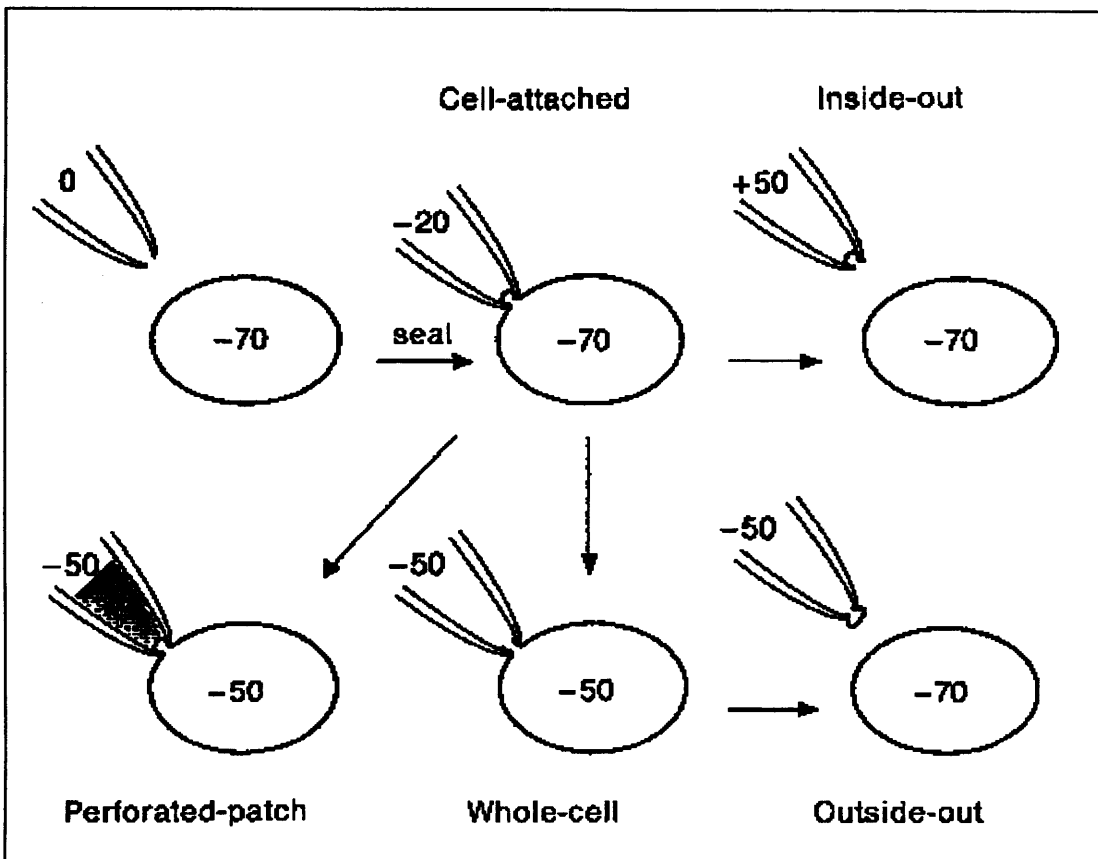


Figure 1.3. Different patch clamp configurations. This figure is taken from Cahalan et al., (1992). A gigaseal is formed between the pipette electrode and cell membrane to give a cell-attached configuration. Withdrawal of the pipette electrode produces an inside-out patch. Breakage of the patch while the pipette is attached to the cell gives whole-cell recording. Withdrawal from this produces an outside-out patch. A perforated patch also produces whole-cell records. The numbers show the electrode voltage required to produce a patch or whole-cell membrane potential of -50 mV if the cell resting potential is initially -70 mV (Cahalan et al., 1992)

1.3. Physiological roles of K_{ATP} channels in different tissues

In pancreatic β -cells, K_{ATP} channels regulate insulin secretion by linking changes in blood glucose concentration to insulin secretion (Ashcroft et al., 1989). Increased blood glucose is taken up and metabolised by β -cells, which alters the ATP/ADP ratio. The increased ATP/ADP ratio inhibits K_{ATP} channels, producing a membrane depolarisation that activates voltage-gated calcium channels. The consequent rise in

intracellular calcium ions stimulates the exocytosis of insulin-containing secretory granules.

In vascular smooth muscles, K_{ATP} channels are involved in regulating basal blood flow by various vasodilators or vasoconstrictors (Quayle et al., 1997). Endogenous vasodilators, like calcitonin gene-related peptide (CGRP), adenosine and β -adrenergic agonists, activate K_{ATP} channels via activation of adenylyl cyclase and PKA causing vasodilation of blood vessels. On the other hand, K_{ATP} channels are inhibited by vasoconstrictors, like 5-HT, histamine, via PKC, which causes the diameter of blood vessels to decrease (Bonev et al. 1996).

In the liver, K_{ATP} channels play a significant role in regulating hepatocyte proliferation (Malhi et al., 2000). Hepatocytes treated with human hepatocyte growth factor (hHGF), to stimulate growth, displayed an increased DNA synthesis 10 fold compared to untreated cells. The addition of potassium channel opener (KCO), minoxidil, cromakalin and pinacidil, increased DNA synthesis even further (20 fold compared to untreated cells). In contrast, in cultures of hepatocytes containing K_{ATP} channel blocker, glibenclamide, hHGF induced DNA synthesis was significantly inhibited. The molecular expression of K_{ATP} channels in rat hepatocytes was also examined (Malhi et al. 2000). Messenger RNA (mRNA) for Kir6.1, SUR1 and SUR2 was detected. Neither hHGF nor glibenclamide altered the overall abundance of Kir6.1 or SUR2 mRNAs in primary rat hepatocytes. In contrast the expression of SUR1 mRNA was reduced.

In the heart K_{ATP} channels are thought to play an important role in ischaemic preconditioning in the heart (discussed in more detail in Section 1.12). Additional physiological roles of the K_{ATP} channels also include epithelial potassium ion transport and the modulation of the electrical activity of different types of neurones (Roeper and Ashcroft, 1995). Perforated-patch whole cell recordings of rat substantia nigra (SN) neurones treated with rotenone (blocker of complex I of the mitochondrial electron transport chain) produced a hyperpolarization and inhibited electrical activity, both of which were reversed by the sulphonylureas, tolbutamide and glibenclamide (Roeper and Ashcroft, 1995). The current-voltage relationship of

the sulfonylurea-sensitive conductance gave a reversal potential value close to that of E_K . To confirm that the activation of K^+ current after mitochondrial metabolic inhibition was due to the activation of K_{ATP} channels, Roeper and Ashcroft, 1995 examined the effects of different intracellular ATP concentration on whole-cell currents in isolated SN neurones, using a whole-cell patch configuration. With low concentrations of ATP in the pipette solution, currents that were blocked on addition of tolbutamide were observed. Tolbutamide had no effect on whole-cell currents when neurones were dialysed with high concentrations of ATP. The current-voltage relationship was similar to the one observed in metabolic inhibition experiments displaying inward rectification, thus confirming K_{ATP} current. The modulation of electrical activity in SN neurones by K_{ATP} channels may be a possible therapeutic target for the mitochondrial complex I defect shown to be present in Parkinson's disease.

1.4. Potassium channels

K_{ATP} channels are members of a large diversity of potassium channels including voltage-gated potassium channels, calcium-activated potassium channels, inward rectifying potassium channels, ether-a-go-go related channels, cyclic-nucleotide-gated potassium channels and others (Hille, 2001). These channels are divided into three main structural classes, those with 2 transmembrane domains, those with four and those with six (Table 1.3). They all contain a conserved pore forming structure, for example in the inward rectifying channel, the M1 and M2 domains together with the H5 region are analogues to the voltage-gated potassium channel (K_V) subunit S5 and S6 domains and S51 S52 (H5) pore region respectively (Kuba et al., 1993).

1.4.1. Voltage-gated potassium channels

All the potassium channels types show diversity, with voltage-gated potassium channels (K_V) having the greatest as shown in Table 1.3. There are three reasons for such a large diversity in K_V channels. Firstly, the K_V gene in *Drosophila* (*Shaker*) contains at least 23 exons, which by alternative splicing leads to 10 different channel variants. In addition there are five different possible N-terminal regions and two different C-terminal domains (Pongs et al 1992). Secondly, *Shaker* is not the only K_V gene present in *Drosophila*, as *Shab*, *Shaw* and *Shal* family genes are also present, which are similar to but not identical to *Shaker*. Further diversity arises because

individual potassium channels can be heteromultimers, assembled from subunits that are not identical with one another (Sheng et al., 1993).

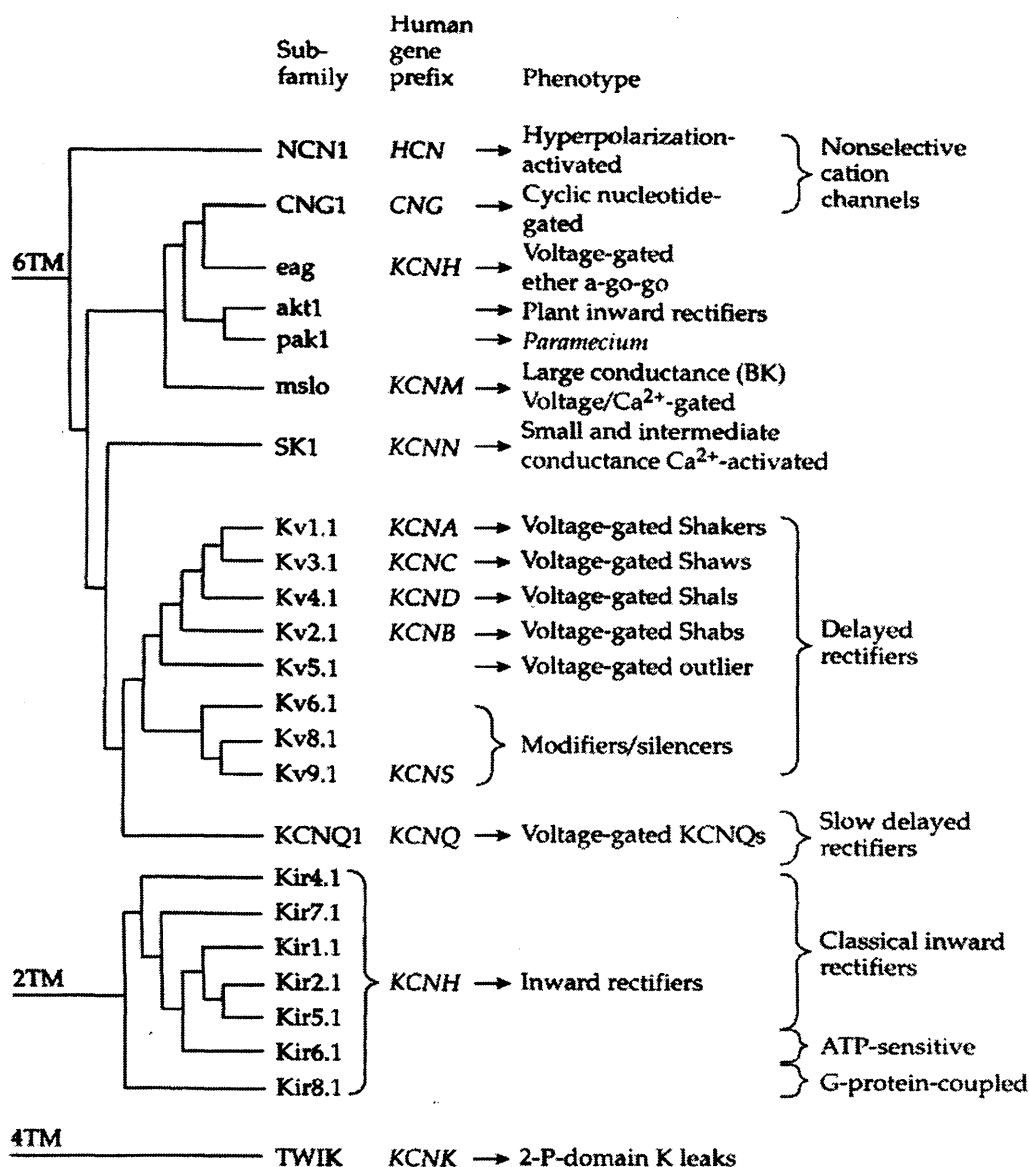


Table 1.3 Diversity of Potassium channels (taken from Hille, 2001).

A detailed model of the transmembrane topology has been developed for K_V (Durrell et al., 1992; Guy et al., 1990) The channel pore of K_V is formed from four subunits, known as α subunits, each having six transmembrane domains, S1 to S6. The section connecting S5 and S6 domains is known as the H5 region, which forms the lining of the pore. The K_{Vα} subunits belong to four subfamilies, whose subunits can assemble into heteromultimers within each subfamily.

The S4 segment is regarded as the voltage-sensor of the channel (Papazian et al., 1991). It contains positively charged arginine or lysine residues at every third position. Replacement of some of the positive residues in the S4 segment with either neutral or negative residues has been shown to alter the relationship between channel opening and membrane potential (Papazian et al., 1991). The S4 segment is likely to be sensitive to changes in membrane potential, leading to protein conformational changes upon depolarisation (Bezanilla et al., 1994).

Voltage-gated potassium channels are inactivated by two mechanisms called N-type and C-type inactivation. K_V channel N-type inactivation is linked to the activity of a cytoplasmic N-terminal blocking particle, which plugs the intracellular mouth of the pore after a prolonged depolarisation, also known as the ball and chain inactivation system (Armstrong and Bezanilla 1977). Evidence for the ball and chain model comes from site-directed mutagenesis investigations on *Shaker* potassium channels (Hoshi et al., 1990). Mutants of the N-terminal cytoplasmic region were made in which various sections had been removed and these were expressed in oocytes. Whole-cell recordings of patched oocytes showed that the deletions in the first 22 residues of the N-terminal slowed or removed inactivation, whereas deletions of sufficient length in the sequence between residues 23 and 83 tended to speed up inactivation. This suggested that the first 22 residues of the N-terminus form the intracellular ball and the next 60, the chain. If the ball is deleted, inactivation cannot occur, if the chain is shortened the ball finds its acceptor in the channel more quickly.

Mammalian K_V channels are unable to undergo N- type of inactivation as described above. In this case the presence of $K_{V\beta}$ accessory subunits allows N-type inactivation to occur (Rettig et al., 1994). Mammalian K_V channels consist of two subunits, α and β . The α subunits are of the familiar *Shaker* related K_V family, but the β subunits are quite different in structure, with no hydrophobic membrane-crossing segments. It seems that they are attached to the cytoplasmic side of the channel, probably with $\alpha_4\beta_4$ stoichiometry. Rettig and colleagues found that β subunits would not form channels when expressed in oocytes, but that they greatly enhanced the inactivation of channels formed from $K_{V\alpha}$ subunits. Deletion of part of the N-terminal region from the β subunit removed its inactivation capability, and a peptide with the same

sequence as the first 24 amino acid residues produced inactivation in the absence of the rest of the β subunit, suggesting that the β subunit carries a ball and chain section that can block the channel.

C-type inactivation is a much slower inactivation system and the mechanism remains to be elucidated. This has been investigated in the *shaker A* and *B* variants in which the time course of C-type inactivation is much slower in the *Shaker B* splicing variant than in *Shaker A*. These two variants have different carboxyl terminals. The other difference is in the S6 segment, where valine residues at 463 and 464 in *Shaker A* are replaced by alanine and isoleucine, respectively, in *Shaker B*. A point mutation valine 463 to alanine makes the inactivation of Shaker A as slow as that of Shaker B and vica-versa (Hoshi et al., 1991). C-type inactivation is also affected by mutations in the H5 region (Lopez-Barneo et al 1993). Mutation of threonine 449 to glutamate or lysine increased inactivation rates.

1.4.2. Calcium sensitive potassium channels

The maxi-calcium sensitive potassium channels (BK) are encoded by the slo gene (Atkinson et al 1991; Pallanck and Ganetzky, 1994), whereas the small calcium sensitive potassium channels (SK) by the SK1, 2 and 3 genes (Litt et al., 1999). BK and SK differ in the conductance of the channels they form, with SK forming small conductance channels that show no voltage dependence, and BK forming channels with larger conductances that are voltage-sensitive.

BK channels are similar in their sequence to K_V channels having a homologous S1-S6 region. Channel activation is dependent upon both direct calcium binding and membrane depolarisation. They are unique at their N and C-termini, possessing calcium-sensitive sites in the C-terminus (Schreiber and Salkoff, 1997; Schreiber et al 1999), and an additional transmembrane segment S0 towards the N terminal (Meera et al 1997). The calcium sensitivities of these channels vary in different tissues and this has been found to be due to their association with accessory beta subunits, which also may provide binding sites for other modulatory compounds (McCobb et al., 1995; Chang et al., 1997; Dick et al., 2001).

1.4.3. *Ether-a-go-go-related channels*

Molecular analysis of mutations affecting membrane excitability in *Drosophila* led to the identification of the gene *eag* (ether-a-go-go) that encodes a polypeptide structurally related to the *Shaker* K_V family (Warmke and Ganetzky, 1994). When expressed the polypeptide assembles into channels that conduct a voltage-activated K^+ and Ca^{2+} selective outward current that is modulated by internal cAMP. Another *eag* related gene, *elk* (*eag*-like K^+ channel) was found in *Drosophila* that was different to *eag* (Wamke and Ganetzky, 1994).

A human *eag*-related gene (HERG) was found on chromosome 7 (Wamke and Ganetzky, 1994). HERG was found to encode an inwardly rectifying current that has an inactivation mechanism that attenuates K^+ efflux during depolarisation (Trudeau et al., 1995; Spector et al., 1996). Mutations in HERG have been shown to cause a form of long QT syndrome, an inherited cardiac disorder resulting in syncope, seizures and sudden death (Benson et al., 1996).

1.4.4. *Cyclic-nucleotide gated K^+ channels*

Cyclic-nucleotide gated K^+ channels are non-selective cation channels. These channels are mainly associated with expression in retinal and olfactory neurones (Nakatani et al., 1995; Leinders-Zufall et al., 1997). They have a pore region that is very similar to that of K_V channels (Heginbotham et al., 1992), display little selectivity among monovalent cations, and are activated by intracellular cyclic nucleotides (Kramer et al., 1994)

1.4.5. *Other potassium channels*

Two pore-domain potassium channels (TWIK and TWEK), also known as leakage channels, possess four transmembrane domains and are active as dimers (Bochenhauer et al., 2000; Lopes et al., 2001). They are widely expressed in excitable and non-excitable cells. Their regulation is varied with different members being sensitive to various physical and chemical stimuli; such as membrane stretch, temperature, pH, and lipids (Reyes et al., 2000; Maingret et al., 2000; Lesage et al., 2000; Patel et al., 2001).

KCNQ1 are cardiac delayed rectifiers, which when mutated can cause inherited LQT disorder (Seeböhm et al., 2001). KCNQ2, 3 and 5 form heteromultimers, which underlie the neuronal M-current. Mutations in the genes encoding these channels cause an inherited form of juvenile epilepsy (Schroeder et al 1998; Selyanko et al., 2000; Lerche et al., 2000). KCNQ4 has been shown to be located in the cochlea with mutations in this gene causing an inherited deafness (Van-Hauwe et al., 2000).

1.5. Cloning and Reconstitution of K_{ATP} channels

1.5.1. Cloning of K_{ATP} channels

The known amino acid sequence of an ion channel can be useful in providing information about the structure of a channel. A hydropathy profile of the amino acid sequence of a channel can give information about the number of transmembrane domains it contains and the topography of the N and C-termini of the channel. Putative glycosylation and phosphorylation sites can be detected by screening the amino acid sequence for consensus sequences.

The protein sequence of K_{ATP} channels have been determined indirectly from the base sequence of the nucleic acids which code for them, using various techniques of recombinant DNA technology. This technique, also known as gene cloning, involves the screening of a DNA library (collection of millions of different DNA molecules held as separate clones in bacteriophage λ or a plasmid vector) with a ^{32}P -labelled oligonucleotide probe (a short stretch of DNA that has a base sequence that is complementary to part of the ion channel DNA fragment of interest). The bacteriophage containing the clones are grown in *E.coli* in a petri dish until visible plaques of lysed cells are formed. Overlaying a filter sheet of nitrocellulose on to the petri dish makes a replica of the pattern of plaques. The DNA is denatured on the nitrocellulose membrane and incubated with ^{32}P -labelled probe. The membrane is then washed and a sheet of X-ray film is laid over the nitrocellulose. The developed film will indicate the position of bound probe, which can be used to pick off plaque from petri dish to produce more DNA of the required channel by purification and propagation of the recombinant clone or by the polymerase chain reaction.

1.5.2. Kir6.1 Subunit

Inagaki et al., (1994) were the first to isolate complementary DNA (cDNA) encoding the Kir6.1 subunit (uK_{ATP-1}). They screened a rat pancreatic islet cDNA library with a ^{32}P -labelled cDNA fragment of Kir3.0 (member of the inwardly rectifying K^+ selective channel subfamily). Five positive clones were obtained and the clone containing the longest DNA insert, designated $\lambda rIK-5$, was cloned and sequenced. The sequenced clone contained 2389 base pairs (bp), which predicted the amino acid sequence of a 424 amino acid residue protein (M_r 47,960). The predicted amino acid sequence of uK_{ATP-1} showed 44% identity with Kir1.1a, Kir3.1 and cK_{ATP-1} (Kir6.2) and 66% identity with Kir2.1, each of which represent a different subfamily of the inwardly rectifying K^+ selective channel family. Inagaki et al., (1994) also examined the electrophysiological properties of uK_{ATP-1} expressed in *Xenopus* oocytes. The cRNA injected oocytes showed inward currents at extracellular K^+ of 45mM, which were blocked by external Ba^{2+} (300 μM). Lowering the extracellular K^+ from 90 to 45mM shifted the inward rectification to more negative voltages and thus decreased conductance. To further characterize the properties of uK_{ATP-1} , Inagaki and colleagues performed single-channel recordings on human embryonic kidney (HEK 293) cells transiently transfected with uK_{ATP-1} . The single-channel conductance recorded was 70 picosiemens (pS). The channel activity was suppressed when intracellular ATP (1 mM) was applied to patched cells; inhibition was also observed when 100 μM nonhydrolyzable ATP (AMP-PNP) was used. Diazoxide, a potent opener of K_{ATP} channels of pancreatic β -cells, activated uK_{ATP-1} channels on inside-out patch membranes. These electrophysiological studies on the $rIK-5$ clone demonstrated it to be member of K_{ATP} channel family, now known as the Kir6.1 subunit.

1.5.3. SUR1 Subunit

Aguilar-Bryan et al., (1995) first cloned a hamster SUR1 cDNA. Hamster insulin-secreting tumour cell (HITT15 cell) membranes were isolated and photolabelled with ^{125}I -labelled iodoglyburide. Gylburide (glibenclamide) is a sulfonylurea drug, which in its iodinated form can be covalently cross-linked by photolabelling to the 140kDa protein, SUR (Kramer et al., 1988). The photolabelled SUR protein was purified,

separated by electrophoresis and transferred to blotting membrane. The blot was stained, bands excised and sequenced by Edman degradation. An NH₂-terminal amino acid sequence of PLAFCGTENHSAA_{YRVDQGV}LNNGC was obtained. Degenerate polymerase chain reaction (PCR) primers were designed on the basis of this sequence and were used to amplify a 67 bp fragment from a random primed cDNA library constructed in λ ZAPII from a mouse glucagonoma- α cell line (α TC-6), which have an abundance of SUR (Rajan et al 1993). The sequence of the 67bp fragment encoded the expected amino acids with codon degeneracy only in the PCR primer regions. A minimally degenerate 47-residue oligonucleotide was synthesized and used to rescreen the α TC-6 cell library. A 1.1kb cDNA was cloned that encoded the 25 amino acids obtained by peptide sequence of the SUR NH₂ terminus. This cDNA fragment was used to screen HIT15 cell λ phage libraries for clones with overlapping sequences to determine the full-length sequence of SUR1. The open reading frame of the hamster SUR cDNA encoded a protein of 1582 amino acids with predicted mass of 177,209 Daltons. The functional analysis of SUR1 coexpressed with Kir6.2 were later done by Inagaki et al., (1995), as discussed below in section 1.4.4.

1.5.4. Kir6.2/SUR1 Channel

Inagaki et al., (1995) later cloned a human Kir6.2 subunit (hBIR), by screening a λ FIXII human genomic library with ³²P-labelled full-length rat Kir6.1 cDNA. Four clones encoded a distinct protein similar to Kir6.1, which was designated BIR. The sequence of the BIR clone revealed a single open reading frame encoding a 390 amino acid protein. Inagaki et al., (1995) also cloned and sequenced a mouse homolog of BIR, isolated from an insulin-secreting cell line cDNA library. The mouse clone showed 96% amino acid identity with hBIR. Inagaki et al., (1995) then looked at the electrophysiological properties of channels formed from BIR and SUR1 when cotransfected in COS-1 cells. The current-voltage relation revealed a weak inward rectification, with a reversal potential value close to that of K⁺ equilibrium potential. The single-channel conductance was recorded to give a value of 76 pS. Currents carried by Kir6.2 were suppressed by 100 μ M ATP and completely inhibited by 1mM ATP. The ATP inhibition of channel activity was concentration-dependent, with a K_i of 10 μ M. Inagaki et al., (1995) also found an increase in inward membrane current in *Xenopus* oocytes co-injected with BIR and SUR cRNA when 100 μ M diazoxide

(potent opener of pancreatic β cell K_{ATP} channels; Trube et al., 1989; Fan et al., 1990) was applied. This current was suppressed when $0.1\mu\text{M}$ glibenclamide (K_{ATP} channel blocker) was introduced. These findings by Inagaki et al., (1995) demonstrated that co-expression of Kir6.2 and SUR1 reconstitute the main characteristic features of the K_{ATP} channel current described in pancreatic β -cells (Cook et al., 1984; Findley et al., 1985).

1.5.5. Kir6.2/SUR2A Channel

Inagaki et al., (1996) cloned the SUR2A subunit by screening a rat brain cDNA library with a ^{32}P -labelled hamster SUR1 cDNA (Aguilar-Bryan et al., 1995). The sequenced SUR2A clone contained a single open-reading frame encoding a protein of 1545 amino acid residues ($M_r = 174,109$) that had 68% identity with SUR1. When SUR2A was expressed with Kir6.2 in COS1 cells, K^+ currents recordings showed essentially identical single channel conductance but different kinetic and pharmacological properties compared with those of the pancreatic β -cell K_{ATP} channel. The current-voltage relation revealed a weak inward rectification, when 140mM K^+ was applied on both sides of the membrane, and the reversal potential value was close to the K^+ equilibrium potential. The single channel conductance recorded was 79.3 pS . Inagaki et al., (1996) also discovered that the sensitivity of SUR2A/Kir6.2 channels to ATP ($K_i = 100\text{ }\mu\text{M}$) was 10 fold less than that of the SUR1/Kir6.2 channel. Potassium channel openers (KCO) of cardiac K_{ATP} channels, cromakalin (Escande et al., 1988) and pinacidil (Escande et al., 1989; Fan et al., 1990) reactivated channels that were inhibited by $100\text{ }\mu\text{M}$ ATP, while diazoxide ($100\text{ }\mu\text{M}$) failed to stimulate the SUR2A/Kir6.2 channel. These studies suggested that the SUR2A/Kir6.2 channel was typical of those of the sarcolemmal cardiac K_{ATP} channel (Terzic et al., 1995; Faivre et al., 1985; Findlay, 1992).

1.5.6. Kir6.2/SUR2B Channel

Isomoto et al., (1996) cloned the SUR2B subunit by screening a mouse heart cDNA library with a ^{32}P -labelled DNA fragment encoding part of rat SUR1 (nucleotide positions 3466-4589). Forty-nine positive clones were obtained, from which a clone, named MCS10, was sequenced. The sequenced clone revealed a single open-reading frame encoding a protein of 1546 amino acid residues. The amino acid sequence of

MCS10 had 67% identity with that of ratSUR1 and 97% identity with that of rat SUR2A, indicating that MCS10 was homologous to SUR2. The SUR2B is identical to SUR2A except from C-terminal amino acids 1500 onwards. The electrophysiological properties of the SUR2B subunit when expressed with Kir6.2 in HEK293 cells were studied using the patch clamp technique (Isomoto et al., 1996). The current-voltage relation of the SUR2B/Kir6.2 channel demonstrated weak inward rectification, with a single channel conductance of 80.3pS. Intracellular ATP inhibited the channel in a concentration-dependent manner with a K_i of 68 μ M and both diazoxide and pinacidil increased channel activity in the presence of ATP. Conversely, channel activity was inhibited by tolbutamide and glibenclamide (SUR blockers). The SUR2B/Kir6.2 channel showed similar properties to those displayed by smooth muscle K_{ATP} channels (Standen et al., 1989; Beech et al., 1993).

Thus the specific properties of a K_{ATP} channel subtype are determined by its subunit composition. **Table 1.4** show the electrophysiological and pharmacological properties of the K_{ATP} channel subtypes.

Subunit	Conductance (pS)	ATP K_i (μ M)	Potassium channel openers EC_{50} (μ M)		
			Diazoxide	Pinacidil	Cromakalin
SUR1/Kir6.2	69-73	8-10	65	High	High
SUR2A/Kir6.2	79	100	n.d.	30	30
SUR2B/Kir6.2	80	-	200	100	n.d.
SUR2B/Kir6.1	33	Activates	n.d.	1×10^5	n.d.

Table 1.4 Electrophysiological and Pharmacological properties of recombinant K_{ATP} channels (adapted from Babenko et al., 1998). n.d.: not determined.

1.6. Molecular assembly and intracellular interactions of K_{ATP} channels

1.6.1. Molecular Assembly of K_{ATP} channels

Giblen et al., (1999) identified a domain in the proximal C terminus (at least amino acids 208-279) in the inwardly rectifying K^+ channel Kir6.2 that appears to interact biochemically with the SUR protein. Kir6.2 chimaeras were constructed containing various parts of the Kir2.1 subunit, which does not interact with the SUR. The chimaera that contained amino acids 208-279 from the Kir2.1 subunit was shown to be unable to co-immunoprecipitate with epitope tagged SUR-Myc after immunoprecipitation with an anti-Myc antibody. Giblen et al. (1999) also established that largely intact Kir6.2 N- and distal C termini were necessary for complete functional reconstitution of the K_{ATP} channel. This was shown in Kir6.2 chimaeras containing part of the N terminus or C-terminus substituted with Kir2.1, where expression of current was abolished on co-expression with the SUR-Myc protein.

Recently, using trafficking based assay approaches, Schwappach et al. (2000) have found that both the first transmembrane segment (M1) and the N terminus of the Kir6.2 inwardly rectifying channel subunit are important for specifying assembly with SUR1. Experiments were based on the need to mask ER retention signals in both Kir6.2 and SUR to ensure surface expression. SUR1 and SUR2A did not express well on the cell surface of *Xenopus* oocytes unless coexpressed with Kir6.2, whereas Kir2.1 expressed on the cell surface by itself and did not stimulate surface trafficking of SUR1. This was shown using a trafficking enhancement assay, where surface coassembly of injected Kir6.2-R (exposed ER retention signal) and extracellular epitope tagged SUR1 (HA-SUR1-R) in oocytes was recorded by incubating oocytes with anti-HA and a secondary anti-rabbit antibody and measuring signal by a luminometer. From this result, Schwappach et al. (2000) created chimaeras between Kir6.2 and Kir2.1 and tested their ability to promote surface expression of extracellular epitope tagged SUR1 using a trafficking trap assay. The trafficking trap assay involves a protein with a strong ER retention signal trapping a membrane targeting protein lacking or containing a weak ER retention signal in the endoplasmic reticulum. Additional ER retention signals were added to Kir6.2-Kir2.1 chimaeras, which were injected in oocytes with mutant SUR proteins (SUR1-HA_{AAA}) lacking the native ER retention signal. Oocytes injected with chimaeras containing the M1 region, and the N and C terminals of the Kir6.2 displayed low surface signals for HA-SUR1

and the N and C terminals of the Kir6.2 displayed low surface signals for HA-SUR1 similar to the ones recorded in oocytes injected with wtKir6.2 implying the importance of these regions in coassembly with SUR1. To determine which domain of SUR1 was important in assembly with the M1 region and cytoplasmic domains of Kir6.2, Schwappach et al. (2000) created a series of chimeras between SUR1 and multi drug resistance-associated protein fragment 1 (MRP1), a homologous ABC protein that does not assemble with Kir6.2, and tested their ability to stimulate the surface expression of epitope tagged Kir6.2HA. Surface expression was reduced when SUR1 transmembrane domains were replaced with those from MBP1 while substitution of the NBF's had little effect showing that the transmembrane domains rather than the NBF's were essential for coassembly with Kir6.2.

1.6.2. Persistent Hyperinsulinemic-Hypoglycemia of Infancy

A number of mutations in the pancreatic K_{ATP} channel subunits SUR1 and Kir6.2 can cause persistent hyperinsulinemic-hypoglycemia of infancy (PHHI); a disease involving hypersecretion of insulin in infants despite low blood glucose levels (Aynsley-Green et al., 1981; Landau et al., 1991). The cause of PHHI is due to the failure of K_{ATP} channels to open in response to glucose deprivation. Genetic studies have identified over 50 PHHI-associated mutations in the K_{ATP} channel genes, most of which are in SUR1 (Kane et al., 1996; Permutt et al., 1996; Sharma et al., 2000). One particular mutation in SUR1, leucine to proline at position 1544 (L1544P), interferes with normal assembly and trafficking of K_{ATP} channels by causing improper shielding of the RKR endoplasmic reticular retention/retrieval trafficking signals in the two channel subunits (Taschenberger et al., 2002). This mutation was detected in an affected patient whose pancreatic DNA was screened for mutations in the Kir6.2 and SUR1 genes after pancreatectomy. When L1544P mutant SUR1/Kir6.2 channels were transiently transfected in COSm6 cells, immunofluorescence-staining experiments showed reduced surface expression of the mutant channels compared to the wild type channels. Cells transfected with mutant channels were treated with lysosomal or proteasomal inhibitors, to increase surface expression, but no effect on expression levels were observed. Taschenberger et al., (2002) then inactivated the RKR motif in L1544P SUR1 (located in the cytoplasmic loop between the 11th TMD and NBF1) by mutating it to AAA and examined expression of mutant SUR1 alone and coexpressed with Kir6.2. They observed increased surface expression of the

the RKR motif was removed from Kir6.2 and coexpressed with L1544P SUR1 the surface expression increased 2 fold. Thus, the results from this study indicate that the mutant L1544P SUR1 prevents the proper shielding of the RKR signal in both subunits after channel assembly and, thus, contributes to reduced surface expression.

In conclusion, it seems that the M1 domain and cytoplasmic domains of the Kir6.2 subunit are essential for SUR1 surface expression and that transmembrane domains in SUR1, especially the cytoplasmic loop, between the 11th TMD and NBF1, rather than the NBF's are required for the coassembly of functional K_{ATP} channels with Kir6.2.

1.6.3. Cytoplasmic domain interactions of Kir6.2 subunit

Physical interactions between the N- and C- termini of individual Kir subunits have been shown to be functionally significant. In the G-protein gated Kir3.0 subunit, the interaction between the two termini has been shown to enhance G $\beta\gamma$ binding, suggesting that both N and C termini form a binding site for G $\beta\gamma$ (Woodward et al. 1997). Similarly, interaction between N and C terminal in Kir1.1 occur as a response to changes in intracellular pH (Schulte et al. 1998). Kir1.1 channel recordings of inside-out patches from oocytes showed closure of channels during acidification. Recovery from inactivation was only seen in channels subjected to short periods of acidification, suggesting that oxidation occurred during long exposure to intracellular acidification, which subsequently prevented channels from recovery. This was confirmed by observation that addition of dithiothreitol (DTT) but not MgATP nor PIP₂ (causes of channel run-down) led to complete recovery of acid-inactivated channels. Schulte et al., (1998) found that addition of Cu (II)-1, 10-phenanthroline (induces formation of disulfide bridges between cysteine residues) reduced the fraction of channels that spontaneously recovered upon realkalinization. Mutating Cys⁴⁹ and Cys³⁰⁸ in the N- and C- terminals, respectively, to alanine prevented the Kir1.1 channel from recovering from pH inactivation on addition of DTT, suggesting formation of disulfide bridges between the N- and C- terminal of Kir1.1 channel during acidification.

Using an *in vitro* protein-protein interaction assay, Tucker et al. (1999) demonstrated physical interaction between the N- and C- termini of Kir6.2. The assay exploited the

ability of a recombinant glutathione S-transferase fusion protein (in this case Kir6.2 N-terminal GST-fusion protein) to interact with [³⁵S] methionine labelled, *in vitro*-translated C-terminal domains of the Kir6.2 subunit. If the two proteins interacted, then the radiolabelled proteins could be purified using glutathione Sepharose beads. Tucker et al. (1999) found that amino acids 30-46 of the N- terminus were critical for the N- terminus to associate with the C terminus. By using the same interaction assay, Tucker et al., (1999) also showed that this conserved interaction domain was capable of interacting with the C- terminus of Kir2.1. A mutation within the interaction domain severely impaired the ability of Kir6.2 to form functional channels with SUR1, suggesting the possible involvement of the cytoplasmic domains of Kir6.2 subunit in channel gating in response to subunit interactions.

1.6.4. Assembly of Heterologous Kir6.0 Channels

As discussed above, it is known that the SUR isoforms can coassemble with different Kir6.0 isoforms to form a functional K_{ATP} channel (section 1.3). However, until recently, it was not known whether Kir6.1 and Kir6.2 could coassemble with each to form a functional channel.

Yi et al., (2000) were the first to demonstrate coassembly of Kir6.1 and Kir6.2 in HEK293 cells. Yi et al., (2000) were able to coimmunoprecipitate Kir6.1 from HEK293 cells coexpressing Kir6.1 and Kir6.2 with an anti-Kir6.2 antiserum. Like Seharaseyon et al., (2000), discussed below, Yi and colleagues made dominant-negative Kir6.1 and Kir6.2 mutants and examined the effects of these mutants on diazoxide-activated I_K currents in HEK293 cells coexpressing Kir6.1/SUR2B. The results showed a 50 % reduction in Kir6.1/SUR2B HEK293 stable cells transfected with either dominant-negative Kir6.1 or Kir6.2 mutant compared to wild type Kir6.1/SUR2B HEK293 stable cell I_K. They then recorded single-channel conductance in the cell-attached configuration in the presence of diazoxide in HEK293 cells coexpressing Kir6.1/SUR2B, Kir6.1+Kir6.2/SUR2B and Kir6.2/SUR2B. The single-channel conductance in HEK 293 cells expressing Kir6.1+Kir6.2/SUR2B gave a value intermediate between those of cells expressing either Kir6.1/SUR2B or Kir6.2/SUR2B. This suggested that a functional heteromultimer of Kir6.1 + Kir6.2/SUR2B can be expressed in HEK293 cells that have intermediate

Kir6.2/SUR2B can be expressed in HEK293 cells that have intermediate electrophysiological properties between Kir6.1/SUR2B and Kir6.2/SUR2B channels when Kir6.1 and Kir6.2 are coexpressed in HEK293 cells.

On the other hand, Seharaseyon et al., (2000) have shown that Kir6.1 and Kir6.2 do not heteromultimerize with each other to form cardiac K_{ATP} channels in rabbit ventricular myocytes or when expressed in a human epithelial cell line (A549). The group constructed dominant-negative Kir6.1 and Kir6.2 mutants, named Kir6.1AFA and Kir6.2AFA, where codon 142 and 144 of the pore forming wild type Kir6.1 and codon 131 and 133 of the pore forming wild type Kir6.2 were mutated to code for alanine instead of glycine respectively. These dominant-negative mutants can inactivate the function of wild-type subunits. A549 cells coexpressing Kir6.2/SUR2A were transfected with the dominant-negative mutants and the effect on pinacidil-activated surface K_{ATP} channel currents (I_K) examined. Only the Kir6.2AFA mutant was able to suppress I_K . The Kir6.1AFA mutant had no effect on pinacidil-activated I_K . In the reverse situation, only Kir6.1AFA mutant was able to suppress I_K in A549 cells coexpressing Kir6.1/SUR2B. The effect of the mutants on I_K in rabbit ventricular myocytes was then examined. Whole-cell patch recordings revealed that I_K was greatly suppressed in Kir6.2AFA transfected myocytes compared with those transfected with wild type Kir6.2, wild type Kir6.1 or Kir6.1AFA mutant transfected myocytes in primary culture. The lack of an effect of wild type Kir6.1 or Kir6.1AFA on sarcolemmal K_{ATP} channel currents, taken together with the lack of suppression of Kir6.1AFA on expressed Kir6.2/SUR2A channel, and of Kir6.2AFA on Kir6.1/SUR2B channel in A549 cells, indicates that Kir6.1 and Kir6.2 do not form functional heteromultimers either in A549 cells or native cells (Seharaseyon et al 2000).

In summary assembly of heterologous Kir6.0 channels is observed in recombinant and not native K_{ATP} channels, suggesting that the assembly is strictly regulated.

1.6.5. Coassembly between SUR subunits

So far, there has been no evidence showing coassembly between SUR subtypes. Giblen et al., (2002) used biochemical and electrophysiological approaches to investigate whether SUR1 and SUR2A coexpressed with Kir6.2 in HEK 293 cells

formed heteromultimers. Immunoprecipitation and Western blotting on HEK293 cells stably expressing Kir6.2/SUR1+SUR2A showed immunoprecipitation of the SUR1 subunit with anti-SUR1 antibody but no co-immunoprecipitation of SUR1 was observed with anti-SUR2 antibody (both antibodies were raised in rabbits to peptides corresponding to isoform-specific sequences in the NBF1). Similarly, the SUR2A subunit showed no co-immunoprecipitation with anti-SUR1 antibody. Examination of the pharmacological properties of HEK 293 cell lines stably expressing Kir6.2/SUR1 and Kir6.2/SUR2A using the whole cell configuration of the patch clamp, showed that diazoxide but not pinacidil activated Kir6.2/SUR1 and that the currents were inhibited by tolbutamide and glibenclamide (Giblen et al., 2002). In contrast, Kir6.2/SUR2A currents were activated by pinacidil but not diazoxide and inhibited by glibenclamide but not tolbutamide. In HEK 293 stably expressing Kir6.2/SUR1+SUR2A, addition of diazoxide activated whole cell currents, which were inhibited on addition of tolbutamide, confirming presence of Kir6.2/SUR1. The cells were then washed and currents activated with pinacidil. In this protocol, tolbutamide had no effect on activated currents, whereas currents were completely inhibited by glibenclamide indicating the presence of Kir6.2/SUR2A channels. No channels with intermediate properties were detected suggesting that heteromeric channels containing SUR1 and SUR2A with Kir6.2 were not found.

The possible assembly of heterologous SUR2A and SUR2B with Kir6.2 to form channels with intermediate properties still remains to be investigated.

1.7. Molecular Entities involved in K_{ATP} channel gating: ATP inhibition

At one time, block of K^+ current on application of ATP to the intracellular face of an excised patch was sufficient to define a K_{ATP} channel (Cook et al. 1984). Now, members of this family of channels are defined by their single-channel current properties and their pattern of regulation by nucleotides and pharmacology as discussed earlier (Babenko et al., 1998).

In excised patches, application of ATP, independent of Mg^{2+} , results in a reduction in the mean open time by prolonging the interburst intervals and shortening the burst duration (Kakei et al. 1984). ADP in the presence of Mg^{2+} stimulates ATP-inhibited channels (Dunne et al. 1986). Dunne et al. (1986) and Misler et al. (1986) have shown

that the ATP/ADP ratio is critical for regulation of K_{ATP} channel activity. They proposed that the application of ADP, in the absence of Mg²⁺, inhibited channel activity, whereas channels pre-inhibited by ATP were activated on stimulation with MgADP.

The inhibitory effects of nucleotides are mediated via the pore-forming Kir6.0 subunit. A range of evidence shows that regions in the Kir6.2 subunit are involved in ATP inhibition. Although both Kir6.2 and SUR subunits are normally required for functional expression of the K_{ATP} channel, Tucker et al. (1997) demonstrated that truncated isoforms of Kir6.2 (Kir6.2 Δ C26 and Kir6.2 Δ C36) alone could express functional channels. These truncated isoforms retain ATP sensitivity, but are not stimulated by MgADP. A single mutation in the C-terminal domain of the Kir6.2 Δ C26 subunit (K185Q) markedly reduced the ability of ATP to inhibit channel activity (Tucker et al. 1997).

Tucker et al., (1998) later found two distinct regions of Kir6.2, the proximal N-terminal sequence and the proximal C-terminal sequence, immediately preceding and following the transmembrane domains M1 and M2, respectively, where mutation in either region caused a change in ATP sensitivity. Some of the mutations (R50G, I167M and T171A) within these regions were compared with the wt Kir6.2 Δ C26 by examining the effect of 100 μ M and 1 mM ATP, which inhibited wt Kir6.2 Δ C26 currents by ~50 % and ~90 %, respectively. The wt and mutant forms of Kir6.2 Δ C26 were expressed in *Xenopus* oocytes and macroscopic currents were recorded from giant excised inside-out patches on addition of 100 μ M and 1 mM ATP. All mutants showed reduced ATP sensitivity compared to wt. It was concluded that the mutations may alter the ATP sensitivity of Kir6.2 Δ C26 by either impairing the ability of the channel to close, interfering with the transduction mechanism by which ATP binding induces pore closure or decreasing the affinity of the ATP-binding site.

Drain et al. (1998) showed that distinct regions of the cytoplasmic C-terminal domain of the Kir6.2 subunit the mouse pancreatic β -cell K_{ATP} channel was important for determining ATP sensitivity, complementary to the findings of Tucker et al., (1998). Chimaeras were constructed between Kir6.2 and the non-ATP-sensitive inward rectifying channel subunit Kir1.1. Swapping both the cytoplasmic N and C terminal

Xenopus oocytes resulted in the formation of a channel that was not inhibited by ATP in a inside-out patch-clamp recordings. Replacement of the N terminal domain of Kir6.2 with the corresponding domain from Kir1.1 (Kir1.1-Kir6.2-Kir6.2) and co-expression the chimaera with SUR1 in *Xenopus* oocytes showed a 2.5 fold reduction of ATP sensitivity compared with wt K_{ATP} channel in patch clamp recordings. The chimaera in which the C terminal domain of Kir6.2 replaced the corresponding residue of Kir1.1 (Kir6.2-Kir1.1-Kir1.1) showed no ATP sensitivity. Drain et al. (1998) also found that replacing 4 residue sequences ³³⁴GNTI³³⁷ from the C-terminal of Kir6.2 with the equivalent segment from either Kir4.1 or Kir2.1 showed a decrease in ATP sensitivity. A second region, amino acids 171-182, which was essential for ATP inhibition in the wt K_{ATP} channel was also identified (Drain et al., 1998), a similar region described by Tucker et al. 1998.

In another study, the cysteine residue at position 166 (C166) of Kir6.2 was implicated in the ATP gating of K_{ATP} channels (Trapp et al., 1998). Mutation of C166, which lies at the cytosolic end of the second transmembrane domain, to serine (C166S) increased the open probability of the truncated isoform of Kir6.2, Kir6.2 Δ C26, sevenfold compared to unmodified Kir6.2 Δ C26. Substitution of C166 with threonine, alanine, methionine or phenylalanine reduced the channel sensitivity to ATP.

In conclusion both N- and C- terminals of the Kir6.2 subunit are required for the determination of ATP sensitivity in K_{ATP} channels. Mutation of selective residues within the cytoplasmic domains, for example R50 in the N-terminal and C166, residues 171-182, and 334-337 in the C-terminal, disrupt ATP-gating in Kir6.2 channels.

1.8. Stimulatory and inhibitory effects of Mg nucleotides and putative Mg nucleotide binding site on K_{ATP} channels

1.8.1. MgADP and K_{ATP} channels

Investigation of the effect of ADP in the presence and absence of Mg^{2+} on K_{ATP} channel currents, using inside-out patches excised from *Xenopus* oocytes coinjected with Kir6.2/SUR1 has shown that ADP stimulates and/or inhibits K_{ATP} channel currents under different conditions (Gribble et al., 1997). ADP potentiated

Kir6.2/SUR1 current in the presence of intracellular Mg^{2+} , while ADP in the absence of Mg^{2+} or at high Mg^{2+} concentration was inhibitory. MgADP acts on K_{ATP} channels by binding to the NBF's of SUR (Gribble et al., 1997). Each NBF contains a highly conserved Walker A (W_A) and Walker B (W_B) motif (Walker et al., 1982). These motifs are known to catalyse ATP hydrolysis. An aspartate in the W_B motif coordinates the Mg^{2+} ion of MgATP and is required for nucleotide binding, while a lysine in the W_A motif interacts with the γ and β phosphate group of ATP and is essential for ATP hydrolysis (Azzarite et al., 1989; Carson et al., 1995; Higgins et al., 1992; Ko et al., 1995; Saraste et al., 1990; Tian et al., 1990). Gribble et al., (1997) made mutants of the SUR1, where the lysine residues in the W_A motif of NBF 1 and NBF 2 were substituted (K719A and K1384M, respectively) and the effect of MgADP on these mutant channel currents was examined. Both of the W_A mutant channel currents (Kir6.2/K719A-SUR1 and Kir6.2/K1384M-SUR1) were inhibited rather than activated by MgADP, indicating that the effect of MgADP is mediated by interaction of the nucleotide diphosphate with the NBDs of SUR1 and that the W_A lysine residues play a critical role in the interaction.

1.8.2. MgATP and K_{ATP} channels

Gribble et al., (1998) later discovered that, like MgADP, MgATP is able to stimulate K_{ATP} channel activity, but that the effect is normally masked by the potent inhibitory effect of the nucleotide. As before, the group recorded large currents in giant inside-out membrane patches excised from *Xenopus* oocytes coinjected with Kir6.2/SUR1. When ATP was applied both in the absence and presence of Mg^{2+} , the large currents were reversibly inhibited, however, ATP was more effective in the absence of Mg^{2+} . They then coinjected *Xenopus* oocytes with Kir6.2 Δ C36 (SUR-independent functional channel) and investigated the effect on currents of ATP in absence and presence of Mg^{2+} . ATP in both the absence and presence of Mg^{2+} showed similar inhibition of current, thus the ATP sensitivity of Kir6.2 Δ C36 current was unaffected by Mg^{2+} removal. This result suggested that the SUR subunit was required for the enhancement of ATP sensitivity by Mg^{2+} . The decrease in the ATP sensitivity of Kir6.2/SUR1 currents in the presence of Mg^{2+} suggests that like MgADP, MgATP is able to stimulate channel activity. So channel inhibition by ATP would occur in the absence of Mg^{2+} , whereas in the presence of Mg^{2+} , channel activity would be

determined by the balance between the inhibitory and stimulatory effects of MgATP. Gribble et al., (1998) also discovered that the aspartate residue of the W_B motif in both NBD's is essential for MgATP binding. Mutation of these aspartate residues to asparagine in both W_B motifs (D853N-NBD1 and D1505N-NBF2) produced channels that were more sensitive to inhibition by ATP in the presence of Mg^{2+} than wild type Kir6.2/SUR1.

Confirmation of the stimulatory effect of ATP came from experiments in which substitution of the arginine residue at position 50 of Kir6.2 with glycine (R50G) produced a mutant channel that was much less sensitive to ATP inhibition when expressed with SUR1 in oocytes and was stimulated by MgATP (Gribble et al., 1998). This suggested that MgATP is able to stimulate K_{ATP} activity, but normally this effect is masked by the potent inhibitory effect of the nucleotide on the Kir6.0 subunit.

Other nucleotides, like GTP and ADP in the presence of Mg^{2+} stimulate K_{ATP} channels by acting on NBF's of SUR (Trapp et al., 1997).

1.9. Sulphonylurea receptor: site for potassium channel openers and blockers

1.9.1. Potassium channel openers (KCO)

The SUR isoforms are the target for potassium channel openers (KCO). These drugs e.g. P1075, pinacidil, diazoxide, exert their effects on cells by opening K_{ATP} channels, thus shifting the membrane potential towards the reversal potential for potassium and reducing cellular electrical activity (Edwards et al. 1993). The binding of KCO to SUR isoforms requires the binding of ATP to the NBFs (Schwanstecher et al., 1998). When non-hydrolysable ATP-analogues were investigated it was found that Mg^{2+} or Mn^{2+} were required to support KCO binding. The affinity of a KCO towards a K_{ATP} channel depends upon the type of SUR isoform present. For example, the smooth muscle isoform, SUR2B, responds to the same openers as the cardiac isoform, SUR2A, but with a significantly higher affinity (Schwanstecher et al., 1998).

Two regions within the 11-17 cluster of transmembrane domains of SUR subunits are reported to be essential for potassium channel opener (KCO) binding and action (Uhde et al. 1999). Chimaeras of the SUR2B isoform substituted with segments of the SUR1 isoform were used to investigate KCO sensitivity. Direct binding experiments

showed that the EC₅₀ of the wt SUR2B for P1075 was approximately 10⁵ fold lower than that of wt SUR1, indicating high affinity of SUR2B towards P1075. Two regions of SUR2B, part of the cytoplasmic loop between TMD 13-14 (Thr1059-Leu1087) and TMD 16-17 (Arg1218-Asn1370), were identified to be essential, with complete loss of detectable [³H] P1075 binding following substitution of these SUR2A segments with those from SUR1. When both of these regions from SUR2B were transferred into SUR1, the chimaera showed a 6,200-fold increase of affinity for P1075, whereas split substitution of either TMD alone mediated only a small increase in affinity. This implied that both domains are required to interact with KCO (Uhde et al. 1999). In another study, the search was narrowed down to two amino acid residues (L1249/T1253 in SUR2A and T1286/M1290 in SUR1) within the 17th TMD that allow KCO (cromakalim) binding (Moreau et al., 2000). Again this was achieved by using SUR1-SUR2A chimaeras and point mutants expressed and characterized (using patch-clamp techniques) in *Xenopus* oocytes. A cromakalim analogue, SR47063, was used in the presence of ATP to stimulate chimeric-constructed K_{ATP} channels.

1.9.2. Potassium channel antagonists: Sulphonylureas

Like KCO, K_{ATP} channel inhibitors, glibenclamide and tolbutamide, also exert their effect by binding to the SUR subunit. Similar to the KCOs, the inhibitory effect of these sulphonylureas depends upon the type of SUR subunit that is present in the K_{ATP} channel (Gribble et al., 1998). For example, tolbutamide blocks Kir6.2/SUR1, but not Kir6.2/SUR2A, currents with high affinity, whereas glibenclamide blocks both types of channels with high affinity. While the effect of glibenclamide is readily reversible for Kir6.2/SUR2A currents, inhibition of Kir6.2/SUR1 currents is very slow to reverse (Gribble et al., 1998). The protein region in the SUR1 subunit that is involved in high-affinity tolbutamide block was discovered by Ashfield et al., (1999). A series of chimaeras between SUR1 and SUR2A was constructed, coexpressed with Kir6.2 in *Xenopus* oocytes and K_{ATP} currents measured using inside-out membrane patches. Results showed that the SUR2A chimaera in which transmembrane domains 14-16 (amino acid residues 1035-1277) were replaced with those of SUR1 expressed channels with high-affinity tolbutamide inhibition, whereas channels with SUR1 chimaera containing transmembrane domains 13-16 of SUR2A, showed abolished high-affinity tolbutamide inhibition. They also demonstrated that by mutating Ser¹²³⁷ to tyrosine within this region of SUR1, both high-affinity tolbutamide inhibition and

to tyrosine within this region of SUR1, both high-affinity tolbutamide inhibition and [H^3]-glibenclamide binding were abolished. In another chimaera study, both the N- and C- terminal domains of SUR1 were shown to be essential for glibenclamide binding (Mikhailov et al., 2000).

These two pharmacological tools, potassium channel openers and sulphonylureas, are an important means of characterizing K_{ATP} channels on the basis of subunit qualitative and quantitative response to these openers and inhibitors (Babenko et al., 1998).

1.10. Modulation of K_{ATP} channels by phosphatidylinositol 4,5 bisphosphate

Besides cytosolic factors, a component of the membrane lipid bilayer, phosphatidylinositol 4,5-bisphosphate (PIP_2), also modulates K_{ATP} channel activity. PIP_2 content increases the open probability and decreases the ATP-sensitivity of the native cardiac and reconstituted Kir6.2/SUR2A K_{ATP} channel (Baukowitz et al. 1998). PIP_2 content increases when phosphatidylinositol and phosphatidylinositol 4-monophosphate are consecutively phosphorylated by phosphatidylinositol 4-kinase and phosphatidylinositol 5-kinase. In COS7 cells expressing the M_1 receptor and Kir6.2/SUR2A, stimulation of the PLC-linked receptor, via addition of ACh caused PIP_2 content to fall and inhibition of K_{ATP} current (Xie et al., 1999). COS7 cells expressing the M_1 receptor and Kir6.2/SUR2A channel in an inside-out patch configuration showed abolished ACh-induced inhibition on addition of $1\mu M$ U-73122, a PLC blocker (Xi et al. 1999). Xie et al. (1999) also investigated the effect of PLC-receptor-mediated inhibition when PIP_2 synthesis was blocked. In their experiments, ACh ($10\mu M$) produced inhibition of K_{ATP} current, which recovered after washout of ACh. On addition of $100\mu M$ wortmannin, an inhibitor of phosphatidylinositol 3-kinase and phosphatidylinositol 4-kinase, the K_{ATP} current no longer recovered after the washout of ACh (Xie et al., 1999). Thus PIP_2 modulates K_{ATP} channel activity.

In another study (Shyng et al. 2000), Kir6.2/SUR1 channels, in inside-out membrane patches from COSm6 cells over-expressing PIP_5 kinase showed a decreased sensitivity to ATP inhibition. PIP_2 has been reported to regulate the activity of the Kir channels, GIRK channels and the $Na^+ - Ca^{2+}$ exchanger (Huang et al. 1998). Therefore,

control of cellular function through the modulation of ion channels and transporters (Xi et al., 2000).

The mechanism by which phospholipids reduce ATP sensitivity to K_{ATP} channels is unclear, but evidence does exist that PIP_2 and ATP may directly compete for binding to the K_{ATP} channel (MacGregor et al., 2001). The fluorescent ATP-analogue, TNT-ATP, has been shown to bind specifically to Maltose binding protein (MBP) fusion protein of the C-terminus of all of the known K_{ATP} channels but not to the C-terminus of an ATP-insensitive inwardly rectifier K^+ channel, Kir2.1. They calculated reduction of total fluorescence (F_T) emitted by binding of the TNT-ATP analogue to an MBP fusion of the C-terminal of Kir1.1 when PIP_2 was added. As expected total TNT-ATP fluorescence increased in a concentration-dependent manner. Addition of PIP_2 reduced F_T in a concentration-dependent fashion. They also found that increasing the phosphorylation state of phosphatidylinositol phospholipid enhanced its potency to compete with TNT-ATP binding to the MBP Kir1.1 C-terminus fusion protein. In addition, polycations, like neomycin, polylysine and spermine, reversed the PIP_2 competition of TNT-ATP binding. Presumably the polycation binds to the negatively charged phosphatidylinositol phospholipids in the cell membrane and prevents them from interacting with the K_{ATP} channel (Fan et al., 1997). Similar results were seen when MBP-C-terminus Kir6.2 and Kir6.2 Δ 36 were used. This study thus suggested that the COOH-terminus of K_{ATP} channels forms a nucleotide and phospholipid modulated channel gate on which ATP and phospholipid compete for binding (MacGregory et al., 2001).

Application of MgATP to excised membrane patches has been shown to reverse the rundown of both native and cloned K_{ATP} channels (Xie et al; 1999). PIP_2 has also been implicated in this effect (Xie et al; 1999). Magnesium nucleotides interact with the NBF's of SUR (Gribble et al; 1998) and most concentrations of MgATP result in K_{ATP} channel inhibition. Since MgATP might act as a PO_4^{-2} donor to produce phosphorylated phospholipids, MgATP might have an opposite effect on K_{ATP} channel activity, i.e. it might decrease rate of channel rundown, cause reactivation of the channel after removal of ATP and reduce the channel ATP sensitivity. Song et al. (2001) examined the effect of 100 μ M MgATP on *Xenopus* oocytes expressing

(2001) examined the effect of 100 μ M MgATP on *Xenopus* oocytes expressing Kir6.2/SUR1 and Kir6.2/SUR2A. Application of MgATP to the intracellular membrane of the excised patch initially inhibited both channels. Inhibition of Kir6.2/SUR1 current did not change over the course of a 10 minute exposure to ATP, whereas there was a gradual decline in ATP sensitivity of Kir6.2/SUR2A current with time. To test whether the reduction of ATP sensitivity of the K_{ATP} channel might be due to the ATP-dependent generation of PIP₂, Song et al (2001) examined the effect of a PI3-kinase inhibitor (LY294002) on the ATP sensitivity of Kir6.2/SUR2A currents. Application of 10 μ M LY294002 blocked the time-dependent decline in ATP sensitivity observed for Kir6.2/SUR2A currents and prevented the reduction in ATP sensitivity produced by preincubation with ATP. To determine the molecular basis of the differential sensitivity of Kir6.2/SUR1 and Kir6.2/SUR2A current to phospholipid Song et al., (2001) constructed chimaeras between SUR1 and SUR2A, and investigated the ability of 100 μ M MgATP to produce a time-dependent activation of K_{ATP} channels containing chimeric SUR. When the first 6 TMDs of SUR1 were transferred into SUR2A, the ability of MgATP to stimulate K_{ATP} channel activity was abolished, suggesting that this region of SUR is critical for the different response of Kir6.2/SUR1 and Kir6.2/SUR2A channels to MgATP.

1.11. Modulation of K_{ATP} channels by phosphorylation

Many ion channels are regulated by protein phosphorylation (Levitan et al. 1994). Phosphorylation is an event in which an enzyme, a protein kinase, transfers a phosphate group from ATP to a specific site(s) on the protein. The reverse of this reaction is called dephosphorylation and requires an enzyme called a protein phosphatase. Both of these reactions require the hydrolysis of a phosphate bond, so both reactions are energetically favourable and will take place rapidly provided the protein kinase or phosphatase is active. The most common mechanisms of phosphorylation of ion channels are mediated by cyclic AMP-dependent protein kinase (PKA) and protein kinase C (PKC). The PKA enzyme molecule is a complex of two regulatory subunits, each binding two molecules of cAMP, and two catalytic subunits which catalyse the phosphorylation of the substrate protein (Taylor et al., 1989). The complex is inactive in the absence of cAMP, but dissociates to release the active catalytic subunits when cAMP is bound. In PKC, the regulatory and catalytic

part of the molecule is in different domains of the same protein chain rather than in separate subunits. The PKC enzyme comprises a highly homologous family of at least ten isozymes (Newton et al., 1995; Dekker et al., 1994; Mahoney et al., 1995). Members of the first group of isozymes (α , β I, β II and γ) are activated by Ca²⁺, phosphatidylserine (PS) and diacylglycerol (DAG), and thus conform to the conventional classification. Members of the second group (δ , ϵ , η and θ) are stimulated by DAG and PS but do not require calcium for activation, and are thus referred to as unconventional PKC isozymes. Members of the third group (ζ and λ) are stimulated by PS alone and are thus considered atypical PKC isozymes (Newton et al. 1995).

The SUR1/Kir6.2 channel has shown to be phosphorylated by PKA (Béguin et al. 1999). Using incorporation of radioactive ³²P, both SUR1 and Kir6.2 have been identified as substrates for PKA phosphorylation. The consensus sites on the Kir6.2 subunit for PKA phosphorylation are Threonine 224 and Serine 372. These two residues were mutated (T224A, S372A and T224A/S372A) and expressed with SUR1 in *Xenopus* oocytes and the phosphorylation capacity of the wt and mutant channels was tested by immunoprecipitation (Béguin et al. 1999). The antibody used was prepared against an unconjugated 24-mer peptide of the C-terminal region of mouse Kir6.2. Phosphorylation was carried out on lysed oocytes in the presence of 100 μ M [γ ³²-P] ATP and 50 μ M cAMP. Béguin et al. (1999) found that after immunoprecipitation of Kir6.2, an increase in the ³²P incorporation upon cAMP addition was detected in wt Kir6.2. On the other hand, the mutant S372A and the double mutant T224A/S372A were shown not to be substrates for PKA phosphorylation, whereas the T224A mutant continued to be phosphorylated by PKA. These results are summarized in **Table 1.5**.

A similar approach was used to identify the phosphorylation sites for PKA in human SUR1. Possible sites on SUR1 for PKA phosphorylation are T949, S1446, S1500 and S1571. Béguin et al. (1999) mutated these residues and expressed the mutants in oocytes. Both the S1500A and S1446A mutants were phosphorylated to the same extent as the wt. In contrast, the phosphorylation in the S1571A mutant in response to PKA was completely abolished (**Table 1.5**). These results indicated that S372 of

Kir6.2 and S1571 of SUR1 were directly phosphorylated by PKA as shown in **Figure 1.1**.

Béguin et al. (1999) then looked at the functional significance of these phosphorylated sites. This was done by investigating the electrophysiological properties of COS-1 cells expressing wt Kir6.2/SUR1, Kir6.2S372A/SUR1, Kir6.2/SUR1S1571A and Kir6.2S372A/SUR1S1571A in excised inside-out membrane patches. Results showed a 2-fold increase in activity for both wt Kir6.2/SUR1 and mutant Kir6.2/SUR1S1571A after application of the PKA catalytic subunit. In contrast, no significant increase in activity was observed in K_{ATP} channels comprising either Kir6.2S372A/SUR1 or Kir6.2S372A/SUR1S1571A. Béguin et al. (1999), thus concluded that the K_{ATP} channel could be activated by direct PKA-mediated phosphorylation of S372 in Kir6.2.

A decrease in channel activity was observed after wt were treated with alkaline phosphatase (dephosphorylation agent). The wt channel displayed a significantly prolonged burst and cluster duration, whereas no significant change was observed in the K_{ATP} channel containing the mutant SUR1 (S1571A). From this Béguin et al. (1999) concluded that the SUR1 subunit displays basal PKA-phosphorylation, which is dephosphorylated by addition of alkaline phosphatase.

Mutants	Kir6.1			SUR1		
	T224A	S372A	T224A/S372A	S1446A	S1500A	S1571A
Phosphorylation on addition of cAMP	+	-	-	+	+	-

Table 1.5 Summary of results obtained from wt and mutant Kir6.2/SUR1 channel PKA-mediated phosphorylation (Béguin et al. 1999). Plus signs represent phosphorylation, whereas the minus signs represent no phosphorylation on addition of cAMP.

In contrast to the *in vitro* findings of Béguin et al. (1999), Lin et al. (2000) demonstrated T224 of Kir6.2 to be the substrate for physiologically relevant PKA phosphorylation rather than S372. Lin et al. (2000) compared single channel currents

of wt Kir6.2 Δ C36 and mutant T224A Kir6.2 Δ C36 expressed in HEK293 cells. Mutant Kir6.2 Δ C36 showed no change in channel activity on treatment with PKA in the presence of Mg-ATP compared to wt Kir6.2 Δ C36, which showed increased activity. Lin et al. (2000) suggested that T224 was the phosphorylation site through which PKA modulated Kir6.2 Δ C36 channel function. The dose-response curves for ATP inhibition of Kir6.2/SUR1 and mutant Kir6.2T224A/SUR1 channels determined after stimulating cells with PKA in inside-out patches showed average K_i of 10.5 μ M for wt channels and 7.2 μ M for mutant channels suggesting that the T224 phosphorylation contributes to a reduction of ATP sensitivity for channel inhibition (Lin et al., 2000).

Neither Béguin nor Lin et al., were able to detect protein kinase C (PKC)-mediated phosphorylation of Kir6.0 or SUR receptor subunits, but there is evidence that PKC-mediated phosphorylation in human, rabbit, dog and swine ventricular myocytes activate K_{ATP} channels (Hu et al. 1996; Liu et al. 1991; Auchampach et al. 1993; Van Winkle et al. 1994). Light et al., (2000) showed PKC-mediated phosphorylation of the truncated C-terminal inwardly rectifying Kir6.2 subunit, Kir6.2 Δ C26. The mutant Kir6.2 Δ C26 forms functional K_{ATP} channels in the absence of SUR subunits when the C-terminal 26 amino acids are removed. The group showed a significant increase in whole-cell current on application of the membrane permeant phorbol 12-myristate 13-acetate (PMA; 100nM) in tsA201 cells (an SV40-transformed variant of the HEK293 cell line) expressing the Kir6.2 Δ C26 mutant. Coexpression of either SUR1 or SUR2A with Kir6.2 in tsA201 cells also yielded currents that were enhanced by PMA, but in both cases the PMA-induced current was sensitive to glibenclamide. These results suggested that the stimulatory effect of PKC occurred via the Kir6.2 subunit. A conserved threonine residue (T180) in the Kir6.2 Δ C26 mutant was determined to be the main site for PKC-mediated phosphorylation. To test the hypothesis that T180 was necessary for PKC-induced modulation of channel function, the effects of replacing this residue with alanine (T180A) or glutamate (T180E) in Kir6.2 Δ C26 constructs was examined. In whole cell perforated-patch recordings of cells expressing Kir6.2 Δ C26 mutant with SUR1, application of 100nM PMA to cells expressing either the T180A or T180E constructs had no significant effect on current increments. An M5-FLAG epitope was engineered onto the N-terminus of the Kir6.2 Δ C26 mutant and the Kir6.2 Δ C26 mutant containing the T180A substitution.

Membrane protein fractions from cells transfected with either the above two constructs were subjected to *in vitro* PKC phosphorylation assays. A phosphorylated 45kDa band was detected in the Kir6.2ΔC26 mutant, identified in Western blots using an M5-FLAG antibody (predicted molecular mass of Kir6.2 subunit), whereas the Kir6.2ΔC26 mutant with the T180A substitution showed no PKC-mediated phosphorylation in the corresponding band. Thus, the results revealed that the Kir6.2 subunit is the primary target site for PKC-mediated phosphorylation at residue T180 in Kir6.2/SUR1 channels (Light et al., 2000).

There are several studies that suggest that cardiac K_{ATP} channels, both in the sarcolemmal and mitochondria, may be regulated by PKC and play a vital role in ischaemic preconditioning (Hu et al., 1998; Liu et al., 1998; Sato et al., 1998; Light et al., 2000). The homologous PKC consensus site is also highly conserved in Kir6.1 (Suzuki et al., 1997), which may form the pore of mitochondria K_{ATP} channel, but it is still not clear whether together both or a particular individual cardiac K_{ATP} channel has a relative importance in the process of ischaemic preconditioning mediated by PKC (see section 1.12).

1.12. Other modulators of K_{ATP} channels

1.12.1 Acidic pH

Besides nucleotides, phospholipids and phosphorylation, evidence also suggests that K_{ATP} channels are modulated by acidic pH (Xu et al., 2001; Piao et al., 2001). Piao et al., (2001) have discovered critical amino acids residues in the N- and C-termini and M2 region of the Kir6.0 subunit that are required for pH regulation. This was investigated by constructing chimaeras between the Kir6.2ΔC36 subunit (activated by acidosis) and Kir1.1 subunit (inhibited by acidosis) and examination of the effect hypercapnia (produced by incubating cells with 15% CO₂) on whole-cell currents when the chimaeras were expressed in *Xenopus* oocytes. Piao et al., (2001) then examined by mutagenesis which residues within the pH- sensitive regions were essential for pH regulation. It had been shown that a lysine residue at position 80 in the N-terminus of Kir1.1 (Tsai et al., 1995) and at position 67 in Kir4.1 is essential for sensitivity to the inhibitory effect of pH (Yang et al., 1999). At the same position, the

Kir6.2 subunit has a threonine (Th-71) instead of lysine residue (Inagaki et al., 1995). Piao and colleagues performed site-directed mutagenesis at this site, mutating threonine to lysine, and examined whole cell current when cells expressing the mutant were exposed to 15% CO_2 . The results showed that the mutant channels became insensitive to hypercapnia. They then mutated the threonine residue to methionine (non-polar residue) and serine (polar-neutral residue). Introduction of the methionine residue reduced pH sensitivity, whereas serine enhanced whole-cell currents under reduced pH conditions. Thus, Piao et al., (2001) suggested that a polar-neutral residue at position 71 in the Kir6.2 subunit was necessary for maintaining pH sensitivity. Similarly, by mutagenesis Piao et al., (2001) discovered a short motif of ~6 amino acids at the intracellular end of the M2 segment centred by the cysteine-166 and a histamine residue at position 175 in the C-terminus that were essential for pH regulation in the Kir6.2 subunit.

1.12.2. Regulation by G-protein-coupled receptors

K_{ATP} channels are also regulated by G-protein-coupled receptors such as galanin (Dunne et al., 1989), adenosine (Kirsch et al., 1990) and somatostatin (Ribalet et al., 1995). The G-protein $\beta\gamma_2$ subunit ($G_{\beta\gamma_2}$) was shown by Wada et al. (2000) to bind directly to the SUR subunit of the K_{ATP} channel. By expressing Kir6.2/SUR1 and Kir6.2/SUR2A channels in COS-1 cells, Wada et al. (2000) examined the effect the $G_{\beta\gamma_2}$ protein had on the two channel activities in the inside-out configuration of the patch clamp technique. Results showed enhancement of Kir6.2/SUR2A channel activity in the presence of 100 μ M ATP on the application of intracellular $G_{\beta\gamma_2}$ that was abolished as soon as the $G_{\beta\gamma_2}$ was washed out. A similar result was seen for the Kir6.2/SUR1 channel, but the pattern of channel activity induced by $G_{\beta\gamma_2}$ in the presence of ATP was different for Kir6.2/SUR2A and Kir6.2/SUR1 channels. $G_{\beta\gamma_2}$ increased the burst length, rather than the opening frequency of Kir6.2/SUR2A channels, whereas $G_{\beta\gamma_2}$ increased the opening frequency of Kir6.2/SUR1 channels without obvious changes in the burst duration. This suggested that the $G_{\beta\gamma_2}$ -induced modulation displayed different effects on K_{ATP} channel activity depending upon the SUR subunit. Experiments were then designed to confirm the binding of $G_{\beta\gamma_2}$ protein to the SUR subunit. The Kir6.2 Δ C26 (functional K_{ATP} channel) was expressed alone and with SUR2A in COS-1 cells and the effect of $G_{\beta\gamma_2}$ was examined. Results showed

cells expressing Kir6.2 Δ C26 alone showed no further enhancement of channel activity, whereas the Kir6.2 Δ C26/SUR2A channels showed increased activity on addition of $G_{\beta\gamma 2}$, suggesting the involvement of the SUR subunit for $G_{\beta\gamma 2}$ binding (Wada et al., 2000).

1.13. Ischaemic Preconditioning

A role for K_{ATP} channel regulation has been implicated in ischaemic preconditioning (IP), an event in which brief periods of conditioning ischaemia paradoxically protect the myocardium against subsequent lethal ischaemia (Gross et al. 1994). Ischaemic preconditioning was first reported in dogs (Murry et al., 1986). Anaesthetized dogs were subjected to four sequential 5-min periods of regional ischaemia, each followed by reperfusion, before a sustained 40-min ischaemic insult. Murry et al., (1986) found that the brief ischaemic periods, which were too brief to cause any myocardium damage, greatly reduced the amount of infarction generated during the subsequent sustained occlusion. Ischaemic preconditioning has since been shown to reduce infarct size in every other species tested including rat (Liu et al., 1992), rabbit (Liu et al., 1991), and pig (Vahlhaus et al., 1996).

Ischaemic preconditioning is a receptor-mediated event, which involves the activation of various G-protein coupled receptors; one of them being the adenosine A_1 receptor (Liu et al., 1991). Ischaemic myocardium rapidly degrades ATP to adenosine, which accumulates in the tissue. To determine whether adenosine might have an effect on the preconditioning phenomenon, Liu et al., (1991) administered adenosine antagonists to preconditioned rabbit hearts. They found that pre-treatment with a non-selective adenosine receptor antagonist (PD-115199) blocked protection induced by a single 5 min cycle of ischaemia and reperfusion before a 30 min occlusion in anaesthetized rabbits. Experiments showing that the A_1 receptor selective agonist (CCPA) but not the A_2 receptor agonist (CGS-21680) mimicked IP in rabbits confirmed the activation of A_1 receptors during IP (Thornton et al., 1992).

In addition to adenosine, the ischaemic heart releases another metabolite, bradykinin. Infusion of the selective bradykinin B_2 receptor antagonist (HOE 140) before a single 5-min ischaemic event completely blocked protection in anaesthetized rabbits (Goto

et al., 1995) suggesting that activation of a bradykinin receptor, as well as the A_1 adenosine receptor, can trigger IP. A third trigger of IP, activation of opioid receptors, has been reported (Huh et al., 2001). Huh et al., (2001) found that a 5-min exposure to the δ_1 -opioid receptor agonist, (-)-TAN-67, followed by a 10 min reperfusion protected cardiac ventricular myocytes isolated from chick embryos against injury induced by the subsequent prolonged ischemia. Besides the involvement of these activated receptors in triggering IP, a non-receptor trigger, oxygen radicals, has also been reported in rabbit heart (Baines et al., 1997). In this case N-2-mercaptopyrionyl glycine, a cell-permeable radical scavenger, completely abolished protection by IP in rabbit heart (Baines et al., 1997).

It would appear that simultaneous activation of adenosine, bradykinin and opioid receptors, as well as the release of oxygen radicals during the brief ischaemia/reperfusion episode, may all contribute to triggering IP. All are thought to act through a PKC pathway because IP in response to bradykinin (Goto et al., 1995), adenosine (Sakamoto et al., 1995), opioids (Huh et al., 2001) and free radicals (Baines et al., 1997), can all be blocked by PKC inhibitors.

1.13.1. Ischaemic Preconditioning and Cardiac K_{ATP} channels

Cardiac myocytes contain two ATP-sensitive potassium channels, the sarcolemmal K_{ATP} channel (sarc K_{ATP} ; Inagaki et al., 1996) and the mitochondria K_{ATP} channel (mito K_{ATP}) found in the inner mitochondria membrane (Inoue et al. 1991). The sarc K_{ATP} channel is suggested to be composed of four SUR2A and four Kir6.2 subunits based on the similarity of K_{ATP} currents expressed by Kir6.2/SUR2A in heterologous expression systems (Inagaki et al., 1996). Little is known about the composition of the mito K_{ATP} channel, however Suzuki et al. (1997) found that an antibody to a C-terminal epitope of Kir6.1 labelled the inner membrane of mitochondria in rat skeletal muscle using immunogold histochemistry and Szewczyk et al. (1997) have described the binding by glibenclamide to a small protein in crude mitochondria extract, possibly representing all or part of a mitochondrial sulphonylurea receptor. These observations hint that the mito K_{ATP} channel consists of a pore-forming subunit with homology to Kir6.1 and an unknown sulphonylurea receptor subunit. Both of these channels respond to many of the same potassium

channel openers, such as pinacidil (Critz et al. 1997) and blockers, such as glibenclamide, however diazoxide opens mito K_{ATP} channels >1000 fold more potently than the Sarc K_{ATP} channel (Garlid et al. 1996). Until recently, the mito K_{ATP} channel was suggested to be inhibited specifically by 5-hydroxydecanoate (5-HD; Garlid et al., 1996; Sato et al. 1998). Recent evidence from Hanley et al., (2002) (discussed later in section 1.13.1) suggests this might not be the case. The sarc K_{ATP} channel is selectively inhibited by HMR-1883 (Gross et al. 1999).

Cardiac K_{ATP} channels are thought to play a vital role in ischaemic preconditioning (IP). Much of the evidence supporting the role of K_{ATP} channels in IP is based on inhibition of the protective effects of both ischaemic and pharmacological preconditioning by inhibitors of K_{ATP} channels (Grover et al., 1997). Administration of bimakalim and cromakalim before ischaemia can reduce infarct size in dogs (Yao et al., 1994; Grover et al., 1995). Armstrong et al., (1995) showed that pinacidil could protect rabbit myocytes against simulated ischaemia. In guinea pig hearts, post-ischaemic recovery of function was greatly improved by either of the K_{ATP} openers BMS-180448 or cromakalim (Grover et al., 1995).

A number of groups have provided evidence of the involvement of PKC and K_{ATP} channels in IP in heart (Liang et al., 1997; Hu et al., 1996; Light et al., 1996). Liang et al. (1997) used chicken embryo ventricular myocytes to investigate the effects of hypoxia on myocytes after the addition of adenosine, the PKC inhibitor chelerythrine, the PKC activator phorbol 12-myristate 13-acetate (PMA) and two K_{ATP} channel blockers, glibenclamide and 5-HD. The percentage of cells killed that were incubated with 1 μ M adenosine prior to a 90-minute period of hypoxia showed a 3-fold decrease compared to unstimulated cells. A similar effect was seen when 0.1 μ M PMA was added, but the percentage of cells killed and the amount of creatine kinase released when cells were incubated with PMA and chelerythrine together was greater than the control. These results suggested a central role for PKC induced IP. When glibenclamide or 5-HD was added with PMA, cells showed an increase in cell death suggesting that PKC acts on K_{ATP} channels directly or indirectly to activate channels to bring about IP.

Hu et al. (1996) has also provided evidence that PKC activates cardiac K_{ATP} channels in rabbit and human ventricular myocytes. This group has shown activation of K_{ATP} current in rabbit myocytes on addition of 0.1 μM phorbol 12,13-didecanote (PDD) in the presence of 400 μM ATP. Cells showed no spontaneous K_{ATP} current in the presence of 400 μM ATP when exposed to 30 nM bisindolylmaleimide (BIM; PKC inhibitor), 5 minutes prior to 0.1 μM PDD. Human myocytes behaved similarly when incubated with 0.1 μM PDD alone and with BIM added. In both rabbit and human myocytes, the PDD activated K_{ATP} current was blocked with 10 μM glibenclamide.

The question still remains concerning whether one or both K_{ATP} channels are involved in IP. Data may suggest T180 being the target for PKC-mediated phosphorylation in sarc K_{ATP} channels (Light et al., 2000 see section 1.10), but the question whether Kir6.2/SUR2A channels are involved in IP remains. Originally, it was proposed that activation of sarc K_{ATP} channels caused a reduction in action potential duration, thereby, decreasing contractility and conserving energy (Takano et al., 1993; Inoui et al., 1991). Contrary to this, however, it has been shown that cardioprotection produced by various potassium channel openers can occur without effect on action potential duration (Yao et al., 1994; Grover et al., 1995).

Some studies suggest that the mito K_{ATP} channel is the key contender in the process of IP (Liu et al. 1998; Toyoda et al. 2000; Liu et al. 1996), although the physiological and pathological roles of the mito K_{ATP} channel are not yet very clear. Opening of mito K_{ATP} channels dissipates the inner mitochondria membrane potential established by the F_0F_1 proton pump (Garlid et al., 1996). This dissipation accelerates electron transfer by the respiratory chain, which leads to net oxidation in the mitochondrial matrix. It is possible to monitor the mitochondrial redox state by recording the fluorescence of FAD-linked enzymes in the mitochondria (Chance et al. 1972; Hajnoczky et al. 1995).

To try to dissect the contribution of the two K_{ATP} channels to IP, Liu et al. (1998) investigated the effect of diazoxide on ventricular myocytes isolated from rabbit heart. Diazoxide at the time of this study was regarded as a selective mito K_{ATP} channel opener (Garlid et al., 1996). Firstly, to investigate the selectivity of diazoxide towards

the $mitoK_{ATP}$ channel, flavoprotein fluorescence and $sarcK_{ATP}$ current in cells exposed to 100 μ M diazoxide and pinacidil (Non-selective KCO) were measured. Reversible oxidation of the flavoproteins but no activation of $sarcK_{ATP}$ current was observed, whereas pinacidil induced mitochondrial oxidation and activated $sarcK_{ATP}$ current. The subcellular site of diazoxide action on rabbit myocytes was further localised by imaging flavoprotein fluorescence. Fluorescence was low under control conditions, but exposure to diazoxide increased fluorescence in strips parallel to the myofibril orientation. Subsequent exposure to dinitrophenol (DNP), a protonophore that uncouples respiration from ATP synthesis and collapses the mitochondrial potential, increased fluorescence in these locations even further. Sodium cyanide (CN), which inhibits the cytochrome oxidase and thus stops electron transfer, reduced fluorescence to the basal level. Liu et al. (1998) found that the distribution of fluorescence induced by diazoxide and DNP was as expected for mitochondria, which occupy approximately 35% of cardiomyocyte volume and are clustered longitudinally between myofibrils (Sommer et al. 1979).

To test the idea that $mitoK_{ATP}$ channels may play a role in cardioprotection, Liu et al. (1998) examined the effect of diazoxide in a cellular ischaemic model. Ventricular myocytes were centrifuged into a pellet to simulate the restricted extracellular space and reduced oxygen supply during ischaemia. Samples were taken from the pellet at 60 and 120 minute time points and stained with trypan blue solution to test the osmotic fragility of the membrane (Vander Heide et al. 1990). Cells permeable to trypan blue were counted as dead. Cells treated with 50 μ M of diazoxide 15 minutes before pelleting showed decreased cell death during simulated ischaemia to about half of that in the controls (untreated cells). The protection by diazoxide was completely blocked when cells were treated with 100 μ M 5-HD and 50 μ M diazoxide together 20 minutes prior to pelleting. From these results, Liu et al. (1998) proposed that the $mitoK_{ATP}$ channels might be the elusive effectors of preconditioning.

In another study, using a similar approach to Liu et al (1998), the effect of a PKC activator, PMA, on the regulation of the $mitoK_{ATP}$ channel on application of diazoxide was examined (Sato et al. 1998). Flavoprotein fluorescence in rabbit ventricular myocytes when stimulated with 100 μ M diazoxide in the presence of 100 nM PMA

was measured. Results showed a 2-fold increase in diazoxide-induced flavoprotein oxidation when the same myocytes were co-stimulated with PMA. Addition of an inactive compound 4α phorbol (100 nM) in the presence of diazoxide showed no increase in flavoprotein oxidation. Addition of 5-HD (2 mM) was able to prevent the diazoxide-induced oxidation, even with a simultaneous application of PMA. These findings indicated that $mitoK_{ATP}$ channels are upregulated by PMA and that the effect of diazoxide is larger and faster when the PKC activator is applied (Sato et al., 1998). Sato et al. (1998) also investigated whether $sarcK_{ATP}$ current was induced by diazoxide and PMA under the same conditions. While they found diazoxide induced flavoprotein oxidation in the presence of PMA, they could not see an effect on surface membrane current in the same cell, thus providing further evidence that the oxidative effect of diazoxide and its upregulation by PKC reflect the selective activation of $mitoK_{ATP}$ channels.

Liu et al (2002) have shown the importance of PKC- ϵ signalling via $mitoK_{ATP}$ channels during preconditioning. They showed that treatment with PMA during ischaemia-reperfusion blocked apoptosis to a similar degree in embryonic chick ventricular myocytes as did in preconditioning, i.e. three cycles of 1 minute ischaemia separated by 5 min of reoxygenation following 10 hours of simulated ischaemia. The protection of preconditioning was blocked by specific PKC- ϵ inhibition with Gö-6976. The effects of preconditioning were reversed when chick myocytes were pretreated with 5-HD, whereas transient administration of diazoxide mimicked preconditioning and blocked apoptosis. The administration of diazoxide also markedly increased PKC - ϵ in particulate fraction, which was detected by immunoprecipitation the fraction with specific anti-PKC - ϵ antibody. The effects of diazoxide were also blocked with Gö-6976 suggesting regulation of $mitoK_{ATP}$ channels mimics the effect of preconditioning to block chick cardiocyte apoptosis via activation of the PKC - ϵ isoform (Liu et al., 2002).

Studies described above (Liu et al., 1998; Sato et al., 1998; Liu et al., 2002) have all used diazoxide and 5-HD in reporting the involvement of the $MitoK_{ATP}$ channel in IP. However, in the presence of high concentrations of ADP, diazoxide can also activate $sarcK_{ATP}$ channels as well (Matsuoka et al., 2000). Recently, Hanley et al., (2002)

have shown no effect on mitochondrial membrane potential in isolated guinea-pig ventricular myocytes with the putative mito K_{ATP} channel opener diazoxide raising doubt over the involvement of mito K_{ATP} in IP. Diazoxide has been reported to inhibit succinate oxidation in liver mitochondria (Schäfer et al., 1969). More recently, diazoxide has been shown to decrease the rate of succinate oxidation in heart mitochondria (Ovide-Bordeaux et al., 2000). To investigate whether diazoxide specifically targeted complex II, the effects of 100 μ M diazoxide on respiratory chain activity using submitochondrial particles was examined (Hanley et al., 2002). In the presence of 5 mM succinate, application of 100 μ M diazoxide reduced the rate of succinate oxidation to 55 % of control rate. Diazoxide was also able to reduce succinate dehydrogenase activity to 58 % of control when the artificial electron acceptor 2, 6-dichlorophenol-indophenol (DCIP) was used to exclude the possible involvement of mito K_{ATP} channels in the measurement. The succinate dehydrogenase activity was measured by monitoring DCIP reduction at 578 nm. In conclusion findings by Hanley et al., (2002) suggest that diazoxide acts independent of Mito K_{ATP} channels and that these channels may not play an essential role in preconditioning as other have shown in ischaemia-reperfusion simulated cardiomyocytes.

5-HD is a hydroxy derivative of decanoate and it may be metabolised like other medium-chain fatty acids in the heart. The ability of acyl-CoA synthetase to synthesize 5-HD-CoA from 5-HD has been investigated recently by liquid chromatography-mass spectrometry (Hanley et al., 2002). Using analytical HPLC, the peaks corresponding to the reactants ATP and CoA but not 5-HD were resolved. When acyl-CoA synthetase was added to the reaction mixture, new peaks corresponding to 5-HD-CoA and its co-product (AMP) were identified. Electrospray ionisation mass spectroscopy was used to confirm the production of 5-HD-CoA. Together these findings suggest that diazoxide and 5-HD have mito K_{ATP} channel-independent targets with mitochondria. Thus, studies using diazoxide and 5-HD as pharmacological agents to show a link between IP and the mito K_{ATP} channel may conversationally be questioned.

Suzuki et al., (2002) have shown that the sarc K_{ATP} channel, rather than the mito K_{ATP} channel, can play a role in cardioprotection against ischaemia/reperfusion in mice.

The group examined the effect that IP had on infarct size in Kir6.2-deficient (knockout mice; KO) ventricular cells. Hearts of control wild type (WT-CON) and KO (KO-CON) mice *in situ* were exposed keeping the animals under ventilation. Ischaemia was achieved by ligating the left anterior descending artery (LAD). Regional ischaemia was confirmed by visual inspection of pale colour in the occluded distal myocardium. After a coronary occlusion of 45 minutes, release of ligature permitted reperfusion of the myocardium, which was confirmed by the appearance of red colour in the previously pale region. Ischaemic preconditioned wild type (WT-IP) and KO (KO-IP) mice underwent three cycles of 3 minutes of coronary occlusion, followed by 5 minutes of reperfusion, before being subjected to 45 minutes of coronary occlusion followed by reperfusion. The infarct (pale) and reperfused (red) regions were measured by computer analysis of heart slices. The results showed a lower percentage of infarct size in WT-IP ventricle compared to WT-CON vehicle, whereas there was no significant difference between the infarct size values of KO-CON and KO-IP. The Mito K_{ATP} channel function was examined in WT and KO mice by methods discussed above (Liu et al., 1998). In both WT and KO mice, diazoxide reversibly induced flavoprotein fluorescence, implying that Mito K_{ATP} channel function was preserved in KO ventricular cells. From these data Suzuki et al., (2002) suggested that the sarc K_{ATP} channel must play a vital role in cardioprotection against ischaemia.

There is recent evidence from Toyoda et al. (2000) suggesting that both the cardiac K_{ATP} channel types may play different roles in adenosine-enhanced IP. Toyoda et al., (2000) investigated the roles of K_{ATP} channels in rabbit heart before ischaemia, during reperfusion and during ischaemia and reperfusion using the non-specific K_{ATP} channel blocker glibenclamide, the mito K_{ATP} channel blocker 5-HD and the sarc K_{ATP} channel blocker HMR-1883 to discriminate channel involvement. It was found that the infarct size was significantly increased in IP hearts treated with glibenclamide before ischaemia and during reperfusion, and in heart cells treated with 5-HD before ischaemia. Glibenclamide treatment before ischaemia and during reperfusion showed significantly decreased functional recovery from IP, whereas cells treated with 5-HD before ischaemia and during reperfusion had no effect on recovery. Cells treated with HMR-1883 during ischaemia and reperfusion significantly decreased postischaemic functional recovery but had no effect on infarct size. From the data, Toyoda et al.,

(2000) suggested that IP infarct size reduction is modulated by mito K_{ATP} channels during ischaemia and that functional recovery is modulated by sarc K_{ATP} channels during ischaemia and reperfusion

1.13.2. Involvement of PKC and other Kinases in IP

The majority of studies imply the importance of PKC in activation of cardiac K_{ATP} channel currents during IP, but there is no evidence suggesting the mechanism of action of PKC on K_{ATP} channels. Whether PKC acts directly on K_{ATP} channels or via a cascade of other kinase phosphorylation steps remains to be resolved.

Experiments by Zhao et al., (2001) showed that adult mice treated with the adenosine mimetic 2-chloro- N^6 -cyclopentyladenosine (CCPA) had improved left ventricular function when subjected to 30 minutes of global ischaemia, which was abolished in mice treated with a p38-mitogen-activated protein kinase inhibitor (SB-203580) in the presence of CCPA. Increased phosphorylation of the p38-mitogen-activated protein kinase (p38MAPK) was discovered in CCPA-treated mice. Zhao et al., (2001) also demonstrated a block of cardioprotection in CCPA treated mice in the presence of 5-HD and a decrease in p38MAPK phosphorylation. This data suggested that p38MAPK is an essential step in mediating the late preconditioning effect due to opening of the K_{ATP} channel, but this study did not show the precise interrelationship of p38MAPK phosphorylation with the opening of the channel. p38MAPK is member of the MAPK (Mitogen-activated protein kinase) family, which is activated by tyrosine receptors and PKC. Phosphorylation of tryrosine-182 residue on p38-MAPK is required for p38-MAPK activation (Weinbrenner et al., 1997). Western blot analysis with phosphospecific p38-MAPK (tyrosine-182) antibody showed decreased phosphorylation during 30 minutes of global ischaemia in non-preconditioned, isolated rabbit hearts, but phosphorylation was enhanced after 10 and 20 minutes of ischaemia in preconditioned hearts, with a peak increase of nearly three-fold at 20 minutes. Furthermore blocking CCPA protection with non-specific adenosine receptor antagonist (SPT) showed no increased phosphorylation of p38-MAPK during ischaemia (Weinbrenner et al., 1997).

Activation of PKC has been shown to elevate MAPK-activated protein kinase-2 (MAPKAPK-2) activity in neonatal rat ventricular cardiomyocytes (Clerk et al.,

1998). MAPKAPK-2 is a primary substrate of p38-MAPK (Freshney et al., 1994), thus it may be possible that during IP, PKC phosphorylates p38-MAPK, which activates MAPKAPK-2 to target K_{ATP} channels. MAPKAPK-2 phosphorylates heat shock protein 27 (Freshney et al., 1994) but no evidence exists showing the regulation of K_{ATP} channels by MAPKAPK-2. This suggests that p38MAPK may exert its cardioprotection affect by phosphorylating heat shock protein 27, which stabilizes actin filaments thus maintaining cardiomyocyte integrity.

Besides p38MAPK, c-Jun N-terminal kinase (JNK) and extracellular signal-regulated kinases 1/2 (ERK1/2), which are also members of the MAPK family, may be possible kinases to target K_{ATP} channels initially following activation by PKC-mediated phosphorylation. Baines et al., (1998) have shown that activation of JNK mimics preconditioning in isolated rabbit hearts. The effect that a strong activator of JNK, anisomycin (Foltz et al., 1998), has on isolated rabbit heart exposed to 30 minutes of regional ischaemia was examined. Anisomycin (50ng/ml) treatment 15 minutes before and during 30 minutes of ischaemia reduced infarct size to a value similar to that observed in ischaemic preconditioned isolated rabbit hearts (Baines et al., 1998). Ping et al., (1998a) have demonstrated recently that transfection of rabbit cardiomyocytes with the wt cDNA of PKC- ϵ induced activation of JNK, whereas the activation of JNK by coronary occlusion and reperfusion in rabbit hearts was abolished by chelerythrine (PKC inhibitor; Ping et al., 1998b). However, there is no evidence suggesting an involvement of ERK1/2 in IP.

The JNK family consists of two isoforms, JNK1 and JNK2, both of which are present in the heart (Clerk et al., 1998). The p38MAPK consists of 6 isoforms (α_1 , α_2 , β_1 , β_2 , γ and δ), of which only p38 α and β isoforms are expressed in the heart (Sudgen et al., 1998). Figure 1.4 summarizes the possible events taking place during the exposure of cells to IP.

Overall, it seems that ischaemic preconditioning involves a complex cascade, which includes receptors, protein kinases and K_{ATP} channels. K_{ATP} channels play an essential role in this mechanism as they are regarded as possible end effectors. The activation of the channels is brought about by the release of adenosine, bradykinin,

opioids and free radicals during ischaemia. Together, they stimulate the phospholipase C signalling pathway, which in turn activates and translocates PKC to the membrane. PKC initiates a complex kinase cascade downstream involving tyrosine kinase, p38MAPK, JNK and possibly ERK1/2, which may eventually activate K_{ATP} channels and other end effectors.

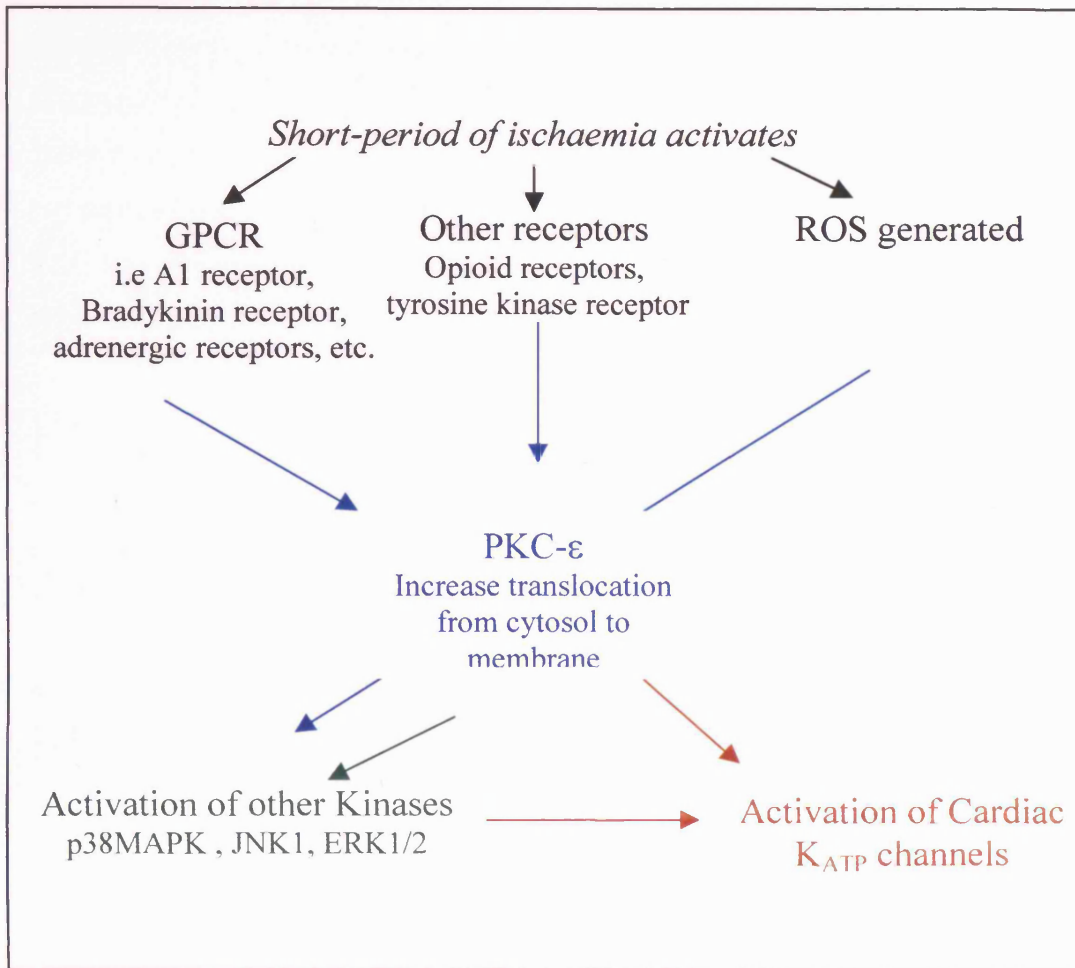


Figure 1.4 Schematic representative of the possible events that take place in cardiac cells during Ischaemic preconditioning. Evidence suggests that during short periods of ischaemia, G-protein-coupled receptors such as adenosine receptors, are activated due to an increase in extracellular adenosine concentration released after nucleotide metabolism. Other receptors such as tyrosine kinase receptors and opioid receptors are activated. There is also an increase production of reactive oxygen species. All of these have been shown to increase activity of PKC, which results in phosphorylations of cardiac K_{ATP} channels either directly or possibly via other kinases such as p38MAPK, JNK1 and ERK1/2. Regulation of the K_{ATP} channels by PKC contributes ischaemic preconditioning.

1.14. Aims

Although studies have implicated the importance of cardiac K_{ATP} channels in ischaemic preconditioning (see section 1.13), the type of K_{ATP} channel involved in this event still remains uncertain. Little is known about the mitochondria K_{ATP} channel subunit composition, which if known would permit comparison of subunit phosphorylation of the two types of cardiac K_{ATP} channels. Also, the issue of whether PKC acts directly or via a cascade of protein kinases on cardiac K_{ATP} channels remains to be investigated.

The main aims of this project were:

- 1) To characterize rabbit antisera raised against epitopes of Kir6.1 and Kir6.2, SUR2A and SUR2B using ELISA, Western blots and immunoprecipitation experiments on *in vitro* expressed Kir6.0 and SUR2 polypeptides, and by immunostaining after expression of Kir6.0 and SUR2 isoforms in human embryonic kidney (HEK 293) cell lines.
- 2) To localize cardiac K_{ATP} channel subunit distribution in cardiomyocytes and to identify the possible subunit composition of mitochondrial K_{ATP} channels by utilizing characterized antibodies in immunocytochemistry experiments and Western blots performed on isolated rat cardiac ventricular myocytes and isolated rat heart mitochondrial fractions.
- 3) To identify K_{ATP} channel subunit substrates for PKA and PKC-mediated phosphorylation and to confirm the findings of Béguin et al. (1999) that the Kir6.2 subunit is phosphorylated by PKA but not PKC. In particular, to examine *in vitro* phosphorylation of Kir6.1 and Kir6.2 proteins by specific kinases.
- 4) To examine K_{ATP} channel subunit phosphorylation events in native tissue by performing *in vivo* phosphorylation experiments on ³²P-inorganic phosphate labelled isolated rat cardiac ventricular myocytes and to identify kinases involved using various kinase inhibitors to inhibit phosphorylation.

- 5) To identify whether serine, threonine or tyrosine residues are phosphorylated in K_{ATP} channel subunits by performing two-dimensional phosphoamino acid analysis on *in vivo* phosphorylated samples using Hunters thin layer electrophoresis apparatus.

- 6) To identify the location of phosphoamino acids in K_{ATP} channel subunits by chimaera studies and site-directed mutagenesis. A longer-term aim of this study will be to examine the effect the phosphorylated subunits have on K_{ATP} channel activity by comparing electrophysiological properties of phosphorylated and normal channels.

Chapter 2: Materials and Methods

2.1. Materials

Nuclease-free water was used in the manipulation of DNA; UHQ (ultra high quality) water for immunocytochemistry and sterile deionised water was used in biochemical solutions and experiments. The Kir6.0 and SUR2 expression constructs in pBF and pBFT were provided by Dr. Lodwick. T-tubule marker, anti-IXE11₂ (Jorgensen et al., 1990) was a gift from Dr Campbell, University of Iowa. Chemicals used in phosphorylation experiments, phorbol-12, myristate-13 acetate (PMA), 2-chloro-N⁶-cyclopentyladenosine (A1 receptor agonist; CCPA), chelerythrine (PKC inhibitor), SB203580 (p38MAPK inhibitor) and U0126 (MEK1/2 inhibitor), were purchased from Sigma (UK). Calbiochem supplied the JNK 1 inhibitor. The Kir6.0 chimaeras were a gift from Dr. H. Kuhlman. Oligonucleotide primers for site-directed mutagenesis were designed with the help of Dr. Lodwick and supplied and purified by MWG-Biotech AG.

2.2. Preparation of polyclonal antibodies

Antisera were raised to peptides corresponding to the C-terminal domains of the rat subunits (Inagaki et al., 1995 and 1996; Isomoto et al., 1996). Peptides were synthesised according to Atherton and Sheppard (1985) and were composed of the following amino acid residues: Kir6.1; (C)KVQFMTPEGNQCPSSES (residues 409-424, PNAACL, University of Leicester, UK), Kir6.2; (C)KAKPKFSISPDSLS (residues 377-390, Research Genetics Inc. Huntsville, USA), SUR2A; PNLLQHKNGLFSTLVMTNK(C) (residues 1527-1545, Pepceuticals Ltd., Leicester, UK), SUR2B; ESLLAQEDGVFASFVRADM(C) (residues 1528-1546, Pepceuticals Ltd). N- or C-terminal cysteines were added to the peptides to facilitate conjugation to ovalbumin (Kir6.1) or Keyhole Limpet Haemocyanin carrier protein (Kir6.2, SUR2A/B) and were not part of the channel subunit sequences. Antisera were raised against peptide carrier protein conjugates in New Zealand White Rabbits (Kir6.1, biomedical services, university of Leicester; Kir6.2, Research Genetics Inc.; SUR2A and SUR2B, Pepceuticals Ltd.). Antibody titre was estimated by ELISA using microtitre plates coated with 1 µg/ml peptide. Plates were blocked with 0.5 % casein, 10 % calf serum, 0.05 % Tween 20 in phosphate buffered saline (PBS; 40 mM

sodium phosphate (pH 7.4), 0.9 % NaCl) for 1 h and then primary antisera were applied at the required dilution for 2 h. Antibody reaction was detected using sequential incubation (1 h) of swine-rabbit IgG (1:1000 dilution, Dakopatts, UK) and anti-rabbit peroxidase conjugate (1:1000 dilution, Amersham) in 1 % calf serum, 0.05 % Tween 20 PBS at room temperature. Positive wells were identified by the development of blue colouration following the application of 10 mg/ml 3,3',5,5'-tetramethyl benzidine (Miles, UK) in 0.1 M sodium acetate/citrate (pH 6.0), 0.0045% H₂O₂. Between steps wells were washed three times with 0.05 % Tween 20 in PBS.

2.3. Expression of K_{ATP} channel subunits

2.3.1 Transformation of Competent cells

Aliquots (50µl) of Epicurian Coli ® XL-Blue subcloning-grade competent cells containing pUC18 plasmid (Stratagene) were transferred to 15 ml centrifuge tube and 0.1-0.5 ng of the K_{ATP} channel subunit expression construct was added after the cells were thawed on ice. These constructs were provided by Dr. D. Lodwick. The mixture was incubated on ice for 20 minutes, heat pulsed for 45 seconds in a 42°C water bath. Following 2 minutes incubation on ice, 0.95 ml of SOC medium (20 g tryptone/l; 5 g yeast extract/l and 0.5 g NaCl/l autoclaved followed by addition of 10 mM MgCl₂, 10 mM MgSO₄ and 20 mM glucose) was added and further incubated for 30 minutes at 37°C. The transformation mixture (200 µl) was then spread onto LB-ampicillin plates (10g NaCl/l; 10 g tryptone/l; 5 g yeast extract/l; 20 g bactoagar/l and 50 mg of ampicillin) using a sterile spreader and incubated at 37°C for 12-16 hours. Single colonies were then used to inoculate 50 ml LB media (0.5 g tryptone/50 ml; 0.25 g Yeast extract/50 ml and 0.25 g NaCl/50 ml) supplemented with 50 µl ampicillin (100 mg/ml).

2.3.2. Purification of plasmid DNA

Plasmids were purified using the QIAfilter™ plasmid midi kit (QIAGEN®). Bacterial cells, harvested by centrifugation at 6000 × g for 15 minutes at 4°C, were resuspended in 6 ml buffer P1 (50 mM Tris-HCl, pH 8.0; 10 mM EDTA; 100 µg/ml RNase A) and lysed with the addition of 6 ml of buffer P2 (200 mM NaOH; 1 % SDS (w/v)). The lysis reaction was neutralised by the addition of 6 ml chilled buffer P3 (3 M potassium acetate, pH5.5) and the cell debris filtered away from the cleared lysate

NaCl; 50mM MOPS, pH 7.0; 15 % isopropanol (v/v)) to remove RNA, proteins, dyes, and low-molecular-weight impurities. The bound plasmid DNA was eluted in a high-salt QF buffer (1.25 M NaCl; 50 mM MOPS, pH 7.0; 15 % isopropanol (v/v)) concentrated and desalted by isopropanol precipitation using the QIAprecipitator, and finally eluted in 500 µl deionised water.

DNA yield was determined by spectrophotometric analysis (see section 2.3.3) and quality by electrophoresis of a sample on an agarose gel.

2.3.3. Spectrophotometric Analysis

The DNA samples were diluted in 10 mM Tris-HCl, pH 8.0 and the absorbance read at 260nm after standardized with 10 mM Tris-HCl, pH 8.0. From this reading the concentration of the DNA sample was calculated.

1 absorbance unit (OD) at 260 nm = 50 µg/ml of double-stranded DNA.

2.3.4. Agarose gel electrophoresis

The DNA samples were run on a 0.8 % Agarose gel (Figure 2.1). Electrophoresis grade agarose was heated in 1× TAE (40 mM Tris-acetate; 1 mM EDTA) until molten, cooled slightly and ethidium bromide added to a concentration of 0.5 µg/ml prior to pouring on to a Perspex gel slab. Ethidium bromide was used to stain the gel enabling the DNA to be visualised under U.V. light. The DNA samples were mixed with DNA loading buffer (65 % w/v sucrose; 10 mM Tris-HCl, pH 7.5; 10 mM EDTA; 0.05 % w/v bromophenol blue) and loaded onto the solidified gel slab. The gel slabs were run in TAE buffer supplemented with 0.5 µg/ml ethidium bromide at 120V. The size of the DNA samples were estimated by comparison with a 1kb DNA ladder, which was loaded alongside.

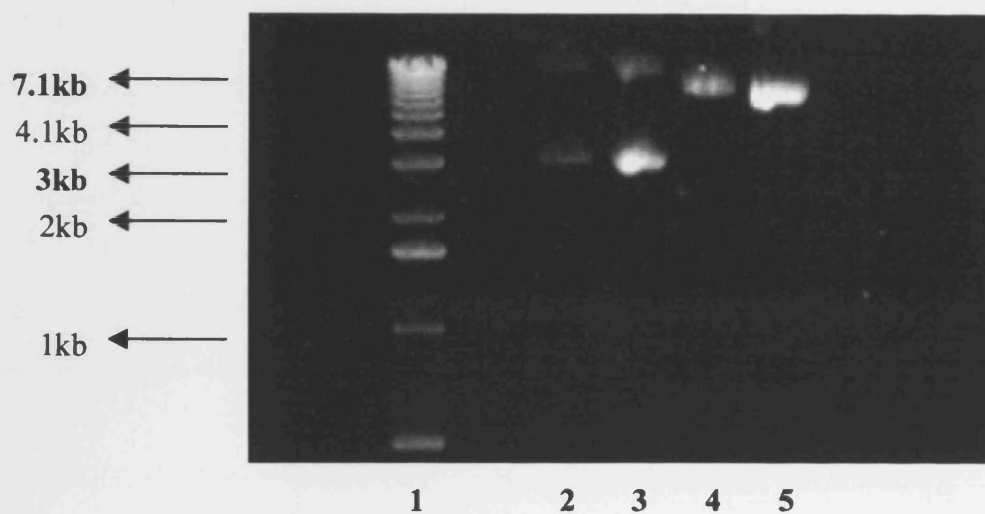


Figure 2.1. Image of agarose gel showing purified plasmid Kir6.0 and SUR2 DNA. Samples were electrophoresed on a 0.8% agarose gel. Lane 1 corresponds to 1 μ g of 1kb DNA ladder marker; lane 2, 5 μ g of Kir6.1 DNA; lane 3, 5 μ g of Kir6.2; lane 4, 5 μ g of SUR2A and lane 5, 5 μ g of SUR2B DNA.

2.3.5. *Proteinase K treated DNA and Phenol Chloroform Extraction*

The treatment of DNA with proteinase K is used to digest RNase protein from nucleic acid solutions. To midi prep DNA samples 200 µg/ml of proteinase K and 0.5 % SDS was incubated at 50°C for 1 hour. An equal volume of phenol and chloroform (1:1 ratio) was added to the proteinase K treated DNA mixture and vortexed until emulsion formed. The sample was then centrifuged at maximum speed in a desktop microcentrifuge for 1 minute at room temperature. The aqueous phase was removed for a second extraction with chloroform to remove traces of phenol and protein. After vortex and centrifugation, the aqueous layer was transferred to a fresh sterile microcentrifuge tube. The aqueous layer was incubated with ethanol for 12-16 hours at -20°C. The DNA precipitate was then recovered from the aqueous solution by centrifugation at maximum speed in a desktop microcentrifuge at 4°C. Recovered DNA pellet was resuspended in nuclease-free water.

The purified DNA yield was determined by spectrophotometric analysis as discussed in section 2.3.3.

2.3.6. *In vitro translation*

Purified DNA at 4 µg per reaction was transcribed and translated in the TNT rabbit reticulocyte lysate Quick coupled transcription/translation system (Promega), in the presence of 0.74 MBq [³⁵S]-methionine (Amersham; SJ1015) and canine pancreatic microsomal membranes (Promega). The reactions were incubated at 30°C for 90 min. Reactions were analysed on 7.5 % polyacrylamide gel and exposed to Kodak film (Section 2.4).

Unlabelled samples used for *in vitro* phosphorylation experiments (section 2.13) were translated with 1 mM methionine instead of [³⁵S]-methionine.

2.4. Electrophoresis

Polyacrylamide mini gels were poured and left to set prior to electrophoresis of samples. Samples were left to denature in denaturing buffer (220 mM sucrose, 2% sodium dodecyl sulphate (SDS), 6 mM dithiothreitol (DTT), 62 mM Tris-HCl (pH 6.8), 0.001 % bromophenol blue stain) for 20-25 minutes before electrophoresis with

high and low protein standards (Sigma; SDS-8H and SDS-7) on a polyacrylamide gel in electrophoresis buffer (25 mM Tris; 192 mM Glycine; 0.1 % SDS). The gels were electrophoresed for 1 hour at 120 volts using power pack 300 (Bio-Rad).

Components	Separating 7.5 % gel	Stacking Gel
Acrylamide	2.5 ml	0.5 ml
Seperating buffer (1.5 M Tris-HCl pH8.8; 0.4 % SDS)	2.5 ml	-
Stacking buffer (0.5 M Tris-HCl pH8.8; 0.4 % SDS)	-	1.25 ml
Water	4.98 ml	3.21 ml
Ammonium peroxidisulphate	60 µl	60 µl
N,N,N',N'-Tetramethylethylenediamine (TEMED)	14 µl	20 µl

Table 2.1. Recipe for pouring 7.5 % polyacrylamide mini gels

Protein standard lanes were stained in Fairbanks 1 stain (140 mg/l each of G250/R250 Coomassie blue stains, 25 % propan-2-ol, 10% acetic acid). The main portion of the gel was fixed in 50 % methanol, 10 % glacial acetic acid solution for 30 min, treated with 1 % methanol, 1 % acetic acid and 7% glycerol solution for 5 minutes and 0.1 M salicylic acid for 30 min before being vacuum dries at 80°C for 2 h. The dried gel was placed against Kodak X-ray film (F-5513; Sigma) and stored at -70°C, for 16-48 h, before development of the film.

2.5 Immunoprecipitation of *in vitro* translated K_{ATP} channel subunit proteins

In vitro translated K_{ATP} channel subunit proteins (5-10 µl) were treated with an equal volume of 2% Triton X-100, 20 mM Tris-HCl (pH 7.5) for 15 min at 4°C. After centrifugation at maximum in a desktop microcentrifuge, the supernatant was incubated for 16 hours at 4°C with 1 µl of anti-K_{ATP} channel subunit antiserum in a final volume of 100 µl made up in 20 mM Tris-HCl (pH 7.5), 10% bovine serum albumin, 500 mM KCl. Protein antibody complex was immunoprecipitated by the addition of 5 mg protein A-Sepharose CL-4B (P-3391; Sigma) with 2 hours

addition of 5 mg protein A-Sepharose CL-4B (P-3391; Sigma) with 2 hours incubation at 4°C. The precipitate was centrifuged at 5000 × g in a desk top microcentrifuge and washed 3 times in 0.1 % Triton X-100, 20 mM Tris-HCl (pH 7.5). The protein/antibody complexes were recovered by the addition of denaturing buffer and centrifugation at 5000 × g. Supernatants were heated to 95°C for 5 min before electrophoresis on a 7 % polyacrylamide mini gel. Gels were electrophoresed for 1.5 h at 120 V with one lane containing 1 µg/ml protein molecular weight standards (section 2.4). The dried gel was placed against Kodak X-ray film (F-5513; Sigma) and stored at -70°C, for 16-48 h, before development of the film. Controls included omission of primary antibody, use of non-specific antibodies and preabsorption of antibody solutions with 10 µg/ml of the specific or non-specific antigenic peptides for 16 h at 4°C.

2.6 Tissue culture

A human embryonic kidney (HEK 293) cell line stably expressing Kir6.2/SUR2A (a gift from Dr. Andrew Tinker, UCL, London, UK) and HEK 293 cell line stably expressing SUR2A were transfected with Kir6.1 alone and Kir6.1 with SUR2B cDNA by Richard Rainbow using the technique described below. These cells were used for immunocytochemistry experiments to characterize the antibodies.

HEK 293 cells were cultured in Minimal Eagles Medium with Earl's salts (MEM-ES), also containing 10% Foetal Calf Serum (FCS) and 10mM L-glutamine (all from GibcoBrl). The antibiotics Zeocin (717 µg/ml) (Invitrogen) and G418 (310 µg/ml) (GibcoBrl) were also included in the medium for selection purposes. Cells were used between passages 12 – 22. Cells were prepared for transfection by aspirating the growth medium and incubation in trypsin-EDTA (GibcoBrl) for 5 minutes at 37°C. Cells were re-suspended in 10ml PBS (GibcoBrl) and centrifuged for 3 minutes at 1000 × g. The supernatant was removed and the cells washed, spun and then re-suspended with 5ml full growth medium. Two millilitres of the cell suspension was used to re-seed a flask for growth; the rest was split into 35mm tissue culture dishes for transfection. FuGENE6™ (Roche) was used as a transfection reagent for the cDNA containing the SUR2A fragments, in accordance with the manufacturers guidelines. Briefly, 3 µl of FuGENE6™ was added to MEM-ES in order to give a

FuGENE6™ and then incubated for 20 minutes. The transfection solution was then added drop-wise to the cells in the tissue culture dish and incubated at 37°C in 95 % O₂/ 5 % CO₂ for 48 hours before use.

2.7 Isolation of single ventricular myocytes

Isolated rat cardiac myocytes were prepared as previously described (Mitra & Morad, 1985; Lawrence & Rodrigo, 1999) with the assistance of Dr. C. Lawrence and Dr. D. Hudman. In brief, adult male Wistar rats (300-400g) were sacrificed by cervical dislocation. The heart was excised, attached to a Langendorff column and perfused (10 ml/min) in a retrograde manner with Ca²⁺-free Tyrode's solution (135 mM NaCl, 5 mM KCl, 0.33 mM NaH₂PO₄, 5 mM Na-pyruvate, 10mM glucose, 1 mM MgCl₂, 10 mM HEPES, pH 7.4 with NaOH) maintained at 37°C and equilibrated with 95% O₂, 5% CO₂ for 5 min and then perfused with a recycling enzyme mixture (30 µg/ml collagenase (Type I), 20 µg/ml protease (Type XIV) and 50µg/ml BSA, in Ca²⁺-free Tyrode's solution) for 8-15 min. Ventricles were cut into small pieces and cells removed by mechanical agitation in 10 ml normal Tyrode's solution (Ca²⁺-free Tyrode's solution containing 2 mM CaCl₂). The isolated cells were washed twice in normal Tyrode's solution before suspension in 10ml of normal Tyrode's solution containing 200 µl of Penicillin-Streptomycin (Sigma; P0906) and stored at 10°C for a maximum of 12 hrs. Typically, there was a 70-90 % yield of quiescent, rod-shaped myocytes.

2.8 Immunocytochemistry

Coverslips (25 mm) were washed with a 1:1 mixture of chloroform and methanol, rinsed once with water, soaked in 0.01 % poly-L-lysine (Sigma) and dried 12-16 hours prior to fixation of cells. HEK 293 stable cell-lines or isolated rat ventricular myocytes were adhered to the glass coverslips at 4°C for 20 min and the cells fixed in 2 % paraformaldehyde at room temperature for 10 min. The fixative was removed and 100 mM glycine added to quench the paraformaldehyde for 10 min. Cells were treated with permeabilisation solution (0.1 % Triton X-100 in PBS; 2.7 mM KCl, 15 mM potassium phosphate, 137 mM NaCl, 8 mM Na phosphate) for 10 min. Finally, the cells were washed 3 times in PBS for 5 min and stored at 4°C for 12-16 h in PBS.

Cells were incubated for 30 min with antibody-diluting buffer (2 % goat serum, 1 % bovine serum albumin (BSA), 0.05 % Triton X-100 in SCC; 150 mM NaCl, 15 mM Na citrate). Antibody diluting buffer was replaced with the same buffer containing primary antibody (anti-Kir6.0 or anti-SUR2 antibodies) at 1:250 or 1/500 dilutions and incubated for one hour at room temperature. Cells were washed for 10 min in 0.05 % Triton X-100 in SCC and then incubated with anti-rabbit IgG fluorescein isothiocyanate (FITC) conjugate (F-0382 Sigma). After three 10 min washes, cells were viewed with a confocal dual laser-scanning microscope at a wavelength of 488nm (see section 2.8).

A mitochondrial tracker, Mitofluor red 589 (Molecular probes; M-22424), and a T-tubule marker, monoclonal antibody IXE1₁₂ raised in mouse (Dr K.P.Campbell; University of Iowa), were used to determine the colocalization of Kir6.0 and SUR2 subunits in stained cardiac myocytes. The T-tubule specific antibody was applied with the primary anti- K_{ATP} channel subunit antibodies at 1:250 dilutions on the same cells and analysed with confocal microscope simultaneously using anti-mouse IgG rhodamine (TRITC) conjugate (T-7782 Sigma) secondary antibody at a wavelength of 525nm at 1/1000 dilution. Cells incubated with anti-Kir6.0 and anti-SUR2A were also incubated with 100 nM Mitofluor 589 in PBS for 10 minutes and analysed on the confocal microscope at 580 nm wavelength. Thus, in each case two images of the same cells, one of the stained primary antibody and the other of the stained colocalization marker, were recorded and analysed.

2.9 Confocal Microscopy

Myocytes were examined using a laser scanning confocal microscope (Perkin-Elmer: Ultra-View™) and imaged using an inverted Olympus oil-immersion objective (x 60) with the assistance of Dr. D. Hudman. Confocal emission fluorescence was captured at wavelengths < 580nm. Images were transferred to a cooled frame transfer CCD camera as full frame images (1392 x 1040 pixels). An acquisition rate of ~ 1 frame per second with 300 ms exposure, binning of pixels 2 x 2 with a 4 s lapse between images was used for all experiments. The readout of images was digitized at 12 bits with data extracted off-line, from the images, using the Ultra-View™ software (Perkin-Elmer). All images were analysed using a background subtraction method

off-line. The background was defined as a region of interest (ROA) proximal to the cell and subtracted automatically from subsequent images.

Data acquisition, image processing

Confocal image processing was performed using the Ultra-view software (v4.0) (Perkin Elmer). All data was exported as an ASCII text file. As a device to represent distribution of fluorescent intensity throughout the cells, data were presented as a line created from one image drawn either horizontally or vertically through the confocal plane. The line graph represents the colour coded fluorescent profile from the whole cell area defined off-line from the confocal images.

Colocalization analysis

Colocalization analysis calculated both the correlation and the colocalization between two images. The two images were mapped to remove the background signals and the images combined to a single colour image. Two forms of results were generated.

The colocalization correlation analysis took into account the intensity of signal within individual pixels, as well as its x, y coordinates. The percentage colocalization was based only on cell area defined off-line from the confocal images, i.e. whether there was any signal from each component in each pixel.

The correlation between the two images image 1 and image 2 was then calculated as

follows: $C = \frac{a * b}{\sqrt{a^2 * b^2}}$ where: C= correlation, a= Image 1-Image 2,

b= Image 2- Image 1 and * = ×.

2.10 Isolation of mitochondria fraction from rat heart

Sprague-Dawley rats (250 g) were killed by cervical dislocation following a Schedule 1 procedure. Hearts were removed into 10 ml ice-cold homogenisation buffer (300 mM sucrose, 0.2 mM ethylenediamine tetraacetic acid (EGTA), 5 mM Tris-HCl (pH 7.5)), cut into small pieces and homogenised in a Potter-Thomas homogeniser. The homogenate was centrifuged at 760 × g for 10 min and the supernatant removed. The nuclei pellet was resuspended in homogenisation buffer and recentrifuged. The two supernatants were combined and centrifuged at 8740 × g for 10 min. The pellet was resuspended in 1 ml homogenisation buffer and layered onto a discontinuous Percoll

gradient consisting 8 ml each of 60 %, 30 % and 18 % Percoll in homogenisation buffer (Santos et al., 1998). After centrifugation at $8740 \times g$ for 10 min, the 30%/60% interface containing mitochondria was collected, diluted 10-fold in homogenisation buffer and centrifuged at $6800 \times g$ for 10 min. The pellet was resuspended in 220 mM mannitol, 68 mM sucrose, 2 mM NaCl, 2.5 mM H_2KPO_4 , 0.5 mM EGTA, 2 mM $MgCl_2$, 5 mM pyruvate, 0.1 mM phenylmethylsulphonyl fluoride, 1 mM dithiothreitol and 1 mM N-2-hydroxyethylpiperazine-N'-2-ethanesulfonic acid (HEPES)-NaOH (pH 7.4).

Cytochrome c Oxidase Assay

The mitochondria fraction, 18-30% fraction and aliquots from other subcellular fractions, supernatant, nuclei fraction and homogenate, were analysed for cytochrome C oxidase activity (marker of mitochondrial inner membrane) as described by Cooperstein et al. (1950).

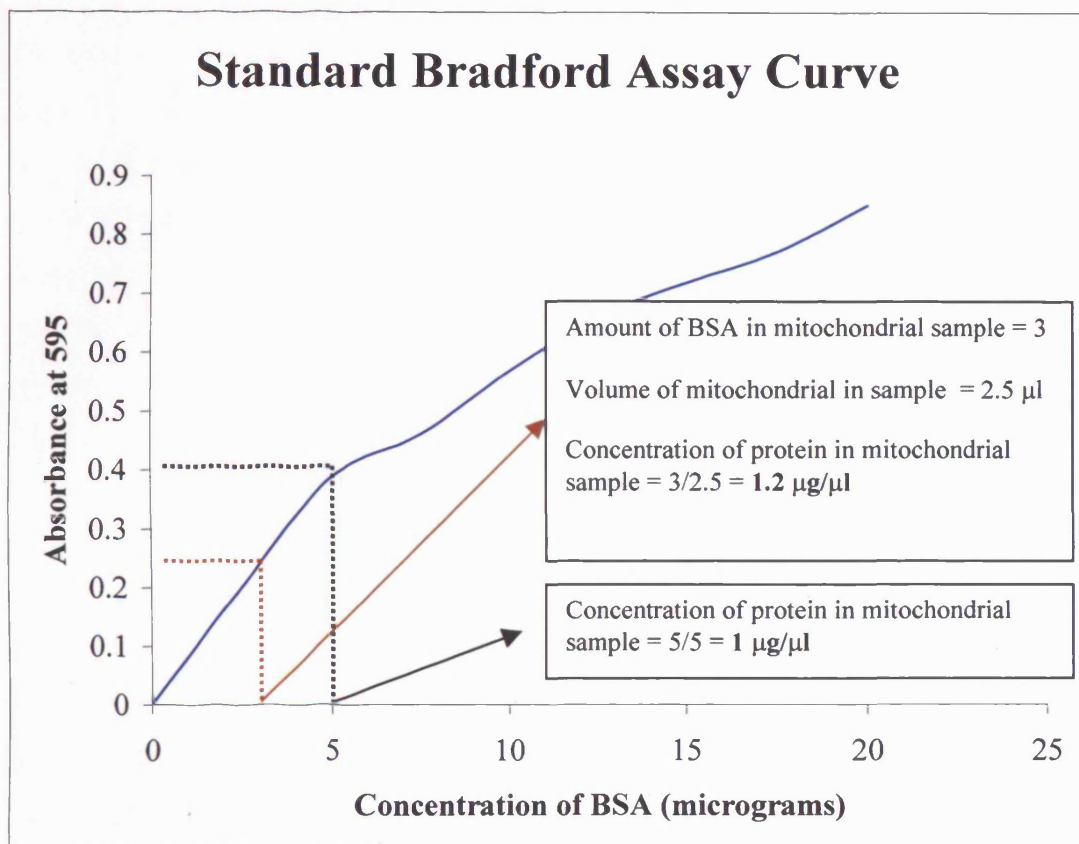
In this assay, the decrease in absorbance of cytochrome c oxidase (in mitochondria fraction) at 550 nm coupled to the oxidation of cytochrome c was measured. Cytochrome c (Sigma; C-7752), 6mg (17 μM), was dissolved in 30 mls of 30 mM NaH_2PO_4 pH 7.4 with NaOH. Freshly prepared sodium dithionite (100 μl from a stock solution of 1.2 M) was added to cytochrome c solution and was shaken vigorously for 2 minutes to remove excess of dithionite. To 1 ml of cytochrome c solution 20 μl of subcellular fractions (1/50 dilution) were added and absorbance was measured at 15 s intervals.

The purity of the mitochondrial fraction was also determined from rest of the subcellular fractions by performing Western blots (Section 2.10) with an anti-cytochrome C polyclonal IgG antibody (Santa Cruz; H-104) and concanavalin A horseradish peroxidase conjugate (ICN; 153246).

2.11. Determination of Protein Concentrations

The protein concentration of the various subcellular fractions was determined using the Bradford assay (Bradford, 1976) also known as the Bio-Rad assay. The absorbance at 595 nm (A_{595}) was measured for known concentrations of bovine serum

albumin (BSA) samples ranging from 0 to 20 μg on addition of 1 ml Bio-Rad Protein Assay Dye Reagent Concentrate (425 ml water; 15 ml 95 % ethanol; 30 ml 88 % phosphoric acid; 30 ml Bradford stock solution (100 ml 95 % ethanol; 200 ml 88 % phosphoric acid; 350 mg Serva Blue G dye)). The standard curve showing the relationship between A_{595} and amount of BSA in μg was constructed to determine protein concentrations after measuring A_{595} of samples containing 1 to 5 μl of unknown protein as shown in graph 2.1.



Graph 2.1. Relationship between A_{595} and amount of BSA in μg .

The concentration of BSA corresponding to the absorbance value of mitochondria sample that intersect the standard curve were divided by the mitochondria volume in that sample to calculate the protein concentration. The average protein concentration from the mitochondrial samples gave the overall estimate.

2.12 Western blotting

Twenty-five microlitres of *in vitro* translated subunit protein reactions (section 2.3), cardiac myocytes (section 2.7) or rat heart isolated mitochondria fractions (section 2.10) were denatured and electrophoresed (section 2.4). Protein was transferred to nitrocellulose membranes (Hybond-C Super, Amersham) with a wet-blot technique (Towbin and Gordon 1984) as described below.

The nitrocellulose membrane was incubated for 10 s in methanol, followed by 5 minutes in water and finally 30 minutes in blotting buffer (0.2 M Glycine; 25mM Tris; 10 % methanol) prior to the electrophoresis with separated protein polyacrylamide gel. The protein gel was placed in blotting cassettes covered with Whatman 3mm paper. The nitrocellulose membrane was placed on top of the gel. The cassettes were then placed in Western blotting tanks and electrophoresed for 2 h at 150 mA in blotting buffer.

Membranes containing protein standards were cut and stained with amido black stain (0.1 % amido black stain, 45 % methanol, 10 % acetic acid) and destained in destain buffer (90 % methanol; 2 % acetic acid; 8 % water). Membranes for immunodetection were incubated with 10 % dried milk in overlay buffer (10 mM Tris-HCl (pH 7.5), 0.9 % NaCl, 0.05 % Tween 20). Individual lanes were isolated in a Decaprobe (Hoefer Scientific Instruments, San Francisco, USA) and treated with anti-K_{ATP} channel subunit antiserum diluted 1:250 in dried milk solution for 16 h at 4°C. The membrane was washed with 10 mM Tris-HCl (pH 7.5), 0.9 % NaCl, 0.05 % Tween 20, 0.25 % N-lauryl sarcosine, 0.25 % nonidet P40 and incubated with horseradish peroxidase conjugated anti-rabbit immunoglobulin (Sigma; A-9169) for 2 h at room temperature. After washing, photoluminometric detection was with Western blot reagent ECL (Amersham; RPN 2106) and data were recorded on Kodak X-ray film.

2.13 *In vitro* phosphorylation

2.13.1. Phosphorylation with Protein Kinase A: *In vitro* translated Kir6.0 proteins (10 µl) were incubated with 0.37MBq [γ -³²P] ATP, 100 µM ATP, 50mM Tris-HCl pH 7.5, and 4 µg/µl of PKA from bovine heart (Sigma P5511), to give a final volume of 50 µl, at 30°C for 30 min. Negative controls contained no kinase in the reaction.

2.13.2. Phosphorylation with Protein Kinase C: *In vitro* translated Kir6.0 proteins, chimaeras and mutants (section 2.16) were incubated at 30°C for 30 minutes with 0.37MBq [γ -³²P] ATP, 100 µM ATP, 10 µl PKC coactivation buffer (1.25 mM EGTA; 2 mM CaCl₂; 0.5 mg/ml BSA), 10 µl PKC activation buffer (1.6 mg/ml phosphatidylserine; 0.16 mg/ml diacylglycerol; 100 mM Tris-HCl pH 7.5; 50 mM MgCl₂) and 3.5 µg/ml of PKC all isoforms from rat brain (Calbiochem; 539494).

In each case, phosphorylated reactions (5 µl) were denatured on addition of denaturing buffer and heated to 95°C for 5 minutes before electrophoresis on a 7% polyacrylamide gel (section 2.4). The dried gel was placed against Kodak X-ray film (F-5513; Sigma) and stored at -70°C, for 5-12 h, before development of the film.

2.13.4. Immunoprecipitation of *in vitro* phosphorylated samples

The phosphorylated reactions were split in half and incubated with equal volume of 2 % TritonX-100 in 20 mM Tris-HCl, pH 7.5 for 15 minutes at 4°C before immunoprecipitating with the anti-Kir6.0 antibodies as described in section 2.4.

2.14. *In vivo* phosphorylation

Approximately 1×10⁶ rat isolated cardiac myocytes per reaction were washed twice in phosphate-free medium (PO₄⁻²-free normal Tyrode's solution) before suspending cells in 2ml of phosphate-free media. The ATP pools of the suspended cells were then labelled with 1mCi of [³²P] inorganic phosphate (Amersham; PBS 13) for 2-3 hours at room temperature. Labelled cells were then stimulated with various agonists and inhibitors alone or in combination as shown in **Table 2.2** for 30 minutes at room temperature.

<i>Agonist (concentration, μM)</i>	<i>Inhibitors (μM)</i>
Phorbol 12-Myristate 13-acetate (50)	-
Adenosine (1000)	-
Adenosine (10)	-
Forskolin (100)	-
CCPA (10)	-
CCPA (10)	Chelerythrine (100)
CCPA (10)	SB203580 (100)
CCPA (10)	U0126 (100)
CCPA (10)	JNK1 inhibitor (100)

Table 2.2 Stimulation of isolated rat cardiac myocytes with protein kinase modulators and inhibitors

The ³²P cell medium was then removed and cells were washed twice with phosphate-free medium before being lysed with 500 μ l cold lysis buffer (50 mM Tris-HCl pH 7.5, 1 mM EDTA, 1 mM EGTA, 1 % TritonX-100, 1 mM sodium orthovanadate, 10 mM sodium glycerophosphate, 50 mM sodium fluoride, 5 mM sodium pyrophosphate, 0.27 M sucrose, 0.1 % β -mercaptoethanol and 0.1 % protease inhibitors cocktail set III (Calbiochem; 539134)). The lysed cells were centrifuged at maximum speed on desk-top microcentrifuge at 4°C for 5 minutes and recovered supernatants were immunoprecipitation with 4 μ l of anti-Kir6.0 and anti-SUR2 (section 2.5).

Immunoprecipitated samples were electrophoresed on 7.5 % polyacrylamide gel (section 2.4). The dried gels were placed against Kodak X-ray film (F-5513; Sigma) and stored at -70°C, for 2-6 h, before development of the film.

2.15 Two Dimensional Phosphopeptide analysis

The precise location of phosphorylated amino acid residues from *in vitro* translated Kir6.0 polypeptides stimulated with PKA and PKC in the presence of [γ -³²P] ATP after immunoprecipitation with specific antisera were detected using thin layer

electrophoresis (first dimension: Hunters thin layer electrophoresis apparatus (HTLE-7000)) and thin layer chromatography (second dimension).

2.15.1. Elution of phosphorylated polypeptides from polyacrylamide gel

Phosphorylated polypeptides were resolved by 7% polyacrylamide mini-gel (section 2.4). Gels were dried and exposed to Kodak film for 12 hours. Identified ³²P-labelled polypeptide bands were cut out from the gel and rehydrated in 400 µl freshly prepared 50 mM ammonium bicarbonate, pH 7.3-7.6 for 5 min at room temperature. The gel pieces were ground until they could be passed through 200 µl disposable tips. The gel suspensions were transferred to screw-cap microcentrifuge tubes. Previous tubes containing residual gel bits were washed with 2 volumes of 250 µl of ammonium bicarbonate and transferred to the tubes containing the gel slurry. To the gel slurry tubes, 50 µl of β-mercaptoethanol (Sigma) and 10 µl of 10 % SDS was added and boiled for 5 minutes before incubating at room temperature while shaking for 12-16 hours. The suspension was then vortexed and centrifuged at 5470 × g at room temperature for 5 min. The supernatant was recovered and transferred to a fresh tube and left to chill at 4°C.

2.15.2. Precipitation of eluted ³²P-labelled polypeptide

To concentrate the phosphorylated polypeptide, 15 % of ice-cold trichloroacetic acid (TCA) was added to the chilled elute and left to incubate at 4°C for 60 min. The TCA precipitate was collected by centrifugation of the elute in a micro-centrifuge for 10 min at 4°C. The precipitate was washed with ice-cold ethanol and left to air-dry.

2.15.3. Oxidation of Eluted ³²P-labelled polypeptide

Oxidation of polypeptides prevents artefactual separation of oxidation isomers during chromatography. Thus the precipitate was dissolved in 50 µl of ice-cold performic acid (900 µl formic acid + 100 µl hydrogen peroxide; incubate at 37°C for 60 min before placing on ice) and oxidized at 0°C for 60 min. After oxidation 400 µl deionised water was added to dilute the performic acid and lyophilized using a freeze-drier (Edward's Modulyo model).

2.15.4. Proteolytic Digestion of ³²P-labelled polypeptide

The polypeptides were digested using trypsin. Trypsin specifically hydrolyses peptide bonds at the carboxylic sides of lysine and arginine residues. Oxidized polypeptide recovered from lyophilization was resuspended in 50 µl of 50 mM ammonium bicarbonate, pH 8.0. Ten microlitres of a stock 1.0 mg/ml solution of TPCK-trypsin (Promega, V5111) was added to suspension and incubated for 12-16 hours at 37°C. An additional 10 µl of stock trypsin was incubated with the digest suspension for another 12-16 hours. After digestion was complete, the samples were washed with 400 µl deionised water, frozen and lyophilized. The digest polypeptide (lyophilized) was once more dissolved in 400 µl deionised water and re-lyophilized before dissolved in 400 µl pH 1.9 buffer (2.5 % formic acid, 7.8 % acetic acid) and freeze-dried. Finally the pellet was dissolved in 10 µl pH 1.9 buffer and was loaded (200-1000 counts per minute; cpm) on to a thin-layer cellulose plate (MERCK) with the marker dye (5 mg/ml ε-DNP-lysine and 1 mg/ml xylene cyanol FF solubilized in water containing 30-50 % (v/v) of pH 4.72 buffer (5 % n-butanol; 2.5 % pyridine; 2.5 % acetic acid)) as shown in Figure 2.2 A.

2.15.5. First Dimension electrophoresis

The TLC plate was dampened with pH 1.9 buffer using a blotter (two layers of Whatman 3MM paper; as shown in Figure 2.2B), placed on the HTLE 7000 apparatus and electrophoresis was carried out in the first dimension for 30 min at 1kV. The TLC plate was air dried for 20 min using a fan.

2.15.6. Second dimension chromatography

A spot of marker dye was loaded to the dried TLC plate in the left margin of the plate at the same level as the sample origin (Figure 2.2 A). The plate was placed in a chromatography tank containing Phospho-Chromatography buffer (37.5 % n-butanol; 25 % pyridine; 7.5 % acetic acid) for 8-12 hours to allow the buffer to run to within 1 cm of the top of the plate. The plates were dried in a fume hood and were exposed to X-ray film for 1-7 days.

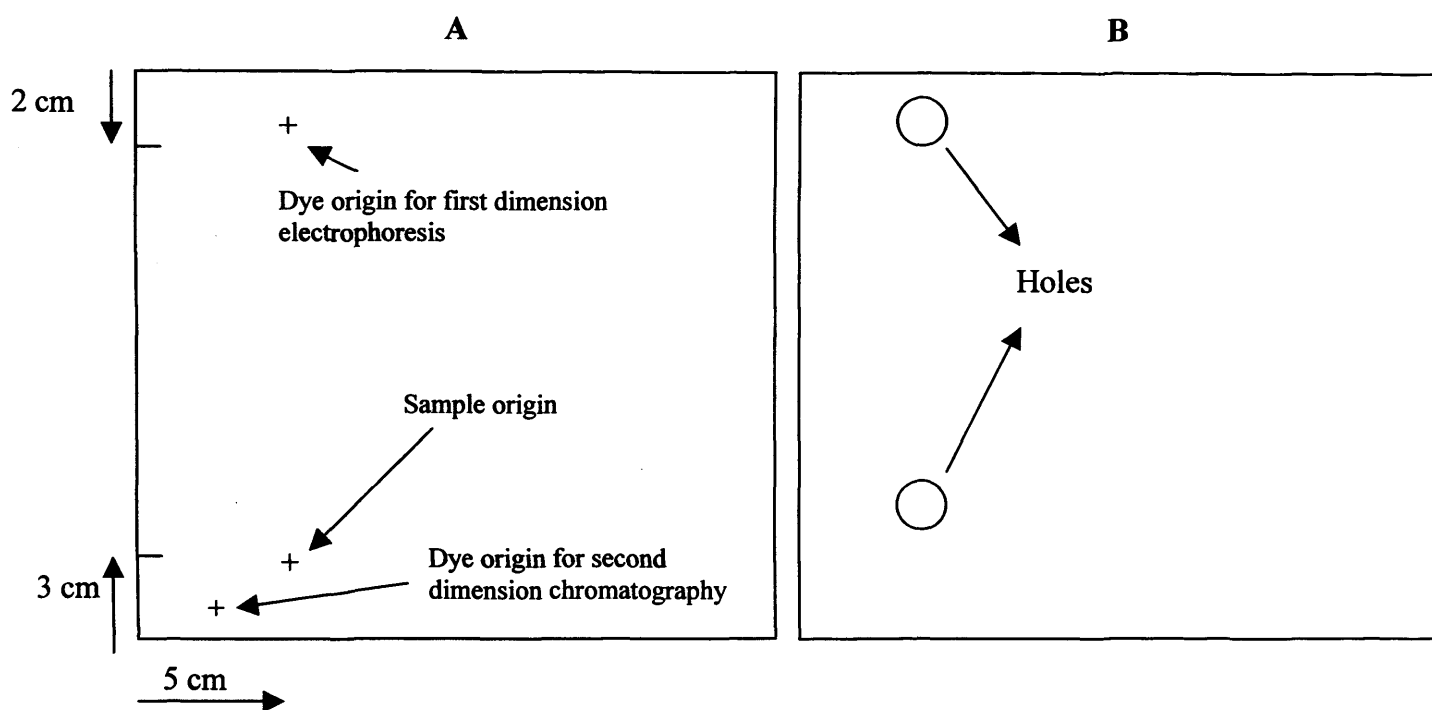


Figure 2.2. A) Location of sample and dye origins for two- dimensional separation of phosphopeptides on TLC plates. B) Blotter for wetting TLC plates before separation of digested peptides by electrophoresis in the first dimension at pH 1.9.

2.16. Phosphoamino acid analysis

Phosphorylated serine, threonine or tyrosine amino acids were detected in PMA/PKC-mediated phosphorylation reactions using a two-dimensional Hunters thin layer electrophoresis apparatus (HTLE-7000). The phosphorylated polypeptide was resolved by 7% polyacrylamide mini-gel (section 2.4) before transfer to Immobilon PVDF (polyvinylidene difluoride) membrane (Millipore; IPVH 10) with a wet- blot technique (Towbin and Gordon 1984, section 2.12). The phosphorylated protein bands were detected on the membrane by exposing the membrane to X-ray film for 2-4 hours at room temperature. Identified bands were then cut from the protein membrane and hydrolysed with 6 M HCl for 12-16 hours at 110°C. Supernatants were removed from samples after centrifugation at 5000 × g for 5 min and dried using a freeze-drier (Edward's Modulyo model). Concentrated hydrolysates were then dissolved in 10 µl of pH 1.9 buffer (2.5 % formic acid, 7.8 % acetic acid) containing

15 parts of buffer to 1 part of unlabelled phosphoaminoacid standards (1 mg/ml each phospho-serine, -threonine and -tyrosine). The pH 1.9 buffer allowed separations of the phosphoserine from the phosphothreonine and phosphotyrosine in the first-dimension electrophoresis, whereas pH 3.5 buffer (0.5 % pyridine, 5 % acetic acid) was used to separate phosphothreonine from phosphotyrosine in the second dimensional electrophoresis. The two electrode tanks of the HTLE-7000 were filled with 500mls of pH 1.9 buffer. The marker dye and samples (10-100 cpm) were loaded onto a thin-layer cellulose (TLC) plate (MERCK) as shown in Figure 2.3A. Four samples could be analysed on one plate. The TLC plate was dampened with pH 1.9 buffer using a blotter (two layers of Whatman 3MM paper) shown in Figure 2.3B and electrophoresis was carried out in the first dimension for 20 minutes at 1.5kV. The plate was dried using a fan for 30 minutes. The buffer in the electrode tanks was replaced with pH 3.5 buffer and the dried plate was dampened with blotter soaked in pH 3.5 buffer as shown in Figure 2.3C. The plate was placed on the apparatus rotated 90°anticlockwise to the previous position and electrophoresis was carried out for 16 minutes at 1.3kV. The plate was dried by baking in an oven at 65°C for 10 minutes. The phosphoamino acid standards were visualized by spraying the dried plate with ninhydrin solution (Sigma; N0587) and baking at 65°C for 15 minutes. Purple spots appeared, corresponding to the phosphoamino standards, Figure 2.2A. The phosphoamino acids were detected by exposing the TLC plate to X-ray film for 2-5 days at -70°C.

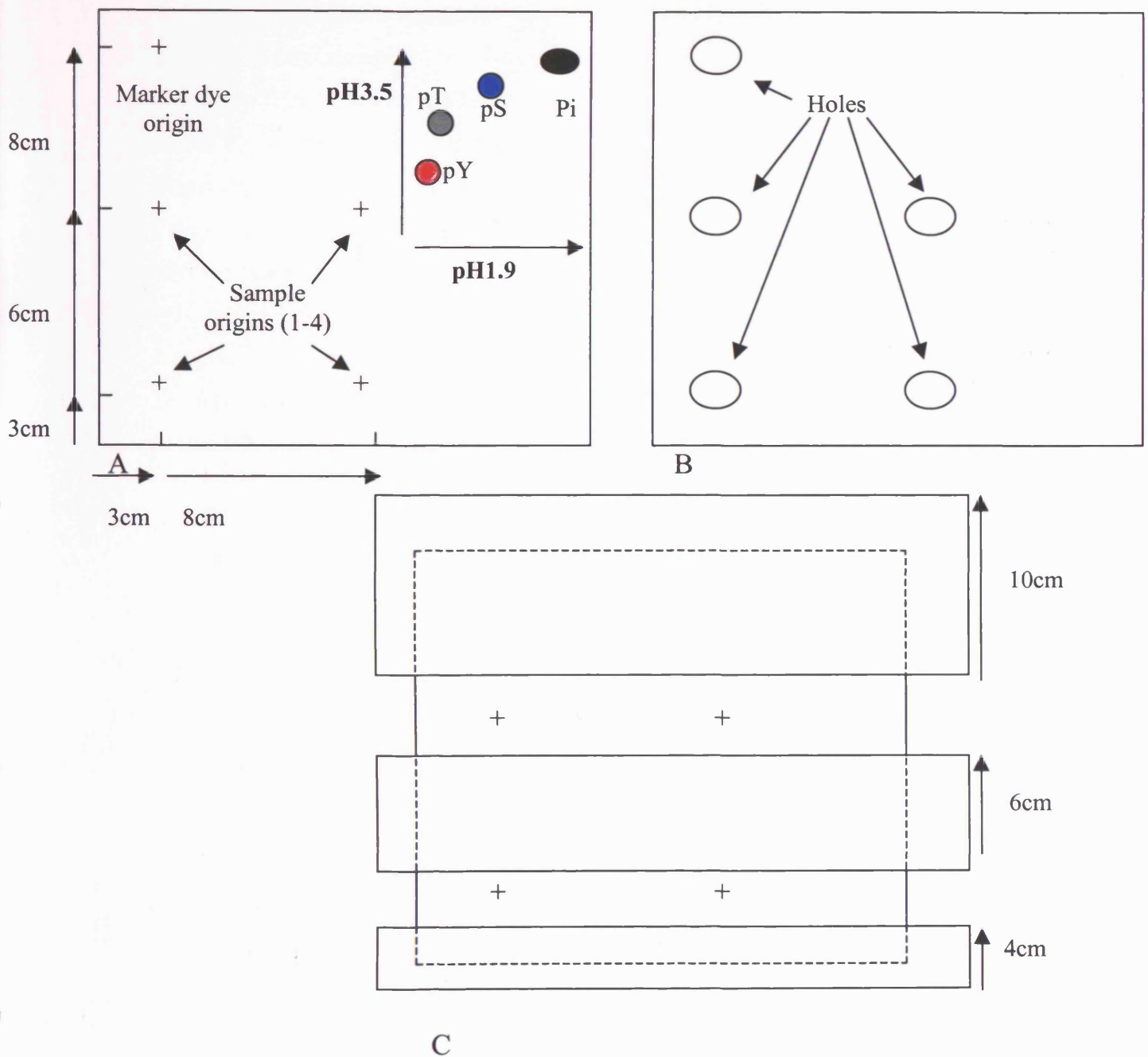


Figure 2.3. A) Locations of samples and dye origins for two-dimensional electrophoresis of phosphoamino acids on TLC plates and positions of the migrated phosphoamino acids after electrophoresis. About 20% of the radioactivity migrated as phosphoserine (pS), phosphothreonine (pT) or phosphotyrosine (pY), the remainder was present as inorganic phosphate (Pi). B) Blotter for wetting TLC plates before separation of phosphoamino acids by electrophoresis in the first dimension at pH 1.9. C) Dimensions of blotter for wetting TLC plates before separation of phosphoamino acids by electrophoresis in the second dimension at pH 3.5.

2.17. Site-directed Mutagenesis

Site-directed mutagenesis was used to mutate serine residues (354, 379, 385, 391 and 397) in the Kir6.1 subunit to alanine residues. The mutants (S354A, S379A, S385A, S391A and S397A) were expressed and utilised in *in vitro* PKC-mediated phosphorylation experiments as described in section 2.13. The QuikChange™ Site-Directed Mutagenesis Kit (Stratagene) was used to create the mutations as described below in sections 2.17.1 and 2.17.2.

2.17.1 Creating Oligonucleotide Primers

The following complementary oligonucleotide primers were designed:

1. **S354A** 5'-CGCCAAGATGCGCAGCCCGGGAGCTGG-3'
5'-CCAGCTCCCGGGCTGCGCATCTTGGCG-3'
2. **S379A** 5'-GTCGCACCAGAATGCTCTGAGGAAGCG-3'
5'-CGCTTCCTCAGAGCATTCTGGTGCAC-3'
3. **S385A** 5'-GAGGAAGCGCAACGCTATGAGAAGAAAC-3'
5'-GTTTCTTCTCATAGCGTTGCGCTTCCTC-3'
4. **S391A** 5'-TGAGAAGAAACAACGCCATGAGGAGGAG-3'
5'-CTCCTCCTCATGGCGTTGTTTCTTCTCA-3'
5. **S397A** 5'-AGGAGGAGCAACGCCATCCGGAGGA-3'
5'-TCCTCCGGATGCCGTTGCTCCTCCT-3'

The oligonucleotides were produced and purified by MWG-Biotech.

2.17.2. QuikChange™ Site-Directed Mutagenesis reaction

Complementary oligonucleotide primers (125 ng), containing 5 µl 10 × reaction buffer (100 mM KCl; 100 mM (NH₄)₂SO₄; 200 mM Tris-HCl, pH 8.8; 20 mM MgSO₄; 1 % Triton® X-100; 1mg/ml nuclease-free BSA), 50 ng of WtKir6.1 parental dsDNA template and 1µl dNTP mix in a final volume of 50 µl made up with distilled water were annealed and extended using a thermal cycler (Hybaid). The cycling parameters are shown in Table 3.2. *Pfu* Turbo DNA polymerase (1µl) was added to

the reaction just before starting the thermal cycler. Generation of mutated plasmid containing staggered nicks was treated with *Dpn* I restriction enzyme, which was incubated at 37°C for 1 hour to digest the parental dsDNA. The new mutated DNA was then transformed into Epicurian Coli® XL-Blue supercompetent cells and colonies grown onto LB-carbencillin plates as described in section 2.3.1.

Segment	Cycles	Temperature	Time
1	1	95°C	30 seconds
2	16	95°C	30 seconds
		55°C	1 minute
		68°C	2 minutes/kb of plasmid

Table 2.3. Cycling parameters for single amino acid change mutagenesis.

In segment 2 the cycles were adjusted to 16 because this was the parameter required to obtain a desirable single amino acid mutation.

2.17.3. Mutant DNA sequencing

Miniprep cultures were grown up in 5 ml LB-ampicillin media inoculated from single colonies after transformation. Mutated plasmid DNA was purified using the Wizard® Plus SV miniprep kit (Promega). The bacterial culture was harvested by centrifugation at 5000 × g for 5 minutes. The bacterial cell pellet was then resuspended in 250 µl Cell Resuspension solution and lysed with 250 µl Cell Lysis solution. Neutralisation solution (750 µl) was then added, which precipitated the cellular debris, and the lysate was centrifuged at maximum speed in desktop microcentrifuge for 10 minutes. The supernatant was then transferred to a spin column and centrifuged at maximum speed in desktop microcentrifuge for 1 minute forcing the cleared lysate through and leaving the mutant DNA bound to the column. The column was washed with an ethanol wash solution, firstly with 750 µl of Column Wash solution and centrifugation for 1 minute at maximum speed in desktop microcentrifuge, followed by 250 µl solution centrifugation for 2 minutes. The DNA was then eluted from the column to a sterilised microcentrifuge tube with 100 µl nuclease-free water. The DNA was precipitated by ethanol-precipitation. The

precipitated DNA was recovered by centrifugation at 1 maximum speed in desktop microcentrifuge for 15 minutes and resuspended in 50 µl of nuclease-free water. The DNA yield was determined by spectrophotometric analysis as described in section 2.3.3.

Purified DNA plasmids were then sequenced to identify mutants (PNACL, University of Leicester) prior to *in vitro* translation.

2.18 Densitometry

Densitometry of *in vitro* and *in vivo* phosphorylated polypeptide bands were performed using the Image MasterTM programme (Pharmacia Biotech).

Autoradiographs exposed for 3 hours to dried polyacrylamide gels were scanned (Sharp JX-330 scanner) and optical density of bands of interest was recorded as highlighted in the manufactures software manual.

Chapter 3: Characterization of anti-Kir6.0 and SUR2 Polyclonal Antisera

3.1 Production of Polyclonal Antisera to K_{ATP} Channel Subunit Isoforms

To provide specific molecular identification of Kir6.0 and SUR2 isoforms in immunocytochemical and biochemical experiments, a range of polyclonal antisera to the rat isoforms were generated. The anti-Kir6.1 polyclonal antiserum was raised by Dr. Robert Norman (Department of Medicine, University of Leicester), the anti-Kir6.2 polyclonal antiserum was prepared by Research Genetics Inc. (Huntsville, USA) and the anti-SUR2 polyclonal antisera were provided by Pepceuticals Ltd (Leicester, UK) against requested target peptide sequences. All four antibodies were raised using C-terminal domain antigenic peptide-carrier protein conjugates as described in Materials and Methods (Section 2.2). By utilizing these antibodies on isolated cardiac myocytes (immunocytochemistry and Western blots) and on purified heart mitochondria fractions (Western blots), the subunit distribution of cardiac K_{ATP} channels was studied. K_{ATP} channel subunit phosphorylation *in vitro* and *in vivo* was also examined with the aid of these antibodies.

Each antibody was shown to recognise immunising peptide in ELISA (Enzyme-Linked Immunosorbent Assay) which were performed by Dr. Robert Norman (Department of Medicine, University of Leicester) and binding of each was displaced from the target antigen by competition with specific antigenic peptide (10 µg/ml) in ELISA). Competition of antibody binding to the immunising peptide was not achieved by other non-specific peptides to related or unrelated antigens. In each case, antisera were shown to be of high titre measured against 20 ng of immobilized immunising peptide, at least to a dilution limit of 1×10^4 .

3.2 Immunoprecipitation of *in vitro* Translated Kir6.0 and SUR2 polypeptides

The specificity of anti-Kir6.0 and anti-SUR2 antisera was verified by immunoprecipitation of [³⁵S]-methionine labelled Kir6.0 and SUR2 proteins. K_{ATP} channel subunit cDNA's (Kir6.1, Kir6.2, SUR2A and SUR2B) were expressed in the TNT rabbit reticulocyte lysate Quick coupled transcription/translation system to produce proteins labelled with [³⁵S]-methionine. The reaction with Kir6.2 cDNA

required canine pancreatic microsomal membranes in order to obtain a high yield of Kir6.2 polypeptide. Satisfactory expression of all four polypeptides was achieved, evidenced by migration of major expressed polypeptides at appropriate molecular weights in 7.5% polyacrylamide gels, i.e. Kir6.1, 48kDa; Kir6.2, 40kDa; SUR2A and SUR2B, 140kDa (Figure 3.1, lanes 1-4 respectively). An additional band corresponding to a molecular weight of approximately 130 kDa was also observed in most Kir6.1 preparations and was assumed to represent a packed tetramer of Kir6.1 subunits. The identity of the polypeptide in this band was not investigated further. The presence of aggregated material was observed at the top of most resolving gels. Electrophoresis of protein samples that were denatured without boiling reduced the amount of aggregation.

Immunoprecipitation of target polypeptides by anti-Kir6.1 and anti-Kir6.2 antisera was demonstrated (Figure 3.2, lanes 3 and 9) by comparison with *in vitro* translated [³⁵S]-methionine labelled Kir6.1 and Kir6.2 proteins that were electrophoresed directly under the same gel conditions (Figure 3.2, lanes 1 and 12).

Immunoprecipitation of the Kir6.0 polypeptides was not seen in reactions incubated with non-specific antisera (Figure 3.2, lanes 4 and 8). Specific immunoprecipitation of [³⁵S]-methionine labelled Kir6.1 and Kir6.2 proteins was prevented by the preadsorption of anti-Kir6.1 and anti-Kir6.2 antibody with 10 µg/ml specific immunizing peptide (Figure 3.2, lanes 5 and 11) but not with non-specific peptides of related antigens (Figure 3.2, lanes 6 and 10). Similarly, *in vitro* translated [³⁵S]-methionine-labelled SUR2A and SUR2B proteins, separated directly by electrophoresis (Figure 3.3, lanes 1 and 12), confirmed specific immunoprecipitation of target polypeptides by anti-SUR2A and anti-SUR2B antibodies (Figure 3.3, lanes 3 and 8). The immunoprecipitation of the target polypeptide was blocked in each case by preadsorption of the antiserum with specific immunizing peptide (Figure 3.3, lanes 6 and 9) but not with non-specific peptides of related antigens (Figure 3.3 lanes, 5 and 10). Some cross-reactivity between the anti-SUR2A and anti-SUR2B antiserum was observed, since the antibodies were able to immunoprecipitate small amounts of non-specific related *in vitro* expressed proteins (Figure 3.3, lanes 4 and 7). No immunoprecipitation was observed in negative control reactions in which primary

antibody was omitted (Figure 3.2, lanes 2 and 7 for Kir6.1 and Kir6.2, respectively; Figure 3.3, lanes 2 and 9 for SUR2A and SUR2B, respectively)

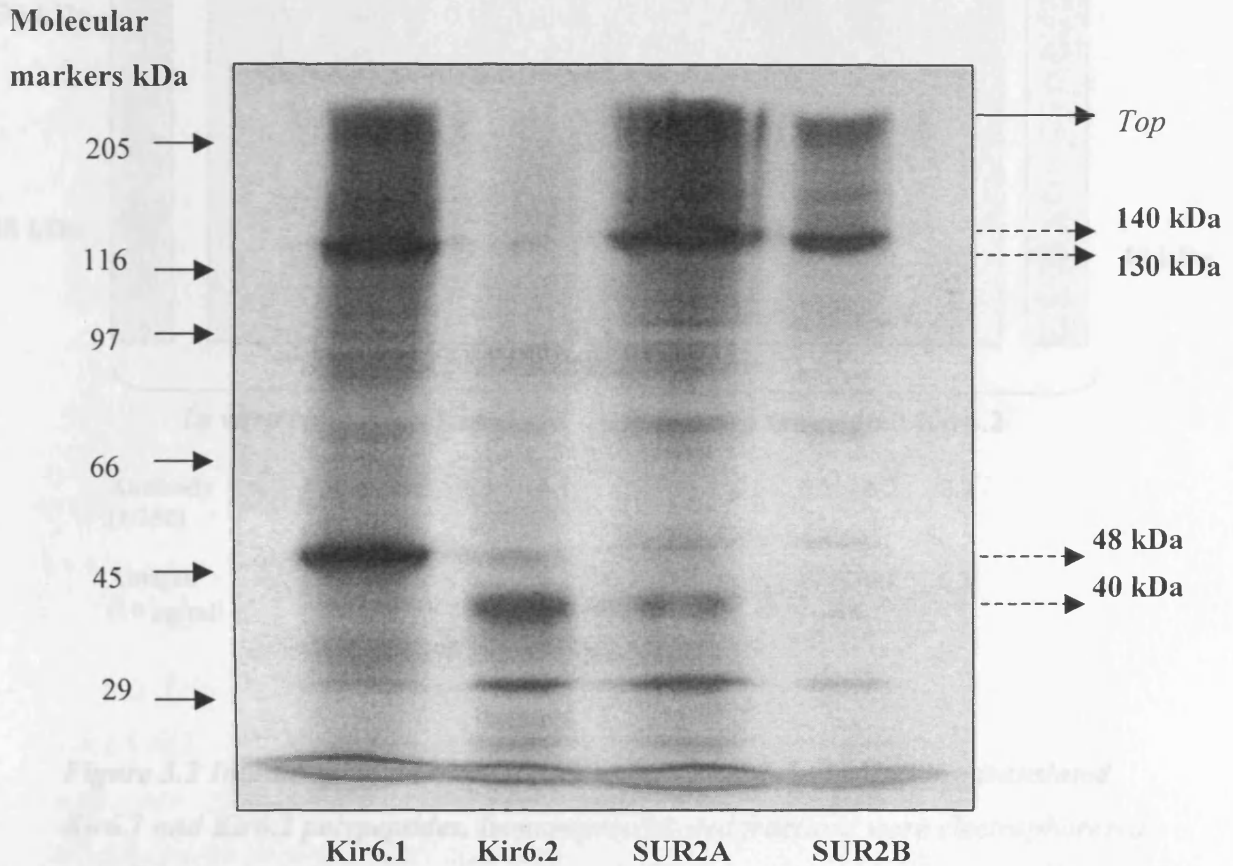


Figure 3.1 *In vitro* translated [³⁵S]-methionine labelled Kir6.0 and SUR2 K_{ATP} channel subunits. Autoradiograph showing electrophoretically separated [³⁵S]-methionine-labelled *in vitro* translated K_{ATP} channel subunit polypeptides on a denaturing 7.5% polyacrylamide mini-gel. K_{ATP} channel subunits were expressed using the SP6 or T7 TNT[®] quick-coupled transcription/translation kit (Promega) from cloned cDNAs. The [³⁵S]-methionine labelled Kir6.1, Kir6.2, SUR2A and SUR2B polypeptides migrated with apparent molecular weights of 48, 40, 140 and 140 kDa, respectively. An additional band of molecular weight of ~ 135 kDa was observed in most Kir6.1 preparations. Aggregated material that did not enter the gel was often observed. Representative experiment (n = 7).

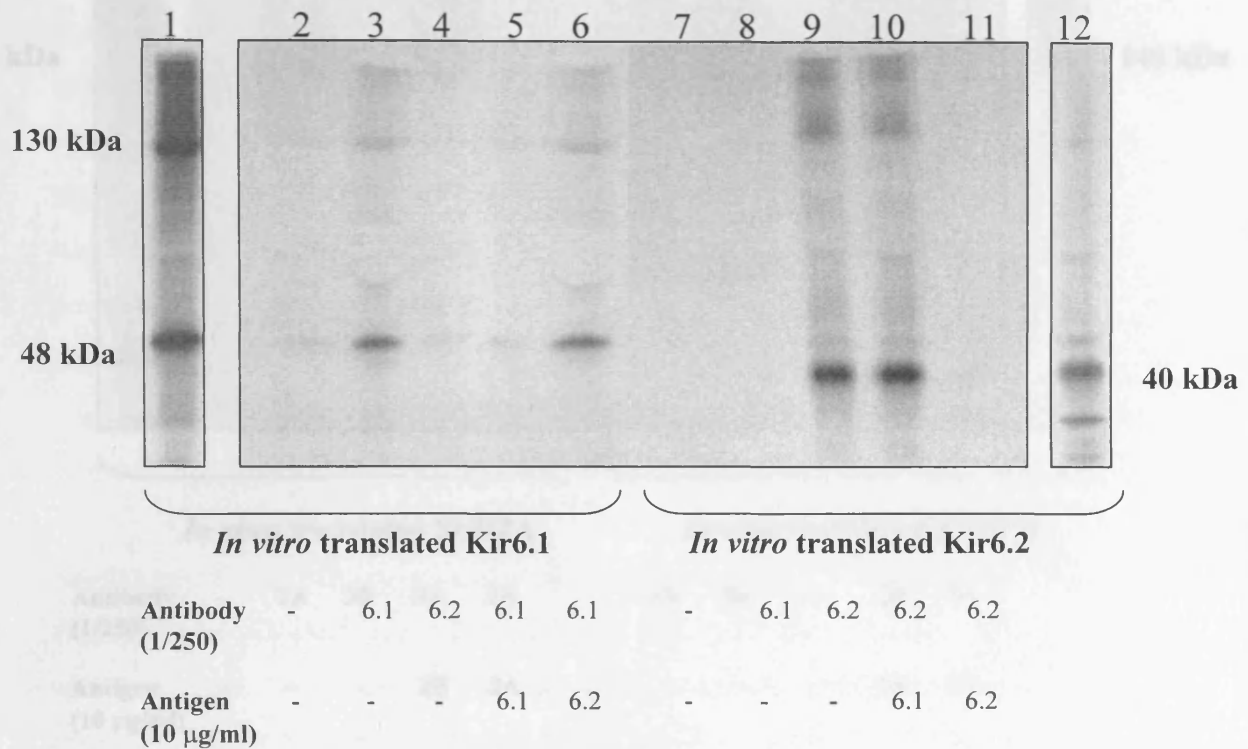


Figure 3.2 Immunoprecipitation of [³⁵S]-methionine-labelled *in vitro* translated Kir6.1 and Kir6.2 polypeptides. Immunoprecipitated fractions were electrophoresed on a 7.5 % polyacrylamide mini-gel. Electrophoresis of *in vitro* translated [³⁵S]-methionine labelled Kir6.1 and Kir6.2 subunits resulted in bands corresponding to polypeptides of 48 (130) and 40 kDa respectively, lanes 1 and 12, which were used to confirm specific immunoprecipitation of target polypeptides by anti-Kir6.0 antisera. Lanes 2 and 7, contained immunoprecipitation fractions with no primary antibody; lanes 3 and 8, anti-Kir6.1 antibody (1/250 dilution); lane 4 and 9, anti-Kir6.2 antibody (1/250 dilution); lane 5, anti-Kir6.1 antiserum (1/250 dilution) plus 10 µg/ml Kir6.1 C-terminal peptide; lane 6, Kir6.1 antibody (1/250 dilution) plus 10 µg/ml Kir6.2 C-terminal peptide; lane 10, Kir6.2 antibody (1/250 dilution) plus 10 µg/ml Kir6.1 C-terminal peptide; lane 11, anti-Kir6.2 antibody (1/250 dilution) plus 10 µg/ml Kir6.2 C-terminal peptide. Representative experiment (n = 5).

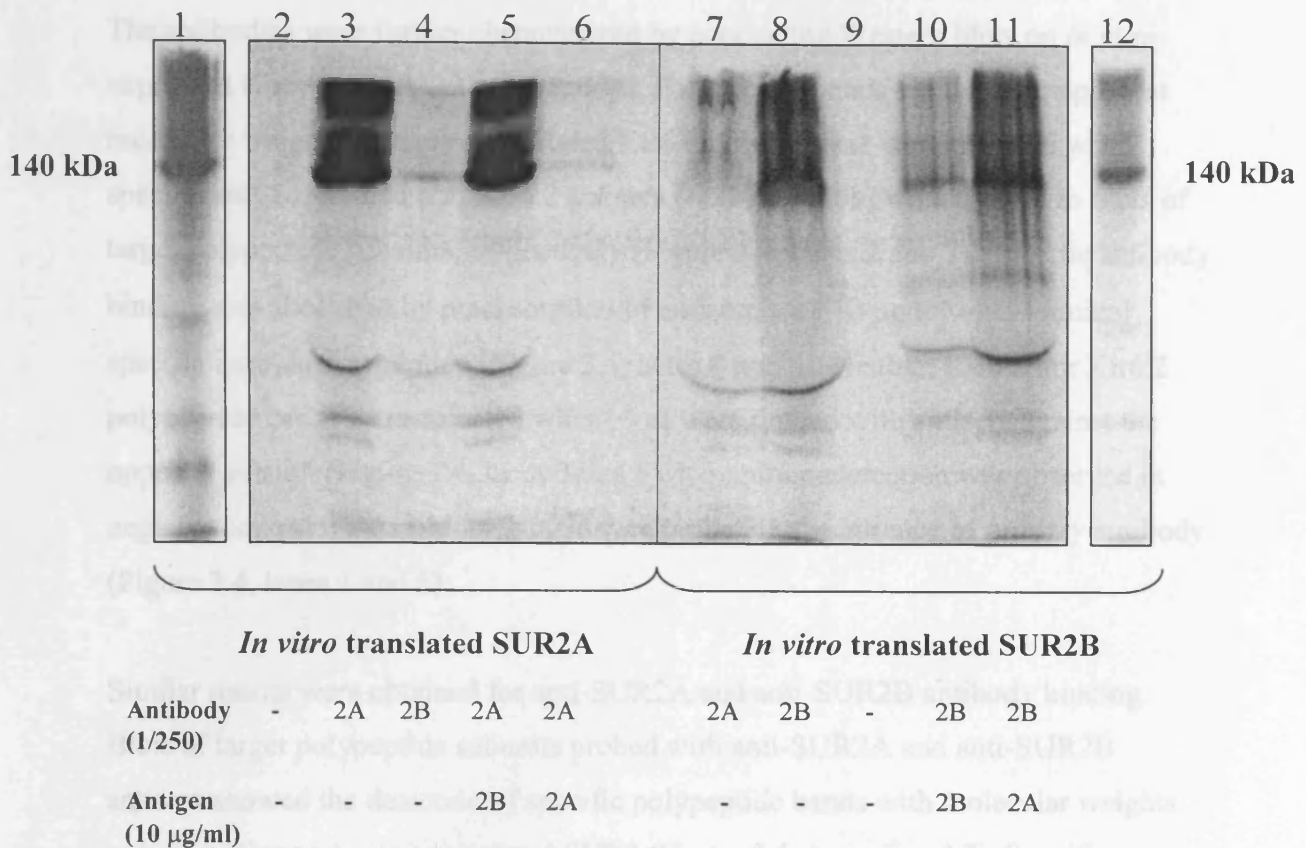


Figure 3.3 Immunoprecipitation of [³⁵S]-methionine-labelled *in vitro* translated SUR2A and SUR2B polypeptides. Autoradiograph represents fractions of immunoprecipitated *in vitro* translated SUR2A and B separated on a 7.5 % polyacrylamide mini-gel. Electrophoresis of *in vitro* translated [³⁵S]-methionine labelled SUR2A and SUR2B resulted in bands corresponding to polypeptides of 140 kDa, lanes 1 and 12, which were used to confirm specific immunoprecipitation of target polypeptides by anti-SUR2A and anti-SUR2B antisera. Lanes 2 and 9, contained immunoprecipitation fractions with no primary antibody; lanes 3 and 7, anti-SUR2A antibody (1/250 dilution); lane 4 and 8, anti-SUR2B antiserum (1/250 dilution); lane 5, anti-SUR2A antiserum (1/250 dilution) plus 10 µg/ml SUR2B C-terminal peptide; lane 6, SUR2A antibody (1/250 dilution) plus 10 µg/ml SUR2A C-terminal peptide; lane 10, SUR2B antibody (1/250 dilution) plus 10 µg/ml SUR2B C-terminal peptide; lane 11, anti-SUR2B antibody (1/250 dilution) plus 10 µg/ml SUR2A C-terminal peptide. Aggregated material, as observed previously (Figure 3.1) was observed at the top of the gels. Representative experiment (n = 5).

3.3 Western blotting of *in vitro* translated Kir6.0 and SUR2 polypeptides

The antibodies were further characterized by conducting Western blots on *in vitro* expressed Kir6.0 and SUR2 polypeptides. Polypeptide bands with similar apparent molecular weights to *in vitro* translated Kir6.0 polypeptides were detected when specific anti-Kir6.1 and anti-Kir6.2 antisera (1/250 dilution) were applied to blots of target polypeptide subunits, respectively (Figure 3.4, lanes 2 and 7). Specific antibody binding was abolished by preabsorption of antisera with 10 $\mu\text{g/ml}$ of C-terminal specific immunizing peptide (Figure 3.4, lanes 4 and 8). Neither, Kir6.1 nor Kir6.2 polypeptide bands were detected when blots were probed with antisera against the opposite subunit (Figure 3.4, lanes 3 and 6). No immunodetection was observed in negative control immunoblots, which were probed in the absence of primary antibody (Figure 3.4, lanes 1 and 5).

Similar results were obtained for anti-SUR2A and anti-SUR2B antibody binding. Blots of target polypeptide subunits probed with anti-SUR2A and anti-SUR2B antisera showed the detection of specific polypeptide bands with molecular weights corresponding to *in vitro* translated SUR2 (Figure 3.5, lanes 2 and 7). Specific antibody binding to target subunits on blots was displaced with specific immunizing peptide (Figure 3.5, lanes 3 and 8). The anti-SUR2 antibodies did not bind to related (non-specific) subunit blots (Figure 3.5, lanes 4 and 9), suggesting Western blots were unable to show any cross-reactivity between the anti-SUR2A and SUR2B antibodies. Negative control immunoblots showed no immunodetection of polypeptides (Figure 3.5, lanes 1 and 6).

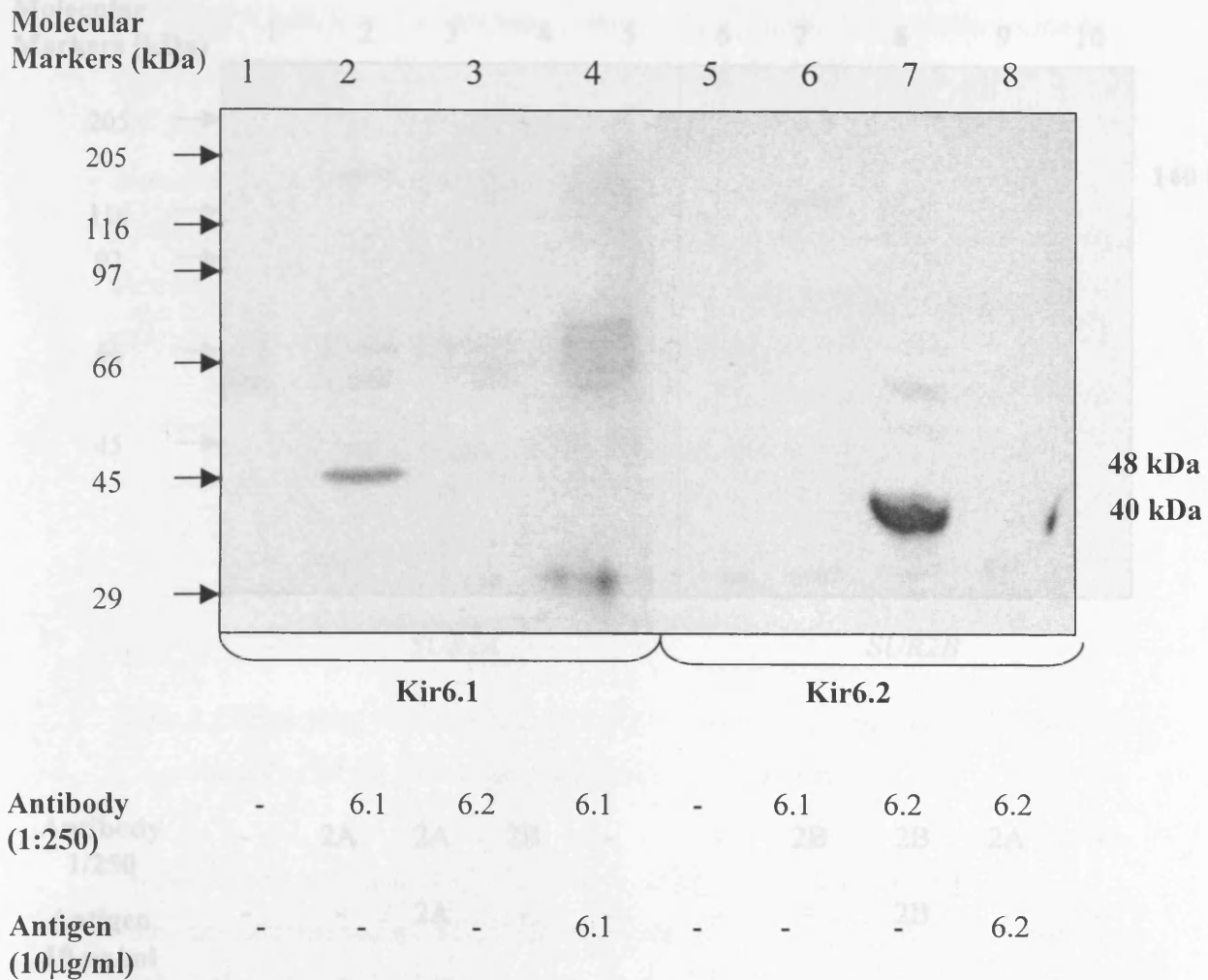


Figure 3.4 Immunoblot of *in vitro* translated Kir6.0 polypeptides probed with anti-Kir6.0 antibodies. Autoradiograph of an immunoblot of *in vitro* translated Kir6.1 and Kir6.2 polypeptides probed with subunit specific and unspecific Kir6.0 antibodies. Antibody binding was detected photoluminometrically using an ECL Western blot detection kit. The blot was exposed to film for 30 seconds. The immunoblots were probed with no primary antibody, lanes 1 and 5; anti-Kir6.1 (1/250 dilution), lanes 2 and 6; anti-Kir6.2 antiserum (1/250 dilution), lane 3 and 7; anti-Kir6.1 (1/250 dilution) plus 10 µg/ml Kir6.1 C-terminal peptide, lane 4; anti-Kir6.2 (1/250 dilution) plus 10 µg/ml Kir6.2 C-terminal peptide, lane 8. Representative experiment (n = 3).

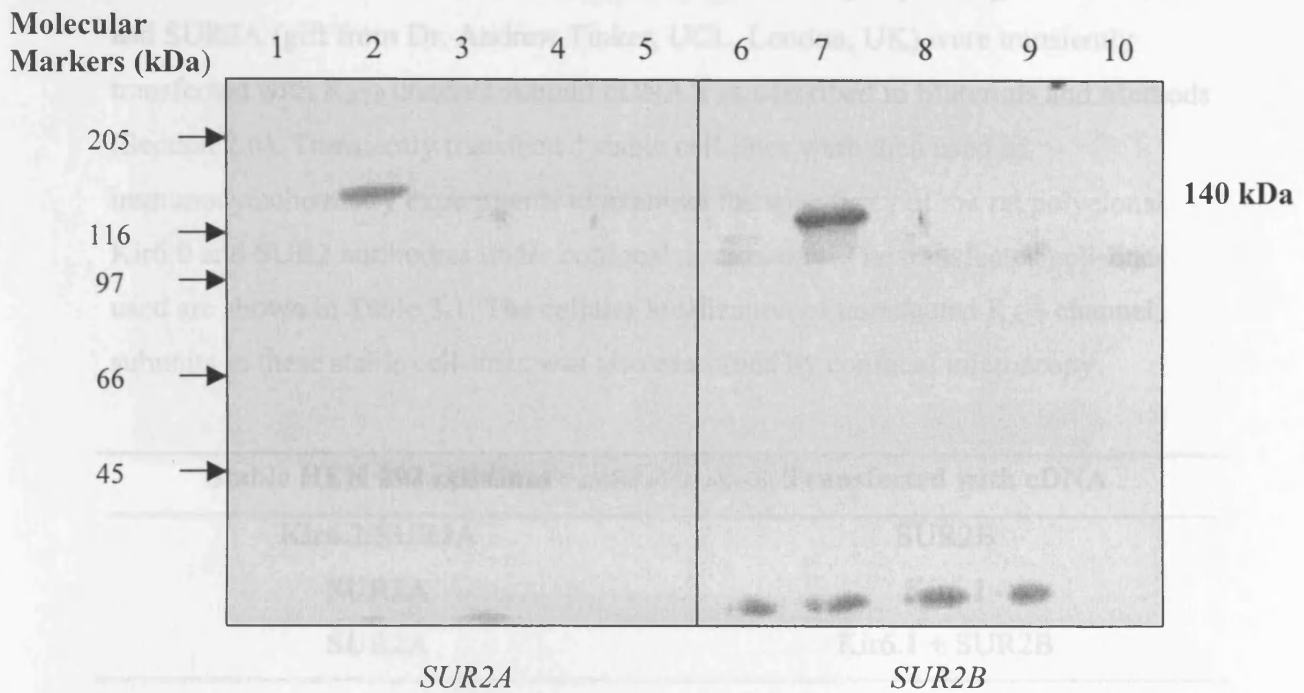


Table 3.1. Transiently transfected HEK 293 cell-lines with various subunits of the K_{ATP} channel used for immunocytochemistry experiments.

Antibody	-	2A	2A	2B	-	-	2B	2B	2A	-
1/250										
Antigen	-	-	2A	-	-	-	-	2B	-	-
10 µg/ml										

Figure 3.5 Immunoblot of *in vitro* translated SUR2 polypeptides probed with anti-SUR2 antibodies. Autoradiograph of an immunoblot of *in vitro* translated SUR2A and SUR2B polypeptides probed with subunit specific and unspecific SUR2 antibodies. Antibody binding was detected photoluminometrically using an ECL Western blot detection kit. The blot was exposed to film for 30 seconds. The immunoblots were probed with no primary antibody, lanes 1 and 6; anti-SUR2A (1/250 dilution), lanes 2 and 9; anti-SUR2B antiserum (1/250 dilution), lane 4 and 7; anti-SUR2A (1/250 dilution) plus 10 µg/ml SUR2A C-terminal peptide, lane 3; anti-SUR2B (1/250 dilution) plus 10 µg/ml SUR2B C-terminal peptide, lane 8.

Representative experiment (n = 3).

3.4 Immunocytochemistry of HEK 293 cells stably expressing Kir6.2/SUR2A or SUR2A transiently transfected with additional K_{ATP} channel subunits

Two human embryonic kidney (HEK) 293 cell lines stably expressing Kir6.2/SUR2A and SUR2A (gift from Dr. Andrew Tinker, UCL, London, UK) were transiently transfected with K_{ATP} channel subunit cDNA's as described in Materials and Methods (Section 2.6). Transiently transfected stable cell-lines were then used in immunocytochemistry experiments to examine the specificity of the rat polyclonal Kir6.0 and SUR2 antibodies under confocal microscopy. The transfected cell-lines used are shown in Table 3.1. The cellular localization of transfected K_{ATP} channel subunits in these stable cell-lines was also examined by confocal microscopy.

Stable HEK 293 cell-lines	Transfected with cDNA
Kir6.2/SUR2A	SUR2B
SUR2A	Kir6.1
SUR2A	Kir6.1 + SUR2B

Table 3.1. Transiently transfected HEK 293 cell-lines with various subunits of the K_{ATP} channel used for immunocytochemistry experiments.

No fluorescent emission of HEK 293 cells stably expressing Kir6.2/SUR2A transiently transfected with SUR2B was detected when cells were probed with anti-Kir6.1 (1/250 dilutions; Figure 3.6 A). The presence of cells detected on slides under transmitted light (Figure 3.6 B) implied that the anti-Kir6.1 antiserum showed no binding to these cells. Even increasing the fluorescent excitation to maximum was unable to elicit cell-associated fluorescence (Figure 3.6 C). When HEK 293 cells stably expressing Kir6.2/SUR2A transiently transfected with SUR2B were analysed with anti-Kir6.2, anti-SUR2A and anti-SUR2B (all at 1/250 dilutions) confocal images showed cell associated fluorescence (Figure 3.7A, Figure 3.8A and Figure 3.9A respectively), which was blocked on addition of 10 μ g/ml of the specific immunizing C-terminal peptide in each case (Figure 3.7 B, Figure 3.8 B and Figure 3.9 B). Transmitted light images of blocked cell-associated fluorescence were recorded showing the existence of cells in each case (Figure 3.7 C, Figure 3.8 C and Figure 3.9 C).

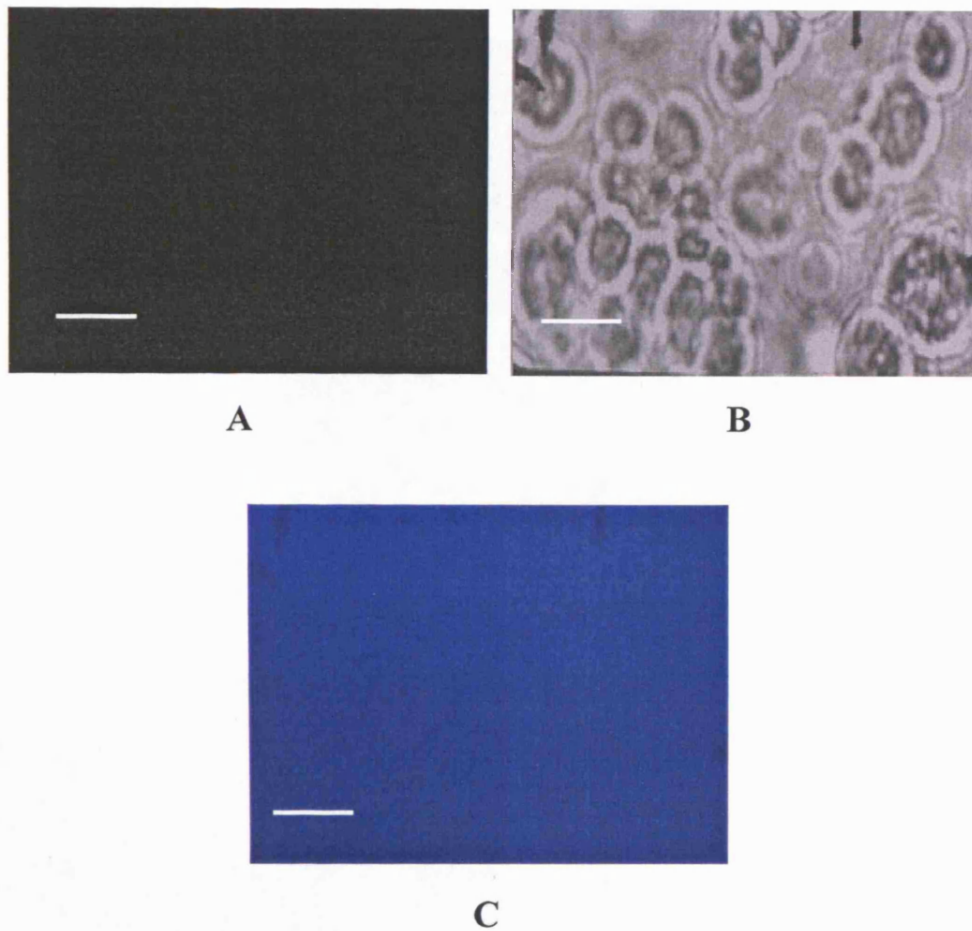
Anti-Kir6.1

Figure 3.6. Immunostained HEK 293 stably expressing Kir6.2/SUR2A transiently transfected with SUR2B to establish the absence of non-specific binding of Kir6.1 antibody under confocal microscopy. (A) FITC fluorescence associated with Kir6.1 antibody (1/250 dilution) binding at 488nm. (B) Transmitted light image of the same cells as in panel A. (C) Recording of FITC fluorescence associated cells in panel A under maximum fluorescent excitation. Horizontal bars = 50 μm . Representative experiment ($n = 2$)

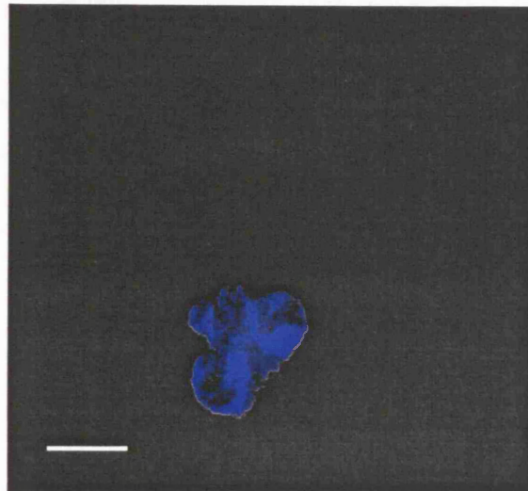
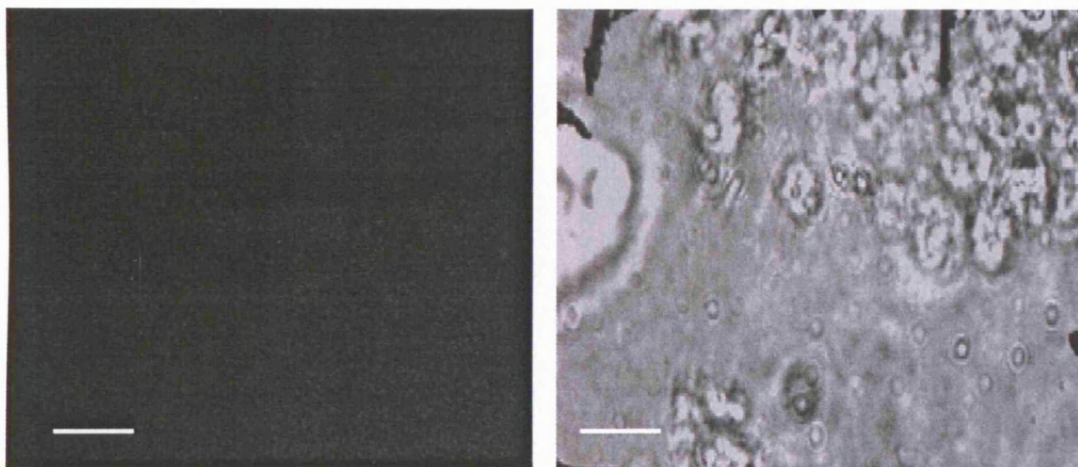
Anti-Kir6.2**Anti-Kir6.2 + Kir6.2 C-terminal peptide Antigen****B****C**

Figure 3.7. Immunostained HEK 293 stably expressing Kir6.2/SUR2A transiently transfected with SUR2B to establish specific binding of Kir6.2 antibody under confocal microscopy. (A) FITC fluorescence associated with anti-Kir6.2 antibody (1/250) binding at 488nm. (B) HEK 293 cell associated FITC fluorescence probed with Kir6.2 antibody (1/250) + 10 µg/ml Kir6.2 C-terminal peptide. (C) Transmitted light image of cells in panel B.

Horizontal bars = 50 µm (n = 2).

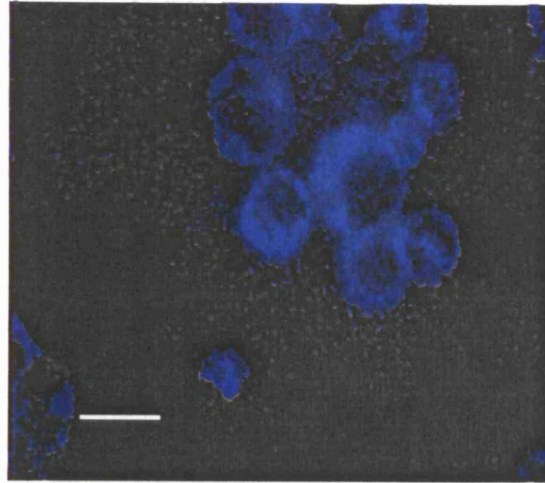
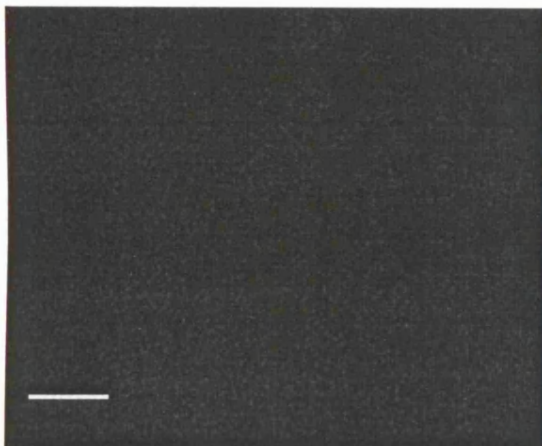
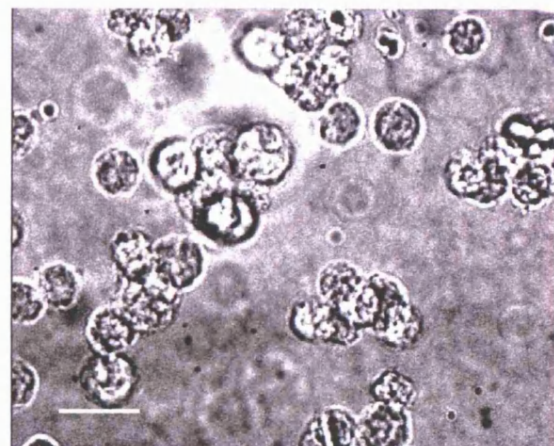
Anti-SUR2A**A****Anti-SUR2A + SUR2A C-terminal peptide****B****C**

Figure 3.8 Immunostained HEK 293 stably expressing Kir6.2/SUR2A transiently transfected with SUR2B to establish specific binding of SUR2A antibody under confocal microscopy. (A) FITC fluorescence associated with anti-SUR2A antibody binding at 488nm. (B) HEK 293 cell associated FITC fluorescence probed with SUR2A antibody (1/250) + 10 $\mu\text{g/ml}$ SUR2A C-terminal peptide. (C) Transmitted light image of the same cells as in panel B. Horizontal bars = 50 μm ($n = 2$)

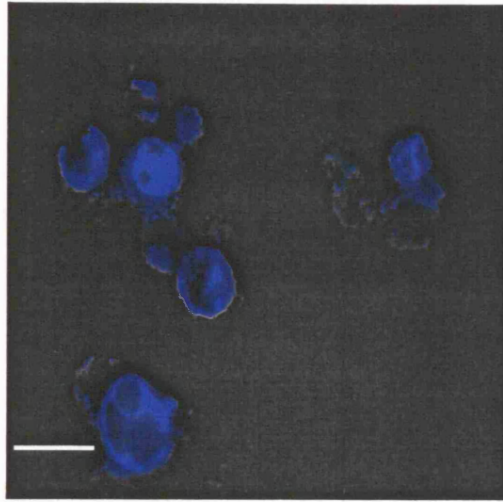
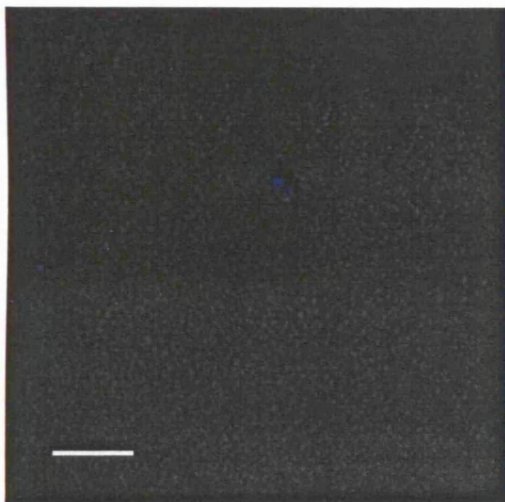
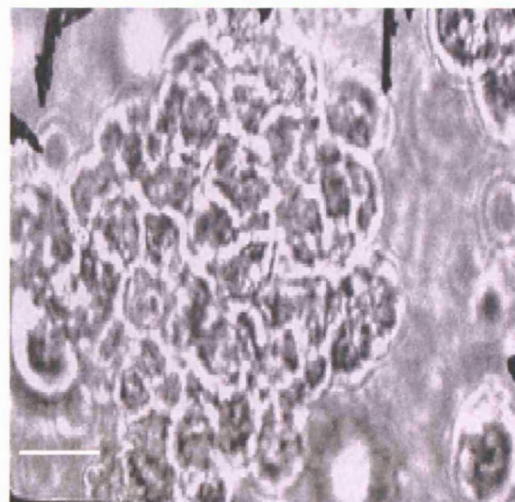
Anti-SUR2B**A****Anti-SUR2B + SUR2B C-terminal peptide****B****C**

Figure 3.9. Immunostained HEK 293 stably expressing Kir6.2/SUR2A transiently transfected with SUR2B to establish specific binding of SUR2B antibody under confocal microscopy. (A) FITC fluorescence associated with anti-SUR2B antibody binding at 488nm. (B) HEK 293 cell associated FITC fluorescence probed with SUR2B antibody (1/250) + 10 μ g/ml SUR2B C-terminal peptide. (C) Transmitted light image of the same cells as in panel B.

Cell-associated fluorescence was also recorded in HEK cells stably expressing SUR2A transiently transfected with Kir6.1 when incubated either with anti-Kir6.1 (1/250 dilution; Figure 3.10A) or anti-SUR2A (1/250 dilution; Figure 3.11). The FITC fluorescence associated with anti-Kir6.1 antiserum binding in the cells was blocked when diluted antiserum was incubated with Kir6.1 C-terminal peptide (10 µg/ml; Figure 3.10 B). The presence of cells in this immunocytochemical reaction was confirmed by transmitted light recordings (Figure 3.10 C). Specific peptide block was not performed on cells incubated with anti-SUR2A in this experiment because the specificity of the SUR2A C-terminal peptide recognition by anti-SUR2A had been determined already in HEK cells stably expressing Kir6.2/SUR2A transiently transfected with SUR2B.

As expected incubation of anti-SUR2B antibody (1/250 dilution) with HEK cells stably expressing SUR2A transiently transfected with Kir6.1 showed no antibody associated fluorescence whatsoever on the cells (Figure 3.12), but when anti-SUR2B antiserum (1/250 dilution) was incubated with HEK cells stably expressing SUR2A transiently transfected with Kir6.1 and SUR2B whole cell-associated fluorescence was observed (Figure 3.12 C) thus confirming specificity of anti-SUR2B. Since the specificity of the anti-SUR2B antibody towards the SUR2B C-terminal peptide had been established in HEK 293 stably expressing Kir6.2/SUR2A transiently transfected with SUR2B, specific peptide block of anti-SUR2B was not performed on HEK cells stably expressing SUR2A transiently transfected with Kir6.1 and SUR2B. No fluorescence was emitted from HEK cells stably expressing SUR2A transiently transfected with Kir6.1 and SUR2B when probed with anti-Kir6.2 (1/250 dilution; Figure 3.13 A). Transmitted images were recorded confirming the existence of cells in immunocytochemical reactions where HEK cells stably expressing SUR2A transiently transfected with Kir6.1 were probed with anti-SUR2B antiserum (Figure 3.12 B) and HEK cells stably expressing SUR2A transiently transfected with Kir6.1 and SUR2B incubated with anti-Kir6.2 antiserum (Figure 3.13 B) thus confirming the absence of non-specific binding of anti-SUR2B and Kir6.2 antiserum in these cells.

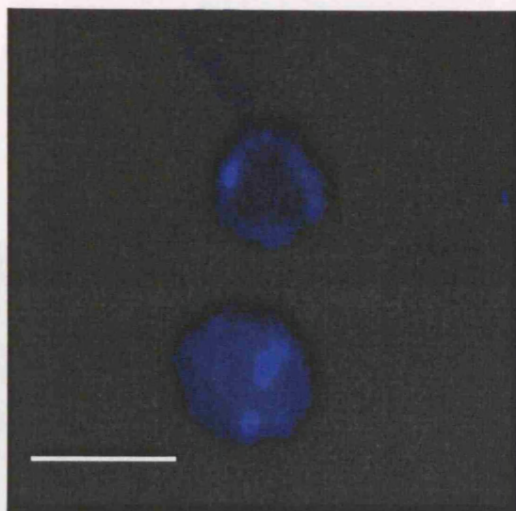
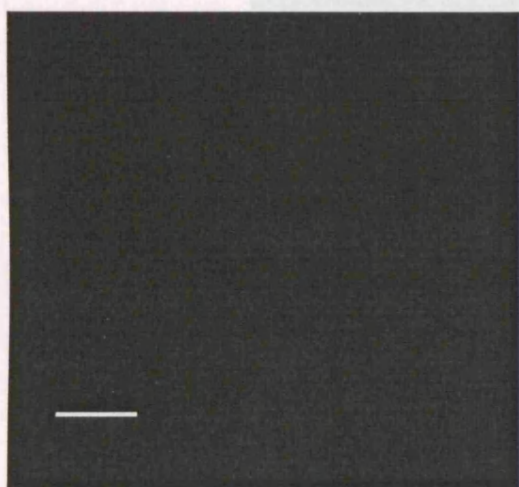
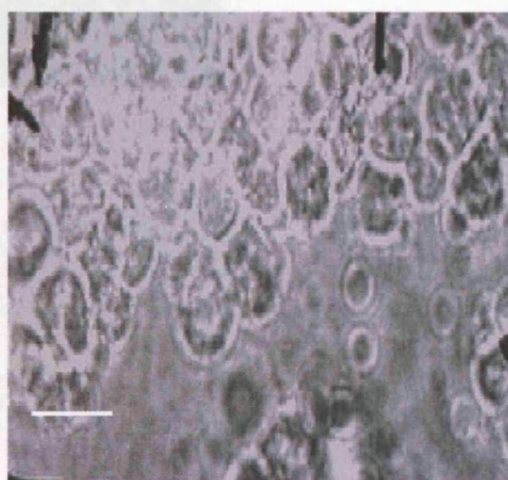
Anti-Kir6.1**A****Anti-Kir6.1 + Kir6.1 C-terminal peptide****B****C**

Figure 3.10 Immunostained HEK 293 stably expressing SUR2A transiently transfected with Kir6.1 to establish specific binding of Kir6.1 antibody under confocal microscopy. (A) FITC fluorescence associated with anti-Kir6.1 antibody binding at 488nm. (B) HEK 293 cell associated FITC fluorescence probed with Kir6.1 antibody (1/250) + 10 µg/ml Kir6.1 C-terminal peptide. (C) Transmitted light image of cells in panel B. Horizontal bars = 50 µm.

Representative experiment (n = 2).



Figure 3.11. Immunostained HEK 293 stably expressing SUR2A transiently transfected with Kir6.1 to establish specific binding of SUR2A antibody under confocal microscopy. FITC fluorescence associated with anti-SUR2A antibody binding (1/250) at 488nm. The specificity of anti-SUR2A towards its specific C-terminal immunizing peptide was not done as it was shown in earlier experiments. Horizontal bar = 50 μm ($n = 2$)

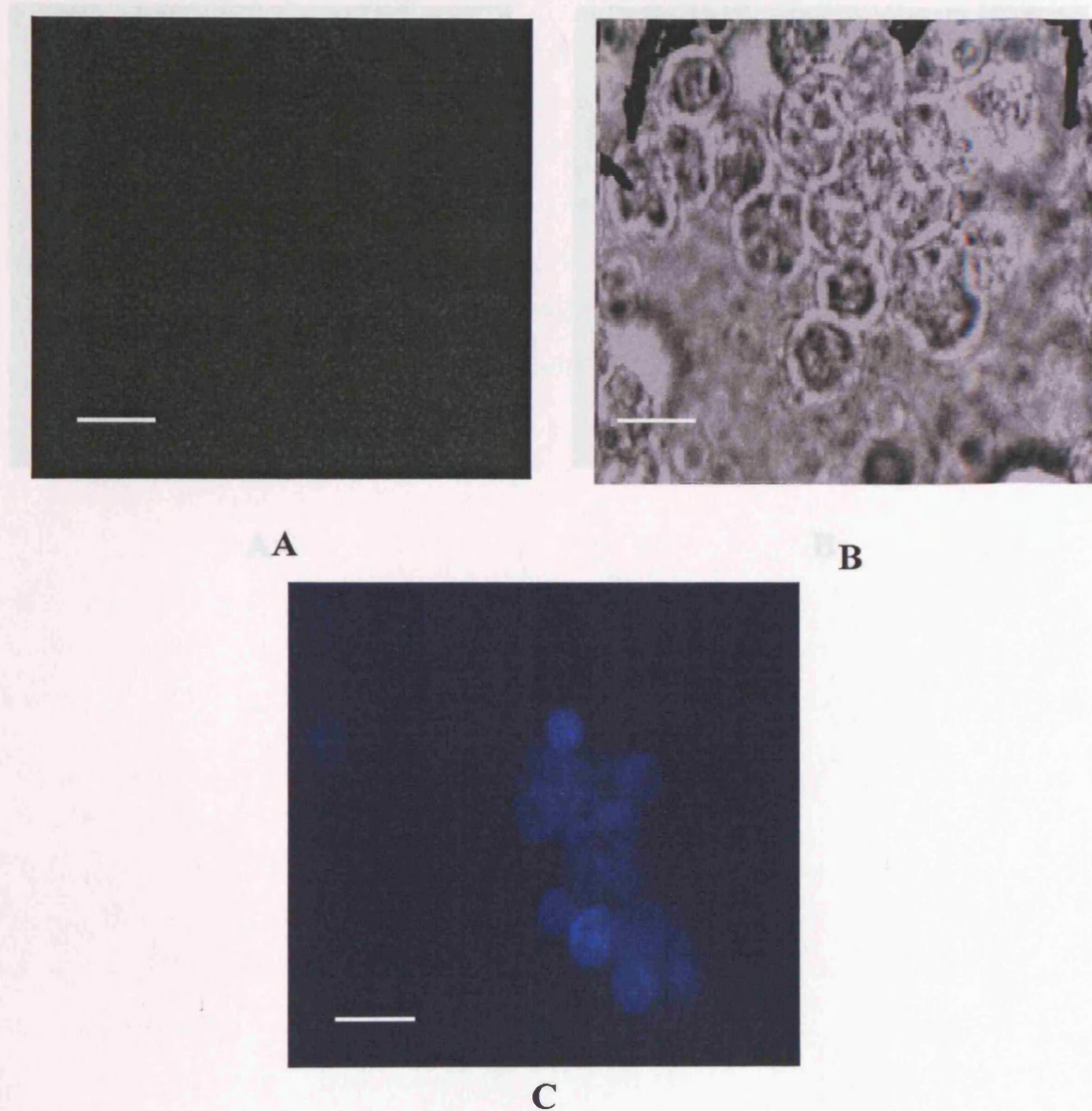
Anti-SUR2B

Figure 3.12 Immunostained HEK 293 cells stably expressing SUR2A transiently transfected with Kir6.1 and the same stable cell-line transiently transfected with Kir6.1 and SUR2B. (A) Fluorescent image of SUR2A expressing stable cell-line transfected with Kir6.1 probed with SUR2B antibody (1/250) at 488nm. The absence of non-specific anti-SUR2B binding was observed. (B) Transmitted light image of cells in panel A. (C) Fluorescence image of stable cell-line transfected with Kir6.1 and SUR2B probed with anti-SUR2B antibody (1/250) at 488nm. Horizontal bars = 50 μ m. Representative experiment ($n = 2$).

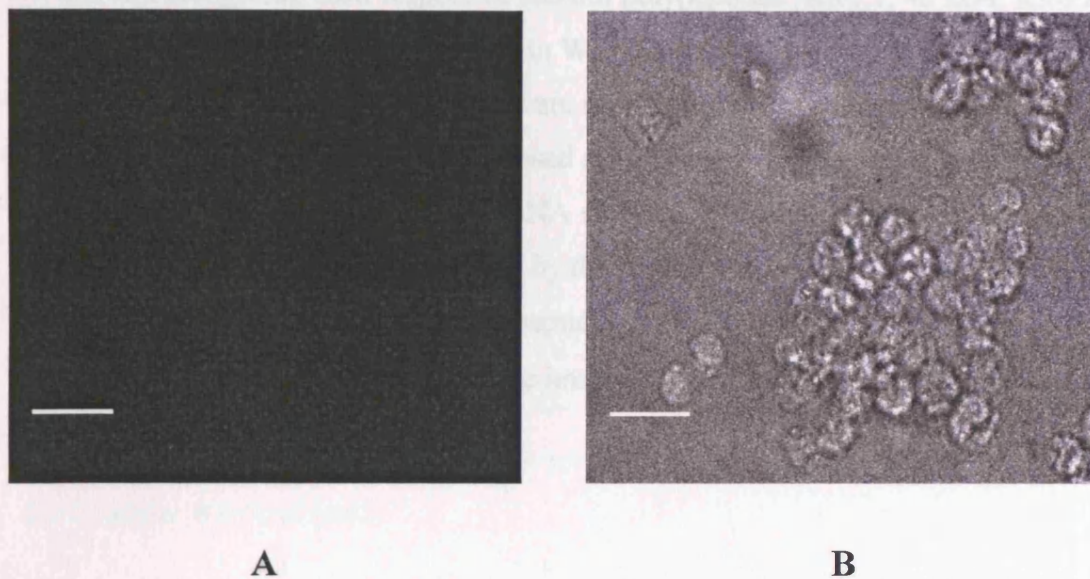
Anti-Kir6.2

Figure 3.13 Immunostained HEK 293 stably expressing SUR2A transiently transfected with Kir6.1 and SUR2B to establish the absence of non-specific binding of Kir6.2 antibody under confocal microscopy. Fluorescent image of cells probed with anti-Kir6.2 antibody (1/250) at 488nm. (B) Transmitted light image of cells in panel A. Horizontal bars = 50 μm ($n = 2$).

3.5 Summary

All antisera recognised their respective subunit polypeptides (Kir6.1, 48 kDa; Kir6.2, 40 kDa, SUR2A and SUR2B, 140 kDa) in Western blots of *in vitro* expressed subunit polypeptides. Moreover, all antibodies were shown to immunoprecipitate specifically [³⁵S]-methionine-labelled *in vitro* expressed subunit polypeptides and to bind to HEK 293 cells only when transfected with cDNA encoding the target polypeptide. In all the above assays, specificity was confirmed by the demonstration of an absence of direct cross-reactivity with other subunit polypeptides and/or block of immunoreaction by preincubation of diluted antisera with the immunizing peptide (10 µg/ml) but not by those derived from related isoforms.

Chapter 4: Localization of Kir6.0 and SUR2 K_{ATP} Channel Subunit Isoforms in Isolated Rat Cardiac Myocytes

The presence of functional K_{ATP} channels has been demonstrated in both cardiac sarcolemmal (Inagaki et al., 1995) and mitochondrial membranes (Inoue et al. 1991). Although studies have implicated the importance of cardiac K_{ATP} channels in ischaemic preconditioning (see section 1.13), the type of K_{ATP} channel involved in this event still remains uncertain. To understand the roles of sarco K_{ATP} and mito K_{ATP} channels in cardiac myocytes, the molecular composition of each needs to be resolved. In this study, characterized site-directed antibodies against K_{ATP} channel subunit peptides were used to investigate the cellular localisation of K_{ATP} channel subunit isoforms in isolated cardiac myocytes by confocal microscopy and Western blotting of subcellular fractionations.

4.1 Localization of the Kir6.1 Subunit in Isolated Rat Cardiac Myocytes

Anti-Kir6.1 C-terminal antiserum was used to localize Kir6.1 subunit distribution in fixed and permeabilised myocytes. A strong intracellular signal was observed with longitudinal streaks of immunofluorescence consistent with an association of this isoform with myofibril structures within the cells (Figure 4.1-A). Anti-Kir6.1 associated fluorescence was also associated in punctated areas under the sarcolemma. Pixel profiles taken across stained myocytes also demonstrated high level of anti-Kir6.1-associated fluorescence associated with internal structures (Figure 4.1-B). The specificity of anti-Kir6.1 antibody binding to these structures was confirmed by the abolition of the fluorescence signal after preadsorption of the anti-Kir6.1 antiserum with 10mg/ml Kir6.1 C-terminal peptide (Figure 4.1-C and D) but not by Kir6.2 C-terminal peptide (not shown).

A predominantly mitochondrial localisation for Kir6.1 subunits has been suggested (Suzuki et al 1997). To investigate whether Kir6.1 subunits were localised in mitochondria associated with myofibrils, mitochondria were labelled with the fluorescent mitochondrial marker, MitoFluor red 589 (Molecular Probes; M-22424) and the co-localization of anti-Kir6.1-associated fluorescence was analysed by comparing fluorescent emissions at 568 and 488 nm, respectively (Figure 4.2-A and

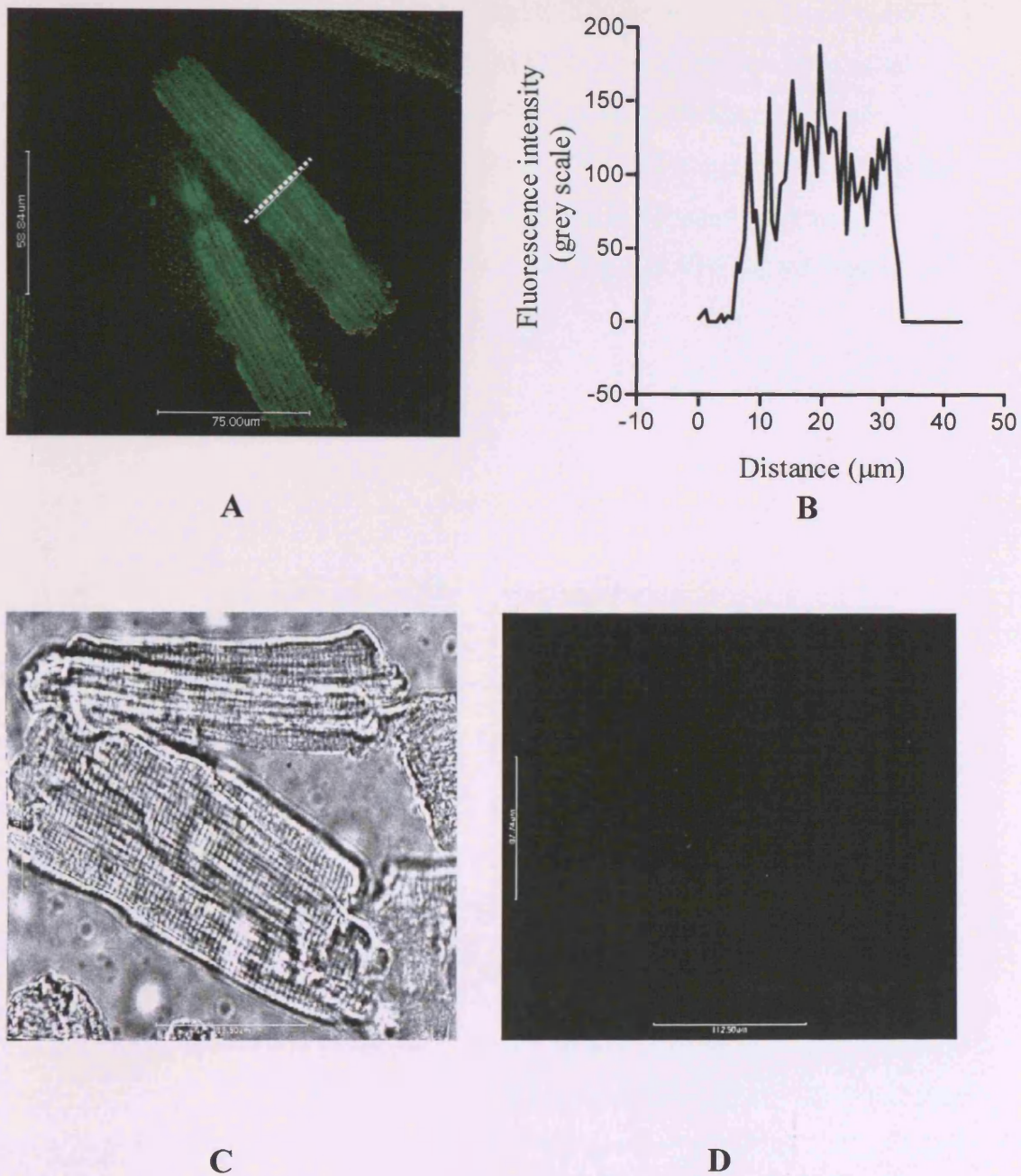


Figure 4.1. Confocal image of the localization of specific Kir6.1 antibody binding (1/250 dilution) on rat isolated ventricular myocytes excited at 488nm. (A) Fluorescence associated with the Kir6.1 antibody binding. (B) Pixel profile along the line defined in A. (C) Transmitted light image of peptide-blocked cell. (D) Specific peptide block of Kir6.1 antibody binding on rat ventricular myocyte. Representative of three experiments ($n = 3$).

B). Green fluorescence corresponding to anti-Kir6.1 and red fluorescence associated with MitoFluor was used to investigate the co-localization of Kir6.1 and mitochondria marker in the same myocyte (Figure 4.2-C). Analysis of the pixel profile (Figure 4.2-D) for the distribution of the two fluorescent labels in six cells revealed that of all pixels positive for anti-Kir6.1, $86 \pm 12\%$ were also positive for MitoFluor red. Conversely, of all pixels positive for MitoFluor red, $74 \pm 17\%$ were also positive for anti-Kir6.1. The correlation coefficient for co-localisation of anti-Kir6.1 and MitoFluor red labelling was 0.63 ± 0.05 . The results suggested strong association of Kir6.1 subunits with the mitochondria membrane.



Figure 4.2. Confocal images of the localization of specific Kir6.1 antibody staining (1/500 dilution) in rat isolated ventricular myocytes incubated with MitoFluor red. (A) Kir6.1 antibody immunofluorescence in yellow. (B) MitoFluor red staining in red. (C) Co-localization of MitoFluor and Kir6.1 antibody associated fluorescence appearing with Kir6.1 distribution shown in green and MitoFluor fluorescence shown in red. (D) Pixel profile of the specific fluorescent intensity of the two probes along the line defined in C. Representative of two experiments ($n = 2$).

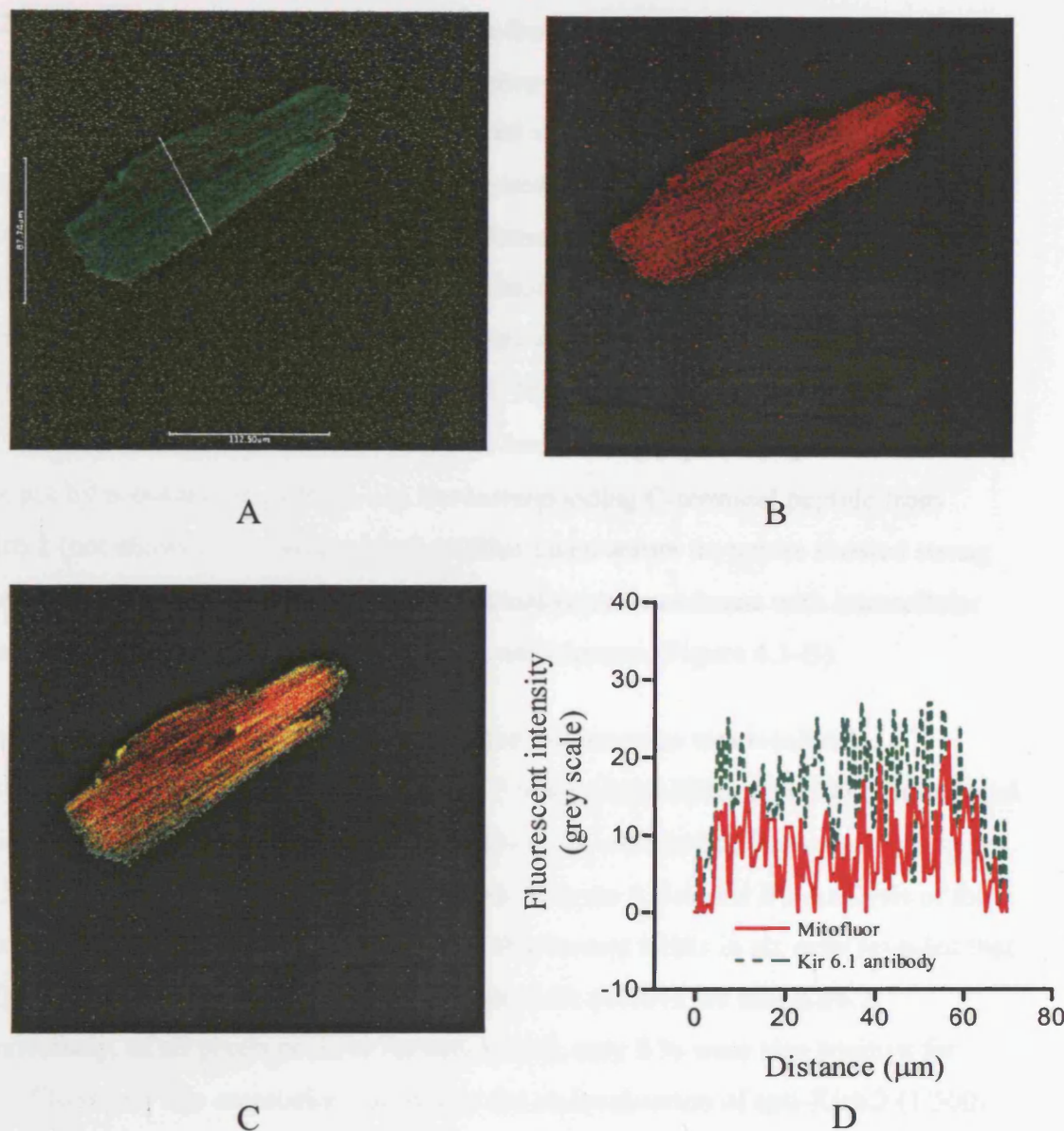


Figure 4.2. Confocal image of the localization of specific Kir6.1 antibody binding (1/500 dilution) on rat isolated ventricular myocytes co-localized with MitoFluor red. (A) Kir6.1 associated immunofluorescence at 488nm. (B) MitoFluor red associated immunofluorescence at 568nm. (C) Co-localization of MitoFluor and Kir6.1 antibody associated fluorescence (yellow) with Kir6.1 fluorescence shown in green and MitoFluor fluorescence in red. (D) Pixel profile of the specific fluorescent intensity of the two probes along the line defined in C. Representative of two experiments (n =2).

4.2 Localization of the Kir6.2 Subunit in Isolated Rat Cardiac Myocytes

The cardiac sarcolemmal K_{ATP} channel is proposed to comprise Kir6.2 and SUR2A subunits from the similarity of the functional and pharmacological properties of K_{ATP} channels when these subunits are co-expressed in heterologous expression systems compared to native cardiac sarcolemmal channels (Inagaki et al., 1995). Consistent with this proposal, anti-Kir6.2-associated fluorescence (1/250 dilution) was localized over the sarcolemma of ventricular myocytes with weaker fluorescence associated with intracellular structures (Figure 4.3-A). This signal was blocked by preadsorption of the anti-Kir6.2 antiserum with 10 µg/ml immunising peptide (Figure 4.3-C and D) but not by non-specific peptide, e.g. the corresponding C-terminal peptide from Kir6.1 (not shown). Transverse pixel profiles taken across myocytes showed strong fluorescence intensity associated with the sarcolemmal membrane with intracellular fluorescence approximately half that at the sarcolemma (Figure 4.3-B).

To investigate internal anti-Kir6.2 associated fluorescence was localized mitochondria, co-localization of anti-Kir6.2 using a high dilution (1/500 dilution) and MitoFluor associated fluorescence was analysed by comparing fluorescent emissions at 568 (red) and 488 nm (green), respectively (Figure 4.4-A and B). Analysis of the pixel profile for the distribution of the two fluorescent labels in six cells revealed that of all pixels positive for MitoFluor red, none were positive for anti-Kir6.2. Conversely, of all pixels positive for anti-Kir6.2, only 9 % were also positive for MitoFluor red. The correlation coefficient for co-localisation of anti-Kir6.2 (1/500) and MitoFluor red was 0.11 ± 0.018 . However, co-localization of anti-Kir6.2 using a low dilution (1/250 dilution) and MitoFluor associated fluorescence in cells showed Kir6.2 localization on the mitochondria (Figure 4.4-C). Analysis of the pixel profile (Fig. 4.4-D) for the distribution of the two fluorescent labels in six cells revealed that of all pixels positive for anti-Kir6.2, 45 ± 3 % were also positive for MitoFluor red. Conversely, of all pixels positive for MitoFluor red, 32 ± 10 % were also positive for anti-Kir6.2 with a correlation coefficient of 0.56 ± 0.05 . These results suggested strong association of Kir6.2 subunits with the sarcolemma and some localization on mitochondria.

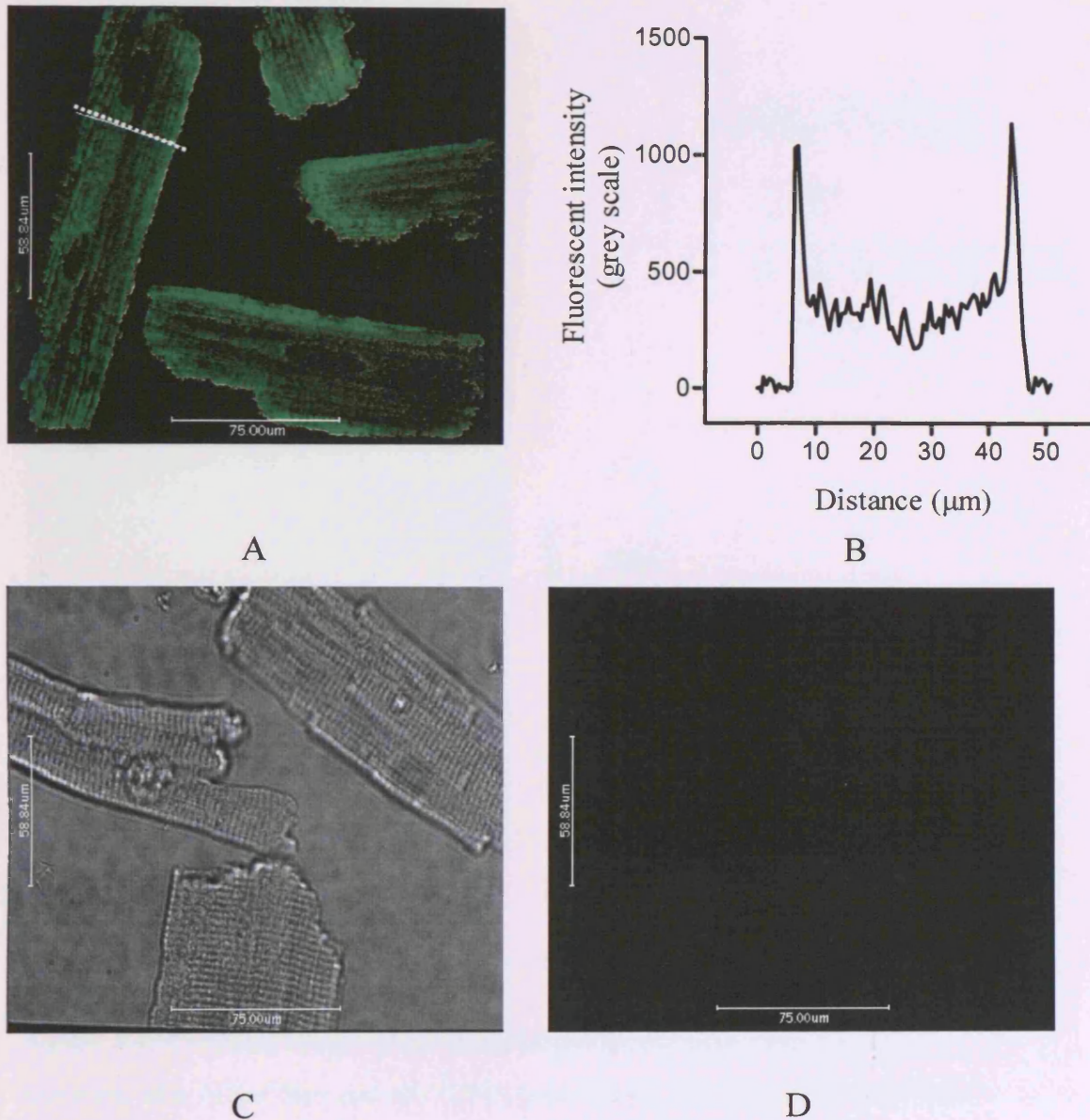


Figure 4.3. Confocal image of the localization of Kir6.2 antibody binding (1/250 dilution) on rat isolated ventricular myocytes excited at 488nm. (A) Fluorescence associated with the Kir6.2 antibody binding. (B) Pixel profile along the line defined in A. (C) Transmitted light image of peptide-blocked cells. (D) Specific peptide block of Kir6.2 antibody binding on rat ventricular myocytes. Representative of three experiments ($n = 3$).

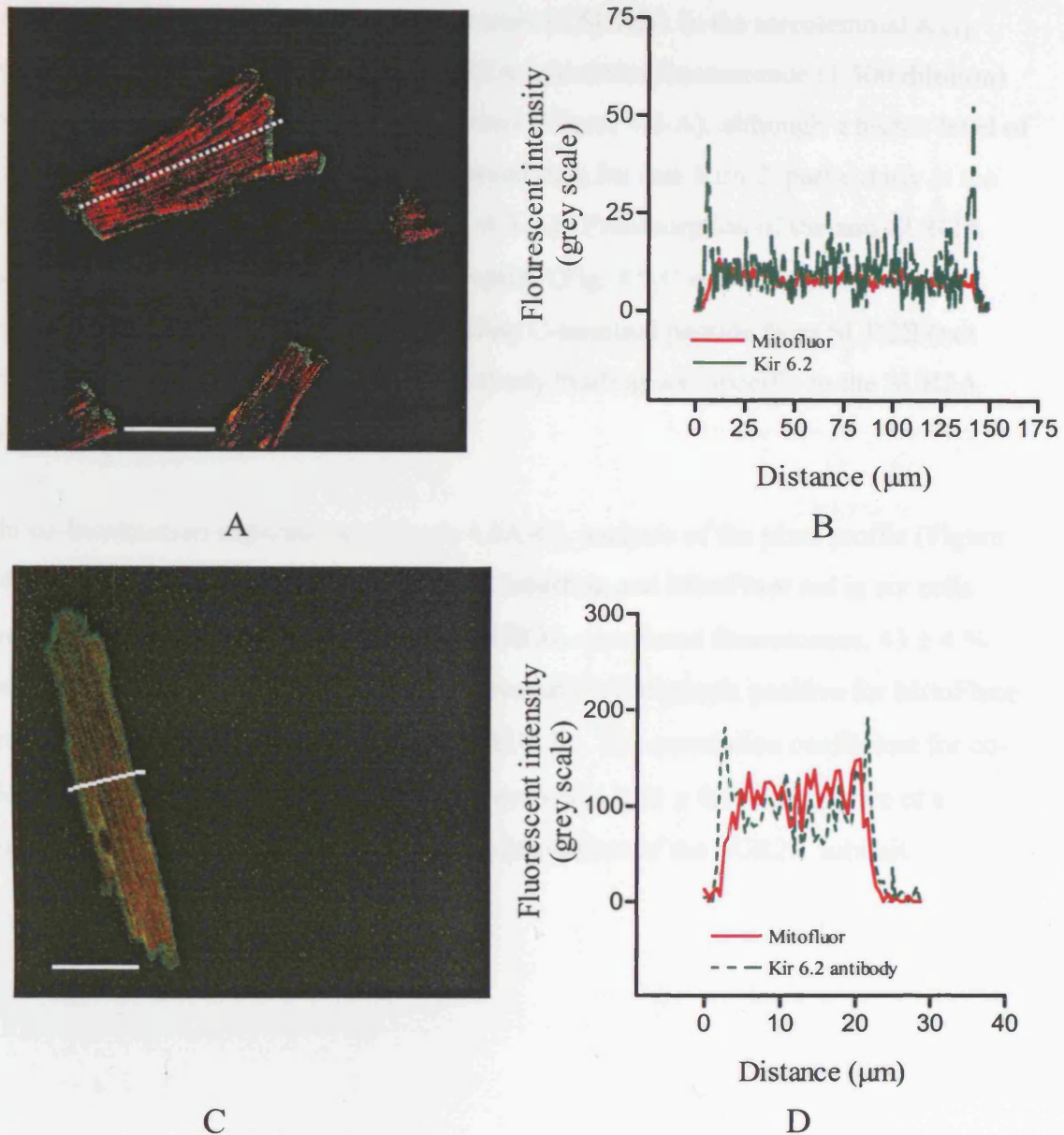


Figure 4.4. Confocal image of the localization of the Kir6.2 antibody co-localized with MitoFluor red. (A) Co-localization of MitoFluor red and Kir6.2 antibody (1/500) associated immunofluorescence (yellow) with Kir6.2 fluorescence shown in green and MitoFluor fluorescence in red. (B) Pixel profile of the specific fluorescent intensity of the two probes along the line defined in A. (C) Co-localization of MitoFluor red and Kir6.2 antibody (1/250) associated immunofluorescence (yellow) with Kir6.2 fluorescence shown in green and MitoFluor fluorescence in red. (D) Pixel profile of the specific fluorescent intensity of the two probes along the line defined in C. Horizontal bars=50µm Representative of two separate experiments (n = 2).

4.3 Localization of the SUR2A Subunit in Isolated Rat Cardiac Myocytes

As predicted from the proposed involvement of SUR2A in the sarcolemmal K_{ATP} channel (Inagaki et al., 1995), anti-SUR2A-associated fluorescence (1/500 dilution) was localised strongly over the sarcolemma (Figure 4.6-A), although a higher level of intracellular fluorescence was also observed than for anti-Kir6.2, particularly at the lower antiserum dilution (1/250; Figure 4.5-A). Preadsorption of the anti-SUR2A antiserum with 10 µg/ml immunizing peptide (Fig. 4.5 C and D) but not non-immunizing peptide, e.g. the corresponding C-terminal peptide from SUR2B (not shown), confirmed that anti-SUR2A antibody binding was specific to the SUR2A polypeptide.

In co-localization experiments (Figure 4.6A-C), analysis of the pixel profile (Figure 4.6 D) for the distribution of anti-SUR2A labelling and MitoFluor red in six cells revealed that all pixels positive for anti-SUR2A-associated fluorescence, $43 \pm 4 \%$ were also positive for MitoFluor red. Conversely, of all pixels positive for MitoFluor red, $72 \pm 5 \%$ were also positive for anti-SUR2A. The correlation coefficient for co-localisation of anti-SUR2A and MitoFluor red was 0.61 ± 0.06 , suggestive of a mitochondrial, as well as, a sarcolemmal distribution of the SUR2A subunit.

Figure 4.5. Confocal image of the localization of specific SUR2A antibody binding (1/500 dilution) on rat isolated ventricular myocytes washed at 422nm. (A) Fluorescence associated with the SUR2A antibody. (B) Pixel profile along the line defined in A. (C) Unimmunized IgG1 image of septin1 blocked cells. (D) Specific peptide block of SUR2A antibody on rat ventricular myocytes. (n = 5)

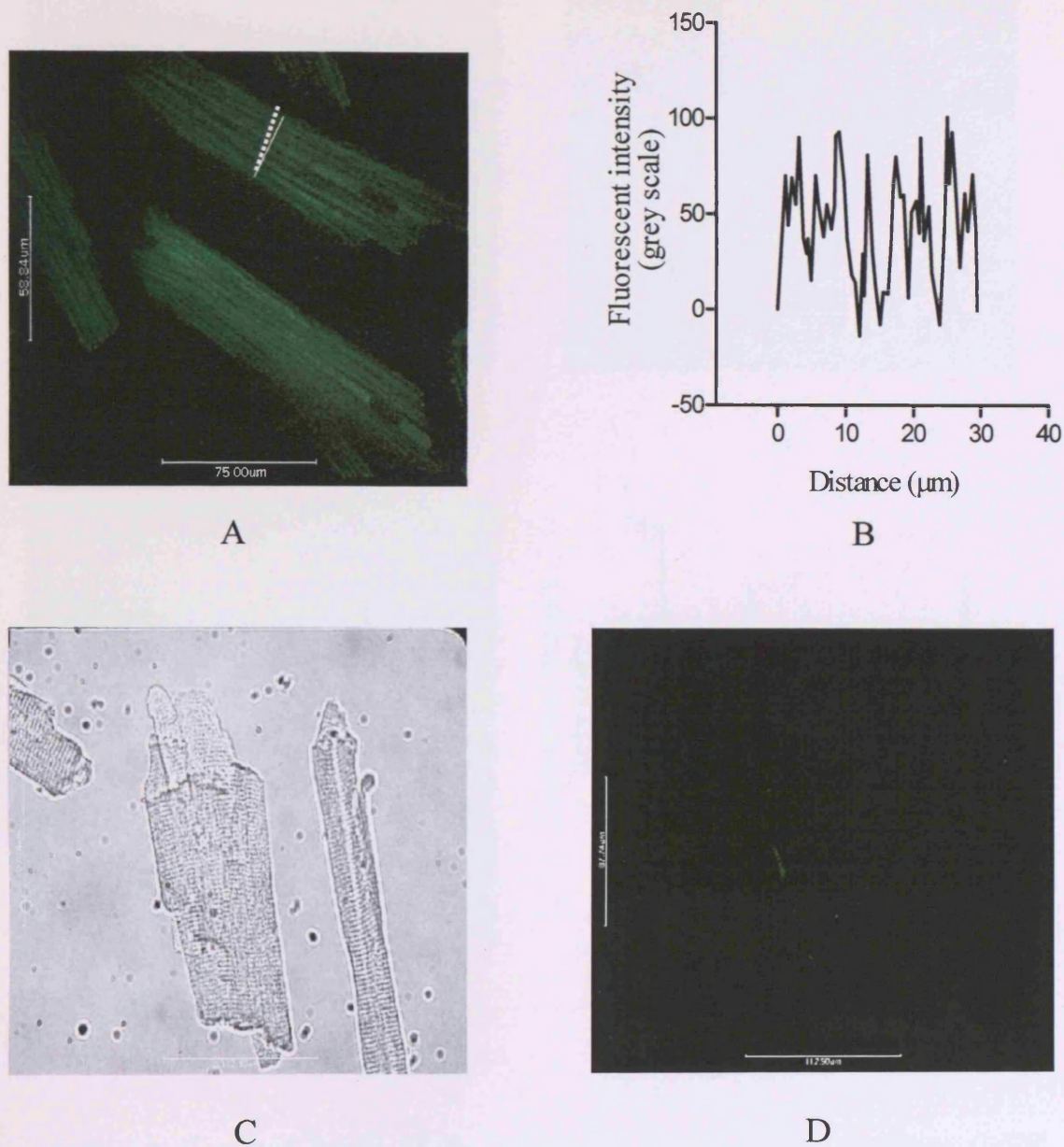


Figure 4.5. Confocal image of the localization of specific SUR2A antibody binding (1/250 dilution) on rat isolated ventricular myocytes excited at 488nm. (A) Fluorescence associated with the SUR2A antibody. (B). Pixel profile along the line defined in A. (C) Transmitted light image of peptide blocked cells. (D) Specific peptide block of SUR2A antibody on rat ventricular myocyte. ($n = 3$)

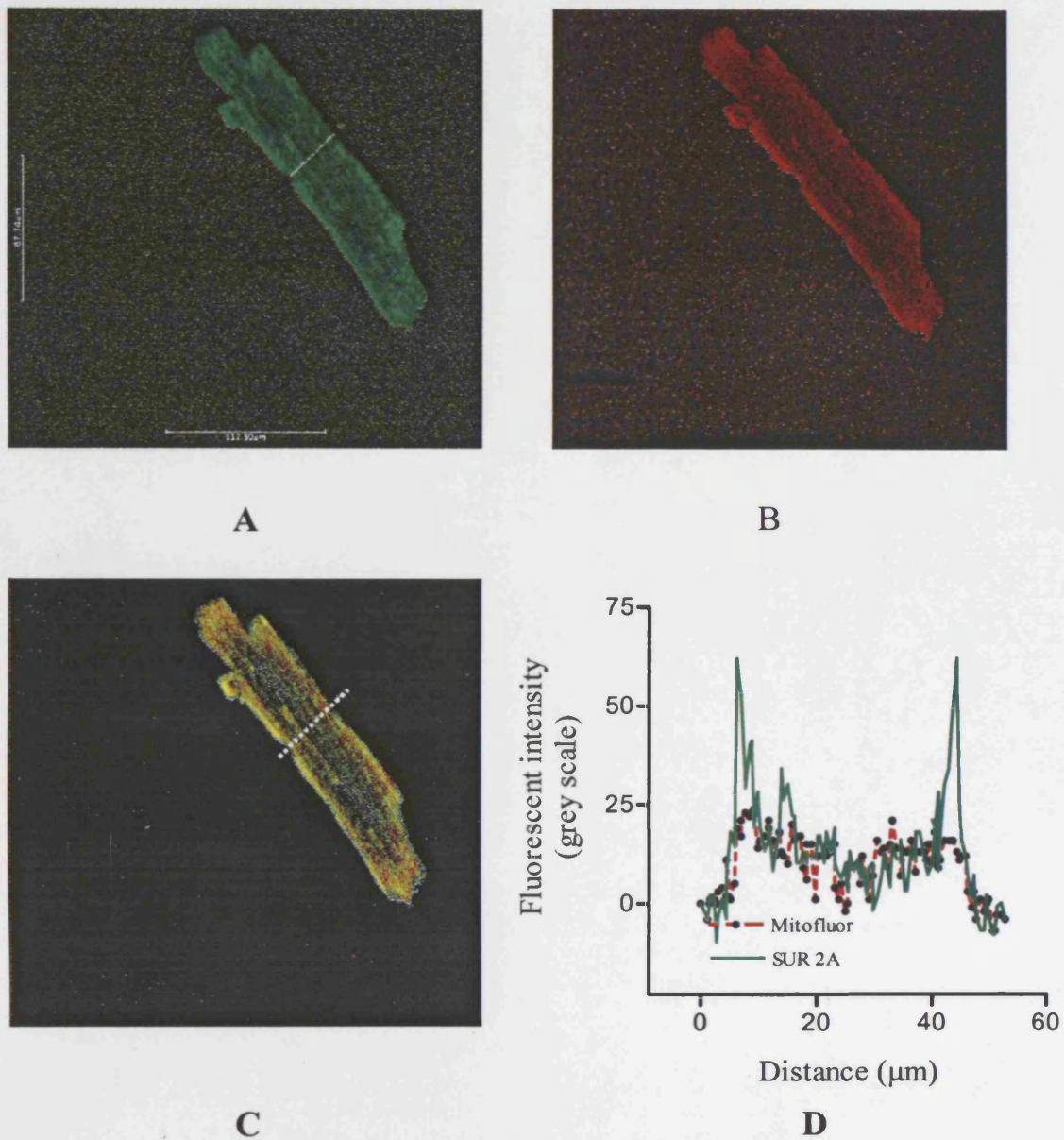


Figure 4.6. Confocal image of the localization of the SUR2A antibody (1/500 dilution) co-localized with MitoFluor red. (A) SUR2A associated fluorescence with excitation at 488nm. (B) MitoFluor red associated fluorescence with excitation at 568nm. (C) Co-localization of MitoFluor red and SUR2A antibody binding (yellow) with SUR2A fluorescence shown in green and MitoFluor red fluorescence in red. (D) Pixel profile of specific fluorescent intensities of the two probes defined from line in C. ($n = 2$)

4.4 Localization of the SUR2B Subunit in Isolated Rat Cardiac Myocytes

Anti-SUR2B-associated fluorescence displayed a distinct regular transverse striated pattern of labelling when viewed directly or an examination of the longitudinal pixel profile of the fluorescent emission with this antiserum (Figure 4.7-A and B).

Preadsorption of the anti-SUR2B antiserum with 10 µg/ml immunizing peptide (Fig. 4.7-C and D) but not non-immunizing peptide, e.g. the corresponding C-terminal peptide from SUR2B (not shown), confirmed that anti-SUR2B antibody detection was specific to the SUR2B polypeptide. To examine whether this pattern of transverse striations corresponded to the localization of transverse tubules (T-tubules), the co-localization of SUR2B labelling with that of a specific 28 kDa T-tubule protein marker recognised by monoclonal IXE11₂ antibody (gift from Dr Campbell; University of Iowa, USA) was investigated (Figure 4.8). Analysis of the pixel profile for the distribution of anti-SUR2B and IXE11₂ antibody labelling in six cells revealed that of all pixels positive for anti-SUR2A-associated fluorescence, 50 ± 5 % were positive for the t-tubule marker. Conversely, of all pixels positive for IXE11₂ binding, 77 ± 7 % were also positive for anti-SUR2B binding. The correlation coefficient for co-localisation of anti-SUR2B and the IXE11₂ t-tubule marker was 0.81 ± 0.05, suggesting that SUR2B subunits are highly localised to the T-tubule system in cardiac myocytes.



Figure 4.7. Confocal images of the localization of anti-SUR2B antibody binding (1:20 dilution) in rat cardiac myocytes (excitation at 488nm). (A) Fluorescence associated with the anti-SUR2B antibody binding. (B) Pixel profile along the line defined in A. (C) Pre-adsorbed cell showing no SUR2B labelling. (D) Specific peptide block of SUR2B antibody binding. Scale bar = 10 µm. Representative of three experiments (n = 3).

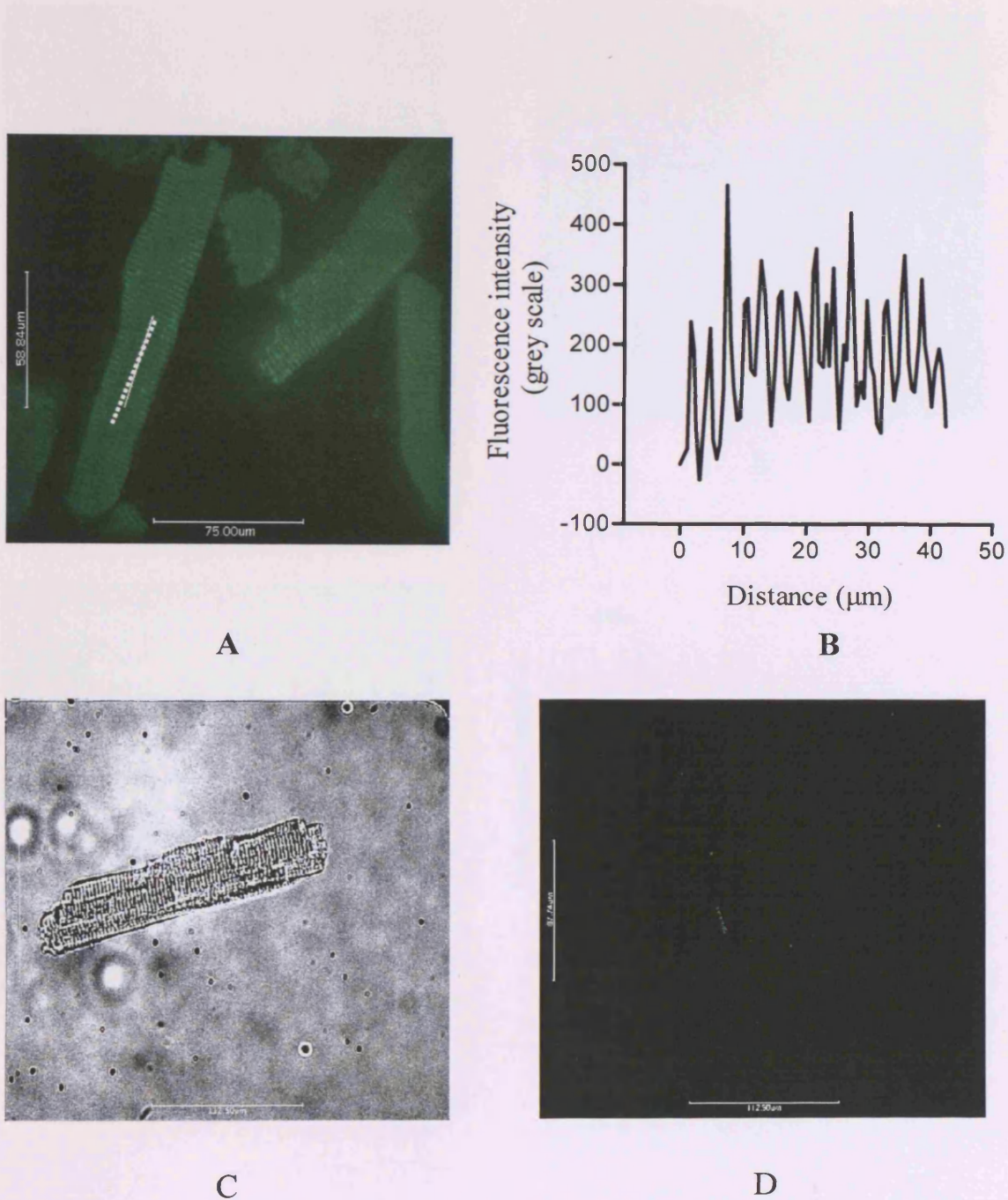


Figure 4.7. Confocal image of the localization of specific SUR2B antibody binding (1/250 dilution) on rat isolated ventricular myocytes excited at 488nm. (A) Fluorescence associated with the SUR2B antibody binding. (B). Pixel profile along the line defined in A. (C) Transmitted light image of a peptide blocked cell. (D) Specific peptide block of SUR2B antibody on a rat ventricular myocyte. Representative of three experiments ($n = 3$).

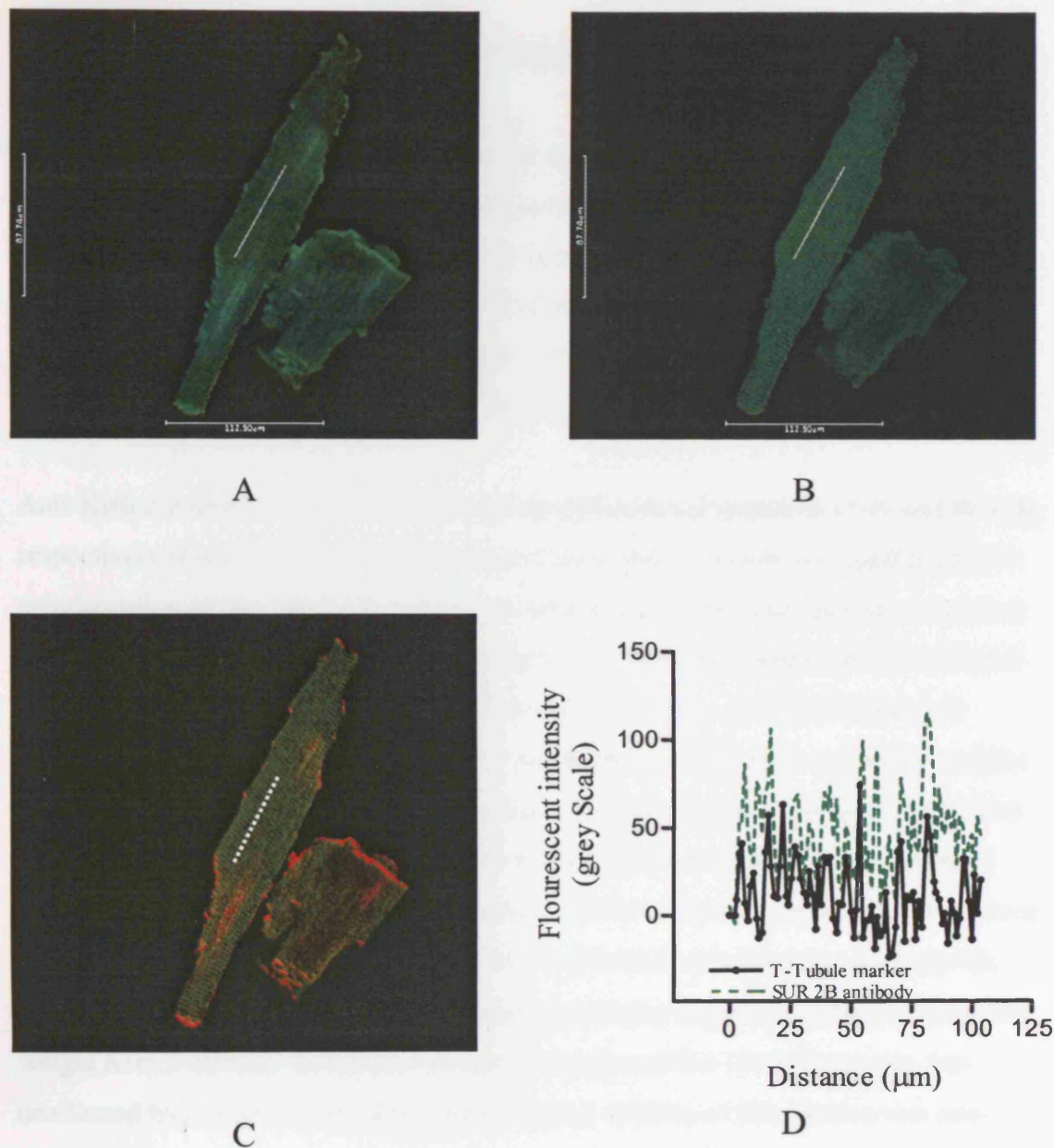


Figure 4.8. Confocal image of the co-localization of the SUR2B antibody (1/500 dilution) with the binding of a T-tubule marker, IXE11₂. (A) Fluorescence associated with the anti-SUR2B binding at 488nm. (B) Fluorescence associated with anti-IXE11₂ antibody binding at 568nm. (C) Co-localization of anti-SUR2B antibody and anti-IXE11₂ antibody binding with SUR2B fluorescence shown in red and anti-IXE11₂ antibody binding fluorescence in green. (D) Pixel profile of fluorescent intensity define from line C. ($n = 2$)

4.5 Western blotting of K_{ATP} channel subunits in isolated cardiac ventricular myocytes

Immunodetection with anti-Kir6.1 revealed a major stained band corresponding to a polypeptide of 45 kDa and minor stained bands of 90 kDa and 130 kDa (Figure 4.9, lane 2). Preadsorption of the diluted antiserum with Kir6.1 C-terminal peptide blocked anti-Kir6.1 recognition of the 45 kDa species completely while staining of the higher molecular weight species, although reduced, was still present suggesting that these species represented possible higher order oligomers of Kir6.1.

Anti-Kir6.2 stained two major bands corresponding to polypeptides of 40 and 80 kDa, respectively (Figure 4.9, lane 4). Staining of each band was reduced significantly on preadsorption of the anti-Kir6.2 antiserum with Kir6.2 C-terminal peptide consistent with specific immunodetection of monomeric (40 kDa) and dimeric (80 kDa) Kir6.2 polypeptides, respectively (Figure 4.9, lane 5). In addition, anti-Kir6.2 detected additional minor bands corresponding to polypeptides of apparent molecular weights of 60, 100 and 180 kDa. Staining of the highest molecular weight species (180 kDa) was blocked by preadsorption of the anti-Kir6.2 antiserum with Kir6.2 C-terminal peptide and may have represented tetrameric Kir6.2 complexes. Staining of the minor 60 kDa polypeptides was also reduced on preadsorption of antiserum with peptide. These species may have represented minor proteolytic fragments of higher molecular weight Kir6.2 channel complexes. Notably, staining of the 100 kDa species was unaffected by competing peptide suggesting that staining of this species was non-specific.

Immunodetection with both anti-SUR2A and SUR2B antisera always resulted in relatively complex staining patterns (Figure 4.9, lane 6 and 8). In particular, a distinct band of the predicted molecular weight was never observed but rather, multiple staining species of apparent molecular weights of approximately 140 kDa were often seen. Moreover, additional polypeptides of lower molecular weights were also stained. Most of the polypeptides were no longer stained after preadsorption of the antiserum with the appropriate immunising SUR2 C-terminal peptide suggesting that staining of the various species of different molecular size was specific. Staining of several polypeptides in the region of the predicted molecular weight (140 kDa), has

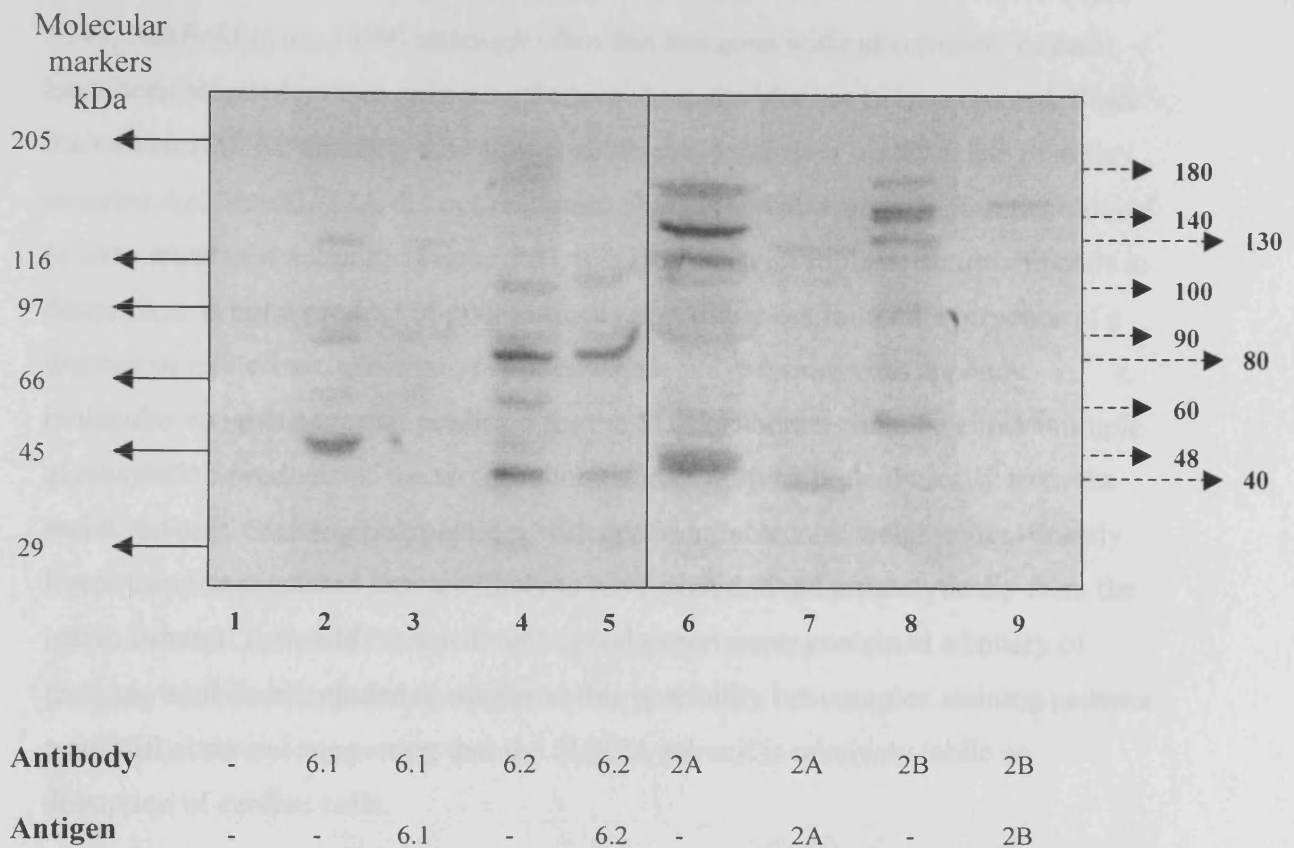


Figure 4.9 Immunoblot staining of isolated rat cardiac myocytes. Cardiac myocytes were lysed and membrane proteins (11 $\mu\text{g}/\text{lane}$) separated on 7.5 % PAGE, transferred electrophoretically to nitrocellulose followed by immunodetection with anti-Kir6.0 and anti-SUR2 antisera. Lane 1, membrane proteins transferred to nitrocellulose incubated with no primary antibody; lane 2, anti-Kir6.1 (1/250 dilution); lane 3, anti-Kir6.1(1/250 dilution) + Kir6.1 C-terminal peptide (10 $\mu\text{g}/\text{ml}$); lane 4, anti-Kir6.2 (1/250); lane 5, anti-Kir6.2(1/250 dilution) + Kir6.2 C-terminal peptide (10 $\mu\text{g}/\text{ml}$); lane 6, anti-SUR2A (1/250); lane 7, anti-SUR2A (1/250 dilution)+ SUR2A C-terminal peptide (10 $\mu\text{g}/\text{ml}$); lane 8, anti-SUR2B (1/250); lane 9, anti-SUR2B (1/250 dilution)+ SUR2B C-terminal peptide (10 $\mu\text{g}/\text{ml}$). Representative of five separate experiments ($n = 5$).

been seen in several other reports of SUR2 detection in Western blots (Giblen et al., 1999; Ashfield et al., 1999) although often this has gone without comment or data have been selected so that only a single band from the blot has been presented. Since the two anti-SUR2 antisera were shown not to recognise their highly related family member, i.e. anti-SUR2A did not recognise SUR2B and vice versa in immunoblots of *in vitro* expressed subunits (Figure 3.5), it is likely that multiple detection of bands in tissue blots is not a product of poor antibody specificity but rather the presence of a number of related antigenic polypeptides. Those polypeptides with apparent molecular weights near that predicted for the SUR2 subunits could be either multiple glycosylation products of the target subunit and/or derived proteolytically from the native subunit. Staining polypeptides with apparent molecular weights significantly lower than the predicted size are likely to have been derived proteolytically from the native subunit. It should be noted that several experiments contained a battery of protease inhibitors included to minimise this possibility but complex staining patterns were still observed suggesting that the SUR2A subunit is relatively labile on disruption of cardiac cells.

4.6. Preparation of Rat Heart Mitochondria Fractions

Immunocytochemistry experiments performed on rat cardiac myocytes displayed a significant correlation between the localisation of Kir6.1 antibody staining and the MitoFluor probe suggesting the presence Kir6.1 subunits in mitochondria (section 4.1). To examine this and to explore the possible mitochondrial localization of other K_{ATP} channel subunits, Western blots were performed on purified mitochondrial fractions.

Rat heart mitochondrial fractions were prepared using Percoll gradients according to the method described by Santos et al., (1998). The relative enrichment of the mitochondrial fraction prepared was compared with other subcellular fractions by measuring the activity of cytochrome oxidase (marker of the inner mitochondrial membrane) as described by Cooperstein et al., (1950). The specific activity of cytochrome oxidase ($\mu\text{moles substrate metabolised/min/mg}$) was greatest in the mitochondrial fraction compared to the other subcellular fractions (Table 4.5) with a least a six-fold enrichment in specific activity over the crude cell homogenate.

Sample	Enzyme activity ($\mu\text{moles/min}$)	Protein content determined by Bradford Assay (mg/ml)	Amount of protein used (mg)	Specific activity ($\mu\text{moles/min/mg}$)
Mitochondria fraction	25.05	1.16	0.023	1089
18-30 % fraction	18.6	1.379	0.027	689
Supernatant from mitochondrial fraction	19.6	5.04	0.1	196
Nuclear fraction	30.16	5.7	0.11	274
Rat heart homogenate	27	7.8	0.156	173

Table 4.5. Specific activity of cytochrome oxidase in subcellular fractions from rat heart mitochondria purification experiment

Western blots of subcellular fractions were probed with a polyclonal anti-cytochrome c antisera (1 $\mu\text{g/ml}$; Santa Cruz; H-104) to provide a second assessment of mitochondrial enrichment (Figure 4.10). Lower amounts of cytochrome c staining were detected in the homogenate, nuclear and 18-30 % interface fraction (Figure 4.10, lanes 1, 2 and 4), whereas no cytochrome c was found from the supernatant from the mitochondrial fraction (Figure 4.10, lane 3). Densitometry revealed 5-fold higher staining of the 12 kDa cytochrome c polypeptide in mitochondrial fractions compared to homogenate, indicative of a significant enrichment of this fraction.

To examine whether the mitochondrial fraction was essentially free from plasma membrane contamination, Western blots of subcellular fractions were probed with Concanavalin A (Con A; 1/2500) horseradish peroxidase conjugate (ICN; 153245). Con A is a lectin protein that binds to mannose moieties within the oligosaccharide modifications on glycoproteins and, thus is a useful plasma membrane marker in detecting glycosylated proteins. A number of polypeptides of 140, 104 and 60 kDa were detected in the supernatant recovered from mitochondrial pellet, suggesting that the supernatant was enriched with glycoproteins and that it contained possible plasma membrane and microsomal membrane fractions (Figure 4.11, lanes 3). Con A binding to glycopolypeptides was not observed in mitochondrial fractions (Figure 4.11, lane 5), but traces of polypeptides of 170 and 85 kDa were detected in nuclear and 18-30 % fraction (Figure 4.11, lanes 2 and 4). Horseradish peroxidase conjugate stained homogenate weakly (Figure 4.11, lane 1). The identity of the polypeptides were not investigated as this experiment was only carried out to determine the purity of mitochondrial fraction.

Results from the cytochrome oxidase assay and Western blots on subcellular fractions with anti-cytochrome c and Concanavalin A horseradish peroxidase showed that a rat mitochondrial fraction had been prepared that was enriched in cytochrome c oxidase activity and essentially free of plasma membrane and Golgi membrane. This fraction was used in immunoblots to examine the possible mitochondrial localization of Kir6.0 and SUR2 subunits.

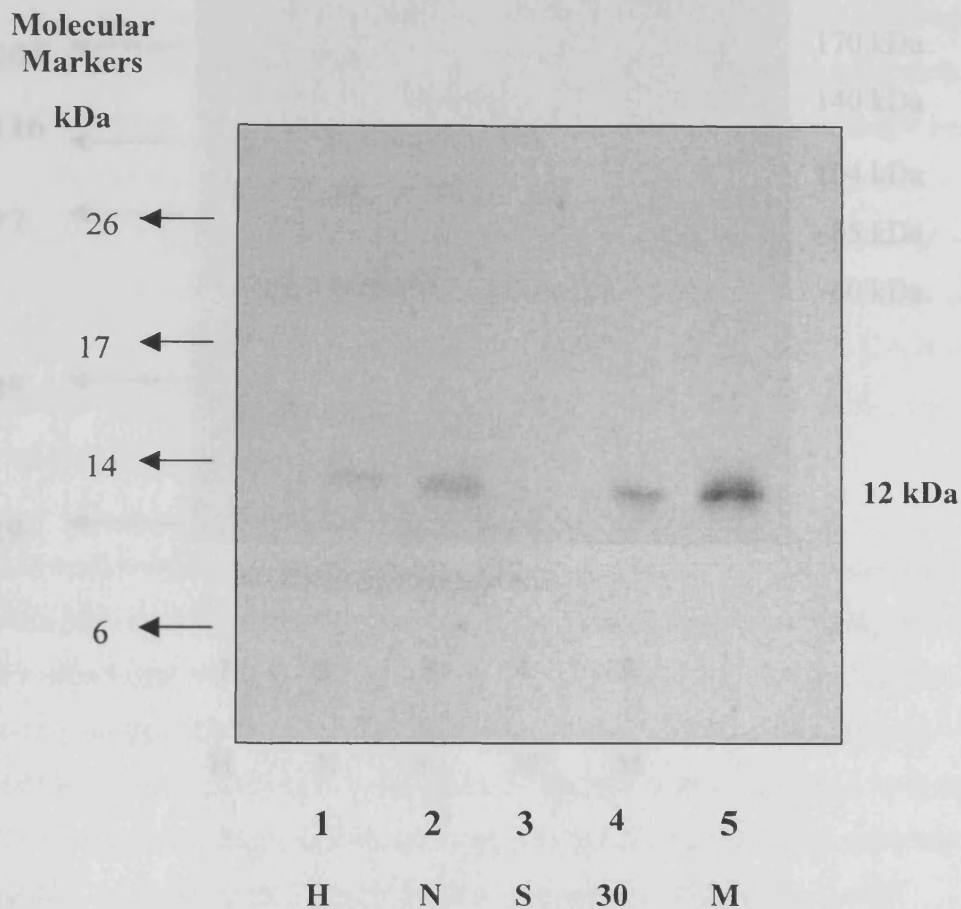


Figure 4.10 Immunoblot staining of a mitochondrial fraction isolated from rat heart to estimate enrichment. Subcellular fractions isolated from rat heart were separated on 14 % polyacrylamide gel and transferred to nitrocellulose membrane. The membrane was incubated with polyclonal anti-cytochrome c antibody (1 µg/ml). Lane 1, heart homogenate (H); lane 2, nuclear fraction (N); lane 3, supernatant recovered from mitochondria pellet (S); lane 4, 30-18 % Percoll interface fraction (30) and lane 5, mitochondrial fraction (M). Representative of two separate experiments (n = 2).

Figure 4.10 Immunoblot staining of a mitochondrial fraction isolated from rat heart to estimate enrichment. Subcellular fractions isolated from rat heart were separated on 14 % polyacrylamide gel and transferred to nitrocellulose membrane. The membrane was incubated with polyclonal anti-cytochrome c antibody (1 µg/ml). Lane 1, heart homogenate (H); lane 2, nuclear fraction (N); lane 3, supernatant recovered from mitochondria pellet (S); lane 4, 30-18 % Percoll interface fraction (30) and lane 5, mitochondrial fraction (M). Representative of two separate experiments (n = 2).

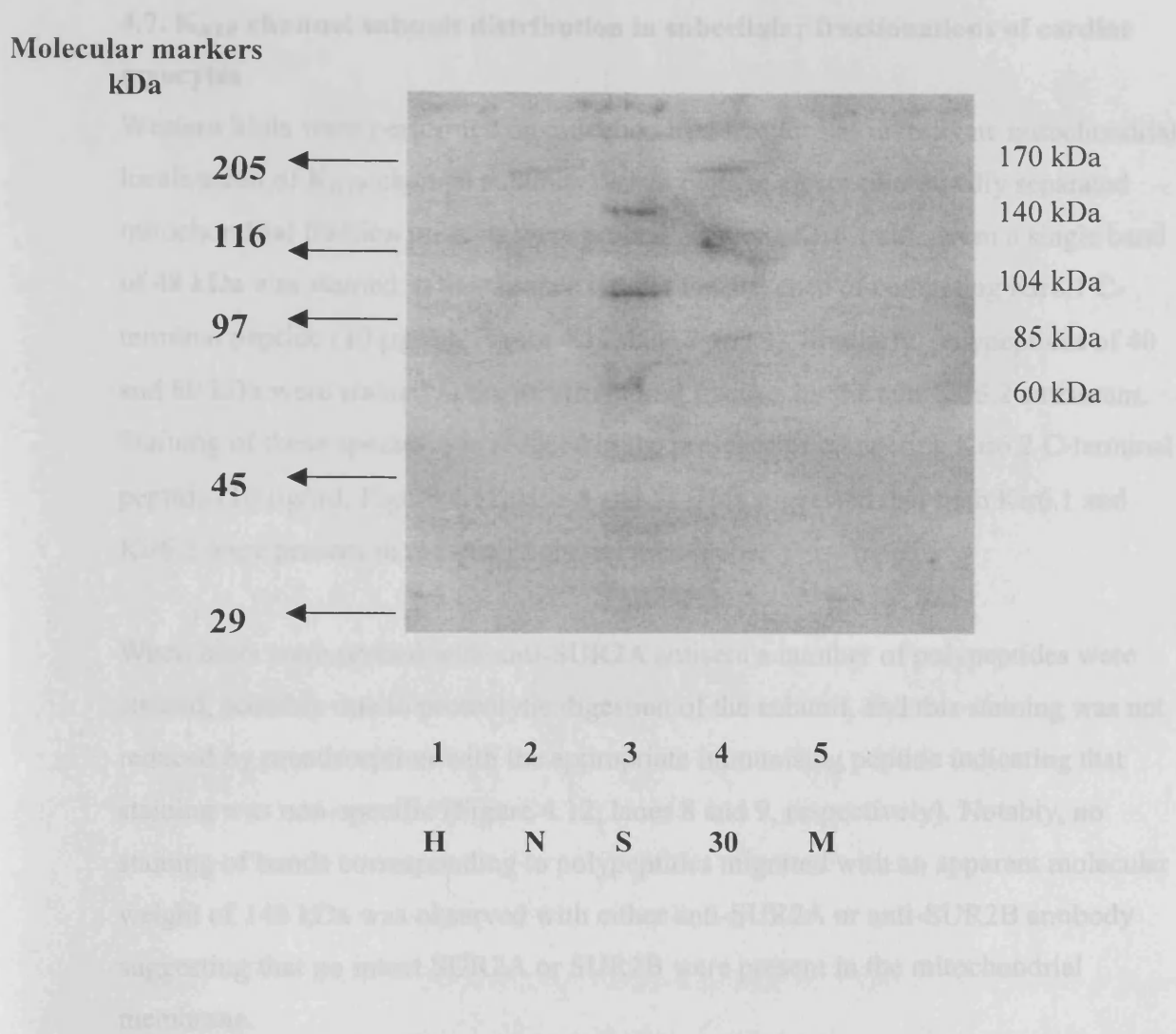


Figure 4.11. Immunoblot staining of a mitochondrial fraction isolated from rat heart with concanavalin A horseradish peroxidase conjugate to estimate enrichment. Subcellular fractions isolated from rat heart were separated on 7.5 % polyacrylamide gels and transferred to nitrocellulose membrane. The membrane was incubated with concanavalin A horseradish peroxidase (1/250). Lane 1, heart homogenate (H); lane 2, nuclear fraction (N); lane 3, supernatant recovered from mitochondrial pellet (S); lane 4, 30-18 % Percoll interface fraction (30) and lane 5, mitochondrial fraction (M). Representative of three experiments ($n = 3$).

4.7. K_{ATP} channel subunit distribution in subcellular fractionations of cardiac myocytes

Western blots were performed on mitochondrial fractions to investigate mitochondrial localization of K_{ATP} channel subunits. When blots of electrophoretically separated mitochondrial fraction proteins were probed with anti-Kir6.1 antiserum a single band of 48 kDa was stained in the absence but not the presence of competing Kir6.1 C-terminal peptide (10 μ g/ml, Figure 4.12, lane 2 and 3). Similarly, polypeptides of 40 and 80 kDa were stained in the mitochondrial fraction by the anti-Kir6.2 antiserum. Staining of these species was reduced in the presence of competing Kir6.2 C-terminal peptide (10 μ g/ml, Figure 4.12, lane 4 and 5). This suggested that both Kir6.1 and Kir6.2 were present in the mitochondrial membrane.

When blots were probed with anti-SUR2A antisera a number of polypeptides were stained, possibly due to proteolytic digestion of the subunit, and this staining was not reduced by preadsorption with the appropriate immunising peptide indicating that staining was non-specific (Figure 4.12, lanes 8 and 9, respectively). Notably, no staining of bands corresponding to polypeptides migrated with an apparent molecular weight of 140 kDa was observed with either anti-SUR2A or anti-SUR2B antibody suggesting that no intact SUR2A or SUR2B were present in the mitochondrial membrane.

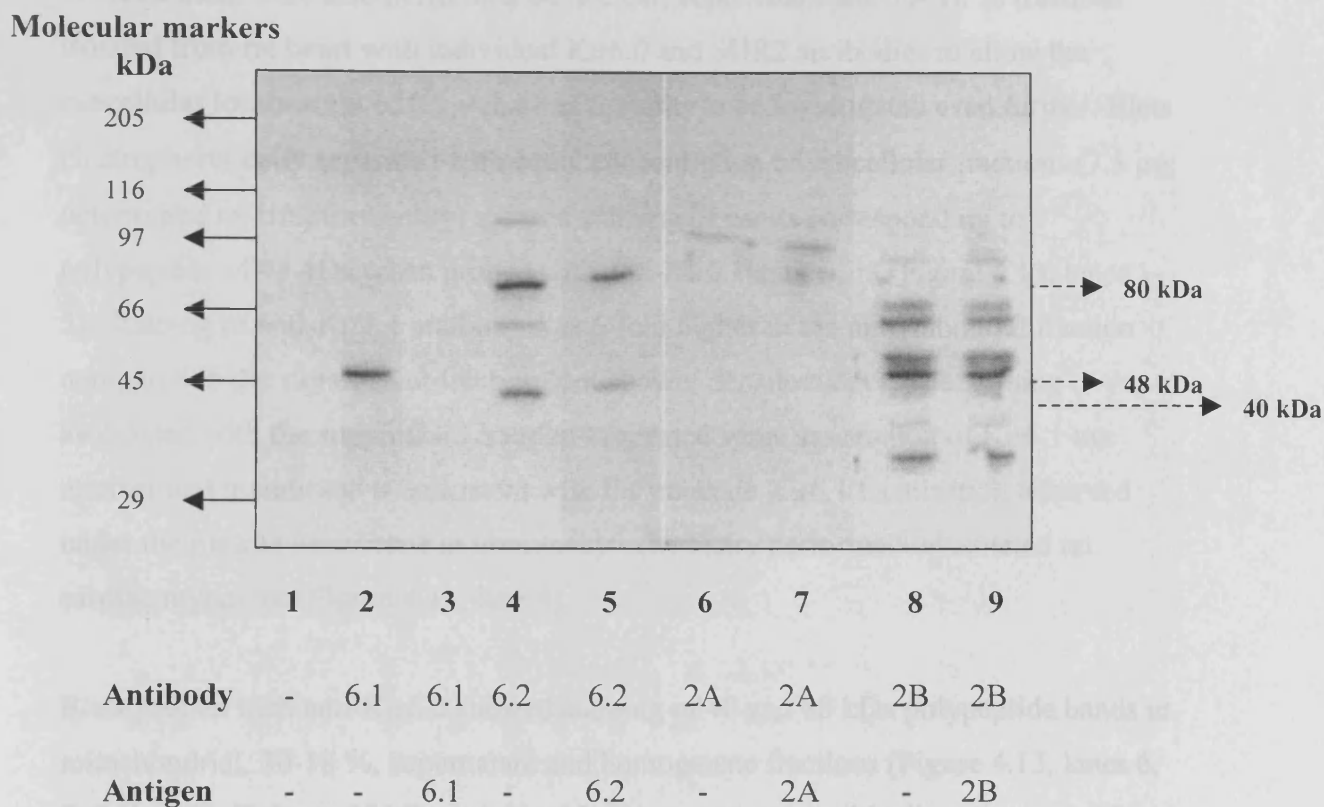


Figure 4.12 Immunoblot staining of mitochondrial fraction isolated from rat heart with anti-Kir6.0 and anti-SUR2 antibodies. Mitochondrial fraction was purified as described in Materials and Methods and separated on 7.5 % PAGE transferred to nitrocellulose and probed with anti-Kir6.0 and SUR2 antibodies. Lane 1, no primary antibody; lane 2, anti-Kir6.1 (1/250); lane 3, anti-Kir6.1 (1/250 dilution) + Kir6.1 C-terminal peptide (10 µg/ml); lane 4, anti-Kir6.2 (1/250); lane 5, anti-Kir6.2 (1/250) + Kir6.2 C-terminal peptide (10 µg/ml); lane 6, anti-SUR2A (1/250); lane 7, anti-SUR2A (1/250) + SUR2A C-terminal peptide (10 µg/ml); lane 8, anti-SUR2B (1/250); lane 9, anti-SUR2B (1/250) + SUR2B C-terminal peptide (10 µg/ml). Representative experiments (n = 4).

Western blots were also performed on nuclear, supernatant and 30- 18 % fractions isolated from rat heart with individual Kir6.0 and SUR2 antibodies to allow the subcellular localisation of K_{ATP} channel subunits to be investigated even further. Blots electrophoretically separated with equal concentration of subcellular fractions (7.5 µg; determined by Bradford assay) showed staining of bands corresponding to polypeptide of 48 kDa when probed with anti-Kir6.1 antiserum (Figure 4.13, lanes 1-5). Staining of anti-Kir6.1 antibody was 6-fold higher in the mitochondrial fraction compared to the supernatant fraction (not shown; densitometry). The staining associated with the supernatant fraction suggested some association of Kir6.1 to microsomal membrane is consistent with the punctate Kir6.1 localization observed under the plasma membrane in immunocytochemistry performed on isolated rat cardiac myocytes (Figure 4.13, lane 4).

Blots probed with anti-Kir6.2 showed staining of 40 and 80 kDa polypeptide bands in mitochondrial, 30-18 %, supernatant and homogenate fractions (Figure 4.13, lanes 6, 7, 9 and 10). Only an 80 kDa polypeptide, representing possible dimerization of the Kir6.2 polypeptide, was detected in the nuclear fraction (Figure 4.13, lane 8).

Densitometry revealed equal staining intensity of 40 and 80 kDa polypeptides in the supernatant and mitochondrial fraction, confirming the localization of Kir6.2 subunit on sarcolemma and mitochondrial membrane, respectively. This result was consistent with immunocytochemical experiments in which distribution of Kir6.2 (immunofluorescence associated with anti-Kir6.2 antibody binding using a low dilution; 1/250 dilution) in sarcolemma and mitochondria was observed (section 4.2).

Non-specific staining of polypeptide bands was observed in subcellular fractions when probed with either anti-SUR2A or SUR2B antibody probably due to proteolytic digestion of native subunits (Figure 4.13, lanes 11-20), however a 140 kDa polypeptide was stained in supernatant fraction (containing microsomal membranes) when probed with anti-SUR2A antiserum, which was consistent with the localization of SUR2A on sarcolemma observed in immunocytochemical experiments (Figure 4.13, lane 14). A trace of polypeptide of 140 kDa was also observed in supernatant fraction when probed with anti-SUR2B antiserum (Figure 4.13, lane 19), suggesting localization of SUR2B microsomal membrane.

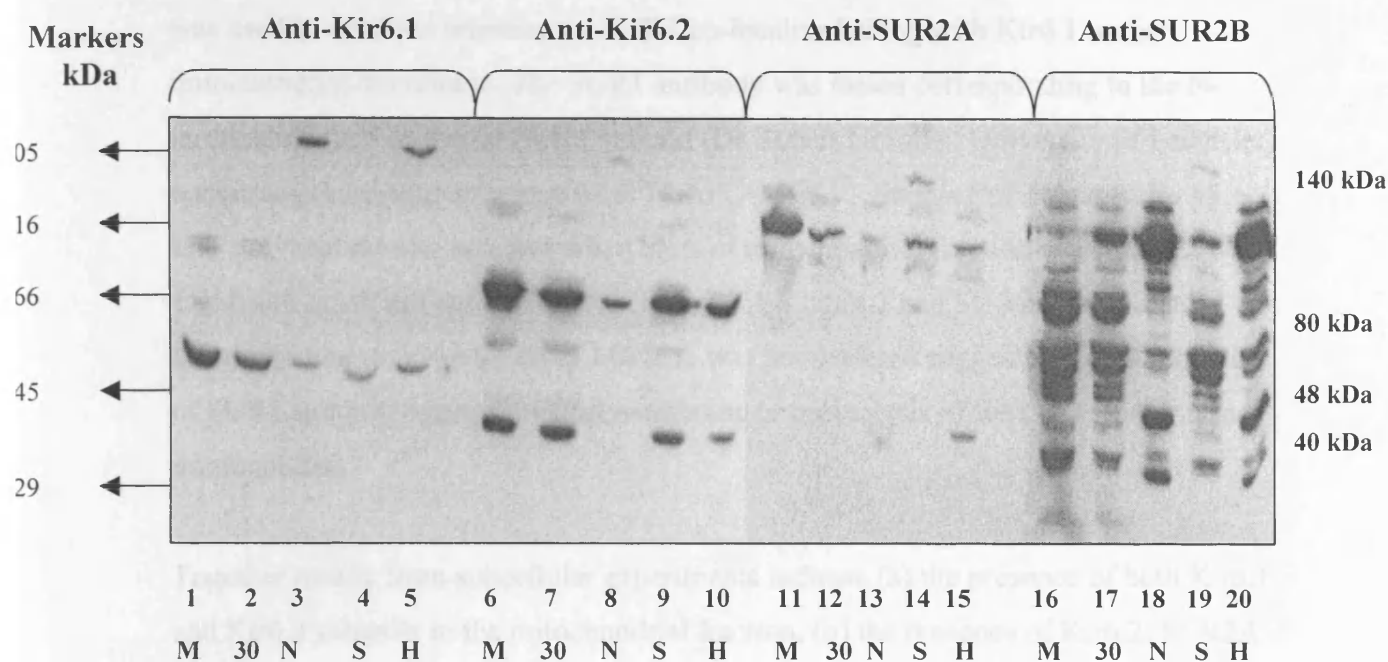


Figure 4.13 Immunoblot staining of subcellular fractions isolated from rat heart using anti-Kir6.0 and SUR2 antibodies. Subcellular fractions (11 μ g protein) were separated on 7.5% PAGE transferred to nitrocellulose and probed with anti-Kir6.0 and SUR2 antibodies. Lanes 1-5 contains mitochondrial (M), 18-30 % (30), nuclear (N), supernatant (S) and homogenate (H). Blots probed with anti-Kir6.1 antibody (1/250); lane 6-10, blots probed with anti-Kir6.2 (1/250); lane 11-15, blots probed with anti-SUR2A (1/250); lane 16-20, blots probed with anti-SUR2B (1/250). Representative experiments ($n = 3$).

Since neither distinct SUR2A nor SUR2B polypeptides were detected in Western blots performed on mitochondrial fractions using anti-SUR2, an anti-SUR1 antibody was used to examine whether the SUR1 co-localized along with Kir6.1 to the mitochondrial membrane. The SUR1 antibody was raised corresponding to the N-terminal domain of the rat SUR1 subunit (Dr Robert Norman; University of Leicester) containing the amino acid sequence ²PLAFCGTEK¹⁰. Staining of non-specific 45 kDa polypeptide was detected when blots of mitochondrial fraction were probed with 1/250 and 1/500 diluted anti-SUR1 (Figure 4.14, lanes 2 and 3), whereas a band corresponding to polypeptide of 140 kDa was not detected suggesting no localization of SUR1 subunit to mitochondrial membrane or proteolysis of the native subunit in immunoblots.

Together results from subcellular experiments indicate (a) the presence of both Kir6.1 and Kir6.2 subunits in the mitochondrial fraction, (b) the presence of Kir6.2, SUR2A, SUR2B and traces of Kir6.1 in the microsomal membrane fraction prepared from rat heart but there was no strong evidence of the presence of any of the three SUR probed subunits (SUR1/2A/2B) in mitochondrial fraction.

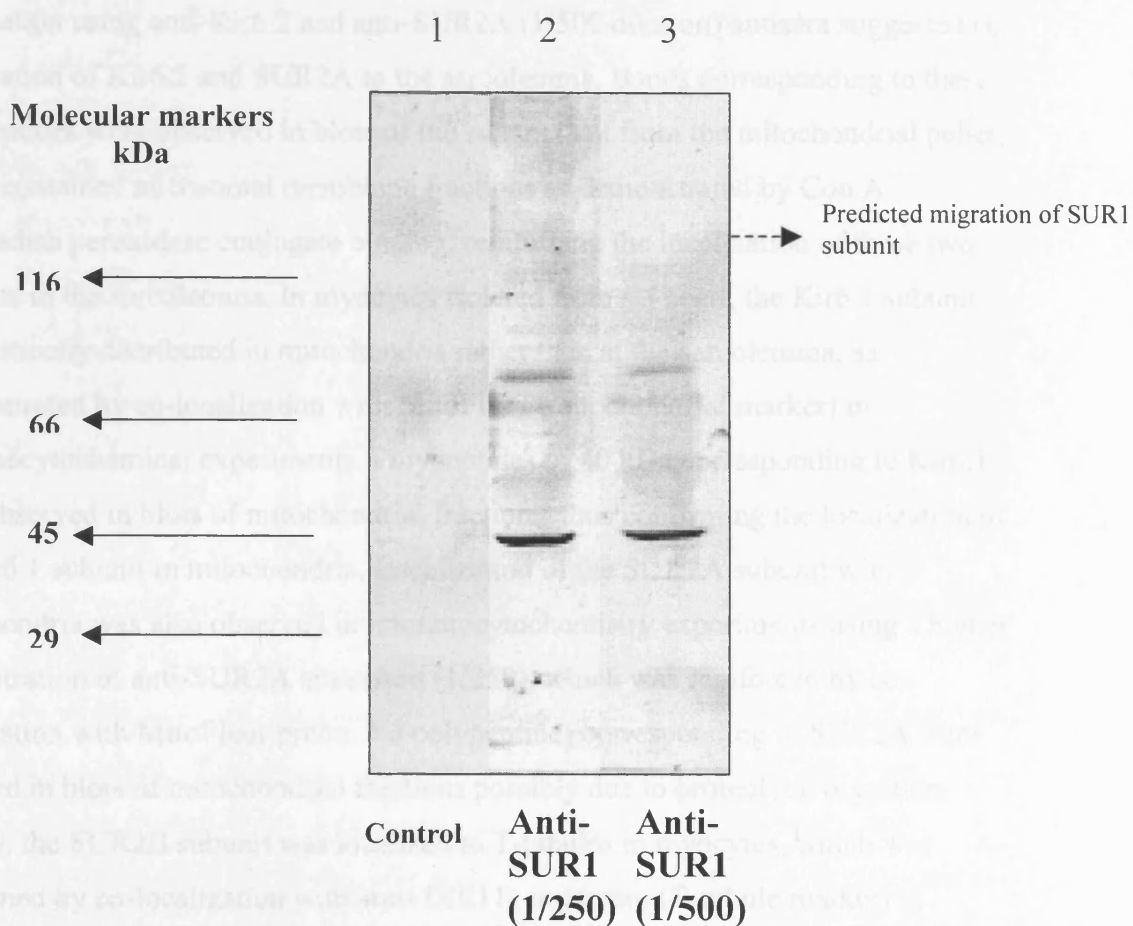


Figure 4.14 Western blot of mitochondrial fraction isolated from rat heart using anti-SUR1 antibody. Mitochondrial fraction was separated on 7.5% PAGE transferred to nitrocellulose and probed with anti-SUR1 antibody. Lane 1 contained mitochondrial fraction probed with no primary antibody; lane 2, mitochondrial fraction probed with anti-SUR1 antibody (1/250); lane 3, mitochondrial fraction probed with anti-SUR1 (1/500). (n = 2).

4.8 Summary

Immunocytochemistry and Western blots on isolated rat cardiac myocytes demonstrated the presence of all four K_{ATP} channel subunits, i.e. Kir6.1, Kir6.2, SUR2A and SUR2B in ventricular myocytes. In myocytes, immunocytochemical localization using anti-Kir6.2 and anti-SUR2A (1/500 dilution) antisera suggested co-localization of Kir6.2 and SUR2A to the sarcolemma. Bands corresponding to these polypeptides were observed in blots of the supernatant from the mitochondrial pellet, which contained microsomal membrane fractions as demonstrated by Con A horseradish peroxidase conjugate binding, reinforcing the localization of these two subunits in the sarcolemma. In myocytes isolated from rat heart, the Kir6.1 subunit was distinctly distributed in mitochondria rather than at the sarcolemma, as demonstrated by co-localization with MitoFluor (mitochondrial marker) in immunocytochemical experiments. Polypeptides of 40 kDa corresponding to Kir6.1 were observed in blots of mitochondrial fractions, thus confirming the localization of the Kir6.1 subunit in mitochondria. Localization of the SUR2A subunit with mitochondria was also observed in immunocytochemistry experiments using a higher concentration of anti-SUR2A antiserum (1/250), which was reinforced by co-localization with MitoFluor probe. No polypeptides corresponding to SUR2A were detected in blots of mitochondrial fractions possibly due to proteolytic digestion. Finally, the SUR2B subunit was localized to T-tubules in myocytes, which was confirmed by co-localization with anti- IXE11₂ antiserum (T-tubule marker) in immunocytochemistry experiments. Traces of bands corresponding to SUR2B were detected in blots of microsomal membrane fractions but none in mitochondrial fractions.

Chapter 5: Phosphorylation of Kir6.0 and SUR2 K_{ATP} channel subunits

The modulation of cardiac K_{ATP} channel activity by PKC-mediated phosphorylation is thought to be one of the many effectors of ischaemic preconditioning in the heart (see section 1.13). The K_{ATP} channel subunit (s) involved in PKC-mediated phosphorylation during IP in native tissue still remains to be investigated. The aim of this study was to identify possible physiological relevant site (s) of PKC phosphorylation within the K_{ATP} subunit (s). Bèguin et al., (1999) and Light et al., (2000) have demonstrated previously that PKA and PKC-mediated phosphorylation of the Kir6.2 subunit, rather than the SUR subunit may modulate recombinant Kir6.2/SUR1 and Kir6.2/SUR2A channels, respectively. In this study initial experiments were designed to challenge *in vitro* expressed Kir6.0 polypeptides with PKA and PKC to establish whether the Kir6.1 is a substrate for these kinases in addition to Kir6.2. To determine cardiac K_{ATP} subunit phosphorylation events in native tissue, experiments were constructed where isolated rat ventricular myocytes were challenged with PKA and PKC activators (forskolin and adenosine, respectively) followed by immunoprecipitation with the characterized anti-Kir6.0 and anti-SUR2 antisera. Two-dimensional chromatographic analysis of thin-layer cellulose plates loaded with tryptic digest polypeptide experiments and mass sequencing of phosphorylated peptides derived from tryptic digest were designed to identify possible phosphorylated site (s) within *in vitro* and *in vivo* K_{ATP} channel subunit (s). Mutants of possible phosphorylation site (s) were constructed using site-directed mutagenesis experiments, which were expressed and subjected to *in vitro* phosphorylation.

5.1 *In vitro* phosphorylation of expressed Kir6.1 and Kir6.2 subunits.

Whether Kir6.1 and Kir6.2 are substrates for phosphorylation by PKA and PKC was investigated in *in vitro* reactions using *in vitro* expressed Kir6.1 and Kir6.2 subunit polypeptides and exogenous PKA and PKC in the presence of [γ ³²P]-ATP. A 48 kDa polypeptide was the major substrate for phosphorylation in *in vitro* expressed Kir6.1 reactions stimulated with exogenous PKA (4 μ g/ μ l) and PKC (3.5 μ g/ μ l; Figure 5.1, Lanes 2, and 3, respectively). A negative control Kir6.1 reaction contained the PKA

assay components (0.37 MBq [γ -³²P] ATP, 100 μ M ATP, 50 mM Tris-HCl pH 7.5) in the absence of added kinase (Figure 5.1, lane 1).

When *in vitro* expressed Kir6.2 was used as substrate for PKA-mediated phosphorylation a 40 kDa polypeptide was phosphorylated (Figure 5.1, lane 5). No phosphorylation of a polypeptide of molecular weight consistent with that of *in vitro* expressed Kir6.2 polypeptide was observed in the PKC assay (Figure 5.1, lanes 4).

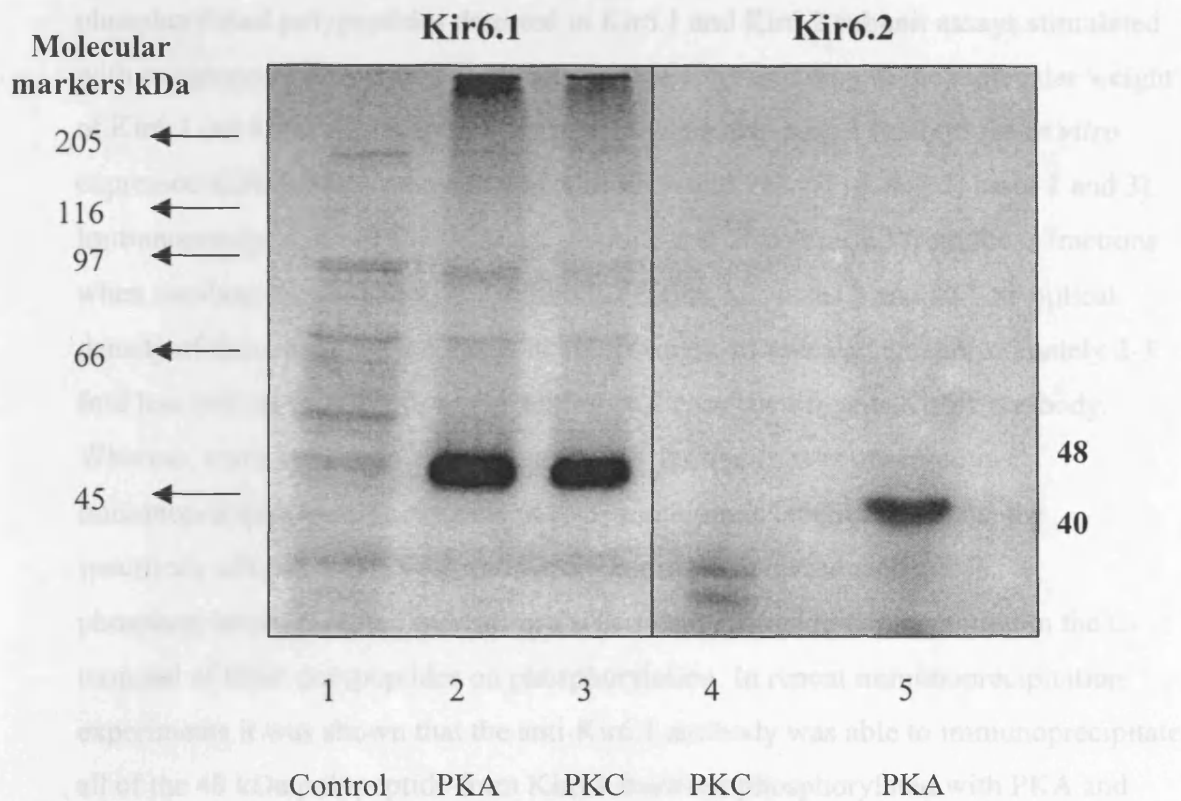


Figure 5.1. Phosphorylation of *in vitro* transcribed/translated Kir6.1 and Kir6.2 polypeptides. Lanes 1-5 represent electrophoresis on a 7.5% polyacrylamide gel of Kir6.0 fractions phosphorylated in the absence or presence of PKA and PKC in the presence of [γ^{32} P]-ATP. Lane 1, Kir6.1 fraction with no added kinase; lane 2, Kir6.1 with PKA (4 μg/μl); lane 3, Kir6.1 fraction with PKC (3.5 μg/μl); lane 4, Kir6.2 with PKA (4 μg/μl); and lane 5, Kir6.2 with PKC (3.5 μg/μl). Rrepresentative of 3 similar experiments.

Immunoprecipitation experiments were employed to confirm the specificity of phosphorylated polypeptides detected in Kir6.1 and Kir6.2 subunit assays stimulated with exogenous PKA and PKC. A polypeptide corresponding to the molecular weight of Kir6.1 (48 kDa) was immunoprecipitated using anti-Kir6.1 antibody in *in vitro* expressed Kir6.1 fractions incubated with PKA and PKC (Figure 5.2, lanes 1 and 3). Immunoprecipitation of a 48 kDa polypeptide was also detected from these fractions when incubated with anti-Kir6.2 antibody (Figure 5.2, lanes 2 and 4). The optical density of these polypeptide bands in autoradiograms revealed an approximately 2-3 fold less immunoprecipitation with anti-Kir6.2 compared to anti-Kir6.1 antibody. Whereas, complete specificity of anti-Kir6.0 antibodies was observed in immunoprecipitation experiments of [³⁵S]-methionine labelled subunits, the specificity of both anti-Kir6.1 and Kir6.2 appeared to be reduced after phosphorylation, possibly indicating a significant change in conformation in the C-terminal of these polypeptides on phosphorylation. In repeat immunoprecipitation experiments it was shown that the anti-Kir6.1 antibody was able to immunoprecipitate all of the 48 kDa polypeptide from Kir6.1 fractions phosphorylated with PKA and PKC, as repeat incubation of these fractions (supernatant extracted from the previous immunoprecipitated experiment) with anti-Kir6.1 antibody precipitated no further 48 kDa polypeptide. On the other hand repeat incubation of anti-Kir6.2 antibody with phosphorylated fractions was able to immunoprecipitate equal amounts of polypeptide as reported in the previous immunoprecipitation experiment suggesting low affinity interaction of the anti-Kir6.2 antibody.

A phospho-polypeptide of 40kDa corresponding to Kir6.2 (Figure 5.2, lane 6) was immunoprecipitated from Kir6.2 fraction after phosphorylation in the presence of PKA. Similarly, the non-specific antibody, anti-Kir6.1, was also able to immunoprecipitate the 40 kDa polypeptide, but only half of the amount compared to anti-Kir6.2 antibody (Figure 5.2, lane 5).

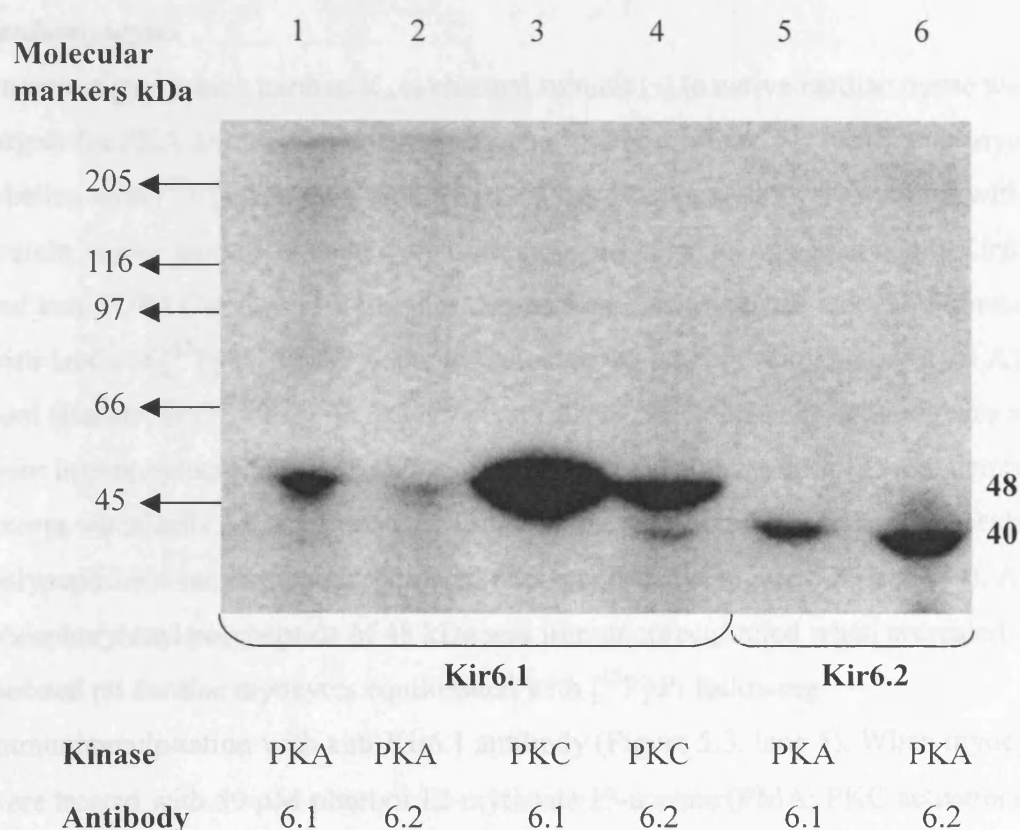


Figure 5.2. Immunoprecipitation of *in vitro* phosphorylated Kir6.1 and Kir6.2 protein. Lanes 1-6 represent SDS-PAGE electrophoresis of phosphorylated Kir6.0 fractions on a 7.5% polyacrylamide gel after immunoprecipitation with anti-Kir6.0 antibody (1/250 dilution). Lane 1, PKA stimulated Kir6.1 fraction immunoprecipitated with anti-Kir6.1; lane 2, PKA stimulated Kir6.1 fraction immunoprecipitated with anti-Kir6.2; lane 3 and 4, PKC stimulated Kir6.1 fraction immunoprecipitated with anti-Kir6.1 and Kir6.2 antibody, respectively; lane 5 and 6, PKA stimulated Kir6.2 fraction immunoprecipitated with anti-Kir6.1 and anti-Kir6.2 antibody, respectively. Representative of three separate experiments ($n = 3$).

5.2 *In vivo* phosphorylation of Kir6.0 and SUR2 subunits in isolated rat cardiomyocytes.

To investigate which cardiac K_{ATP} channel subunit (s) in native cardiac tissue were targets for PKA and PKC-mediated phosphorylation, isolated rat ventricular myocytes labelled with [³²P] orthophosphate ([³²P] Pi) were challenged for 30 minutes with protein kinase modulators and were immunoprecipitated using specific anti-Kir6.0 and anti-SUR2 C-terminal antibodies. Isolated cardiac myocytes were equilibrated with 1mCi of [³²P]-Pi for 2-3 hours to radioactively label the cardiac myocyte ATP pool (Hardie, D.G., 1993). In negative controls, in which primary antibody was absent from immunoprecipitation reactions, no phosphorylated polypeptides were detected, except when cells were stimulated with forskolin where a number of phosphorylated polypeptides were immunoprecipitated non-specifically (Figure 5.3, lane 1-4). A phosphorylated polypeptide of 48 kDa was immunoprecipitated when untreated isolated rat cardiac myocytes equilibrated with [³²P] Pi following immunoprecipitation with anti-Kir6.1 antibody (Figure 5.3, lane 5). When myocytes were treated with 50 μM phorbol 12-myristate 13-acetate (PMA; PKC activator), 1 mM adenosine (PKC activator) and 100 μM forskolin (PKA activator) phosphorylation of this polypeptide was increased (Figure 5.3, lanes 6, 7 and 8). In addition to the Kir6.1 polypeptide, a number of other phosphorylated polypeptides were observed in the forskolin immunoprecipitate. The additional polypeptides were considered to have been immunoprecipitated non-specifically as they were also observed when control immunoprecipitates reacting no primary antibody were conducted (Figure 5.3, lane 4) after stimulation with forskolin.

No evidence was found for phosphorylation of Kir6.2 or SUR2B in unstimulated ³²P-labelled rat cardiac myocytes or in myocytes stimulated with PMA, adenosine and forskolin (Figure 5.3, lanes 9-12 and 17-20, respectively). Immunoprecipitation of cell extract from ³²P-labelled cardiac myocytes with anti-SUR2A antibodies immunoprecipitated phosphorylated polypeptide of 48kDa corresponding to Kir6.1 from unstimulated and PMA, adenosine and forskolin-stimulated myocytes (Figure 5.3, lanes 13, 14, 15 and 16, respectively) suggesting association of the SUR2A subunit with Kir6.1.

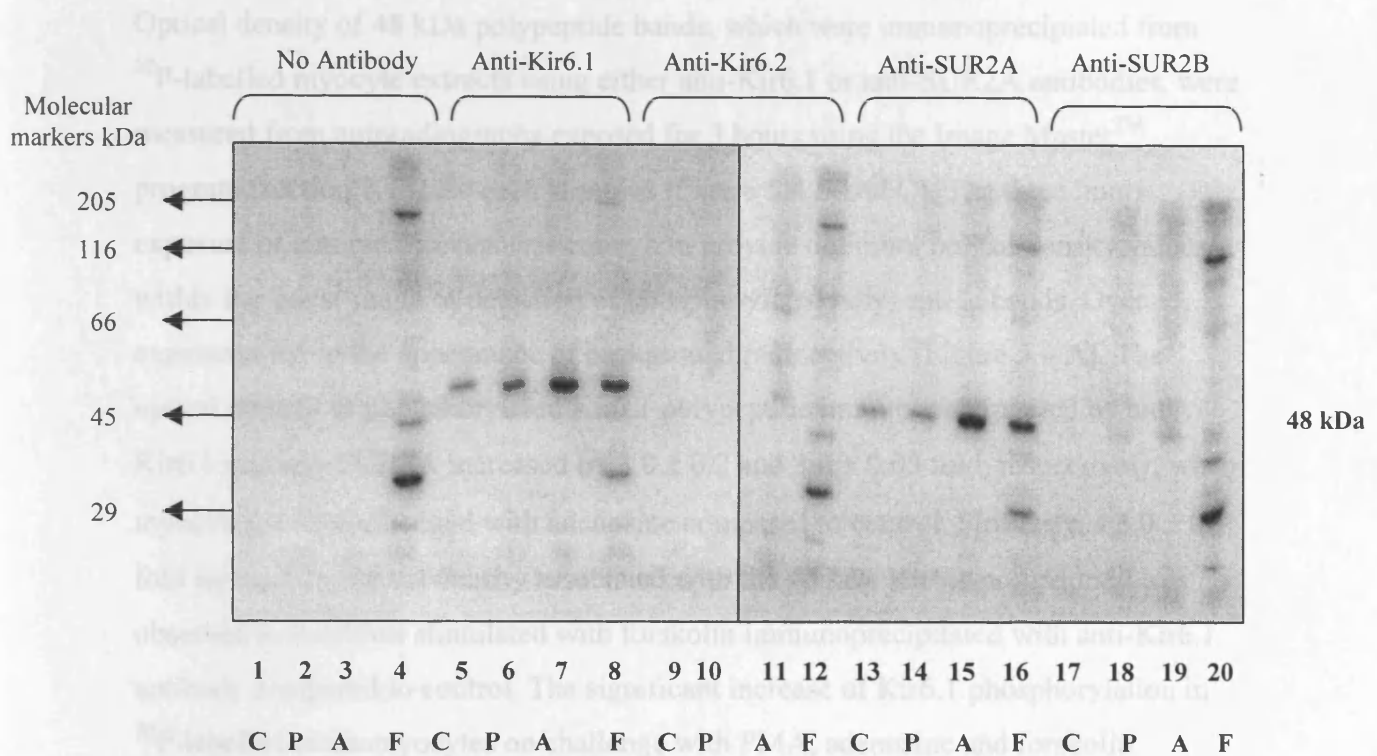
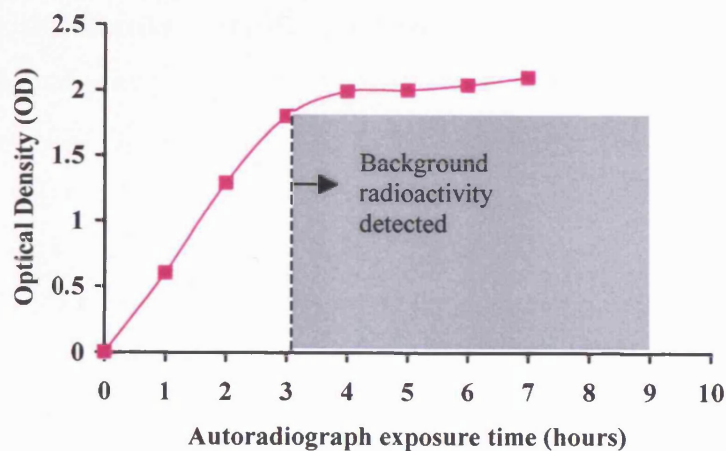


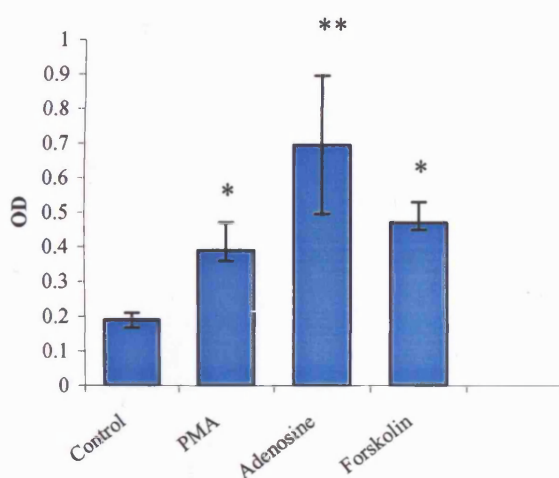
Figure 5.3 Immunoprecipitation of *in vivo* phosphorylated rat isolated cardiac myocytes. Lanes 1-20 represent immunoprecipitation of polypeptides from extracts of ³²P-labelled cardiac myocytes by anti-Kir6.0 and anti-SUR2 antibodies that were either unstimulated (C) or stimulated with 50 μM PMA (P), 1mM adenosine (A) and 100 μM forskolin (F) for 30 minutes. Lanes 1-4, immunoprecipitation of ³²P-labelled polypeptides from unstimulated cells in the absence of primary antibody (C), PMA (P), Adenosine (A) and Forskolin (F), respectively; lanes 5-8, immunoprecipitation of ³²P-labelled polypeptides with anti-Kir6.1 antibody from C, P, A and F reactions, respectively; lanes 8-12, immunoprecipitation of ³²P-labelled polypeptides with anti-Kir6.2 antibody from C, P, A and F, respectively; lanes 13-16, immunoprecipitation of ³²P-labelled polypeptides with anti-SUR2A antibody from C, P, A and F, respectively; lanes 17-20, immunoprecipitation of ³²P-labelled polypeptides with anti-SUR2B antibody from C, P, A and F reactions, respectively. Representative of 3 similar experiments (n = 3).

Optical density of 48 kDa polypeptide bands, which were immunoprecipitated from ³²P-labelled myocyte extracts using either anti-Kir6.1 or anti-SUR2A antibodies, were measured from autoradiographs exposed for 3 hours using the Image Master™ program (section 2.18) for each stimulus (Figure 5.4 B and C). The three hours exposure of autoradiographs was enough to provide optimum optical density values within the linear range of detection of phosphorylated polypeptide bands. Over exposures led to the appearance of background radioactivity (Figure 5.4 A). The optical density of phosphorylated Kir6.1 polypeptide immunoprecipitated by anti-Kir6.1 and anti-SUR2A increased by 3.0 ± 0.2 and 3.0 ± 0.05 fold, respectively, when myocytes were challenged with adenosine compared to control. Similarly, a 5.0 ± 0.1 fold increase in optical density associated with the 48 kDa Kir6.1 polypeptide was observed in reactions stimulated with forskolin immunoprecipitated with anti-Kir6.1 antibody compared to control. The significant increase of Kir6.1 phosphorylation in ³²P-labelled cardiomyocytes on challenge with PMA, adenosine and forskolin compared to basal phosphorylation was shown to be statistically significant (Figure 5.4 B and C; unpaired Student's T-test with Bonferroni correction).

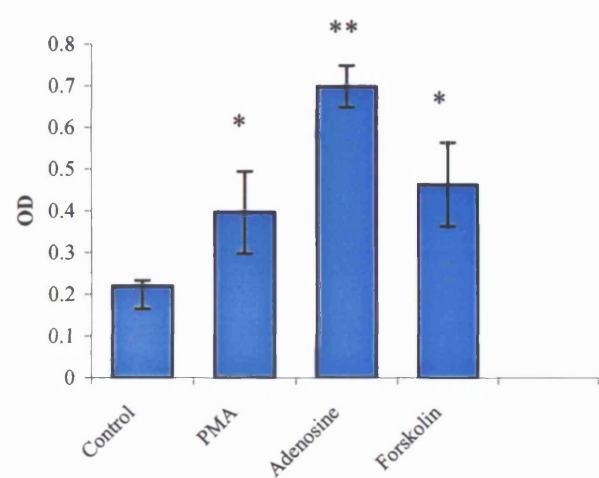
Overall these results show that the Kir6.1 subunit in isolated cardiac myocytes is the predominant target K_{ATP} channel subunit for both PKA and PKC-mediated phosphorylation.



A



B



C

Figure 5.4 A) Optical density from autoradiographs of phosphorylated Kir6.1 polypeptide bands immunoprecipitated from ³²P-labelled myocytes stimulated with adenosine against different autoradiograph exposure times.

B) and C) Optical density from autoradiographs of phosphorylated Kir6.1 polypeptides immunoprecipitated with anti-Kir6.1 and anti-SUR2A antibody, respectively. Experiments were conducted as in Figure 5.3 and optical density values were measured of phosphorylated Kir6.1 polypeptides using Image MasterTM program (Pharmacia Biotech) from autoradiographs that were exposed for 3 hours. (n = 3). Statistical significance was tested using the unpaired t-test with Bonferroni multi-comparison correction against the control reaction. p < 0.01*, p < 0.001**.

5.3. Dependence on adenosine concentration of *in vivo* phosphorylation of the Kir6.1 subunit in isolated rat cardiac myocytes.

The concentration of adenosine (1 mM) used to stimulate phosphorylation of Kir6.1 subunit in initial experiments on isolated rat cardiomyocytes was much higher than the concentration (10 μ M) that triggers changes in K_{ATP} channel activity (Lawrence et al., 1999) and ischaemic preconditioning in the heart (Liu et al., 1991; Thornton et al., 1992). Thus, concentrations of adenosine ranging from 1 μ M to 1 mM were used to stimulate ³²P-labelled isolated rat cardiac myocytes to determine the concentration dependence of Kir6.1 polypeptide phosphorylation. Isolated rat cardiac myocytes labelled with [³²P] orthophosphate were challenged with 1 μ M, 10 μ M, 100 μ M, 500 μ M and 1 mM adenosine and immunoprecipitated with anti-Kir6.1 antibody (Figure 5.5-A). Phosphorylation of the Kir6.1 polypeptide was observed in all the reactions including some basal phosphorylation in the control reaction.

The level of phosphorylation of immunoprecipitated and electrophoretically separated Kir6.1 polypeptides were quantified by densitometry of autoradiograph exposed for 3 hours (Figure 5.5-B). Basal phosphorylation of the Kir6.1 polypeptide band determined in unstimulated myocytes was nominated as background phosphorylation (Figure 5.5-B). The highest optical density of phosphorylated Kir6.1 polypeptides was recorded in reactions stimulated with 10 μ M adenosine with a 4 ± 0.05 fold increase of phosphorylation compared to background phosphorylation (Figure 5.5-B). Phosphorylation of the Kir6.1 subunit was still over background but lower than that of 10 μ M adenosine level in reactions stimulated with 1 μ M, 100 μ M, 500 μ M, and 1 mM adenosine.

This experiment suggests that maximum phosphorylation of the Kir6.1 polypeptide in isolated rat cardiac myocytes is observed in the presence of 10 μ M adenosine.

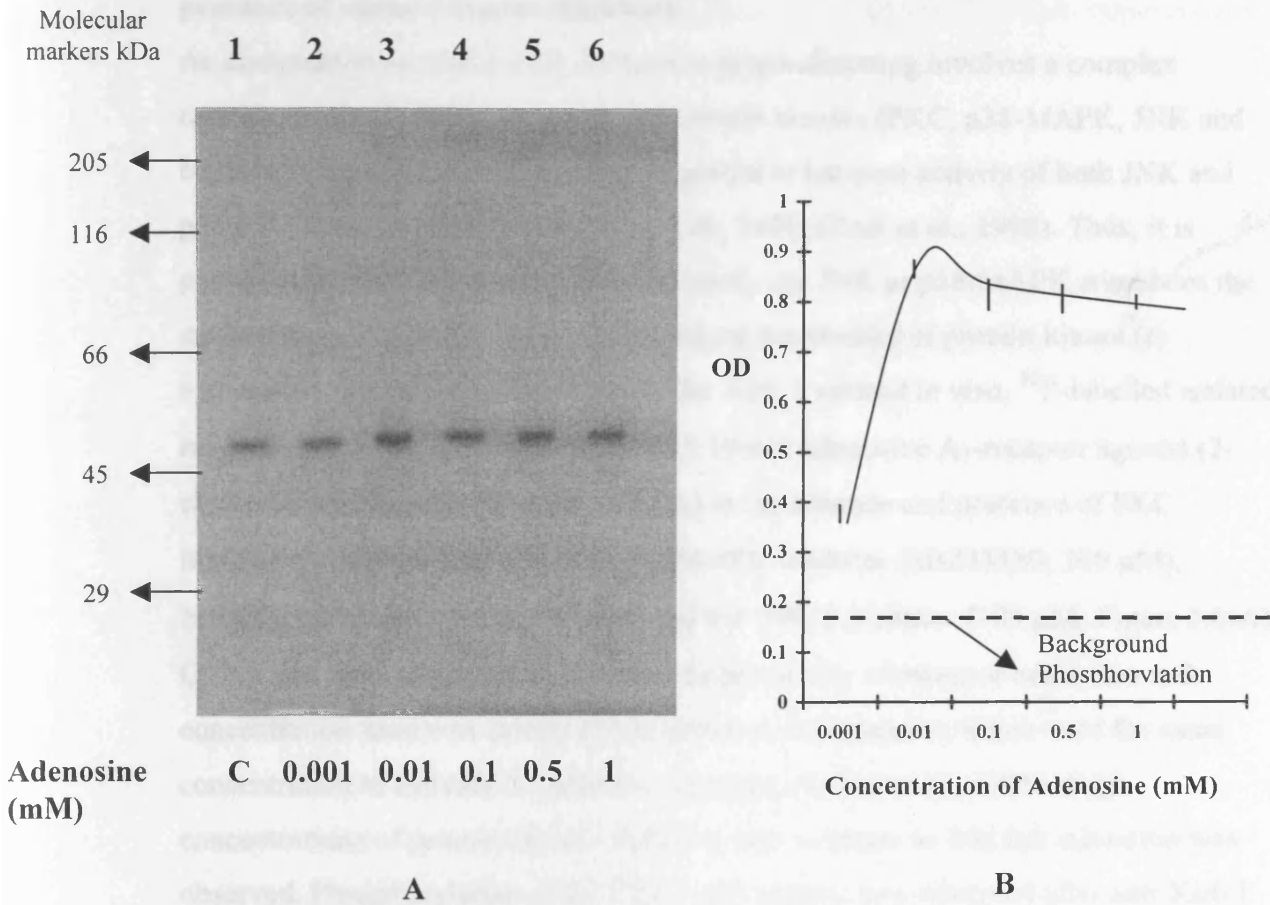


Figure 5.5A) Immunoprecipitation of Kir6.1 polypeptide from [³²P] labelled rat isolated cardiac myocytes stimulated with adenosine. Lanes 1-6 represent immunoprecipitated Kir6.1 polypeptide using anti-Kir6.1 antibody from extracts of ³²P-labelled cardiac myocytes stimulated with different concentrations of adenosine. Lane 1, unstimulated; lane 2, 1 μM adenosine; lane 3, 10 μM adenosine; lane 4, 100 μM adenosine; lane 5, 500 μM adenosine and lane 6, 1 mM adenosine. Representative of three experiments.

B) Densitometric analysis of adenosine-stimulated phosphorylation of Kir6.1 polypeptide. Background phosphorylation represents basal phosphorylation of immunoprecipitated Kir6.1 polypeptide observed from unstimulated ³²P-labelled cardiac myocytes. (n = 3).

5.4. *In vivo* phosphorylation of the Kir6.1 subunit in isolated rat cardiac myocytes stimulated by 2-chloro- N^6 -cyclopentyladenosine (CCPA) in the presence of various kinase inhibitors.

As discussed in section 1.13.2, ischaemic preconditioning involves a complex cascade, which includes receptors and protein kinases (PKC, p38-MAPK, JNK and MEK1/2). Protein kinase C has been reported to increase activity of both JNK and p38-MAPK in cardiomyocytes (Ping et al., 1998; Clerk et al., 1998). Thus, it is possible that PKC either directly or indirectly via JNK or p38-MAPK stimulates the cardiac K_{ATP} channel. In order to investigate the identity of protein kinase (s) responsible for the phosphorylation of the Kir6.1 subunit *in vivo*, ^{32}P -labelled isolated rat cardiomyocytes were stimulated with 10 μ M adenosine A_1 -receptor agonist (2-chloro- N^6 -cyclopentyladenosine; CCPA) in the absence and presence of PKC inhibitor (Chelerythrine; 100 μ M), p38MAPK inhibitor (SB203580; 100 μ M), MEK1/2 inhibitor (U0126; 100 μ M) and the JNK 1 inhibitor (100 μ M; Figure 5.6-A). CCPA was used as agonist to increase the specificity of receptor activation and concentration used was selected from previous experiments, which used the same concentration to activate A_1 -selective receptors (Lohse et al., 1988). High concentrations of protein kinase inhibitors were selected so that full inhibition was observed. Phosphorylation of the Kir6.1 polypeptide was observed after anti-Kir6.1 and anti-SUR2A antiserum immunoprecipitation when cardiomyocytes were stimulated with 10 μ M CCPA (Figure 5.6-A and 5.7-A, lane 1). Phosphorylation of the Kir6.1 subunit was inhibited when myocytes were incubated with 100 μ M Chelerythrine during the stimulation of 10 μ M CCPA (Figure 5.6-A and 5.7-A, lane 2). Phosphorylation of the Kir6.1 subunit was essentially unaffected when isolated rat cardiac myocytes were challenged with CCPA in the presence of SB203580, U0126 and JNK 1 inhibitor (Figure 5.6-A and 5.7-A, lane 3, 4 and 5, respectively).

For each of the reactions the optical density corresponding to Kir6.1 bands immunoprecipitated by anti-Kir6.1 and SUR2A on autoradiographs was measured (Figure 5.6-B and 5.7-B). In experiments using immunoprecipitation with either anti-Kir6.1 or anti-SUR2A antibody chelerythrine was observed to inhibit Kir6.1 phosphorylation by approximately 80% irrespective of immunoprecipitation conditions employed (Figure 5.6 –B and 5.7-B). Phosphorylation examined in

myocyte fractions stimulated with CCPA in the presence of other inhibitors was not significantly different from the cell fraction treated with CCPA alone, apart from the JNK I inhibitor which showed some inhibition ($p < 0.05$) but less than chelerythrine (Figure 5.6 –B and 5.7-B).

These results suggest that the activation of the A₁-receptor in isolated rat cardiac myocytes modulates the K_{ATP} channel Kir6.1 subunit predominately via PKC and that none of the other kinases tested play a large part in the signalling between A₁-receptor activation and the phosphorylation of the K_{ATP} channel Kir6.1 subunit.

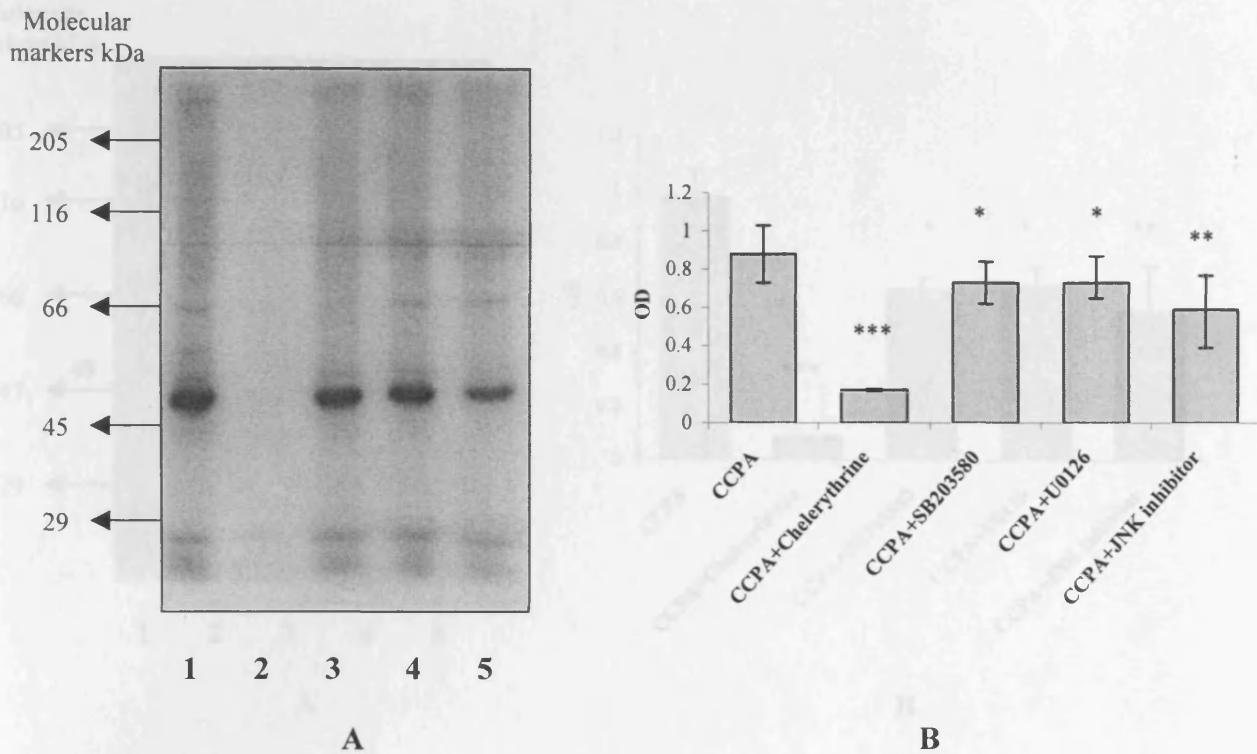


Figure 5.6 A) Immunoprecipitation of Kir6.1 polypeptide from ³²P-labelled cardiac myocytes stimulated with CCPA using anti-Kir6.1 antiserum.

Autoradiograph shows anti-Kir6.1 immunoprecipitation of the Kir6.1 polypeptide from ³²P-labelled rat isolated cardiac myocytes stimulated with CCPA in the absence and presence of various kinase inhibitors. Lane 1, ³²P-labelled myocytes stimulated with 10 μ M CCPA alone; lane 2, 10 μ M CCPA + 100 μ M chelerythrine; lane 3, 10 μ M CCPA + 100 μ M SB203580; lane 4, 10 μ M CCPA + 100 μ M U0126; lane 5, 10 μ M CCPA + 100 μ M JNK 1 inhibitor. Representative experiment ($n = 3$).

B) Densitometry from autoradiographs of phosphorylated Kir6.1 polypeptide bands immunoprecipitated using anti-Kir6.1 antibody. Optical density values were measured using Image MasterTM program (Pharmacia Biotech) from autoradiographs that were exposed for three hours. ($n = 3$). Statistical significance was tested using the unpaired *t*-test with Bonferroni multi-comparison correction against the CCPA reaction. *, $p > 0.1$; **, $p < 0.05$; ***, $p < 0.001$.

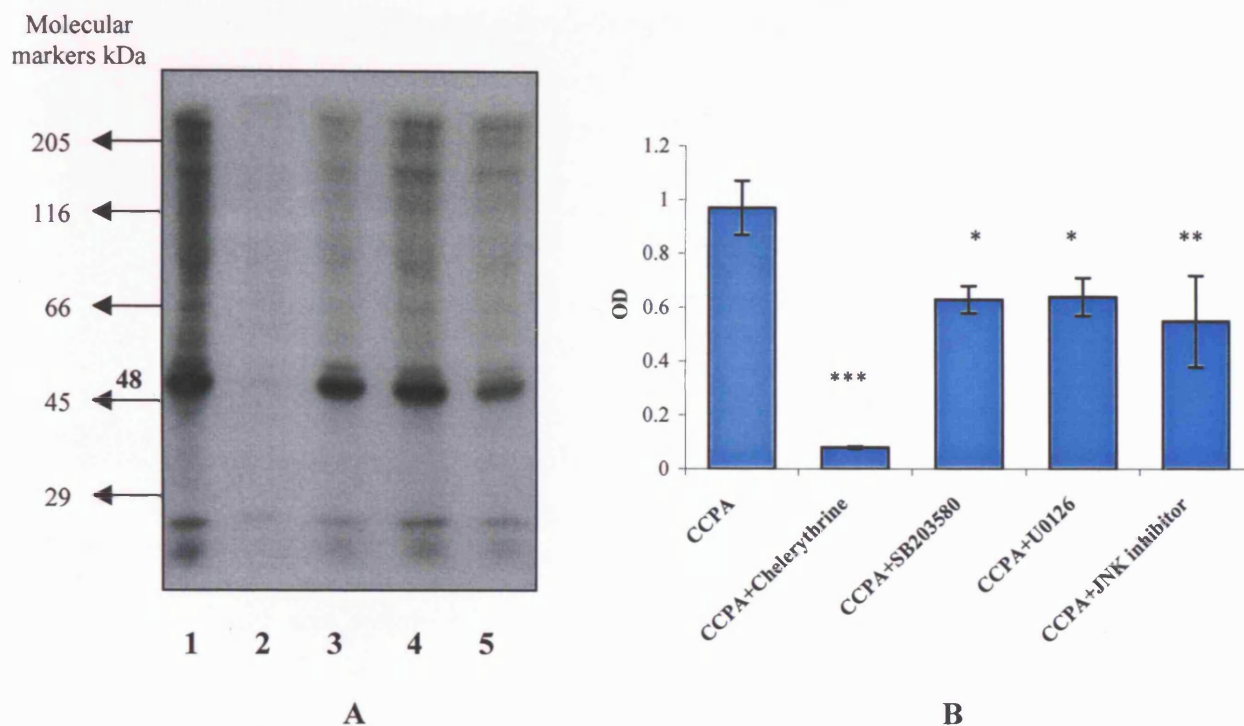


Figure 5.7A) Immunoprecipitation of Kir6.1 polypeptide from [³²P]-labelled cardiac myocytes stimulated with CCPA using anti-SUR2A antiserum.

Autoradiograph shows anti-SUR2A immunoprecipitation of the Kir6.1 polypeptide from ³²P-labelled rat isolated cardiac myocytes stimulated with CCPA in the absence and presence of various kinase inhibitors. Lane 1, [³²P]-labelled myocytes stimulated with 10 μM CCPA alone; lane 2, 10 μM CCPA + 100 μM chelerythrine; lane 3, 10 μM CCPA + 100 μM SB203580; lane 4, 10 μM CCPA + 100 μM U0126; lane 5, 10 μM CCPA + 100 μM JNK 1 inhibitor. Representative experiment (n = 3).

B) Densitometry from autoradiographs of phosphorylated Kir6.1 polypeptide bands immunoprecipitated using anti-SUR2A antibody. Optical density values were measured using Image Master™ program (Pharmacia Biotech) from autoradiographs that were exposed for three hours. (n = 3). Statistical analysis by unpaired Student's t-test with Bonferroni Multi-comparison see Figure 5.6.

5.5. Mapping of sites on Kir6.1 phosphorylated by *in vitro* using 2D-phosphopeptide mapping

To locate PKC-mediated phosphorylation sites on the Kir6.1 polypeptide, *in vitro* translated Kir6.1 polypeptide phosphorylated in the presence of exogenous PKC in the presence of [γ ³²P]-ATP was subjected to immunoprecipitation using anti-Kir6.1 antiserum, polyacrylamide (7%) gel electrophoresis, band isolation, tryptic digestion, separation of phosphopeptides by FeCl₃ column chromatography and 2D-electrophoretic analysis on TLC plates. Yields of phosphopeptides applied to TLC plates after phosphopeptide isolation were low (#50 counts per minute measured by liquid scintillation counting) and proved to be undetectable on autoradiography of TLC plates exposed to X-ray film for 2 to 30 days (not shown). This experimental approach was performed three times without success.

To observe separation of [³²P]-labelled tryptic digest polypeptide (s) on exposed autoradiographs, it is necessary to load samples with radioactivity of 200-1000 cpm on to the TLC plates. Even more counts would be required in the sample if the polypeptide were to contain multiple phosphorylation sites. Due to the amount of time (5-7days) required to prepare tryptic digest phosphopeptides, the low radioactivity in samples and high possibility of contamination of the digest polypeptides with keratin (keratin contamination makes the phosphopeptide very difficult to distinguish in mass sequencing), a different strategy was used to identify sites on the Kir6.1 polypeptide responsible for PKC phosphorylation.

5.6. Two-dimensional phosphoamino acid analysis of *in vivo* Kir6.1 subunit phosphorylated in isolated rat cardiomyocytes by PKC

³²P-phosphoamino acids can be detected from acid hydrolysed polypeptide samples containing very low radioactivity (10-100 cpm) by phosphoamino acid analysis (Hardie, D.G., 1993). Phosphoamino acid analysis using an HTLE-7000 2D electrophoresis apparatus, as described in materials and methods (section 2.16), was used to determine which amino acid residue (s), tyrosine, threonine or serine, was phosphorylated in response to PKC activation on Kir6.1 polypeptides immunoprecipitated from ³²P-labelled myocytes stimulated with 50 μ M PMA. Immunoprecipitated [³²P]-Kir6.1 was subjected to polyacrylamide (7%) gel

electrophoresis, blotting to Immobilon PVDF membrane. PVDF membrane bearing the [^{32}P]-Kir6.1 band was cut out and the polypeptide hydrolysed with 6M HCl before 2D-phosphoamino acid analysis (see section 2.16). [^{32}P]-phospho-serine residue (p-SER) was resolved from acid hydrolysed Kir6.1 polypeptides immunoprecipitated with anti-Kir6.1 and anti-SUR2A antisera (Figure 5.8). The migration of unlabelled phosphoamino acid standards as used to identify p-SER as the phosphorylated residue in the Kir6.1 polypeptide. Neither [^{32}P]-phosphothreonine nor [^{32}P] phosphotyrosine was detected in any 2D electrophoresis, even when the TLC plate was exposed to film for up to 14 days (not shown).

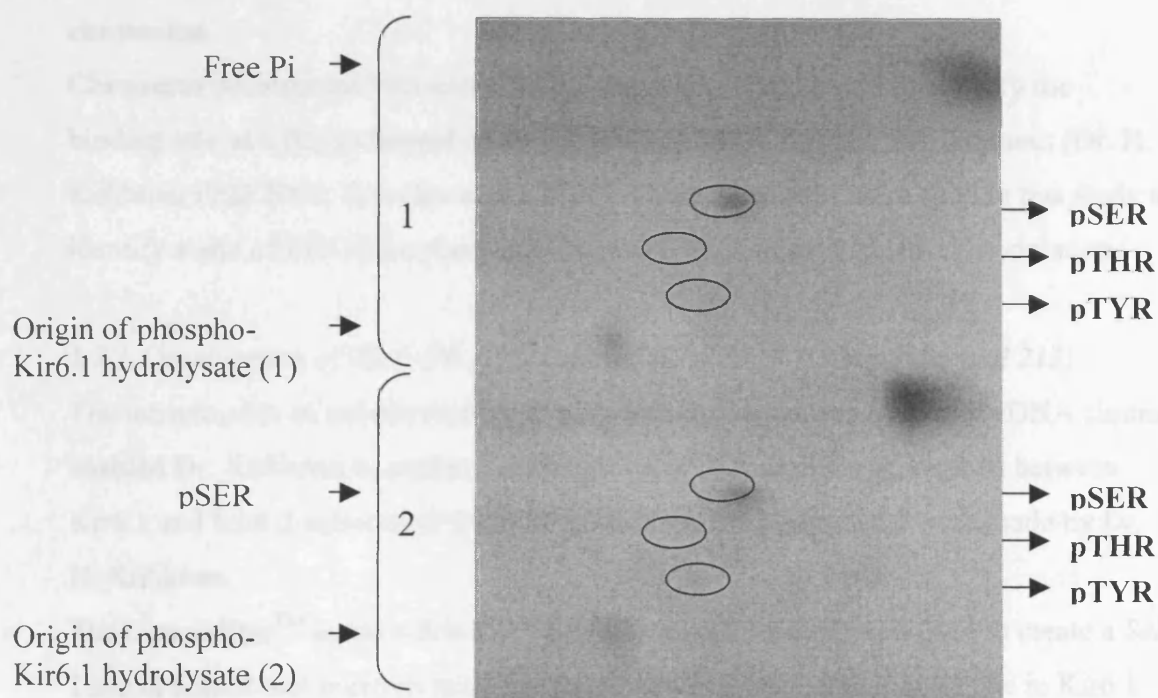


Figure 5.8 . 2D-phosphoamino acid analysis of immunoprecipitated Kir6.1 polypeptide stimulated with PMA. Immobilon PVDF (polyvinylidene difluoride) membrane slices bearing ^{32}P -Kir6.1 polypeptide immunoprecipitated by either anti-Kir6.1 (1) or anti-SUR2A (2) from ^{32}P -labelled cardiac myocytes stimulated with PMA were incubated in 6 M HCl. The Kir6.1 derived phosphoamino acids were then separated by 2D thin layer electrophoresis. The autoradiograph shows phosphorylation of Kir6.1 proteins on serine residues in both cases. The migration of phosphoamino acid standards is shown by circles. Representative experiment ($n = 2$).

5.7 Mapping of a PKC phosphorylation site in Kir6.1 using Kir6.1/Kir6.2 chimaeras

Chimaeras constructed between Kir6.0 subunits have been used to identify the binding site of a K_{ATP} channel inhibitor, PNU-37883A, on the Kir6.1 subunit (Dr. H. Kuhlman PhD 2002; Kovalev et al., 2001). These chimaeras were used in this study to identify a site of PKC phosphorylation on the Kir6.1 subunit for PKC modulation.

5.7.1 Construction of Kir6.1/6.2 3' swap and Kir6.2/6.1 3' swap (123 and 213)

The introduction of unique restriction sites into the sequences of Kir6.0 cDNA clones enabled Dr. Kuhlman to perform a straight swap of four different regions between Kir6.1 and Kir6.2 subunits (Figure 5.9). All Kir6.1/6.2 constructs were made by Dr. H. Kuhlman.

The GeneEditor™ *in vitro* Site-Directed Mutagenesis system was used to create a *Sal* I site in Kir6.2 that corresponded to one present in Kir6.1, and a *Sph* I site in Kir6.1 that corresponded to one present in Kir6.2 (Kuhlman, 2002). Mutagenic oligonucleotides (*Sph* I mutant oligo: 5' TTT TCA GCC ATG CTG TAA 3', *Sal* I mutant oligo: 5' CCA CGC TGG TCG ACC TCA AG 3') were annealed to the template DNA with subsequent synthesis and ligation of the mutant strand linking the two oligonucleotides. After transforming DNA into JM109 cells [e14⁹McrA⁰end A1 recA1 gyrA96 thi hsdR17 (r_k⁻m_k⁻) rel A1 supE44 L-Δ(lac-proAB)(F' traΔ36 proA⁺B⁺ lacI^qΔm150] mutants were selected by plating onto ampicillin plates containing GeneEditor™ Antibiotic Selection Mix. Resistance to the selection mix encoded by the mutant DNA strand facilitated selection of the desired mutation. DNA sequencing was used to identify the mutants. Identified mutant Kir6.1 (*Sph* I) and Kir6.2 (*Sal* I) DNA was digested with *Sph* I restriction enzyme to obtain fragments corresponding to the C-terminal ends and rest of the Kir6.0 subunits. Obtained fragments were gel purified from 1% agarose gel. The opposing fragments were ligated to form constructs of Kir6.1 with the C-terminal end of Kir6.2 (123) and the equivalent opposite construct (213). Transformation of the constructs into Epicurian Coli ® XL-Blue subcloning-grade competent cells (Stratagene) were performed, which were plated onto LB-carb plates. DNA from single colonies (mini-preps; section 2.15.3) were analysed by DNA sequencing.

5.7.2 Construction of Kir6.2/6.1 pore swap (21P)

Kir6.2 (*Sal* I) clone and Kir6.1 (*Sph* I) clone DNA were digested with *Sal* I and *Sph* I, with the resulting fragments gel purified following agarose gel electrophoresis. The opposing fragments were ligated together (in this case the M1-H5-M2 fragment of Kir6.1 ligated into the N and C-terminal region of Kir6.2). After transformation of the ligation reactions clones were confirmed by sequencing.

5.7.3 Construction of Kir6.2/6.1 5' swap (215)

Kir6.2 (*Sal* I) and Kir6.1 (*Sph* I) DNA was digested with *Sal* I to obtain fragments corresponding to the N-terminal end and the rest of Kir6.0. These fragments were gel purified following agarose gel electrophoresis and the opposing fragments were ligated to form constructs of Kir6.2 with the N-terminal end of Kir6.1. After transformation the correct clone was confirmed by DNA sequencing.

5.7.4 Construction of Kir6.1/Ki6.2 *Sph*-*EcoRV* and Kir6.2/Ki6.1 *Sph*-*EcoRV* (1121 and 2212)

The QuickChange™ Site-Directed Mutagenesis Kit as described in materials and methods (section 2.17) was used to create an *EcoRV* site in the Kir6.2, 87 amino acids downstream from the *Sph* I site (Dr. Kuhlman, PhD 2002). The primers used were 5' AGC CCG CTC TAC GAT ATC GCT CCT AGT GAC 3' (forward) and 5' GTC ACT AGG AGC GAT ATC GTA GAG CGG GCT 3' (reverse). The mutant which was identified by restriction enzyme digests was then digested with *Sal* I and this fragment ligated into the original Kir6.2 (*Sal* I) clone in order to lessen the chance of an accidental mutation being present in the clone. This new Kir6.2 (*Sal* I, *EcoRV*) clone was then sequenced to further confirm the presence of the desired mutation. The mutant Kir6.2 (*Sal* I, *EcoRV*) and Kir6.1 (*Sph* I) clones were digested with *EcoRV*. The resulting fragments were purified from an agarose gel and the C-terminal fragment of Kir6.1 was ligated to the rest of Kir6.2 and visa -versa. The swaps were confirmed by sequencing. These Kir6.0 chimaeras were then digested with *Sph* I. The resulting fragments were ligated into the opposite constructs, to produce constructs, which were Kir6.1 with *Sph* I to *EcoRV* fragment of Kir6.2 and the equivalent opposite construct. The constructed clones were confirmed by DNA sequencing (section 2.17.3).

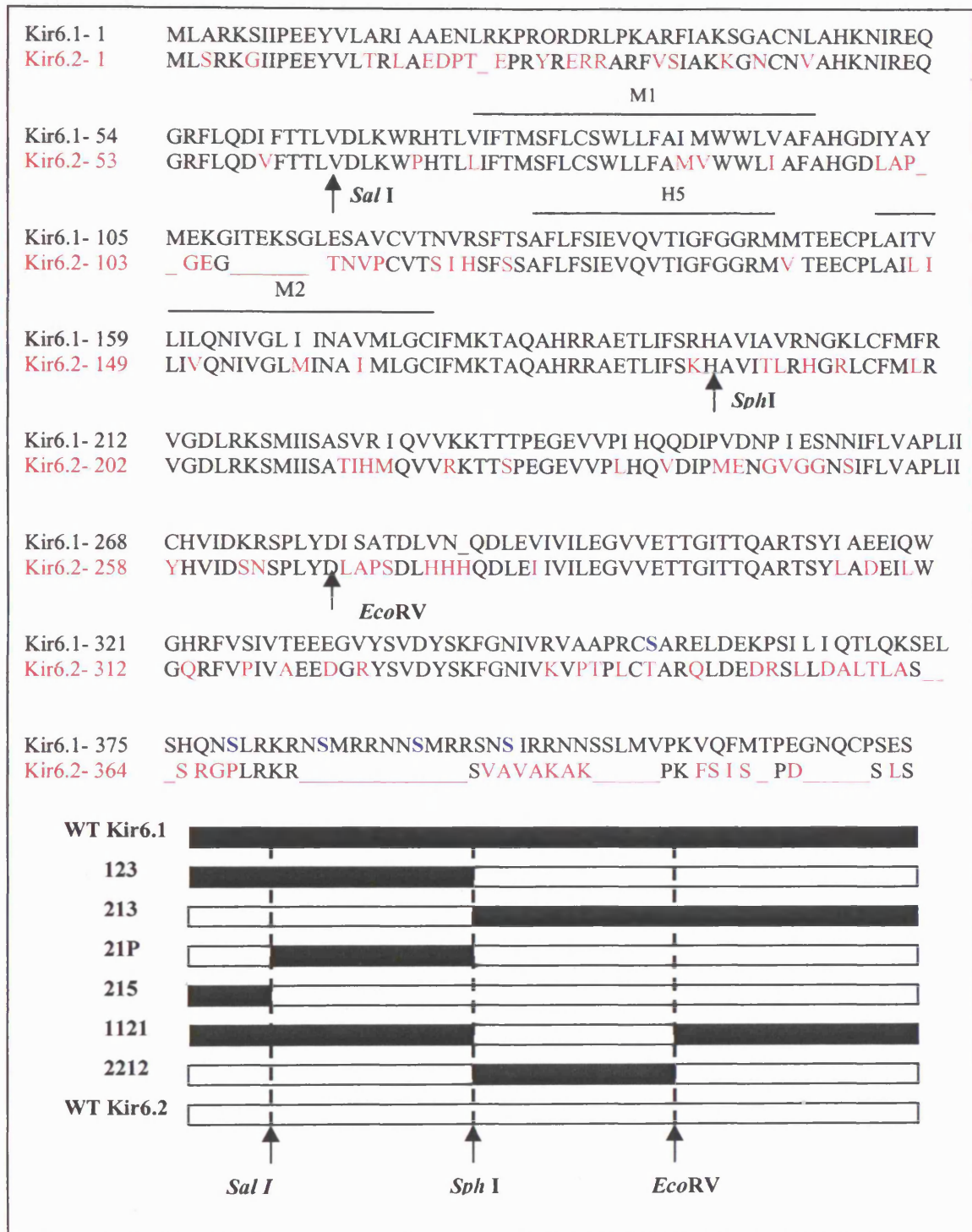


Figure 5.9. Amino acid sequence of rat Kir6.0 subunits and schemata of constructed chimaeras. The Kir6.2 amino acid residues highlighted in red differ from those of the Kir6.1 subunit. Arrows represent the position of restriction sites used for cloning. Serine residues in blue represent potential PKC mediated phosphorylation sites in the Kir6.1 polypeptide. The Kir6.0 coding region in chimaeras is indicated by rectangular box with the Kir6.1 and Kir6.2 subunits being presented either black or white, respectively (Dr. H. Kuhlman PhD 2002).

5.7.5. *In vitro* expression of the chimaera clones

Expression of sequenced chimaera clones as verified by using the TNT® Quick Coupled Transcription/Translation kit. Chimeric DNA (2µg) was incubated with SP6 TNT® Quick Master Mix in the presence of 0.37MBq of [³⁵S]-methionine. *In vitro* translation of all the [³⁵S]-methionine chimaeras was observed (Figure 5.10). All the polypeptides migrated to predicted molecular weights as shown below in Table 5.3.

Nomenclature of chimaera clones	Constituent	Migrated molecular weight on 7.5 % polyacrylamide gel (kDa)
123	Kir6.1 with Kir6.2 C-terminal	40
213	Kir6.2 with Kir6.1 C-terminal	48
21P	Kir6.2 with pore region swapped with Kir6.1	40
215	Kir6.2 with N-terminal Kir6.1	40
1121	Kir6.1 with region between restriction sites <i>Sph</i> I to <i>EcoRV</i> swapped with Kir6.2	48
2212	Kir6.2 with region between restriction sites <i>Sph</i> I to <i>EcoRV</i> swapped with Kir6.1	48

Table 5.3 Apparent molecular weights of Kir6.0 chimaeras from electrophoretic analysis on 7.5 % polyacrylamide gel

Kir6.0 chimaeras were then expressed in the absence of [³⁵S]-methionine, i.e. in the presence of 1mM unlabelled methionine, and utilized for *in vitro* PKC-mediated phosphorylation experiments.

Molecular markers

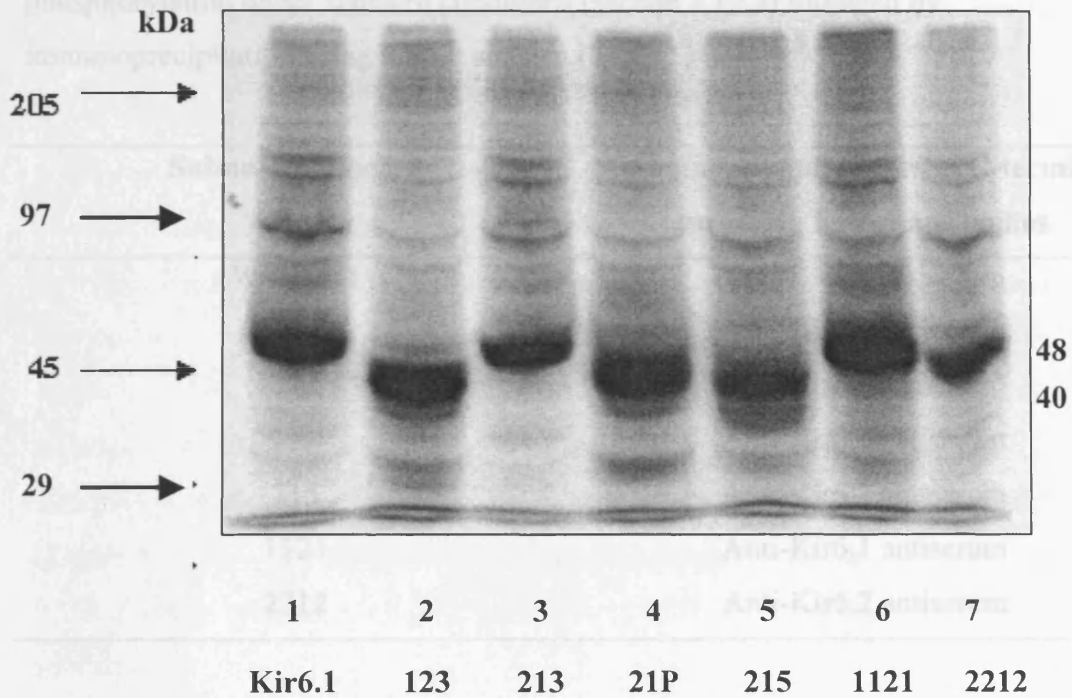


Table 5.4. Kir6.0 antisera used for the immunoprecipitation of polypeptides from *in vitro* expressed chimaeras following incubation with PKC in the presence of [³⁵S]-ATP.

Immunoprecipitation of a phosphopeptide of 48 kDa was observed in reactions

Figure 5.10 *In vitro* translated [³⁵S]-methionine-labelled Kir6.0 constructed chimaeras. Autoradiograph showing migrated [³⁵S]-methionine labelled *in vitro* translated chimeric polypeptides on a 7.5% polyacrylamide mini-gel. The subunits were expressed using the SP6 TNT[®] quick-coupled transcription/translation kit (Promega). The [³⁵S]-methionine-labelled WtKir6.1, 213 and 1121 polypeptides migrated to molecular weights of 48 kDa, whereas chimaeras 123, 21P, 215 and 2212 migrated to molecular weights of 40kDa. Representative experiment (n = 2)

EcoRV site in Kir6.2 were substituted with Kir6.1 (Figure 5.11-A, line 7), which further localized the amino acid (s) responsible for PKC phosphorylation of the Kir6.1 polypeptide between isoleucine²⁸⁹-serine³⁰² (I²⁸⁹-S³⁰²)

5.7.6. *In vitro* PKC-mediated phosphorylation of Kir6.0 chimaeras

In vitro translated unlabelled Kir6.0 chimaeras were subjected to PKC-mediated phosphorylation under standard conditions (section 2.12.2) followed by immunoprecipitation using Kir6.0 antisera (Table 5.4).

Subunit/ chimeara	Immunoprecipitated with C-terminal targeting Kir6.0 antibodies
Wt Kir6.1	Anti-Kir6.1 antiserum
123	Anti-Kir6.2 antiserum
213	Anti-Kir6.1 antiserum
21P	Anti-Kir6.2 antiserum
215	Anti-Kir6.2 antiserum
1121	Anti-Kir6.1 antiserum
2212	Anti-Kir6.2 antiserum

Table 5.4. Kir6.0 antisera used for the immunoprecipitation of polypeptides from *in vitro* expressed chimaeras following incubation with PKC in the presence of [γ^{32} P]-ATP.

Immunoprecipitation of a phosphopolypeptide of 48 kDa was observed in reactions containing WT Kir6.1, 213 and 1121 chimaeras only (Figure 5.11-A, lanes 1, 3 and 6, respectively) using the anti-Kir6.1 antiserum. No detectable immunoprecipitation of a phosphopolypeptide (40 kDa) using anti-Kir6.2 antiserum was detected from reactions containing 123, 21P and 215 chimaeras (Figure 5.11-A, lanes 2, 4, and 5, respectively) suggesting that the Kir6.1 phosphorylation must occur in the C-terminal half of the protein. No phosphorylation was seen in the reaction containing the 2212 chimaera, where the amino acids included in the coding region between *Sph* I to *EcoRV* sites in Kir6.2 were substituted with Kir6.1 (Figure 5.11-A, lane 7), which further localized the amino acid (s) responsible for PKC phosphorylation of the Kir6.1 polypeptide between isoleucine²⁸⁰-serine⁴²⁴ (I²⁸⁰-S⁴²⁴).

The optical density of phosphorylated polypeptide bands measured from autoradiographs exposed for 3 hours showed a similar level of PKC-mediated phosphorylation in WT Kir6.1, 213 and 1121 reactions (Figure 5.11).

5.8. Two-dimensional phosphoamino acid analysis of *in vitro* PKC-mediated phosphorylation of Kir6.0 chimaeras.

Phosphoamino acid analysis was performed on immunoprecipitated polypeptides from chimaera reactions incubated with PKC in the presence of [$\gamma^{32}\text{P}$]-ATP to see whether serine was the target residue for PKC as observed in *in vivo* experiments where Kir6.1 polypeptide was phosphorylated by PKC in rat isolated ventricular myocytes (section 5.6). Phosphorylation of serine residues was detected in immunoprecipitated polypeptide from WT Kir6.1 and 1121 chimaera reactions (Figure 5.12). No serine, threonine nor tyrosine phosphorylation was detectable in the 2212 chimeric reaction even after the exposure of the TCL plate to film for 14 days (not shown).

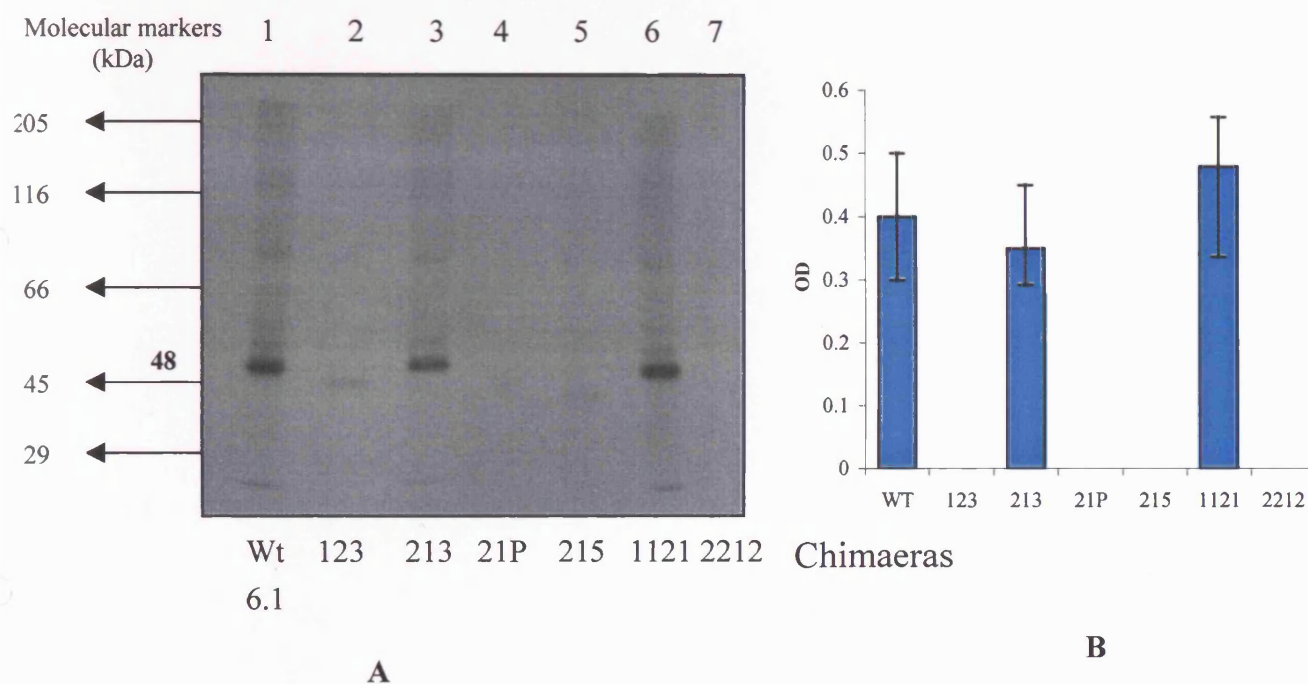


Figure 5.11A) *In vitro* PKC-mediated phosphorylation of constructed Kir6.0 chimaeras. *In vitro* expressed Wt Kir6.1 and chimaeras were incubated with PKC (3.5 $\mu\text{g/ml}$) in the presence of [^{32}P]-ATP, resolved by SDS-PAGE and visualized by autoradiography. Lane 1, WT Kir6.1 immunoprecipitation using anti-Kir6.1 antisera; lane 2, 123 chimaera immunoprecipitation using anti-Kir6.2 antisera; lane 3, 213 chimaera immunoprecipitation using anti-Kir6.1 antisera; lane 4, 21P chimaera immunoprecipitation using anti-Kir6.2 antisera; lane 5, 215 chimaera immunoprecipitation using anti-Kir6.2 antisera; lane 6, 1121 chimaera immunoprecipitation using anti-Kir6.1 antisera; lane 7, 2212 chimaera immunoprecipitation using anti-Kir6.2 antisera. Representative experiment ($n = 3$)

B) Densitometry of polypeptide bands detected from autoradiograph shown in A. Optical density values were measured using Image Master programTM (Pharmacia Biotech) from autoradiographs that were exposed to X-ray film for three hours. ($n = 3$)

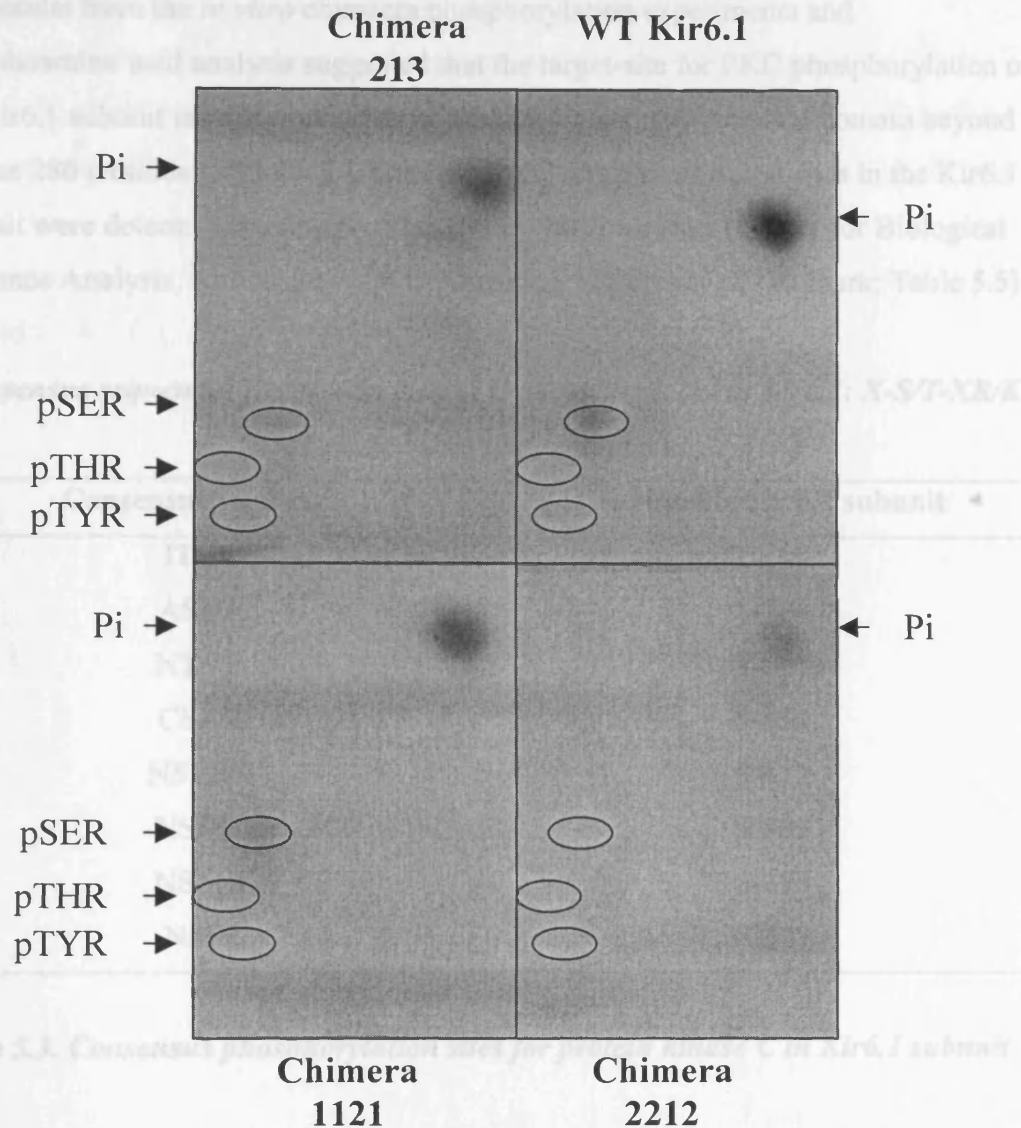


Figure 5.12. 2D-Phosphoamino acid analysis of phosphorylated WT Kir6.1 and Chimeras 213, 1121 and 2212. Immobilized PVDF membrane strips bearing immunoprecipitated polypeptides from WT Kir6.1, chimeras 213, 1121 and 2212 reactions incubated with PKC (3.5 $\mu\text{g/ml}$) in the presence of ^{32}P -ATP were incubated with 6 M HCl to hydrolyse the peptide. Phosphoamino acids were separated by 2D-thin layer electrophoresis (section 2.16). The autoradiograph shows phosphorylation of serine residues in WT Kir6.1 and 1121. The migration of unlabelled phosphoamino acid standards are shown by the circles. ($n = 1$)

5.9 *In vitro* phosphorylation of expressed point mutants of Kir6.1.

The results from the *in vitro* chimaera phosphorylation experiments and phosphoamino acid analysis suggested that the target-site for PKC phosphorylation on the Kir6.1 subunit is located on a serine residue (s) in the C-terminal domain beyond residue 280 (residues 280-424). Consensus PKC target amino acid sites in the Kir6.1 subunit were determined using NetPhos 2.0 Prediction server (Center for Biological Sequence Analysis, BioCentrum-DTU, Technical University of Denmark; Table 5.5).

*Consensus sequences for protein kinase C phosphorylated in Kir6.1: X-S/T-XR/K
(where X is any amino acid)*

Consensus sequence	Residue in Kir6.1 subunit
ITEK	T-110
ASVR	S-224
NTVR	T-345
CSAR	S-354
NSLRK	S-379
NSMR	S-385
NSMR	S-393
NSIR	S-397

Table 5.3. Consensus phosphorylation sites for protein kinase C in Kir6.1 subunit

Five serine and one threonine residue, represented in bold in Table 5.5, are present between amino acids I²⁸⁰-S⁴²⁴ in the Kir6.1 subunit. Since threonine phosphorylation was undetected in phosphoamino acid analysis performed on the Kir6.0 chimaeras, attention was directed to the serine residues at position 354, 379, 385, 393 and 397, which were mutated to alanine and examined for PKC-mediated phosphorylation. The Kir6.1 mutants (S354A, S379A, S385A, S393A and S397A) were constructed using the QuikChangeTM Site-Directed Mutagenesis kit as described in section 2.14.

5.9.1. *In vitro* expression of Kir6.1 mutants

Kir6.1 mutants were expressed using the TNT® Quick Coupled Transcription/Translation kit in the presence of 0.37 MBq [³⁵S]-methionine. The migration of [³⁵S]-methionine-labelled polypeptides on polyacrylamide gels verified the expression of the mutants, with a molecular weight similar to WT Kir6.1 (Figure 5.13).

The mutants were then expressed in the presence of 1mM unlabelled methionine and utilized for *in vitro* PKC-mediated phosphorylation experiments.

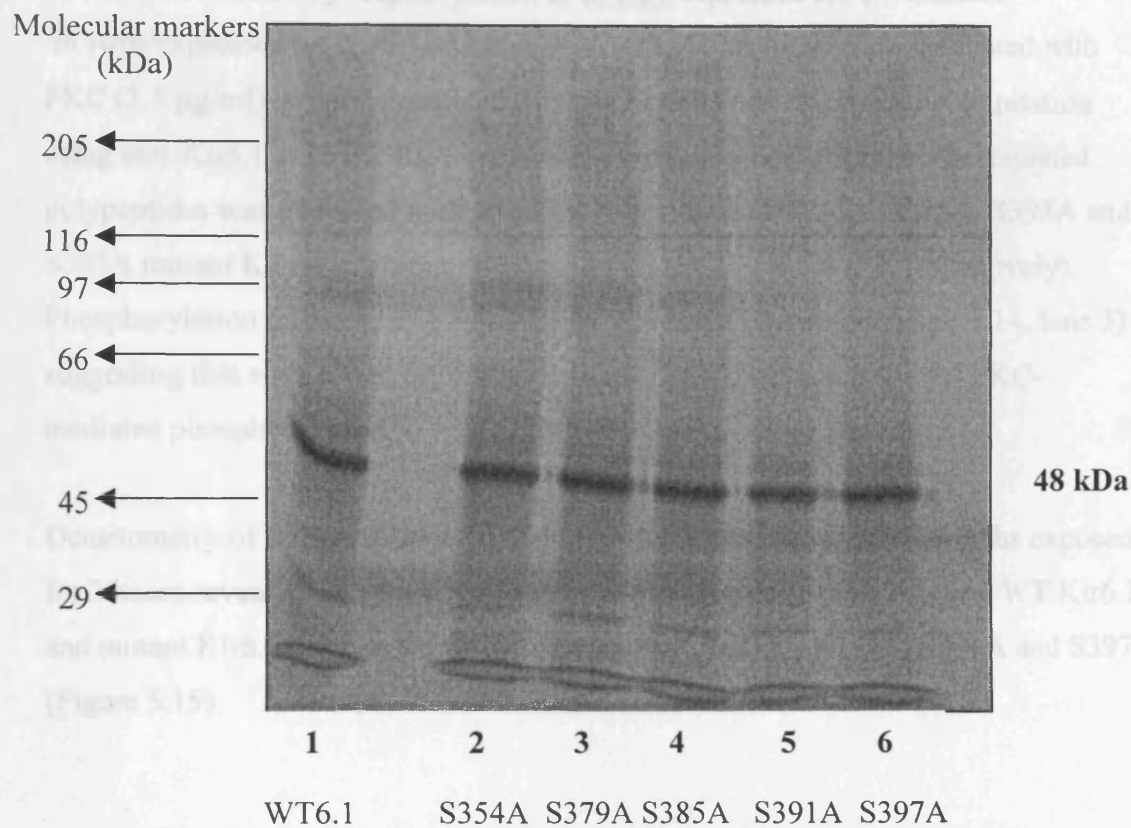


Figure 5.13. *In vitro* translated [³⁵S]-methionine labelled Wt and Kir6.1 mutants. Autoradiograph showing migrated [³⁵S]-methionine labelled *in vitro* translated wt and mutant Kir6.1 polypeptides electrophoresed on a 7.5% polyacrylamide mini-gel. The subunits were expressed using the SP6 TNT[®] quick-coupled transcription/translation kit (Promega). The [³⁵S]-methionine labelled WT and Kir6.1 mutants, S354A, S379A, S385A, S393A and S397A polypeptides all migrated with an apparent molecular weight of 48 kDa. (n = 2).

5.9.2. PKC-mediated phosphorylation of *in vitro* expressed Kir6.1 mutants

In vitro expressed wt Kir6.1 and mutant Kir6.1 polypeptides were incubated with PKC (3.5 µg/ml) in the presence of [γ ³²P]-ATP followed by immunoprecipitation using anti-Kir6.1 antisera. PKC-mediated phosphorylation of immunoprecipitated polypeptides was observed in the wt Kir6.1 reaction and S354A, S385A, S393A and S397A mutant Kir6.1 reactions (Figure 5.14, lanes 2, 3, 5,6 and 7, respectively). Phosphorylation of the S379A mutant Kir6.1 was not observed (Figure 5.14, lane 3) suggesting that serine³⁸⁵ is the residue in Kir6.1 subunit responsible for PKC-mediated phosphorylation.

Densitometry of immunoprecipitated polypeptide bands on autoradiographs exposed for 3 hours revealed no significant difference in phosphorylation between WT Kir6.1 and mutant Kir6.1 *in vitro* expressed polypeptides, S354A, S385A, S391A and S397A (Figure 5.15).

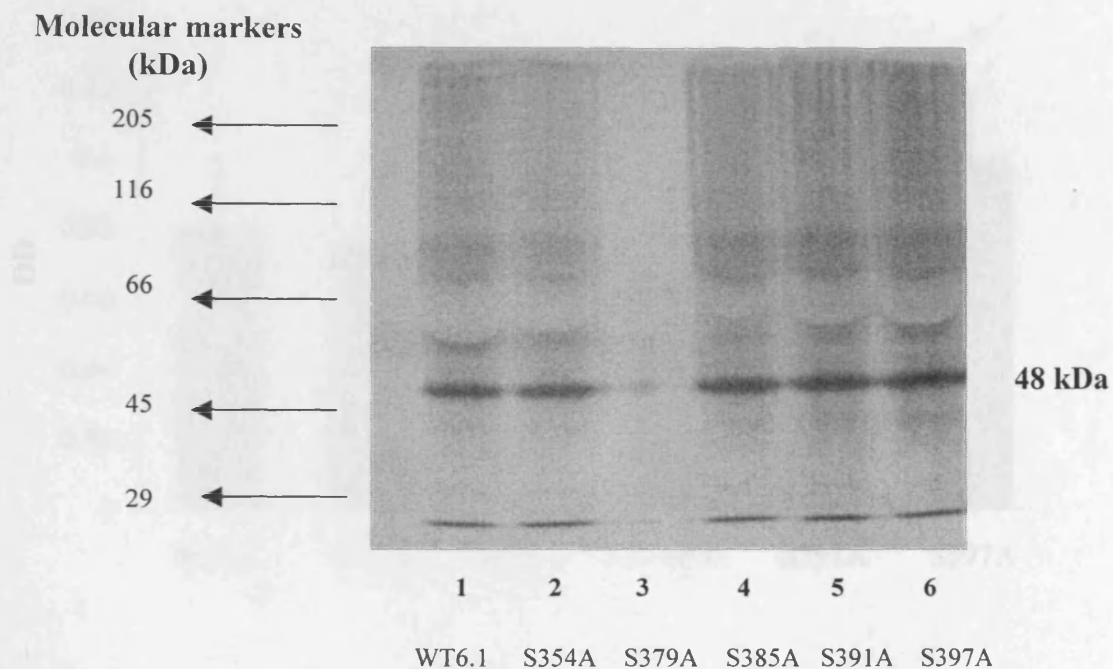


Figure 5.14. *In vitro* PKC-mediated phosphorylation of expressed Kir6.1 mutants. *In vitro* expressed Wt Kir6.1 and Kir6.1 mutants were phosphorylated in the presence of PKC (3.5 μ g/ml) and [32 P]-ATP, immunoprecipitated with anti-Kir6.1 antiserum, resolved by SDS-PAGE and visualized by autoradiography. Lane 1, WT Kir6.1; lane 2, S354A Kir6.1; lane 3, S379A Kir6.1; lane 4, S385A Kir6.1; lane 5, S391A Kir6.1; lane 6, S397A Kir6.1 mutant. Representative experiment ($n = 3$).

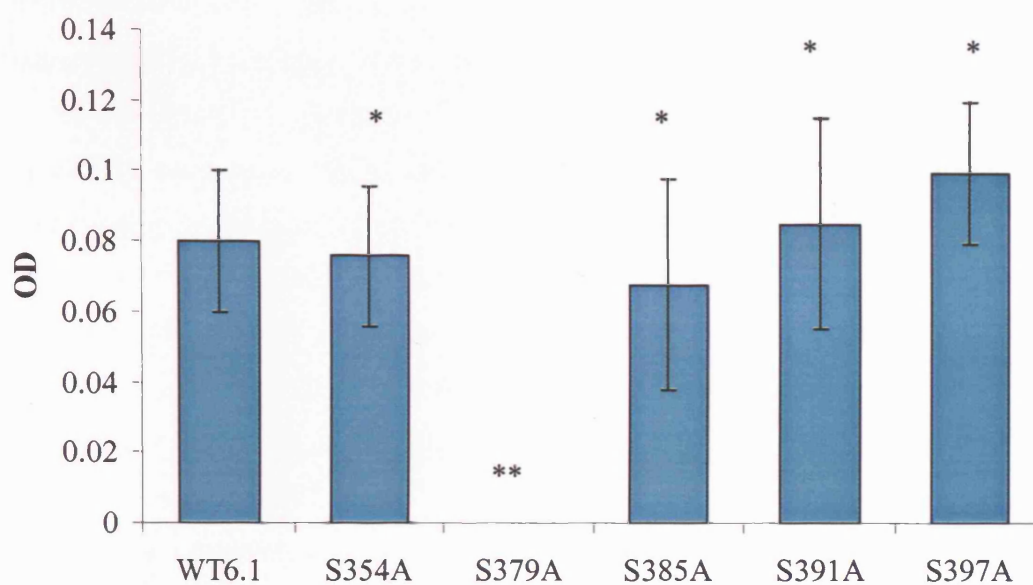


Figure 5.15. Densitometry of autoradiographs of immunoprecipitated Kir6.1 polypeptide bands. Optical density values were measured using Image MasterTM program (Pharmacia Biotech) from autoradiographs that were exposed for three hours. ($n = 3$). Statistical analysis was by unpaired Student's t -test with Bonferroni Multi-comparison. * $p =$ non-significant, ** $p < 0.01$.

5.10 Summary

In vitro expressed Kir6.1 was phosphorylated by PKA and PKC, whereas Kir6.2 was phosphorylated by PKA only. The Kir6.1 polypeptide in rat isolated ventricular myocytes was the only K_{ATP} channel subunit phosphorylated on stimulation with activated PKC (adenosine; PMA) and PKA (Forskolin). Complete inhibition of phosphorylation with cheleythrine (PKC inhibitor), but not with SB203580 (p38MAPK), U0126 (MEK1/2) and JNK 1 inhibitor indicate a probably direct PKC mediated phosphorylation of the Kir6.1 polypeptide in native tissue. *In vitro* phosphoamino acid analysis and phosphorylation of expressed Kir6.1/6.2 chimaeras showed PKC-mediated phosphorylation of the Kir6.1 polypeptide located on a serine residue between amino acids 280-424. *In vitro* phosphorylation experiments on expressed Kir6.1 mutants, confirmed serine 379 as the site for PKC phosphorylation.

Chapter 6: Discussion

Cardiac myocytes contain two ATP-sensitive potassium channels, the sarcolemmal K_{ATP} channel (sarc K_{ATP} ; Inagaki et al., 1996) and the mitochondrial K_{ATP} channel (mito K_{ATP}) found in the inner mitochondrial membrane (Inoue et al. 1991). The regulation of cardiac K_{ATP} channels by PKC in ischaemic preconditioning (IP) has been shown to be potentially important (Liang et al., 1997; Hu et al., 1996; Light et al., 1996; Liu et al., 1998; Sato et al., 1998; Liu et al., 2002). Evidence supporting a role for PKC regulated sarc K_{ATP} and mito K_{ATP} channels in IP has been examined by blocking and mimicking the protective effects of both ischaemic and pharmacological preconditioning by selective K_{ATP} channel inhibitors and agonists in the presence and absence of PKC inhibitors (Suzuki et al., 2002; Sato et al., 1998; Liu et al., 2002). To date, these studies have been unable to provide strong evidence for whether regulation of one or both cardiac K_{ATP} channels via PKC is involved in IP.

Protein kinase C-mediated phosphorylation of the Kir6.2 threonine residue at position 180 in Kir6.2/SUR2A transfected HEK 293 cells has been determined (Light et al., 2000), but PKC-mediated phosphorylation of the sarcolemmal K_{ATP} channel subunits in native tissue still remains to be investigated. On the other hand, activation of PKC has been linked specifically to the protective role of the mitochondrial K_{ATP} channel (Sato et al., 1998). Like the Kir6.2 subunit, the PKC consensus sites are also highly conserved in the Kir6.1 subunit, the putative mito K_{ATP} subunit (Suzuki et al., 1997), which suggests the possibility of regulation of the mitochondrial K_{ATP} channel subunit. Again, there is no evidence to date that the Kir6.1 subunit is substrate for PKC in cardiac tissue. To investigate PKC-mediated phosphorylation of these cardiac K_{ATP} channel components and to understand their importance in cardiac myocytes during IP, the molecular composition of sarc K_{ATP} and mito K_{ATP} needs to be resolved.

To resolve the molecular composition of these channels isoform specific site-directed antibodies against K_{ATP} channel subunit peptides were produced to investigate the cellular localization of K_{ATP} channel subunit isoforms in isolated cardiac myocytes by confocal microscopy and in subcellular fractions by Western blotting. The same

antibodies were then used to investigate *in vivo* PKC-mediated phosphorylation of resolved cardiac K_{ATP} channel subunits.

6.1. Antibody Characterization

Anti-Kir6.0 and SUR2 antibodies were prepared against the C-terminal sequences of rat K_{ATP} channel subunits, as shown in Figure 6.1. Each antibody was shown to recognise immunising peptide in ELISA, which was displaced from the target antigen by competition with specific antigenic peptide. Their specificity towards their target peptide sequence in expressed K_{ATP} channel subunits were confirmed by immunoprecipitation, Western blots and immunocytochemistry. The anti-Kir6.0 and anti-SUR2 antibodies were able to immunoprecipitate target specific peptide sequences on [³⁵S]-methionine labelled Kir6.0 and SUR proteins, respectively, which were, in each case, blocked by preadsorption of the antiserum with specific immunizing peptide. Limited cross-reactivity between anti-SUR2A and anti-SUR2B antibody was observed at high serum concentrations, as these antibodies were able to immunoprecipitate non-specific related peptide on expressed *in vitro* proteins.

Western blots performed on *in vitro* expressed K_{ATP} channel subunits were also able to show specific binding of antibodies to specific target peptides, which in each case was abolished by preadsorption of antisera with 10 µg/ml of C-terminal specific immunizing peptide. Cross-reactivity between the anti-SUR2A and anti-SUR2B antibodies was not seen in Western blots, as these antibodies were unable to target related subunits, implying that anti-SUR2 antisera along with anti-Kir6.0 antisera were subunit specific and could be used to investigate localization of K_{ATP} channel subunits in isolated rat heart subcellular fractions using Western blots.

The demonstration of specific binding of antibodies to stably expressing Kir6.2/SUR2A and SUR2A HEK293 cell-lines transfected with appropriate K_{ATP} channel subunits using immunocytochemistry and confocal microscopy established the subunit specificity of each of the antibodies in this application and permitted the application of these antibodies in the examination of the localization of Kir6.0 and SUR2 subunits in rat isolated cardiac myocytes.

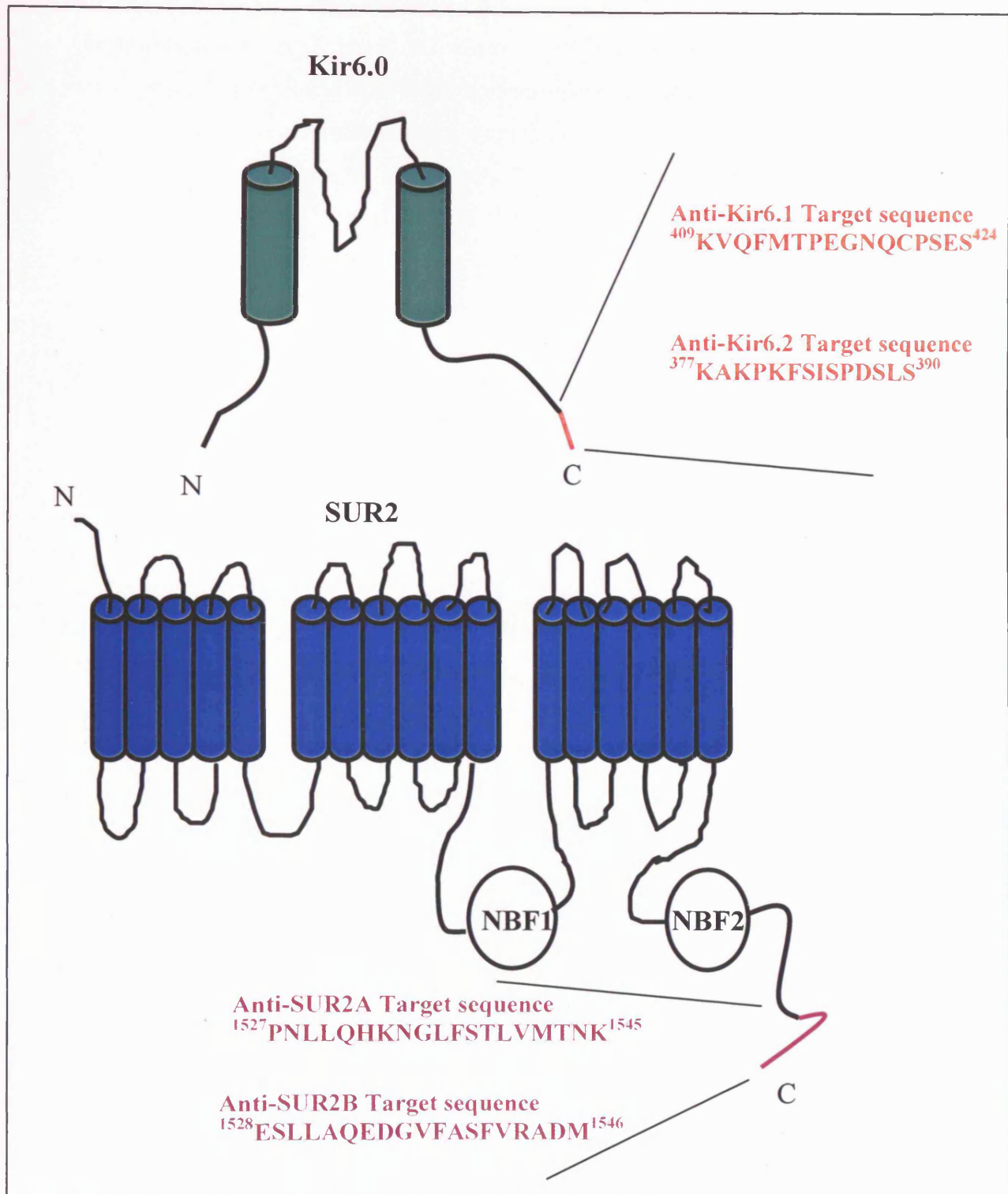


Figure 6.1. Primary antibodies and their target epitope. The antibodies were utilized in immunocytochemistry and phosphorylation experiments. All antibodies were raised in rabbit to target peptide in the C-terminal of the K_{ATP} channel subunits.

6.2. Localization of Kir6.0 and SUR2 subunits

The application of Kir6.0 and SUR2 subunit specific antibodies in immunocytochemistry and Western blot experiments of isolated rat cardiac myocytes and subcellular fractions, respectively, was employed to investigate the localization of cardiac K_{ATP} channel subunits and identify the possible molecular composition of sarc K_{ATP} and mito K_{ATP} channels. Antibody-associated immunofluorescence observed in confocal microscopy and staining in Western blots of isolated rat cardiac myocytes showed that all four K_{ATP} channel subunits were present.

6.2.1 Kir6.1 subunit

The Kir6.1 subunit was shown to be associated predominantly with the mitochondria of cardiac ventricular myocytes. Confocal microscopy using the anti-Kir6.1 antiserum revealed an intracellular distribution of the Kir6.1 subunit associated with myofibril structures. Mitochondria are known to associate with myofibril structures and, since anti-Kir6.1 immunofluorescence was significantly co-localised with the mitochondrial marker MitoFluor red, these findings suggest that Kir6.1 is the predominant K_{ATP} channel pore forming subunit in the mitochondria of ventricular myocytes. This result was corroborated by the strong staining by anti-Kir6.1 antiserum of a polypeptide of 48 kDa in Western blots of mitochondrial fractions. Occasional punctate localization of Kir6.1 just under the sarcolemma was observed immunocytochemically and staining of a polypeptide of 48 kDa in Western blots of microsomal membrane fractions isolated from rat heart was consistent with a localization in another non-mitochondrial vesicular or sarcolemmal structure.

The presence of Kir6.1 proteins in mitochondrial fractions prepared from rat skeletal muscle and liver has been determined previously using an anti-Kir6.1 antibody raised to a different epitope (amino acid residues corresponding to 375-386 of rat Kir6.1; Suzuki et al., 1997). Their findings confirm the mitochondrial localization of the Kir6.1 subunit suggested from immunoblots performed on mitochondrial fractions, which the anti-Kir6.1 antibody revealed a 47 kDa polypeptide corresponding to the Kir6.1 subunit. Immunostaining of ultrathin tissue sections by the immunogold method determined the distribution of anti-Kir6.1 antibody binding to the mitochondrial inner membrane in skeletal muscle (Suzuki et al., 1997). Gold staining

was observed over the matrix and cristae in mitochondria, but not along the outer membrane.

Electrophysiological properties of mitochondrial K_{ATP} channels have been reported in a purified mitochondrial inner membrane protein fraction, which were inhibited by sulfonylureas and activated by KCO (Takata et al., 1990). From their localization study, Suzuki et al., (1997) suggested that the Kir6.1 subunit might constitute a possible isoform of the mitochondrial K_{ATP} channel present on the inner membrane. In a recent test of whether the Kir6.1 subunit is an essential component of the mito K_{ATP} , adenovirus encoding either dominant-negative Kir6.1 or Kir6.2 subunits, in which the pore signature sequence GFG was mutated to AFA, were constructed to knock out current carried by SUR/Kir6.0 channels (Seharaseyon et al., 2000a). The AFA mutation eliminates the ability of the channel to conduct K^+ but does not prevent the mutant subunit from co-assembling with native K_{ATP} channel subunits. The Kir6.2AFA virus, but not the Kir6.1AFA virus, could suppress native sarc K_{ATP} current in isolated rabbit cardiomyocytes, but transfection of adult myocytes with the dominant-negative Kir6.1AFA subunit had no effect on the mitochondrial redox response to diazoxide (Seharaseyon et al., 2000b), which was interpreted to indicate that Kir6.1 is not a part of mito K_{ATP} . However, a recent study has shown no effect on mitochondrial membrane potential in isolated guinea-pig ventricular myocytes with the putative mito K_{ATP} channel opener diazoxide and that diazoxide regulates succinate oxidation rather than mito K_{ATP} channel, causing a changing in mitochondrial redox state (Hanley et al., 2002; section 1.13.1). This suggests that the Kir6.1 subunit could still contribute to the mito K_{ATP} channel structure, since the selectivity of diazoxide as a mito K_{ATP} channel, suggested by Seharaseyon et al., (2000b), remains questionable.

The Kir6.1 subunit has been shown to associate with the actin cytoskeleton in mouse ventricular myocytes (Rosner et al., 2002). Clear expression of Kir6.1 was observed in the sarcolemma when isolated mouse cardiac myocytes were stained with Kir6.1 antibody by immunocytochemistry. Kir6.1 proteins co-localized strongly with the actin cytoskeleton after staining with FITC-phalloidin but no co-localization was observed with actinin or tubulin. As mentioned earlier the dominant-negative Kir6.1AFA mutant had no apparent effect on sarc K_{ATP} channel current in rabbit

ventricular myocytes (Seharaseyon et al., 2000b), suggesting that the localization of the Kir6.1 subunit to sarcolemma in isolated mouse cardiac myocytes is a species issue, where localization of Kir6.1 in cardiac myocytes might vary between species. While Yokoshiki et al., (1997a) indicated that there is a link between the F-actin cytoskeleton and K_{ATP} channels in mice, the role of Kir6.1 subunits associated with actin in mouse cardiac function and excitability still remains to be investigated.

In this study, a significant correlation observed between anti-Kir6.1-associated immunofluorescence and Mito-tracker distribution in isolated rat cardiac myocytes, plus the detection of Kir6.1 polypeptide in mitochondrial fractions strongly suggest Kir6.1 a part of the mito K_{ATP} channel.

6.2.2. Kir6.2 subunit

Kir6.2 subunits are widely held to comprise the pore of the sarc K_{ATP} channel from the resemblance of the properties of co-expressed Kir6.2/SUR2A expressed in heterologous systems with those of the native sarc K_{ATP} (Liu et al., 2001; Ashcroft et al., 2000) and from the reduction in functional sarc K_{ATP} channels in Kir6.2 knockout mice (Suzuki et al., 2002). Anti-Kir6.2 subunit associated immunofluorescence at low antiserum dilution (1/250) was observed predominantly on the cell boundary, but some weak internal localization was also observed. This is the first direct evidence in support of the contention that Kir6.2 subunits are present in the sarc K_{ATP} channel. Western blots on microsomal membrane fractions also revealed anti-Kir6.2 staining of a 40 kDa polypeptide corresponding to Kir6.2, consistent with a plasma membrane localization. The presence of the Kir6.2 subunit in mitochondria was also confirmed for the first time by recognition of a polypeptide of 40 kDa by anti-Kir6.2 antiserum in Western blots of isolated mitochondrial fractions. When the anti-Kir6.2 antiserum dilution was increased (1/500), the low immunofluorescence associated with intracellular structures became undetectable while a strong immunofluorescence was still associated with the sarcolemma. Together, these results suggest that Kir6.2 is the predominant Kir6.0 isoform in the sarcolemma and that it is also present at lower levels in mitochondria.

The presence of both Kir6.0 subunits in mitochondria in isolated cardiac myocytes suggests the possibility of co-assembly between the two subunits. Recently

heteromultimerization between Kir6.1 and Kir6.2 subunits in the presence of SUR2A has been shown (Pountney et al., 2001). Either dominant-negative Kir6.1 or Kir6.2 subunits (GFG residues of the pore region mutated to AAA) were able to suppress both wt Kir6.1/SUR2A and Kir6.2/SUR2A currents in transfected HEK293 cells. In co-immunoprecipitation experiments, Kir6.2 subunit was immunoprecipitated with Kir6.1 antibody and conversely, immunoprecipitation with Kir6.2 antibody co-immunoprecipitated Kir6.1 subunit from HEK 293 cell extracts. However, as discussed above, Seharaseyon et al., (2000a) were unable to demonstrate functional heteromultimeric Kir6.0 recombinant or native channels. Immunocytochemical studies are able to give an idea of the possible channel combinations which may arise in any one tissue but do not determine whether mixed oligomer channels are being functionally expressed. The determination of the presence of the Kir6.1 and Kir6.2 subunits together on the mitochondrial inner membrane does not necessarily suggest they can form heterologous functional channels. Co-immunoprecipitation experiments on detergent extracts of isolated mitochondrial fractions are required to resolve this tissue. Pilot experiments carried out in this study were inconclusive and restricted by yield of mitochondria from isolated myocytes.

6.2.3. SUR2A subunit

Consistent with the contention that SUR2A subunits comprise the sulphonylurea accessory subunit of the sarcK_{ATP} channel, from comparisons of functional properties of heterologously expressed Kir6.2/SUR2A channels and native channels (Liu et al., 2001; Ashcroft et al., 2000), a distinct localisation of anti-SUR2A-associated immunofluorescence to the cell boundary was observed in confocal microscopy of isolated cardiac myocytes. Consistent with a plasma membrane localization, anti-SUR2A staining was observed in Western blots on microsomal membrane fractions. Anti-SUR2A-associated immunofluorescence was also localised to intracellular structures when a lower dilution was used. This showed was a significant correlation with the distribution of the mitochondrial marker MitoFluor red indicative of a mitochondrial localisation of this subunit also.

Immunoblot analysis of isolated myocyte proteins with both anti-SUR2 subunit antisera resulted in the specific detection of multiple polypeptides. Staining of several polypeptides in the region of the predicted molecular weight (140 kDa), has been

observed in previous reports of SUR2 detection in Western blots (Giblen et al., 1999; Ashfield et al., 1999) but has either not been discussed or the data selected by letterboxing of selected bands. Since cross-reactivity between the two anti-SUR2 antisera was not seen in Western blots of expressed SUR2 subunits, it was likely that multiple detection of bands in tissue blots was not a product of low antibody specificity but rather the presence of a number of related antigenic polypeptides. Those polypeptides with apparent molecular weights near that predicted for the SUR2 subunits may have been either multiple glycosylation products of the target subunit or derived proteolytically from the native subunit. Staining of polypeptides with apparent molecular weights significantly lower than the predicted size are likely to have been derived proteolytically from the native subunit. Inclusion of protease inhibitor cocktails in all steps following myocyte dissociation did not reduce the number of polypeptides detected, suggesting that the SUR2A subunit is relatively labile on disruption of cardiac cells.

When the presence of SUR2A in mitochondria was further examined directly in immunoblots of mitochondrial proteins, anti-SUR2A antiserum was unable to detect polypeptides corresponding to SUR2A subunit under routine staining conditions. The inability to detect the presence of SUR2A, suggested from confocal microscopy, may have been due to the proteolytic lability of the SUR2A subunit. In *in vivo* phosphorylation experiments on isolated rat cardiac myocytes, the anti-SUR2A antiserum was able to immunoprecipitate [³²P]-labelled Kir6.1 polypeptide suggesting an association between Kir6.1 with SUR2A. Even though SUR2 was undetectable in Western blots of mitochondrial fractions to confirm localization of SUR2A in mitochondria, the immunofluorescence patterns displayed by both anti-SUR2A and anti-Kir6.1 and the co-immunoprecipitation of [³²P]-incorporated Kir6.1 polypeptide using anti-SUR2A strongly suggest the association between the two subunits and thus, localization of SUR2A in inner membrane of mitochondrial. Further experiments (section 6.3) are required to validate SUR2A as a subunit of the mitoK_{ATP} channel.

6.2.4. SUR1 subunit

Work by Liu et al., (2001) indicated that among the combinations of known SUR and Kir subunits expressed heterologously as surface channels, only Kir6.1/ SUR1 fits the

pharmacological profile for mitoK_{ATP}. The pharmacological profiles of the native mitoK_{ATP} channels in rabbit ventricular myocytes were compared with heterologously expressed K_{ATP} channels in HEK293 cells. All possible combinations of Kir6.0 and SUR1/2 subunits (Kir6.1/SUR1, Kir6.1/SUR2A, Kir6.1/SUR2B, Kir6.2/SUR1, Kir6.2/SUR2A and Kir6.2/SUR2B) were heterologously expressed in HEK293 cells, and the effect of the KCOs, diazoxide, pinacidil, P-1075, and blockers, glibenclamide, 5HD and HMR-1098, was characterized with the whole-cell, patch-clamp technique. The effect of these agents on mitoK_{ATP} channel activity in myocytes was monitored by mitochondrial oxidation. Table 6.2 summarises the results obtained by Liu et al., (2001).

Diazoxide activated Kir6.1/SUR1 and native mitoK_{ATP} channels with an EC₅₀ value of 10 μM and 27 μM, respectively. The EC₅₀ value of 10 μM to activate Kir6.1/SUR1 was close to the value that was reported by Garlid et al., (1996) on isolated mitochondria (2.3 μM). 5HD blocked diazoxide-induced Kir6.1/SUR1 channels with

Table 6.1. Pharmacology of heterologously expressed K_{ATP} channels (adapted from Liu et al 2001)

Tissue	Molecular Composition	Dia	Pina	P-1075	Gly	5HD	HMR-1098
	Kir6.1/SUR1	O	O	NE	C	C	NE
	Kir6.1/SUR2A	NE	O	O	C	NE	NE
VSM	Kir6.1/SUR2B	O	O	O	C	NE	NE
Pancreatic	Kir6.2/SUR1	O	O	O	C	C	C
Sarcolemmal	Kir6.2/SUR2A	NE	O	O	C	NE	C
VSM	Kir6.2/SUR2B	NE	O	O	C	NE	NE
Mitochondria	Unknown	O	O	NE	C	C	NE

VSM, vascular smooth muscle; Dia, diazoxide (100 μM); Pina, pinacidil (100 μM); P-1075 (100 μM); Gly, glibenclamide (10 μM); 5HD, 5-hydroxydecanonic acid (200 μM); HMR-1098 (10 μM); O, open; C, close; NE, no effect.

an IC_{50} value of 66 μ M, which was close to that required to block native mito K_{ATP} channels (95 μ M). These results showed diazoxide to be a selective mito K_{ATP} channel opener and 5HD a mito K_{ATP} channel blocker, which is consistent with results published by Garlid et al., (1996) and Sato et al., (1998), respectively. Together, the results of Liu et al., (2001) imply that mito K_{ATP} channels may contain structural motifs involved in drug binding similar to that of Kir6.1/SUR1.

In this study no staining of myocytes was seen with an anti-SUR1 subunit antiserum targeting amino acid residues 2-10 on the N-terminal domain of this subunit in immunocytochemistry experiments (not shown). Immunoblots performed on mitochondrial fractions using anti-SUR1 antiserum were unable to detect polypeptides corresponding to SUR1. It can be argued that anti-SUR1 antibody was poorly characterized and like SUR2A, it is possible that SUR1 was proteolytically labile in the mitochondrial fraction. Further work in characterizing the current anti-SUR1 antibody, together with preparation of a new anti-SUR1 antiserum to a different epitope is required before a conclusion can be made whether SUR1 is localized in mitochondria or not.

Recent studies by Hanley et al.,(2002) have demonstrated diazoxide and 5-HD act independent of mito K_{ATP} channels (section 1.13.1). Diazoxide was shown to inhibit succinate oxidation in submitochondrial particles isolated from pig heart rather having an effect on mito K_{ATP} targeting. The inhibitor of mito K_{ATP} , 5-HD was also shown to be a substrate for acyl-CoA synthetase, which is present on the outer mitochondrial membrane and matrix. Thus, the inferences from flavoprotein oxidation, seen as autofluorescence, that these drugs were acting pharmacologically via mito K_{ATP} channels may be in error (Liu et al., 1998; Sato et al., 1998; Liu et al., 2002). Likewise, the implication of a Kir6.1/SUR1 mito K_{ATP} channel from its similar pharmacological profile might also be misguided. Although the presence of Kir6.1 in mitochondria was confirmed in this study, the identity of any SUR partner (s) remains an open question.

6.2.5. *SUR2B* subunit

The distribution of anti-SUR2B-associated immunofluorescence in isolated cardiac myocytes was distinctly different to that observed with any of the other three anti- K_{ATP} channel subunit antisera. In this case, a distinct regular transverse striated pattern of labelling which coincided with the t-tubular structures (IXE11₂ antibody associated immunofluorescence) was observed.

The complex structure of cardiac muscle has made interpretation of early electrophysiological studies of the membrane currents in multicellular tissue difficult. One of the most important problems in cardiac multicellular tissue is the accumulation of K^+ in the intercellular clefts. These changes in the extracellular K^+ concentrations can distort the magnitude and time course of K^+ currents (Almers, 1972; Attwell and Cohen, 1977; Attwell et al., 1979). Many of these problems have been reduced by the use of enzymatically isolated single cardiac cells. However, single myocytes have numerous invaginations of the sarcolemmal membrane that could act as restricted spaces in which ions might accumulate during activation of transmembrane currents. For example, mouse ventricular myocytes have an extensive transverse tubule (t-tubule) system whose surface area makes up approximately 50 % of the total sarcolemmal membrane of the cells (Forbes et al., 1984). These tubules are about 50-100nm in diameter and, hence, the tubule lumen could readily accumulate ions during current flow across the t-tubule membrane.

Clark et al., (2001) were able to show the presence of a slow transient current (I_{tail}) following depolarisation of voltage-clamped mouse ventricular myocytes. The slow inward I_{tail} was blocked by 0.25mM $BaCl_2$, a blocker of inwardly rectifying K^+ current, I_K . Using a specific antibody against Kir2.1, Clark et al., (2001) were able to localize Kir2.1 in the t-tubules of mouse ventricular myocytes. The staining of Kir2.1 to the t-tubules, verified by co-localization with t-tubule membrane marker (wheat germ agglutinin conjugated to Oregon Green 488) was consistent with the electrophysiological data obtained in these cells. This strongly suggested that I_{tail} in mouse ventricular myocytes was produced by the activation of inward I_K in the t-tubules, resulting from K^+ accumulation in these membrane structures. Other studies have also supported these findings. Leonoudakis et al., (2001) showed that Kir2.2 is also localized to t-tubules in rat ventricular myocytes. When the gene encoding Ki2.2

was knocked out, I_K was reduced by 50 % (Zaritsky et al., 2001). Christé (1999) has reported that cultured rabbit ventricular myocytes lose a large portion of I_K and ATP-sensitive potassium current (I_{K-ATP}) conductance in parallel when cell membrane capacitance decays (Christé, 1999). A reduction in membrane capacitance has been attributed mainly to the disappearance of the t-tubules (Lipp et al., 1996; Mitcheson et al., 1996), thus suggesting that a major part of I_K and I_{K-ATP} are located in the t-tubule of rabbit ventricular myocytes.

The immunocytochemical evidence from the present study localizes the SUR2B subunit to t-tubules in rat isolated cardiac myocytes and provides direct evidence for the presence of a distinct ATP-sensitive K^+ channel in the t-tubule membrane. Additional studies exploring the physiological consequences of the t-tubule localization of K_{ATP} channels are required and may provide important insights into the functional role of these channels under physiological and pathological conditions. In addition, co-immunoprecipitation experiments will be required to determine the Kir6.0 partner for SUR2B in the T-tubule.

6.3. Future experiments regarding localization of K_{ATP} channel subunits:

In this study, immunocytochemistry and Western blots have demonstrated localization of Kir6.0 and SUR2 subunits to various cellular compartments of isolated rat cardiac myocytes and to some extent shown the possible subunits associated to sarc K_{ATP} and mito K_{ATP} channel. To validate the molecular composition of these channels determined by immunocytochemistry and Western blots, future biochemical experiments need to be performed.

Since in *in vivo* phosphorylation experiments the anti-SUR2A antibody was able to immunoprecipitate [^{32}P]-labelled Kir6.1 polypeptide from isolated cardiac cells labelled with [^{32}P] orthophosphate that had been challenged with adenosine, PMA, CCPA or even forskolin, suggesting an association between Kir6.1 with SUR2A in the mito K_{ATP} channel, trial co-immunoprecipitation experiments were performed on [^{35}S]-methionine-labelled cardiac myocytes using the characterized antibodies to investigate the association between Kir6.0 and SUR2 subunits. Cells were incubated with [^{35}S]-methionine (380 μ Ci) for 24 hours, lysed and immunoprecipitations performed as described in section 2.5. The result (not shown) was inconclusive as the

incorporation of [^{35}S]-methionine into Kir6.0 and SUR2 polypeptide was so low that it was hard to distinguish specific polypeptides from the background non-specifically precipitated polypeptides. A series of immediate experiments for the future would be:

- To improve [^{35}S]-methionine labelling of the polypeptides in isolated rat cardiac myocytes perhaps by extending the labelling period to allow K_{ATP} subunit labelling to come to steady state.
- To improve immunoprecipitation conditions to remove non-specific precipitated polypeptides. Possible solutions for this would be to preclear the cell lysate with appropriate control IgG corresponding to the host species of the primary antibody, in this case anti-rabbit IgG, with protein A-agarose before applying the primary antibodies. Alternatively, covalent coupling of primary antibody-protein A agarose or protein A-Sepharose conjugate could be adopted.

In addition, trial immunoprecipitation/Western blot experiments were carried out on lysed cardiac myocytes to determine the association of K_{ATP} channel subunits. The cell lysate was initially immunoprecipitated with anti-Kir6.0 and anti-SUR antibodies in the absence and presence of C-terminal specific peptides. Immunoprecipitated samples were electrophoresed and transferred to nitrocellulose membrane, followed by immunoblot staining using anti-Kir6.0 antibodies only. The anti-SUR2 antisera were not used in immunoblots, since secondary antibody alkaline phosphatase detection of primary antibody binding on the immunoblot also stained the immunoprecipitating anti- K_{ATP} channel subunit IgG that was present in the resolving gel for the precipitated subunits. Relatively large amounts of incompletely denatured IgG ran with similar electrophoretic mobilities to SUR2 subunits, thus masking the detection of the latter. Also, previous experiments had shown complex staining patterns due to proteolytic digest of native polypeptides (section 4.5), which would have made identification of specific bands difficult to detect amongst the background of high staining of immunoprecipitate IgG. Results obtained after immunodetection of anti-Kir6.0 were inconclusive. Although there was some evidence of antibody specific immunoprecipitation of Kir6.0 subunits, low yields of immunoprecipitation of target antigen with specific antibodies made confirmed identification of subunits in immunoblots problematic. Potential future experiments regarding the

immunoprecipitation/Western blot approach in detecting the molecular composition of cardiac K_{ATP} channels would be:

- To optimise conditions for the immunoprecipitation part of the experiment so that maximum immunoprecipitation of specific targeted polypeptide with specific antibodies could be achieved.
- To reduce binding of non-specific polypeptides in immunoblots by using a different detection system to alkaline phosphatase. For example, a biotin-avidin detection system.

Once the conditions for the above experiments are optimised, they will need to be performed also on mitochondrial fractions to confirm the presence of Kir6.1 and SUR2A subunit localization in mitochondria and to resolve the molecular composition of the mito K_{ATP} channel.

In this study, experiments were focused on the localization of Kir6.0 and SUR2A subunits, with less attention on SUR1. However, trial experiments were performed using a poorly characterized anti-SUR1 antibody in immunocytochemistry and Western blots to look for localization of SUR1 subunit in cardiac myocytes. In both trial immunocytochemistry and Western blots the SUR1 subunit was not detected and, thus, the association of the SUR1 subunit in cardiac myocytes was not investigated further. Characterizing the existing anti-SUR1 antibody or preparation of new antibody is necessary to establish whether SUR1 subunit is present in cardiac myocytes and especially in mitochondria.

In this study, Kir6.1 localization was predominantly in mitochondria with some traces under the plasma membrane associated with non-mitochondrial transport vesicles in isolated rat cardiac myocytes. A study by Rosner et al., (2001) has shown localization of Kir6.1 on sarcolemma associated with actin filaments and not in mitochondria in isolated mouse ventricular myocytes. This suggests that the distribution of Kir6.1 or even other K_{ATP} channels subunits may possibly vary in cardiac cells depending upon the species. To investigate if this is the case or not future immunocytochemistry experiments need to be performed on cardiac myocytes isolated from different species like mouse and human with the characterized K_{ATP} channel subunit specific antibodies.

6.4. Phosphorylation of cardiac K_{ATP} channels

Recent studies have shown that the activity of Kir6.2/SUR1 and Kir6.2/SUR2A channels can be regulated via PKA and PKC-mediated phosphorylation of the Kir6.2 subunit, respectively (Béguin et al., 1999; Light et al., 2000). In both cases, phosphorylation of the Kir6.2 subunit increased K_{ATP} channel current. Basal PKA-mediated phosphorylation has been observed in the SUR1 subunit, which on dephosphorylation reduces Kir6.2/SUR1 channel activity (Béguin et al., 1999). Phosphorylation of the SUR2A subunit has been reported not to be required for regulation of Kir6.2 by PKC as tsA201 cells expressing Kir6.2 Δ C26 alone (functional K_{ATP} channel in the absence of SUR) have been reported to show an increase in whole-cell K_{ATP} current on application of PMA (Light et al., 2000). Whether SUR2A is a substrate for PKA still remains to be investigated. Both Kir6.1 and Kir6.2 subunits have a number of consensus PKA and PKC phosphorylation sites within their amino acid sequence (Table 6.2). While PKA and PKC phosphorylation of Kir6.2 has been demonstrated, similar phosphorylation events on Kir6.1 have not been identified as yet.

	Kir6.1	Kir6.2
Consensus PKA sites	S-6, T-72, T-128, T149, T-190, S-218, S-312, S-326, S-354, S-385, S-391, S-395, S-403	T-28, S-37, T-139, T-180, S-208, T-224, S-303, S-327, S-372
Consensus PKC sites	T-110, S-224, T-345, S-354, S-379, S-385, S-391, S-397	S-37, T-190, T-336, T-345, S-363

Table 6.2. Kir6.0 phosphorylation consensus sites for PKA and PKC determined by using NetPhos 2.0 Prediction server (Center for Biological Sequence Analysis, BioCentrum-DTU, Technical University of Denmark).

6.4.1. *In vitro* phosphorylation of expressed Kir6.0 subunits

In this study, incubation *in vitro* with PKA and PKC resulted in phosphorylation of *in vitro* expressed Kir6.1 polypeptide, whereas the Kir6.2 polypeptide displayed phosphorylation with PKA and none whatsoever when incubated with PKC. Béguin et al., (1999) were also unable to observe PKC-mediated phosphorylation of the Kir6.2 subunit when coexpressed with SUR1 in oocytes. On the other hand, Light et al., (2000) have reported phosphorylation of a threonine residue at position 180 on the Kir6.2 Δ C26 subunit with PKC. Whether the removal of the 26 amino acids from the C-terminal affects the ability of PKC to act on Kir6.2 has not been investigated.

6.4.2. Kir6.1 as the major target for phosphorylation in cardiac K_{ATP} channels

Results obtained in *in vitro* experiments were consistent with those from phosphorylation experiments conducted *in vivo* on native cardiomyocytes. The Kir6.1 subunit was phosphorylated when isolated rat ventricular myocytes were stimulated with adenosine, forskolin or PMA. Adenosine acts on A_1 G_i -protein coupled-receptors, activation of which has been shown to protect the heart in anaesthetized rabbits during ischaemia (Thornton et al., 1992). A_1 receptor activation results in activation of PKC via the phospholipase C, DAG pathway. Forskolin, an activator of PKA, and PMA, an activator of PKC, both resulted in phosphorylation of the Kir6.1 in cardiomyocytes showing that PKA and PKC-mediated phosphorylation of the Kir6.1 subunit observed *in vitro* can be mirrored *in vivo*. No detectable phosphorylation of Kir6.2 or SUR2 subunits was observed when cardiac myocytes were stimulated with adenosine, forskolin or PMA suggesting that the Kir6.1 subunit is the major K_{ATP} channel substrate for phosphorylation in native cardiac myocytes. While SUR2A was not itself a substrate for PKA or PKC-mediated phosphorylation, immunoprecipitation with anti-SUR2A antisera after cell stimulation resulted in the immunoprecipitation of [32 P] labelled –Kir6.1. This observation provides the first direct evidence of the formation of Kir6.1/SUR2A oligomers in cardiomyocytes and since Kir6.1 was localised to mitochondria predominantly, SUR2A may represent the SUR subunit in the mito K_{ATP} channel, in spite of the inability to show this directly in immunoblot experiments in this study.

The Kir6.2 subunit from recombinant Kir6.2/SUR1 channels expressed in *Xenopus* oocytes has been shown to be phosphorylated by PKA on serine residue at position

372 (C-terminal; Béguin et al. 1999). In the present study neither PKA nor PKC-mediated phosphorylation of the Kir6.2 subunit was observed in native cardiac cells. The M1 domain and cytoplasmic domains of the Kir6.2 subunit are essential for surface expression of Kir6.0/SUR oligomers (Schwappach et al. 2000). It may be that the PKA consensus site at position 372 on Kir6.2 is masked by SUR2A in surface expressed Kir6.2/SUR2A cardiac channels making it difficult for PKA to act on Kir6.2 subunits in cardiac myocytes.

Ischaemic preconditioning (IP) may require phosphorylation of K_{ATP} channels by PKC or other kinases (Liu et al., 1996). In isolated rabbit cardiomyocytes, PMA potentiated the opening of K_{ATP} channels by pinacidil (non-selective KCO) when ATP levels were reduced by metabolic inhibition with potassium cyanide (Liu et al., 1996). Liu et al., (1996) also reported that adenosine has little effect on unstimulated myocytes, but it opens K_{ATP} channels after pretreatment with PMA, which suggests that PKC participates to open the channels. From co-localization and *in vivo* phosphorylation studies on rat isolated cardiac myocytes and biochemical analysis on rat mitochondrial fractions performed in this study, the localization of the Kir6.1 subunit to the mitochondria and its phosphorylation in response to a known mediators of ischaemic preconditioning suggests that the hypothesis involving mitoK_{ATP} in IP should be considered, in spite of contrary suggestion of Hanley et al., (2002).

Recent studies by Suzuki et al., (2002) (section 1.13.1) have shown that the sarcK_{ATP} channel, rather than the mitoK_{ATP} channel, can play a role in cardioprotection against ischaemia/reperfusion in mice. The group examined the effect that IP had on infarct size in Kir6.2-deficient (knockout mice; KO) ventricular tissues. Infarct size was substantially higher in KO compared to wild type mice ventricular cells. In both WT and KO ventricular cells, mitoK_{ATP} channel function was preserved suggesting that the sarcK_{ATP} channel must play a vital role in cardioprotection against ischaemia. In the present study, mediators of IP, appeared to be unable to phosphorylate either subunits of the sarcK_{ATP} channel, Kir6.2/SUR2A, suggesting regulation of sarcK_{ATP} channel activity during IP from a mechanism other than direct phosphorylation. It may be possible that phosphorylation of the mitoK_{ATP} channel on the Kir6.1 subunit regulates the activity of the sarcK_{ATP} channel, which causes IP. How the phosphorylation event in the mitochondrial channel may be transduced to modify the

activity of the sarc K_{ATP} remains enigmatic but could involve modulation of the levels of ATP.

6.4.3. Protein kinase C phosphorylates Serine 379 directly in the Kir6.1 subunit in rat isolated ventricular myocytes

As discussed in section 1.13.2, both PKC and tyrosine kinases are involved in ischaemic preconditioning, which probably activate a much larger kinase cascade. One of the major kinase cascades in the mammalian heart is the highly conserved mitogen activated protein kinase MAPK family. These enzymes can be activated by receptor tyrosine kinases, PKC, G-protein-coupled receptors and cellular stress. The three major MAPK pathways identified in the heart are the extracellular signal-regulated kinases (ERK1/2) and the two stress-activated MAPK families, c-JUN N-terminal kinases (JNK) and the p38MAPK (Robinson et al., 1997) (Figure 6.2).

The ERK1/2 kinase pathway is activated by growth and G-protein-coupled receptors (Sugden et al., 1995), but there is no evidence of its involvement in IP (Maulik et al., 1998). The JNK family (JNK1 and JNK2) are activated by upstream MAPK kinase (MKK4 and MKK7, Clerk et al., 1998; Deacon et al., 1997). MKK4 is also capable of activating p38MAPK, as well as JNK (Deacon et al., 1997). Brief periods of ischaemia/reperfusion have been shown to activate the JNK pathway (Clerk et al., 1998). Furthermore, activation of G_q -coupled receptors and subsequent activation of PKC has been shown to activate JNK (Nagao et al., 1998). In addition, rabbit cardiomyocytes transfected with cDNA encoding PKC- ϵ have induced activation of JNK (Ping et al., 1998).

The p38MAPK is activated by MKK3, MKK4 and MKK6 (Sugden et al., 1998), which targets MAPK-activated protein kinase 2 (MAPKAPK-2, Freshney et al., 1994). The activity of MAPKAP-2 has been reported to increase in preconditioned rat hearts (Maulik et al., 1996). Evidence also suggests that activation of PKC elevates MAPKAPK-2 activity in neonatal rat ventricular cardiomyocytes (Clerk et al., 1998). However, there is still considerable controversy over whether PKC is capable of activating the p38MAPK pathway (Raingeaud et al., 1995; Zanke et al., 1996). These observations suggest that there may be a link between PKC activation and the stress-activated protein kinase cascade and that PKC activation might result in

phosphorylation of the mito K_{ATP} channel via activation of the JNK or p38MAPK kinase pathway.

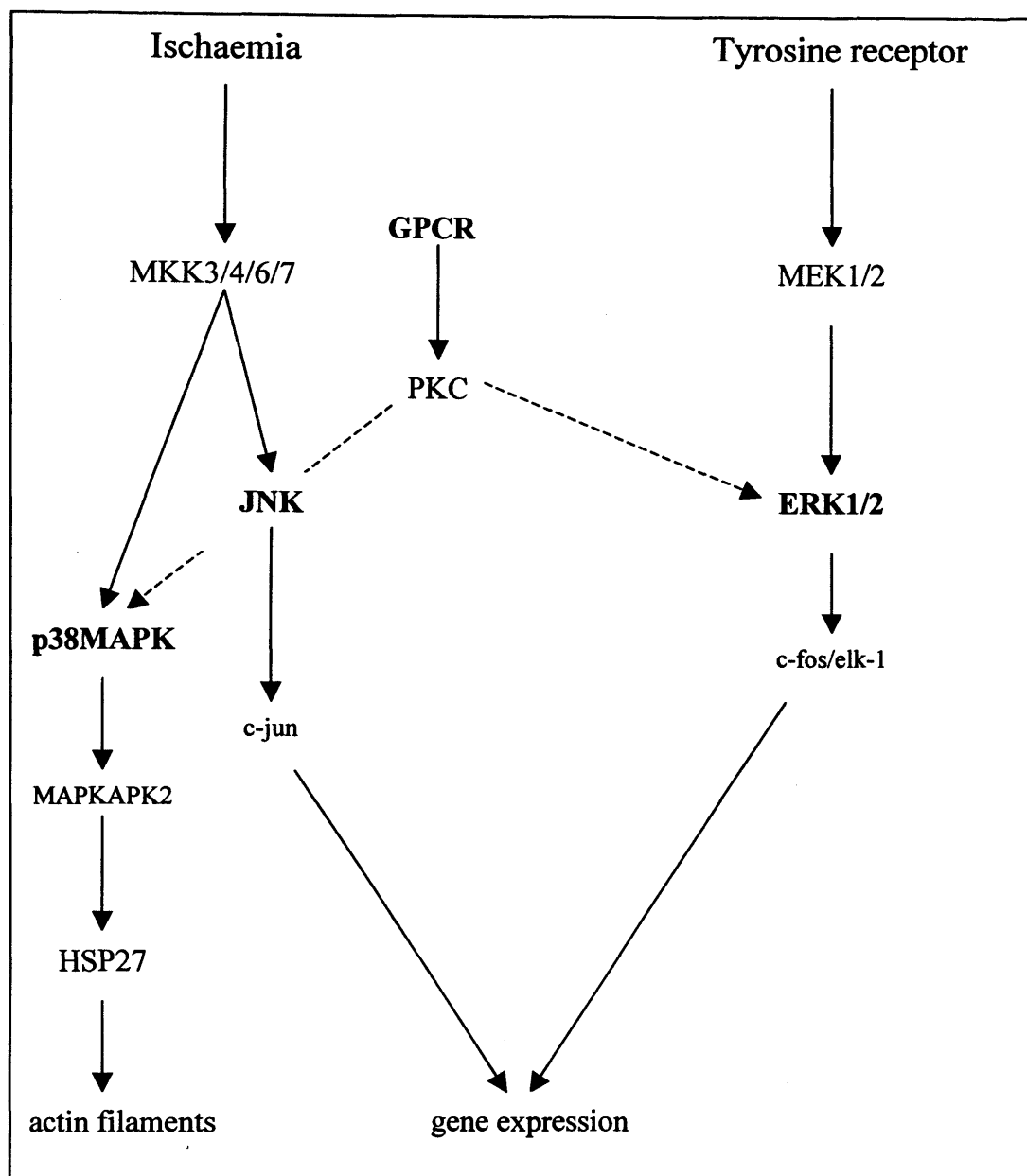


Figure 6.2. A simplified scheme of the three major mitogen-activated protein kinase (MAPK) cascades (adapted from Cohen et al., 2000). The three MAPKs, p38/RK, JNK, and extracellular signal-regulated kinases 1/2, are indicated in bold-faced type. Activation of either of the two stress-activated protein kinases, p38 MAPK or JNK, has been implicated in ischaemic preconditioning.

Stimulation of rat cardiomyocytes with the adenosine A₁-receptor agonist, CCPA, in the presence of PKC inhibitor, chelerythrine, resulted in significantly reduced phosphorylation of the Kir6.1 subunit compared to myocytes stimulated with CCPA alone. The p38MAPK inhibitor (SB203580) and MEK1/2 inhibitor (U0126) at saturating concentrations had no effect on Kir6.1 phosphorylation when applied in conjunction with CCPA on cells. On the other hand the JNK inhibitor did display some inhibition (20 %) of Kir6.1 phosphorylation but this was much less than that observed by chelerythrine. From the effects of the three kinase selective inhibitors on K_{ATP} channel Kir6.1 subunit phosphorylation, it was concluded that the stress-activated JNK and p38MAPK pathways and the G-protein-coupled receptor activated ERK pathway are unlikely to be involved in the direct regulation of cardiac K_{ATP} channels in native tissue. This implies strongly that PKC acts directly on the mitoK_{ATP} channel Kir6.1 subunit in rat isolated ventricular myocytes and is consistent with this subunit being a direct substrate *in vitro*.

Phosphorylation *in vitro* of Kir6.1/Kir6.2 chimaeras (constructed by Dr H. Kuhlman, PhD, 2002) was employed to narrow the action of PKC on Kir6.1 to amino acids I²⁸⁰-S⁴²⁴ (Figure 5.9). PKC-mediated phosphorylation was observed in reactions containing the 1121 chimaera (where amino acids encoding in the region between the *Sph* I and *EcoRV* sites (Figure 5.9) in Kir6.1 coding sequence were substituted with Kir6.2) and 213 chimaera (where amino acids encoding region between the *Sph* I site and the C-terminal of Kir6.2 were substituted with Kir6.1). Conversely, phosphorylation was not seen in reactions containing 1121 and 123 chimaeras (the reverse of 1121 and 213 chimaeras). Phosphoamino acid analysis on Kir6.1 polypeptide phosphorylated *in vitro* with PKC revealed a serine residue (s) as the phosphate acceptor. Five potential PKC serine sites (S354, S379, S385, S391 and S397) within PKC consensus sequence in the Kir6.1 amino acid region I²⁸⁰-S⁴²⁴ were mutated to alanine residues, expressed using *in vitro* transcription/translation and subjected to the *in vitro* PKC phosphorylation assay. All single serine mutants were phosphorylated to approximately the same levels as WT Kir6.1 except for the S379A mutant, indicating this residue as the phosphate acceptor for PKC phosphorylation.

6.4.4. Possible implication of PKC-mediated phosphorylation of the Mito K_{ATP} channel Kir6.1 subunit in ischaemic preconditioning

Immunocytochemistry on isolated rat ventricular myocytes and immunochemical staining of electrophoretically separated proteins from subcellular fractions suggest Kir6.1 as a component of the mito K_{ATP} channel. If PKC phosphorylation of the Kir6.1 subunit in the mito K_{ATP} channel is relevant to protection of the heart during periods of prolonged ischaemia, the question is raised concerning the likely functional outcome of the phosphorylation event to cellular function. It is still not clear why opening of mito K_{ATP} channels is cardioprotective but three main hypotheses have been proposed to explain the possible protective effect of mito K_{ATP} channel opening, possibly in response to PKC phosphorylation of Kir6.1 (Figure 6.3). These hypotheses may all contribute to cardioprotection, but it is still undetermined whether they play a role in either acute or delayed preconditioning *in vivo*.

Mitochondrial swelling: In steady-state conditions, K^+ influx into the mitochondrial matrix is balanced by K^+ efflux via a K^+/H^+ exchanger, which possibly maintains mitochondrial volume (Garlid et al., 1996b). However, opening of mito K_{ATP} channels would cause a net influx of K^+ and, hence, increase matrix volume causing mitochondrial swelling outcome. Alternatively, because of the K^+/H^+ exchanger, K^+ influx would tend to dissipate the potential across the inner membrane and uncouple electron transfer. This may be beneficial in ischaemia as it may prevent wasteful ATP hydrolysis (Garlid et al., 1997). Alternatively, improved ATP production in mitochondria as a common feature during preconditioning is also shown by Fryer et al., (2000), where mitochondria isolated from the area at risk in preconditioned hearts had higher rates of ATP synthesis than those of hearts subjected to long ischaemia alone. ATP production in IP hearts was partially inhibited by 5-HD. Matrix swelling has also been shown to activate fatty acid oxidation, respiration, and ATP production (Halestrap et al., 1989), thus improving the rate of oxidative metabolism in mitochondria.

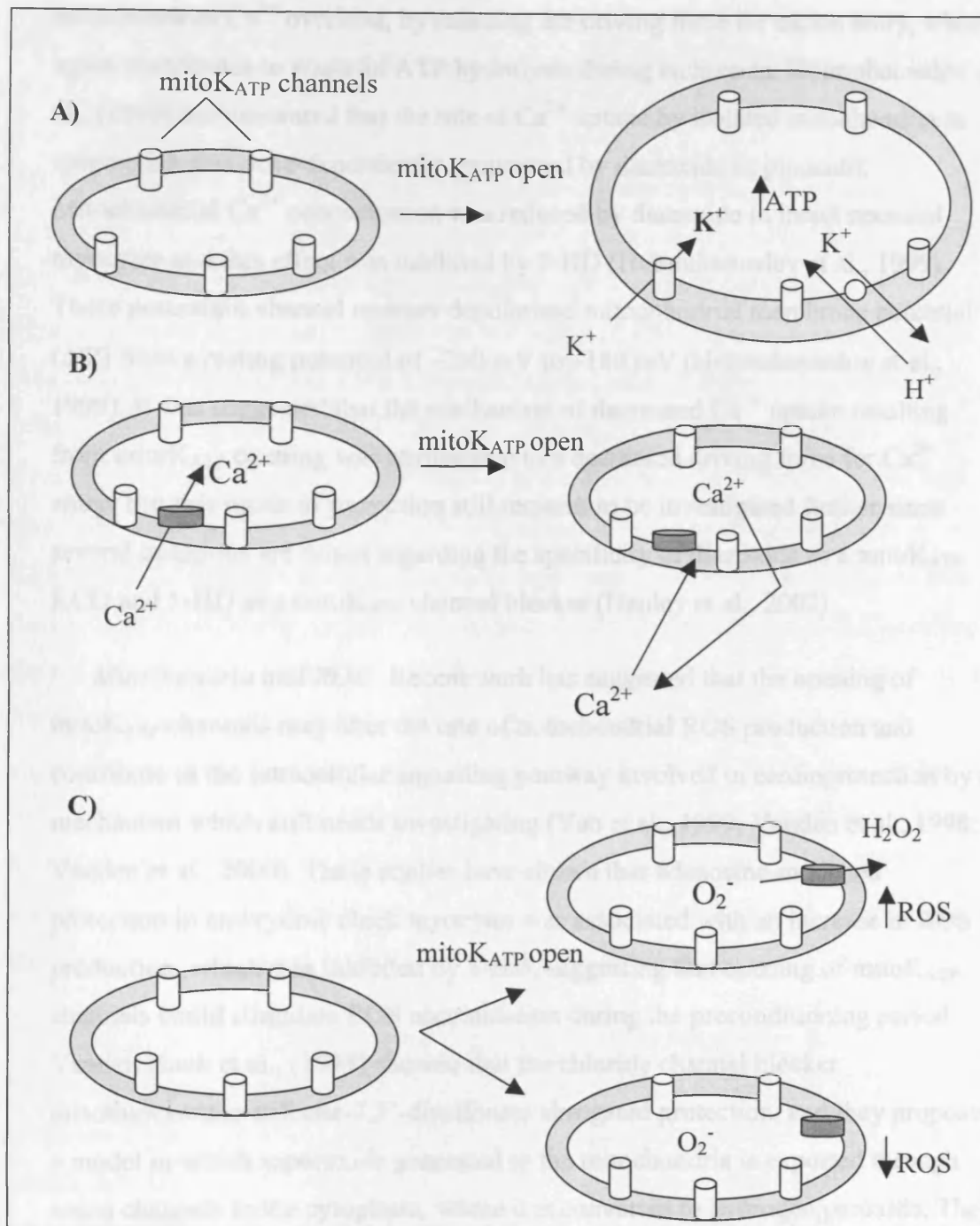


Figure 6.3. Putative mechanisms of protection mediated by mitoK_{ATP} channel opening adapted from O'Rourke et al., 2000. A, Mitochondrial volume, determined by the balance between salt influx and efflux from the matrix, may be adjusted to optimise energy production during ischaemia and reperfusion. B, Mitochondrial Ca^{2+} overload during ischaemia or reperfusion may be slowed by depolarisation of the mitochondrial membrane potential, and Ca^{2+} release may be initiated by permeability transition pore opening. C, ROS production by the mitochondria may be enhanced during early ischaemia to trigger protection but inhibited during reperfusion to mitigate damage (O'Rourke et al., 2000).

Mitochondrial Ca^{2+} handling: The opening of $mitoK_{ATP}$ decreases mitochondrial Ca^{2+} overload, by reducing the driving force for cation entry, which again contributes to wasteful ATP hydrolysis during ischaemia. Holmuhamedov et al., (1999) demonstrated that the rate of Ca^{2+} uptake by isolated mitochondria in suspension was dose-dependently suppressed by diazoxide or pinacidil. Mitochondrial Ca^{2+} concentration was reduced by diazoxide in intact neonatal myocytes and this effect was inhibited by 5-HD (Holmuhamedov et al., 1999). These potassium channel openers depolarised mitochondrial membrane potential ($\Delta\Psi$) from a resting potential of -200 mV to -180 mV (Holmuhamedov et al., 1999). It was suggested that the mechanism of decreased Ca^{2+} uptake resulting from $mitoK_{ATP}$ opening was attributable to a decreased driving force for Ca^{2+} entry. But this mode of protection still remains to be investigated further since several questions are raised regarding the specificity of diazoxide as a $mitoK_{ATP}$ KCO and 5-HD as a $mitoK_{ATP}$ channel blocker (Hanley et al., 2002).

Mitochondria and ROS: Recent work has suggested that the opening of $mitoK_{ATP}$ channels may alter the rate of mitochondrial ROS production and contribute in the intracellular signalling pathway involved in cardioprotection by a mechanism which still needs investigating (Yao et al., 1999; Vanden et al., 1998; Vanden et al., 2000). These studies have shown that adenosine-mediated protection in embryonic chick myocytes was associated with an increase in ROS production, which was inhibited by 5-HD, suggesting that opening of $mitoK_{ATP}$ channels could stimulate ROS accumulation during the preconditioning period. Vanden Hoek et al., (1998) showed that the chloride channel blocker diisothiocyanato-stilbene-2,2'-disulfonate abrogated protection, and they proposed a model in which superoxide generated in the mitochondria is exported through anion channels to the cytoplasm, where it is converted to hydrogen peroxide. They have also shown that hydrogen peroxide was capable of significantly protecting chick embryonic ventricular cells from cell death during subsequent ischaemia/reperfusion and that this protection against cell death was inhibited on application of Cu,Zn-superoxide dismutase inhibitor, diethyldithiocarbamic acid suggesting hydrogen peroxide causes protection in chick cardiomyocytes. Interestingly, mitochondrial ROS production was attenuated by pinacidil (KCO) when applied just at the time of reperfusion, but this effect was eliminated in the

presence of 5-HD or a PKC inhibitor, suggesting that mito K_{ATP} opening during reperfusion attenuates ROS production (Vanden Hoek et al., 1998). The link between mito K_{ATP} opening, ROS generation, and PKC remains incompletely defined at present.

All the above hypotheses argue that it is essential for the mito K_{ATP} channel to be open, probably via activation in response to PKC (Wang et al., 1999; Liu et al., 2002; Sato et al., 1998; section 1.13.1), to cause preconditioning. Recent studies by Thorneloe et al., (2002) have shown that the action of PKC on Kir6.1 inhibits, rather than activates, recombinant Kir6.1/SUR2B channel activity expressed in HEK 293 cells. The effect of the PKC activator, phorbol ester (PdBu), on recombinant Kir6.1/SUR2B and Kir6.2/SUR2B channel current induced by 50 μ M pinacidil was examined in HEK 293 cells. PdBu (50 nM) caused a time-dependent decrease in Kir6.1/SUR2B channel activity, which was suppressed following pre-treatment with the PKC inhibitor, chelerythrine (Thorneloe et al., 2002). In contrast, PdBu increased the activity of recombinant Kir6.2/SUR2B, implying that a site (s) on the pore-forming subunits, Kir6.1 and Kir6.2, were the target for PKC. No biochemical experiments were performed to confirm phosphorylation of the Kir6.0 subunits by PKC, whereas in this study PKC-mediated phosphorylation was observed biochemically on the Kir6.1 but not Kir6.2. It may be possible that the SUR2A subunit is masking the PKC phosphorylation site on the Kir6.2 in cardiac myocytes, thus preventing phosphate labelling of the Kir6.2 subunit in this study.

Thorneloe et al., (2002) also showed that PKC, activated in response to vasoconstrictors like angiotensin II, also showed inhibition of Kir6.1/SUR2B current in the presence of pinacidil, suggesting PKC-mediated phosphorylation of the Kir6.1 inhibit vascular smooth muscle Kir6.1/SUR2B K_{ATP} channels causing vasoconstriction of these cells by enhancing Ca^{2+} influx through voltage-gated L-type Ca^{2+} channels. This conflicts with the proposed mechanism in this study, which suggests phosphorylation of Kir6.1 by IP mediators, via PKC, must activate rather than inhibit K_{ATP} channels to cause an IP event. Until the regulatory effect of PKC on mito K_{ATP} channels, which from this study is suggested to be Kir6.1/SUR2A, in native cardiac cells is investigated electrophysiologically, the exact role of Kir6.1 phosphorylation in cardiomyocytes cannot be determined.

6.5. Future experiments regarding phosphorylation of K_{ATP} channel subunits:

To discover if PKC-mediated phosphorylation of the Kir6.1 subunit in native mitoK_{ATP} channels plays a vital role in ischaemic protection, a number of electrophysiological experiments need to be performed.

- First of all, the electrophysiological and pharmacological properties of the proposed mitoK_{ATP} channel, Kir6.1/SUR2A, needs to be investigated. In the past co-expression of this pair of subunits has failed to induce K⁺ conductance that can be activated by metabolic inhibition (Aguilar-Bryan et al., 1997). However Kir6.1/SUR2A channels transiently transfected in HEK 293 cells have been reported to activate on application of pinacidil and P-1075, and to be inhibited on addition of glibenclamide (Liu et al., 2001).
- The regulatory effect of PKC on wild type and mutant mitoK_{ATP} channel needs to be investigated by performing electrophysiological studies on recombinant Kir6.1/SUR2A and Kir6.2S379A/SUR2A channels expressed in mammalian cell lines as well as in native cardiomyocytes.
- If electrophysiological studies show PKC activates wild type mitoK_{ATP} channels (Kir6.1/SUR2A) and has no effect on mutant channels, experiments need to be performed confirming PKC phosphorylation of the Kir6.1 subunit in mitoK_{ATP} are involved in some sort of cardioprotection. Experiments need to be designed where protection can be compared between wild type cardiac cells expressing Kir6.1/SUR2A and cells expressing Kir6.1S379A/SUR2B channels (probably by looking at cell survival) from a hypoxic preconditioning model after stimulating the cells with a PKC activator, like PMA. This is a complicated procedure since the WT Kir6.1/SUR2A needs to be suppressed in myocytes transfected with mutant mitoK_{ATP} channels. The use of small interfering RNA (siRNA) would be one way to overcome this problem. Like dsRNA, siRNA has proven to suppress gene expression that is homologous to its sequence through a process known as RNA interference (RNAi). However, in most mammalian cells dsRNA provokes a non-specific cytotoxic response. siRNAs appears to suppress gene expression without producing a non-specific cytotoxic response.

In this study PKA-mediated phosphorylation of the Kir6.1 subunit *in vivo* was observed in isolated rat cardiac myocytes. The site (s) of PKA action on the Kir6.1 remains to be investigated. Initial experiments would employ methods used in identifying serine 379 as a PKC phosphorylation site on Kir6.1 subunit. Also the functional significance of PKA phosphorylation of the Kir6.1 subunit in cardiac K_{ATP} channels will need to be examined.

In vivo phosphorylation of the SUR2 subunits was not observed in cardiac myocytes in this study. However both SUR1 and SUR2 have been shown to contain consensus sites for PKA and PKC phosphorylation (Aguilar-Bryan et al., 1995; Inagaki et al., 1996; Isomoto et al., 1996). Béguin et al., (1999) have identified the PKA phosphorylation site on a serine residue at position 1571 in the SUR1 subunit but were unable to show SUR1 phosphorylation by PKC. Immediate future experiments would be to investigate *in vitro* PKA and PKC-mediated phosphorylation of SUR1 and SUR2 polypeptides. Phosphorylated polypeptides then need to be explored further to identify site (s) responsible for phosphorylation and their regulatory significance.

Finally it would be interesting to mimic inhibition of Kir6.1/SUR2B channel activity on application of PKC activator in a mammalian cell line, like HEK 293, as shown by Thorneloe et al., (2002), and to investigate the potential role of S379 in this response both by phosphopeptide mapping and mass spectrometry or by expression of mutant S379A in cells where WT S379 is suppressed.

6.6. Summary and Conclusion

In this study the molecular composition and PKC-mediated phosphorylation site of cardiac K_{ATP} channels was investigated. The subunit composition of sarcolemma K_{ATP} channel (sarc K_{ATP}) and mitochondrial K_{ATP} channel (mito K_{ATP}) was further elucidated by immunocytochemistry on isolated rat ventricular myocytes using characterized C-terminal specific anti-Kir6.0 and anti-SUR2 antibodies. Staining of these antibodies revealed predominant localization of the Kir6.1 subunit in mitochondria, which was confirmed by co-localization using MitoFlour red. The Kir6.2 subunit was found in abundance in sarcolemma, with some present in mitochondria as well. The SUR2A subunit was not only localized in sarcolemma but was also found in mitochondria,

shown by co-localization with MitoFlour red, whereas the SUR2B subunit was distinctively present on T-tubules, confirmed by co-localization with anti-IXE11₂ (T-tubule marker). These findings were further established by Western blots, which were performed on subcellular fractions isolated from rat heart. The presence of polypeptides corresponding to Kir6.2 and SUR2A proteins in microsomal membrane fractions, which contained plasma membrane, suggest Kir6.2 association with SUR2A to form a typical sarcK_{ATP} channel. The sulfonylurea receptor subunit associated with Kir6.1 and, thus, the molecular composition of mitoK_{ATP} channel was not determined as Western blots on mitochondria fractions did not reveal specific staining for SUR2A/2B or 1, possibly due to lability of the SUR in this preparation. Interestingly, [³²P]-Kir6.1 was co-immunoprecipitated by anti-SUR2A from whole myocyte extracts after stimulation of PKA and PKC suggesting that these subunits are associated. The mitochondrial localization of Kir6.1 suggests that SUR2A could be its partner in this organelle.

PKC-mediated phosphorylation of cardiac K_{ATP} channel subunits was investigated in *in vitro* and *in vivo*. In *in vitro* experiments, expressed Kir6.1 polypeptide was phosphorylated with PKA and PKC, whereas Kir6.2 was phosphorylated by PKA alone. The Kir6.1 polypeptide in isolated rat ventricular myocytes was the only K_{ATP} channel subunit phosphorylated on stimulation of PKC (adenosine; PMA) or PKA (Forskolin). Complete inhibition of phosphorylation with chelerythrine (PKC inhibitor), but not with SB203580 (p38MAPK), U0126 (MEK1/2) and JNK 1 inhibitor suggest a direct PKC-mediated phosphorylation of the Kir6.1 polypeptide in native tissue. *In vitro* phosphoamino acid analysis and phosphorylation of expressed Kir6.1/6.2 chimaeras showed PKC-mediated phosphorylation of the Kir6.1 polypeptide located on a serine residue between amino acids 280-424, which later, by *in vitro* phosphorylation experiments on expressed Kir6.1 point mutants, confirmed Serine 379 residue as the site for PKC action.

References

- Aguilar-Bryan L, Nichols CG, Wechsler SW, Clement JP IV, Boyd AE III, et al. 1995. Cloning of the beta cell high-affinity sulfonylurea receptor: a regulator of insulin secretion. *Science* **268**:423–26
- Almers, W. (1972) The decline of potassium permeability during extreme hyperpolarization in frog skeletal muscle. *Journal of physiology*, **225**, 57-83
- Armstrong, C.M. and Bezanilla, F. (1977) Inactivation of the sodium channel. II. Gating current experiments. *J. General Physiology* **70**, 567-590
- Armstrong, S.C., Liu, G.S., Downey, J.M., Ganote, C.E. (1995) Potassium channels and preconditioning of isolated rabbit cardiomyocytes: effects of glyburide and pinacidil. *J. Mol. Cell. Cardiol.* **27**, 1765-1774
- Ashcroft FM, Kakei M. 1989. ATP-sensitive K⁺ channels in rat pancreatic beta-cells: modulation by ATP, Mg²⁺ ions. *J. Physiol.* **416**:349–67
- Ashfield, R., Gribble, F.M., Ashcroft, S.J.H., Ashcroft, F.M. (1999) Identification of the high-affinity tolbutamide site on the SUR1 subunit of the K_{ATP} channel. *Diabetes* **48**, 1341-13347
- Atherton E, Sheppard RC 1985 Solid-phase peptide synthesis using N-alpha-fluorenylmethoxycarbonylamino acid pentafluorophenyl esters. *J. Chem. Soc.* **3**:165-166
- Atkinson, N., Robertson, G. and Ganetzky. (1991) A component of calcium-activated potassium channels encoded by the *Drosophila* slo locus. *Science* **253**, 551-555
- Attwell, D.E. and Cohen, I.S. (1977) The voltage clamp of multicellular preparations. *Progress in Biophysics and molecular Biology*, **31**, 201-245

- Attwell, D.E. and Cohen, I.S. (1979) Voltage clamp and tracer flux data: effects of a restricted extracellular space. *Quarterly Review of Biophysics* **12**, 213-263
- Auchampach J.A., Gross GJ. 1993. Adenosine A₁ receptors, K_{ATP} channels, and ischemic preconditioning in dogs. *Am J Physiol.* **264**: H1327-H1336
- Aynsley-Green, A., Polak, J. M., Bloom, S. R., Gough, M. H., Keeling, J., Ashcroft, S. J. H., Turner, R. C., and Boum, J. D. (1981) Nesidioblastosis of the pancreas: definition of the syndrome and the management of the severe neonatal hyperinsulinaemic hypoglycaemia. *Arch. Dis. Child.* **56**, 496-508
- Azzaria, M., Schurr, E. and Gros, P. (1989) Discrete mutations introduced in the predicted nucleotide binding sites of the *mdr-1* gene abolish its ability to confer multidrug resistance. *Mol. Cell. Biol.*, **9**, 5289-5297
- Babenko A.P., Aguilar-Bryan L. and Bryan J. 1998 A view of SUR/K_{IR} 6.X, K_{ATP} channels. *Annu. Rev. Physiol.* **60**:667-687
- Baines, C.P., Wang, L., Cohen, M.V., Downey, J.M. (1998) Protein tyrosine kinase is downstream of protein kinase C for ischemic preconditioning's anti-infarct effect in the rabbit heart. *J. Mol. Cell. Cardiol.* **30**, 383-392
- Baines, C.P., Goto, M. and Downey, J.M. (1997) Oxygen radicals released during ischemic preconditioning contributes to cardioprotection in the rabbit myocardium. *J. Mol. Cell. Cardiol.* **29**, 207-216
- Baukowitz, T., Schulte, U., Oliver, D., Herlitz, S., Krauter, T., Tucker, S. J., Ruppersberg, J. P. & Fakler, B. (1998) *Science* **282**, 1141-1144

- Beavis, A.D. (1992) Properties of the inner membrane anion channel in intact mitochondria. *J Bioenerg Biomembr.* **24**: 77-90.
- Beech, D. J., Zhang, H., Nakao, K., Bolton, T. B. (1993) K channel activation by nucleotide diphosphate and its inhibition by glibenclamide in vascular smooth muscle cells. *Br. J. Pharmacol.* **110**, 573-582
- Benson, D.W., MacRae, C.A., Vesely, M.R., Walsh, E.P., Seidman, J.G., Seidman, C.E. and Salter, C.A. (1996) Missense mutation in the pore region of HERG causes familial long QT syndrome. *Circulation* **93**, 1791-1795
- Benzanilla, F. and Stefani, E. (1994) Voltage-dependent gating of ionic channels. *Annual Review of Biophysics* **23**, 819-846
- Béguin P, Kazuaki Nagashima, Motoi Nishimura, Tohru Gono, and Susumu Seino. PKA-mediated phosphorylation of the human K_{ATP} channel: separate roles of Kir6.2 and SUR1 subunit phosphorylation . *EMBO J.* 1999 **18**: 4722-4732.
- Bond, C.T., Pessia, M., Xia, X.M., Lagrutta, A., Kavanaugh, M.P. and Adelman, J.P. (1994) Cloning and expression of a family of inward rectifier potassium channels. *Receptors and Channels* **2**, 183-191
- Bonev A.D, and Nelson M.T. (1996) Vasoconstrictors inhibit ATP-sensitive potassium channels in arterial smooth muscle through protein kinase C. *J. Gen. Physiol.* **108**:315-323.
- Browne, D.L., Gancher, S.T., Nutt, J.G., Brunt, E.R.P., Smith, E.A., Kramer, P and Litt, M. (1994) Episodic ataxia/myokymia syndrome is associated with point mutations in the human potassium channel gene, *KCNA1*. *Nature Genetics* **8**, 136-140

- Cahalan, M. and Neher, E. (1992) Patch clamp techniques: an overview. *Methods in Enzymology*, **23**, 141-165.
- Carson, M.R., Travis, S.M. and Welsh, M.J. (1995) The two nucleotide binding domains of the cystic fibrosis transmembrane conductance regulator (CFTR) have distinct functions in controlling channel activity. *J. Biol. Chem.*, **270**, 1711-1717
- Chance B, Salkovitz IA, Kovach AG. Kinetics of mitochondrial flavoprotein and pyridine nucleotide in perfused heart. *Am. J Physiol.* 1972; **223**:207–218.
- Chang, C.Y., Dworetzky, S.I., Wang, J. and Goldstein, M.E. (1997) Differential expression of the alpha and beta subunits of the large conductance calcium-activated potassium channel: implication for channel diversity. *Brain research. Molecular Brain Research* **45**, 33-40
- Christé, G. (1999) Localization of K⁺ channels in the t-tubules of cardiomyocytes as suggested by the parallel decay of membrane capacitance, I_K and I_{KATP} during culture and by delayed I_{K1} response to barium. *Journal of Molecular and Cellular Cardiology* **31**, 2207-2213.
- Chutkow WA, Simon MC, Le Beau MM, Burant CF. 1996. Cloning, tissue expression, and chromosomal localization of SUR2, the putative drug-binding subunit of cardiac, skeletal muscle, and vascular K_{ATP} channels. *Diabetes* **45**:1439–45
- Clark, R.B., Tremblay, A., Melnyk, P., Allen, B.G., Giles, W.R. and Fiset, C. (2001) T-tubule localization of the inward-rectifier K⁺ channel in mouse ventricular myocytes: a role in K⁺ accumulation. *Journal of Physiology* **537.3**, 979-992

- Clement, J.P. IV, Kunjilwar, K., Gonzalez, G., Schwanstecher, M., Panten, U., Aguilar-Bryan, L. and Bryan, J. (1997) Association and stoichiometry of K_{ATP} channel subunits. *Neuron*, **18**, 827-838
- Clerk, A., Michael, A., Sugden, P.H. (1998) Stimulation of the p38 mitogen-activated protein kinase pathway in neonatal rat ventricular myocytes by the G protein-coupled receptor agonists, endothelin-1 and phenylephrine: a role in cardiac myocyte hypertrophy? *J. Cell Biol.* **142**: 523-535
- Clerk, A., Fuller, S.J., Michael, A., Sugden, P.H. (1998). Stimulation of “stress-regulated” mitogen-activated protein kinase in perfused rat hearts by oxidative and other stresses. *J. Biol. Chem.* **273**, 7228-7234
- Conti, L.R., Radeke, C.R., Shyng, S.L. and Vandenberg, C.A. (2001). Transmembrane topology of the sulfonylurea receptor SUR1. *J Biol. Chem.*, **276**, 41270-41278.
- Cook DL, Hales CN. 1984. Intracellular ATP directly blocks K⁺ channels in pancreatic B-cells. *Nature* **311**:271–73
- Cooperstein SJ, Lazarow A (1950). A microspectrophotometric method for the determination of cytochrome oxidase. *J Biol. Chem* **186**: 129-139
- Critz S, Liu GS, Chujo M, Downey JM. Pinacidil but not nicorandil opens ATP-sensitive K₁ channels and protects against simulated ischemia in rabbit myocytes. *J. Mol Cell Cardiol.* 1997; **29**, 1123–1130.
- Deacon, K., Blank, J.L. (1997). Characterization of the mitogen-activated protein kinase kinase 4 (MKK4)/c-Jun NH₂-terminal kinase 1 and MKK3/p38 pathways regulated by MEK kinases 2 and 3: MEK kinase 3 activates MKK3 but does not cause activation of p38 kinase in vivo. *J. Biol. Chem.* **272**, 14489-14496.

- Dekker, L.V. and Parker, P.J. (1994) Protein kinase C- a question of specificity. *Trends Bioch. Sci.* **19**, 73.
- Dick, G.M., Rossow, C.F., Smirnov, S., Horowitz, B. and Sanders, K.M. (2001) Tamoxifen activates smooth muscle BK channels through the regulatory beta 1 subunit. *Journal of Biological Chemistry* **276**, 34594-34599
- Doupnik CA, Lim NF, Kofuji P, Davidson N, Lester HA. 1995. Intrinsic gating properties of a cloned G protein-activated inward rectifier K⁺ channel. *J. Gen. Physiol.* **106**:1–23
- Dunne MJ, Petersen OH. 1986. Intracellular ADP activates K⁺ channels that are inhibited by ATP in an insulin-secreting cell line. *FEBS Lett.* **208**:59–62
- Dunne, M.J., Bullett, M.J., Li, G., Wollheim, C.B. and Petersen, O.H. (1989) Galanin activates nucleotide-dependent K⁺ channels in insulin-secreting cells via a pertussis toxin-sensitive G-protein. *EMBO J.*, **8**, 413–420
- Durrell, S.R. and Guy, R. (1992) Atomic scale structure and functional models of voltage-gated potassium channels. *Biophys.J.* **62**, 238-250
- Edwards, G., and Weston, A. H. (1993) *Annu. Rev. Pharmacol. Toxicol.* **33**, 597-637
- Escande, D., Thuringer, D., Le Guern, S., and Cavero, I. (1988) The potassium channel opener cromakalin activates ATP-dependent K⁺ channels in isolated cardiac myocytes. *Biochem. Biophys. Res. Commun.* **154**, 620-625
- Escande, D., Thuringer, D., Le Guern, S., Courteix, J., Laville, M., and Cavero, I. (1989) Potassium channel openers act through an activation of ATP-sensitive K⁺ channels in guinea-pig cardiac myocytes. *Pflügers Arch.* **414**, 669-675

- Faivre, J. F., Findlay, I. (1989) Effects of tolbutamide, glibenclamide and diazoxide upon action potentials recorded from rat ventricular muscle. *Biochim. Biophys. Acta.* **984**, 1-5
- Fan, Z., Nakayama, K., and Hiraoka, M. (1990). Multiple actions of pinacidil on ATP-sensitive K⁺ channels in guinea-pig ventricular myocytes. *J. Physiol.* **430**, 273-295.
- Fan, Z. & Makielski, J. C. (1997) Anionic Phospholipids Activate ATP-sensitive Potassium Channels. *J. Biol. Chem.* **272**, 5388-5395
- Findlay, I., Dunne, M. J., Petersen, O. H. (1985) ATP-sensitive inward rectifier and voltage- and calcium-activated K⁺ channels in cultured pancreatic islet cells. *J. Membr. Biol.* **88**, 165-172
- Findlay, I., and Dunne, M. J. (1986) ATP maintains ATP-inhibited K⁺ channels in an operational state. *Pfluegers Arch. Eur. J. Physiol.* **407**, 238-240
- Findlay, I. (1992) Inhibition of ATP-sensitive K⁺ channels in cardiac muscle by the sulphonylurea drug glibenclamide. *J. Pharmacol. Exp. Ther.* **261**, 540-545
- Foltz, I.N., Gerl, R.E., Wieler, J.S., Luckach, M., Salmon, R.A., Schrader, J.W. (1998) Human mitogen-activated protein kinase 7 is a highly conserved c-JUN N-terminal kinase/stress-activated protein kinase activated by environmental stresses and physiological stimuli. *J. Biol. Chem.* **273**, 9344-9351
- Forbes, M.S., Hawkey, L.A. and Sperelakis, N. (1984) The transverse-axial tubular system (TATS) of mouse myocardium: its morphology in the developing and adult animal. *American Journal of Anatomy* **170**, 143-162

- Fresney, N.W., Rawlinson, L., Guesdon, F., Jones, E., Cowley, S., et al (1994) Interleukin-1 activates a novel protein kinase cascade that results in the phosphorylation of hsp27. *Cell* **78**, 1039-1049.
- Fryer, R.M., Eells, J.T., Hsu, A.K., Henry, M.M., Gross, G.J. (2000) Ischemic preconditioning in rats: role of mitochondrial K_{ATP} channel in preservation of mitochondrial function. *Am J Physiol Heart Circ Physiol.* **278**: H305-H312.
- Garlid KD, Paucek P, Yarov-Yarovoy V, Sun X, Schindler PA. The mitochondrial KATP channel as a receptor for potassium channel openers *J Biol Chem.* 1996;**271**:8796 –8799.
- Garlid, K.D. (1996b). Cation transport in mitochondria-the potassium cycle. *Biochim. Biophys. Acta* **1275**, 123-126
- Garlid KD, Paucek P, Yarov-Yarovoy V, Murray, H.N., Darbenzio, R.B., et al. (1997). Cardioprotection effect of diazoxide and its interaction with mitochondrial ATP-sensitive K⁺ channels: possible mechanism of cardioprotection. *Circ. Res.* **81**: 1072-1082
- Garlid, K.D. (2000). Opening mitochondrial K(ATP) in the heart-what happens and what does not happen. *Basic Res. Cardiol.* **95**, 275-279
- Giblin J, Joanne L. Leaney, and Andrew Tinker The Molecular Assembly of ATP-sensitive Potassium Channels. DETERMINANTS ON THE PORE FORMING SUBUNIT *J. Biol. Chem.* 1999 **274**: 22652-22659
- Giblin, J.P., Cui, Y., Clapps, L.H. and Tinker, A. (2002) Assembly limits the pharmacological complexity of ATP-sensitive potassium channels. *JBC*, **277**, 13717-13723

- Gribble FM, Tucker SJ, Ashcroft FM. 1997. The essential role of the Walker A motifs of SUR1 in K-ATP channel activation by Mg-ADP and diazoxide. *EMBO J.* **16**:1145–52
- Gribble FM, Tucker SJ, Seino, S., Ashcroft, FM (1998) Tissue specificity of sulfonylureas: studies on cloned cardiac and beta-cell K_{ATP} channels. *Diabetes* **47**, 1412-1418
- Gross GJ, Yao Z, Auchampach JA. Role of ATP-sensitive potassium channels in ischemic preconditioning. In: Przyklenk K, Kloner RA, eds. *Ischemic Preconditioning: The Concepts of Endogenous Cardioprotection*. Boston, Mass: Kluwer Academic Publishers; *Developments in Cardiovascular Medicine*, vol **148**; 1994:125–135.
- Grover GJ, Sleph PG, Dzwonczyk S. 1992. Role of myocardial ATP-sensitive potassium channels in mediating preconditioning in the dog heart and their possible interaction with adenosine A₁ receptors. *Circulation.* **86**: 1310-1316
- Grover, G.J. (1997) Pharmacology of ATP-sensitive potassium channel openers in models of myocardial ischemia and reperfusion. *Can. J. Physiol. Pharmacol.* **75**, 309-315
- Grover, G.J., D'Alonzo, A.J., Parham, C.S., Darbenzio, R.B. (1995) Cardioprotection with the K_{ATP} opener cromakalim is not correlated with ischemia myocardial action potential duration. *J. Cardiovasc. Pharmacol.* **26**, 145-152
- Grover, G.J., D'Alonzo, A.J., Hess, T., Sleph, P.G. and Darbenzio, R.B. (1995) Glyburide-reversible cardioprotective effect of BMS-180448 is independent of action potential shortening. *Cardiovasc. Res.* **30**, 731- 738
- Guy, H.R. and Conti, F. (1990) Pursuing the structure and function of voltage-gated channels. *Trends Neurosci.* **13**, 201-206

- Halestrap, A.P. (1989) The regulation of the matrix volume of mammalian mitochondria in vivo and in vitro and its role in the control of mitochondrial metabolism. *Biochim Biophys Acta*. **973**: 355-382
- Hanley, P.J., Mickel, M., Löffler, M., Brandt, U. and Daut, J. (2002) ATP-sensitive K⁺ channel-independent targets of diazoxide and 5-hydroxydecanoate in the heart. *Journal of Physiology*.
- Hardie, D.G. (1993) Protein phosphorylation: a practical approach. Oxford, Oxford University Press.
- Higgins, C.F. (1992) ABC transporters: from microorganisms to man. *Annu. Rev. Cell Biol.*, **8**, 67-113
- Hille, B. (2001) Ion channels of excitable membranes. Sunderland, Massachusetts USA.
- Ho, K., Nichols, C.G., Lederer, W.J., Lytton, J., Vassilev, P.M., Kanazirska, M.V. and Hebert, S.C. (1993) Cloning and expression of an inwardly rectifying ATP-regulated potassium channel. *Nature* **362**, 31-38
- Holmuhamedov, E.L., Wang, L., Terzic, A. (1999) ATP-sensitive K⁺ channel openers prevent Ca²⁺ overload in rat cardiac mitochondria. *J Physiol (Lond)*. **19**: 347-360.
- Hoshi, T., Zagotta, W.N. and Aldrich, R.W. (1990) Biophysical and molecular mechanisms of *Shaker* potassium channel inactivation. *Science* **250**, 553-538
- Hoshi, T., Zagotta, W.N. and Aldrich, R.W. (1991) Two types of inactivation in *Shaker* K⁺ channels: effects of alterations in the carboxy-terminal region. *Neuron* **7**, 547-556

- Hu K, Duan D, Li G, Nattel S (1996) Protein Kinase C activates ATP-sensitive potassium current in human and rabbit ventricular myocytes. *Circulation research* 78:492-497
- Huang, C. L., Feng, S. & Hilgemann, D. W. (1998) *Nature (London)* 391, 803-806
- Huh, J., Gross, G.J., Nagase, H. and Liang, B.T (2001). Protection of cardiac myocytes via δ_1 -opioid receptors, protein kinase C, and mitochondrial K_{ATP} channels. *Am. J. Physiol. Heart Circ. Physiol.*, 280, H377-H383
- Inagaki N, Inazawa J, Seino S. 1995. cDNA sequence, gene structure, and chromosomal localization of the human ATP-sensitive potassium channel, uKATP-1, gene (KCNJ8). *Genomics* 30:102-4
- Inagaki N, Gono T, Clement JP IV, Namba N, Inazawa J, et al. 1995. Reconstitution of IK_{ATP}: an inward rectifier subunit plus the sulfonylurea receptor. *Science* 270:1166-70
- Inagaki N, Gono T, Clement JP IV, Wang CZ, Aguilar-Bryan L, et al. 1996. A family of sulfonylurea receptors determines the pharmacological properties of ATP-sensitive K⁺ channels. *Neuron* 16:1011-17
- Inoui, I., Nagase, H., Kishi, K. and Higuti, T. 1991 ATP-sensitive K⁺ channel in the mitochondrial inner membrane. *Nature* 352, 244-247
- Isomoto S, Kondo C, Yamada M, Matsumoto S, Higashiguchi O, et al. 1996. A novel sulfonylurea receptor forms with BIR (Kir6.2) a smooth muscle type ATP-sensitive K⁺ channel. *J. Biol. Chem.* 271:24321-24
- Jorgensen, A.O., Arnold, W., Shen, A.C.Y., Yuan, S., Gaver, M. and Campbell, K.P. (1990). Identification of novel proteins unique to either

transverse tubules (TS28) or the sarcolemma (SL50) in rabbit skeletal muscle. *The Journal of Cell Biology*, **110**, 1173-1185.

- Kakei M, Noma A. 1984. Adenosine-5'-triphosphate-sensitive single potassium channel in the atrioventricular node cell of the rabbit heart. *J. Physiol.* **352**:265–84
- Kane, C., Shepherd, R. M., Squires, P. E., Johnson, P. R. V., James, R. F. L., Milla, P. J., Aynsley-Green, A., Lindey, K. J., and Dunne, M. J. (1996) Loss of functional K_{ATP} channels in pancreatic beta-cells causes persistent hyperinsulinemic hypoglycemia of infancy. *Nat. Med.* **2**, 1344-1347
- Kirsch, G.E., Codina, J., Birnbaumer, L. and Brown, A.M. (1990) Coupling of ATP-sensitive K⁺ channels to A₁ receptors by G proteins in rat ventricular myocytes. *Am. J. Physiol.*, **259**, H820–H826
- Ko, Y.H. and Pedersen, P.L. (1995) The first nucleotide binding fold of cystic fibrosis transmembrane conductance regulator can function as an active ATP-ase. *J. Biol. Chem.*, **270**, 22093-22096
- Kopustinskiene, D.M., Pollesello, P., Saris, N.L. (2001). Levosimendan is a mitochondrial K_{ATP} channel opener. *European Journal of Pharmacology* **428**, 311-314.
- Kovalev, H., Lodwick, D. and Quayle, J.M. (2001). Inhibition of cloned K_{ATP} channels by the morpholinoguanidine PNU-37883A. *Journal of Physiology* **531**, S173 (abstract)
- Kowaltowski, A.J., Seetharaman, S., Pauczek, P., Garlid, K.D. (2001). Levosimendan, a new positive inotropic drug, decreases myocardial infarct size via activation of K(ATP) channels. *Anesth. Analg.* **90**, 5-11.

- Kubo, Y., Baldwin, T.J., Jan, Y.N. and Jan, Y.Y. (1993) Primary structure and functional expression of a mouse inward rectifier potassium channel. *Nature* **362**, 127-133
- Kuhlman, H. (2002) An investigation into the molecular identity of the K_{ATP} channel of vascular smooth muscle. *Ph.D.* University of Leicester.
- Landau, H., and Schiller, M. (1991) in *Pediatric Surgery of the Liver, Pancreas, and Spleen* (Landau, H. , and Schiller, M., eds) , pp. 187-201, W. B. Saunders Co., Philadelphia, PA
- Lawrence, C. & Rodrigo, G. C. (1999). A Na⁺-activated K⁺ current (IK,Na) is present in guinea-pig but not rat ventricular myocytes. *Pflugers Archiv-Euro.J.Physiol.* **437**, 831-838.
- Lederer WJ, Nichols CG, Smith GL (1989) The mechanism of early contractile failure of isolated rat ventricular myocytes subjected to complete metabolic inhibition. *J Physiol.* **413**: 329-349
- Leonoudakis, D., Mailliard, W., Wingerd, K., Clegg, D. and Vandenberg, C. (2001) Inward rectifier potassium channel Kir2.2 is associated with synapse-associated protein SAP97. *Journal of Cell Science* **114**, 987-998
- Levitan, I.B. (1994) Modulation of ions channels by protein phosphorylation and dephosphorylation. *Annu. Rev. Physiol.*, **56**, 193-212
- Liang BT (1997) Protein kinase C-mediated preconditioning of cardiac myocytes: role of adenosine receptor and K_{ATP} channel. *Am j Physiol.* **272**: H847-H853.
- Light, P.E., Sabir, A. B., Allen, B.G., Walsh, M.P. and French, R.J. (1996) Protein kinase C-Induced changes in the stiochimetry of ATP binding activate cardiac ATP-sensitive K⁺ channels. *Circ Res* **79**, 399-406

- Light PE, Bladen C, Winkfein RJ, Walsh MP, French RJ (2000) Molecular basis of protein kinase c-induced activation of ATP-sensitive potassium channels. *PNAS* **97**: 9058-9063
- Lin Y, Yuh Nung Jan, and Lily Yeh Jan. Regulation of ATP-sensitive potassium channel function by protein kinase A-mediated phosphorylation in transfected HEK293 cells. *EMBO J.* 2000 **19**: 942-955
- Lipp, P., Hüsher, J., Pott, L. and Niggli, E. (1996) Spatially non-uniform Ca²⁺ signals induced by the reduction of transverse tubules in citrate-loaded guinea-pig ventricular myocytes in culture. *Journal of Physiology* **497**, 589-597
- Litt, M., LaMorticella, D., Bonel, C.T. and Adelman, J.P. (1999) Gene structure and chromosome mapping of the human small-conductance calcium-activated potassium channel SK1 gene (KCNN1). *Cytogenet cell genet* **86**, 70-73
- Liu GS, Thornton J, Van Winkle DM, Stanley AWH, Olsson RA, Downey JM. 1991. Protection against infarction afforded by preconditioning is mediated by A₁ adenosine receptors in rabbit heart. *Circulation.* **84**: 350-356
- Liu, Y. and Downey, J.M. (1992) Ischemic preconditioning protects against infarction in rat heart. *Am. J. Physiol.* **263**, H1107-H1112.
- Liu Y, Gao WD, Rourke BO, Marbán E (1996) Cell-type specificity of preconditioning in an in vitro model. *Basic Res Cardiol* **91**: 450-457
- Liu Y, Gao WD, Rourke BO, Marbán E (1996). Synergistic modulation of ATP-sensitive K⁺ currents by protein kinase C and adenosine: implications for ischemic preconditioning. *Circ. Res.* **78**, 443-453

- Liu, Y., Sato, T., Rourke, B.O, Marbán, E. (1998) Mitochondrial ATP-dependent potassium channels: Novel effectors of cardioprotection? *Circulation*, **97**, 2463-2469.
- Liu, Y., Ren, G., O'Rourke, B., Marbán, E., Seharaseyon, J. (2001) Pharmacological comparison of native mitochondrial K_{ATP} channels with molecularly defined surface K_{ATP} channels. *Mol. Pharmacol.*, **59**, 225-230
- Liu, H., Zhang, H.Y., Zhu, X., Shao, Z. and Yao, Z. (2002) Preconditioning blocks cardiocyte apoptosis: role of K_{ATP} channels and PKC-ε. *AM. J. Physiol. Heart Circ Physiol.* **282**, H1380-H1386.
- Lochner, A., Colesky, F., Genade, S. (2000). Effect of a calcium-sensitizing agent, levosimendan on the postcardioplegic inotropic response of the myocardium. *Cardiovasc. Drugs Ther.* **14**, 271-281
- Lohse, M.J., Klotz, K.N., Schwabe, U., Cristalli, G., Vittori, S., Grifantini, M. (1988) 2-Chloro-N⁶-cyclopentyladenosine: A highly selective agonist at A₁ adenosine receptors. *Naunyn-Schmiedeberg's Arch. Pharmacol.* **337**, 687-689.
- Lopez-Barneo, J., Hoshi, T., Heinemann, S.H. and Aldrich, R.W. (1993) Effects of external cations and mutations in the pore region on C-type inactivation of *Shaker* potassium channels. *Receptors and Channels* **1**, 61-71
- Lustig KD, Conklin BR, Herzmark P, Taussig R, Bourne HR (1993) Type II adenylylase integrates coincident signals from G_s, G_i, and G_q. *J Biol Chem* **268**: 13900-13905
- MacGregor, G.G., Dong, Ke., Vanoye, C.G., Tang, L., Giebisch, G. and Hebert, S.C. (2002) Nucleotides and phospholipids compete for binding to the C terminus of K_{ATP} channels. *PNAS*, **99**, 2726-2731

- Mahoney, C.W. et al (1993) Phosphorylation of MARCKS, neuromodulin, and neurogranin by protein kinase C exhibits differential responses to diacylglycerols. *Cell. Signal.* **7**, 679.
- Malhi, H., Irani, A.N., Rajvanshi, P., Suadicani, S.O., Spray, D.C., McDonald, T.V., and Gupta, S. (2000) K_{ATP} channels regulate mitogenically induced proliferation in primary rat hepatocytes and human liver cell lines. *JBC*, **34**, 26050-26057.
- Matsuoka, T., Matsushita, K., Katayam, Y., Fujita, A., Inagenda, K., Tanemoto, M., Inanobe, A., Yamashita, S., Matsuzawa, Y. and Kurachi, Y. (2000) C-terminal tails of sulphonylurea receptors control ADP-induced activation and diazoxide modulation of ATP-sensitive K⁺ channels. *Circulation Research* **87**, 873-880.
- Maulik, N., Yoshida, T., Das, D.K. (1998). P38 MAP kinase and not MEK1 kinase is involved in ischemic preconditioning. *J. Mol. Cell. Cardiol.* **30**, A264.
- McCobb, D.P., Fowler, N.L., Featherstone, T., Lingle, C.J., Saito, M., Krause, J.E. and Salkoff, L. (1995) A human calcium-activated potassium channel gene expressed in vascular smooth muscle. *American Journal of Physiology* **269**, H767-777.
- Meera, P., Wallner, M., Song, M. and Toro, L. (1997) Large conductance voltage and calcium-dependent K⁺ channels, a distinct member of voltage-dependent ion channels with seven N-terminal transmembrane segments (S0-S6), an extracellular N terminus, and an intracellular (S9-S10) C terminus. *Proceedings of the National Academy of Sciences* **94**, 14066-14071
- Mikhailov, M.V., Ashcroft, S.J.H. (2000) Interactions of the sulfonylurea receptor 1 subunit in the molecular assembly of β-cell K_{ATP} channels. *J.Biol.Chem*, **275**, 3360-3364

- Misler S, Falke LC, Gillis K, McDaniel ML. 1986. A metabolite-regulated potassium channel in rat pancreatic B cells. *Proc. Natl. Acad. Sci. USA* **83**:7119–23
- Mitcheson, J.S., Hancox, J.C. and Levi, A.J. (1996) Action potentials, ion channel currents and transverse tubule density in adult rabbit ventricular myocytes maintained for 6 days in cell cultures. *Pflügers Archiv* **431**, 814-827.
- Mitra, R. & Morad, M. (1985). A uniform enzymatic method for dissociation of myocytes from hearts and stomachs of vertebrates. *Am.J.Physiol.* **249**, H1056-H1060.
- Miura, T., Liu, Y., Kita, H., Ogawa, T., Shimamoto, K. (2000) Roles of mitochondrial ATP-sensitive K channels and PKC in anti-infarct tolerance afforded by adenosine A1 receptor activation. *J Am Coll Cardiol.* **35**: 238-245.
- Moreau, C., Jacquet, H., Prost, A.L., D'hahan, N. and Vivaudou, M. (2000) The molecular basis of the specificity of action of K_{ATP} channel openers. *Embo. J*, **19**, 6644-6651.
- Morishige, K., Takahashi, N., Jahangir, A., Yamada, M., Koyama, H., Zanelli, J.S. and Kurachi, Y. (1994) Molecular cloning and functional expression of a novel brain-specific inward rectifier potassium channel. *FEBS Letters* **346**, 251-256
- Murry, C.E., Jennings, R.B. and Reimer, K.A. (1986). Preconditioning with ischemia: a delay of lethal cell injury in ischemic myocardium. *Circulation*, **74**, 1124-1136.
- Nagao, M., Yamauchi, J., Kaziro, Y., Itoh, H. (1998). Involvement of protein kinase C and Src family tyrosine kinase in G $\alpha_{q/11}$ -induced activation of c-Jun

N-terminal kinase and p38 mitogen-activated protein kinase. *J. Biol. Chem.* **273**, 22892-22898.

- Newton, A.C. (1995) Protein kinase C: structure, function and regulation. *J. Biol. Chem.* **270**, 28,495.
- Nichols, C. G., Shyng, S. L., Nestorowicz, A., Glaser, B., Clement, J. P. IV., Gonzalez, G., Aguilar-Bryan, L., Permutt, M. A., and Bryan, J. (1996) Adenosine Diphosphate as an Intracellular Regulator of Insulin Secretion *Science* **272**, 1785-1787
- Noma A. 1983. ATP-regulated K⁺ channels in cardiac muscle. *Nature* **305**:147-48
- Ohno-Shosaku, T., Zunkler, B. J., and Trube, G. (1987) Dual effects of ATP on K⁺ currents of mouse pancreatic beta-cells. *Pfluegers Arch. Eur. J. Physiol.* **408**, 133-138
- O'Rourke, B. (2000) Myocardial K_{ATP} channels preconditioning. *Circ Res.* **87**, 845-855.
- Pallanck, L. and Ganetzky, B. (1994) Cloning and characterization of human and mouse homologs of the *Drosophila* calcium-activated potassium channel gene, slowpoke. *Human Molecular Genetics* **3**, 1239-1243
- Papazian, D.M., Timpe, L.C., Jan, Y.N. and Jan, L.Y. (1991) Alteration of voltage-dependence of *Shaker* potassium channel by mutations in the S4 sequence. *Nature* **349**, 305-310
- Permutt, M. A., Nestorowicz, A., and Glaser, B. (1996) *Diabetes Rev.* **4**, 347-355

- Piao, H., Cui, N., Xu, H., Mao, J., Rojas, A., Wang, R., Abdulkadir, L., Li, L., Wu, J. and Jiang, C. (2001) Requirement of multiple protein domains and residues for gating K_{ATP} channels by intracellular pH. *J. Biol. Chem.*, **276**, 36673-36680
- Ping, P., Zhang, J., Cao, X., Qui, Y., Tang, X.L, et al (1998a) Activation of the p38MAPK and the p46/p54 JNKs after brief episodes of ischemia/reperfusion in the heart of conscious rabbits. *J. Mol. Cell. Cardiol.* **30**, A263
- Ping, P., Cao, X., Kong, D., Zhang, J., Li, R.C.X, et al (1998b) PKC isoform induces activation of the p42/p44 MAPKs and the p46/p54 JNKs in adult rabbit cardiac myocytes. *J. Mol. Cell. Cardiol.* **30**, A263
- Pongs, O. (1992) Molecular biology of voltage-dependent potassium channels. *Physiological Reviews* **72**, S69-S88
- Pountney, D.J., Sun, Z.Q., Porter, L.M., Nitabach, M.N., Nakamura, T.Y., Holmes, D., Rosner, E., Kaneko, M., Manaris, T., Holmes, T.C. and Coetzee, W.A. (2001) Is the molecular composition of K_{ATP} channels more complex than originally thought? *Journal of Molecular and Cellular Cardiology*, **33**, 1541-1546
- Quayle JM, Nelson MT, and Standen NB. 1997. ATP-sensitive and inwardly rectifying potassium channels in smooth muscle. *Physiol Review.* **77**: 1165-1215
- Raingeaud, J., Gupta, S., Roggers, J.S., Dickens, M., Han, J, et al. (1995). Pro-inflammatory cytokines and environmental stress cause p38 mitogen-activated protein kinase activation by dual phosphorylation on tyrosine and threonine. *J. Biol. Chem.* **270**, 7420-7426.

- Raymond LA, Tingley WG, Blackstone CD, Roche KW, Huganir RL (1994) Glutamate receptor modulation by protein phosphorylation. *J Physiol Paris* **88**: 181-192
- Rettig, J., Heinemann, S.H., Wunder, F., Lorra, C., Parcej, D.N., Dolly, J.O. and Pongs, O. (1994) Inactivation properties of voltage-gated K⁺ channels altered by presence of β-subunit. *Nature* **369**, 289-294
- Ribalet, B. and Eddlestone, G.T. (1995) Characterization of the G protein coupling of a somatostatin receptor to the K⁺_{ATP} channel in insulin-secreting mammalian HIT and RIN cell lines. *J. Physiol.*, **485**, 73–86
- Robinson, M.J., Cobb, M.H. (1997). Mitogen-activated protein kinase pathways. *Curr. Opin. Cell Biol.* **9**, 180-186.
- Roeper, J. and Ashcroft, F.M. (1995) Metabolic inhibition and low central ATP activate K-ATP channels in rat dopaminergic substantia nigra neurons. *Pflügers Arch.*, **430**, 44-54
- Sakamoto, J., Miura, T., Goto, M. and Imura, O. (1995) Limitation of myocardial infarct size by adenosine A₁ receptor activation is abolished by protein kinase C inhibitors in the rabbit. *Cardiovasc. Res.* **29**, 682-688
- Santos, A.S., Nathanael, L., Maurice, G. and Guido, K. Purification of Mitochondria for apoptosis assays. *Methods of enzymology* 205-208
- Saraste, M., Sibbald, P.R. and Wittinghofer, A. (1990) The P-loop_ a common motif in ATP- and GTP-binding proteins. *Trends Neurosci.*, **15**, 430-434
- Sasaki, N., Sato, T., Ohler, A., O'Rourke, B., Marbán, E. (2000) Activation of mitochondrial ATP-dependent potassium channels by nitric oxide. *Circulation.* **101**: 439-445.

- Sato T, O'Rourke B, and Marban E. Modulation of mitochondria ATP-dependent K⁺ channels by protein kinase C. *Circ Res* **83**: 110–114, 1998.
- Schreiber, M. and Salkoff, L. (1997) A novel calcium-sensing domain in the BK channel. *Biophysical Journal* **73**, 1355-1363
- Schreiber, M., Yuan, A. and Salkoff, L. (1999) Transplantable sites confer calcium sensitivity to BK channels. *Nature Neuroscience* **2**, 416-421
- Schulte, U., Hahn, H., Wiesinger, H., Ruppertsberg, J. P., and Fakler, B. (1998) pH-dependent Gating of ROMK (K_{ir}1.1) Channels Involves Conformational Changes in Both N and C Termini. *J. Biol. Chem.* **273**, 34575-34579
- Schwanstecher, M., Sieverding, C., Dörshner, H., Gross, I., Aguilar-Bryan, L., Schwanstecher, C. and Bryan, J. (1998) Potassium channel openers require ATP to bind to and act through sulfonylurea receptors. *embo. J*, **17**, 5529-5535
- Schwappach B, Zerangue N, Jan YN, and Jan LY. 2000. Molecular basis for K_{ATP} assembly: Transmembrane interactions mediate association of a potassium channel with ABC transporter. *Neuron*. **26**: 155-167
- Seharaseyon, J., Sasaki, N., Ohler, A., Sato, T., Fraser, H., Johns, D.C., Rourke, B.O. and Marbán, E. (2000a) Evidence against functional heteromulimerization of the K_{ATP} channel subunits Kir6.1 and Kir6.2. *JBC*, **275**, 17561-17565.
- Seharaseyon, J., Ohler, A., Sasaki, N., Fraser, H., Sato, T., Johns, D.C., Rourke, B.O. and Marbán, E. (2000b) Molecular composition of mitochondrial ATP-sensitive potassium channels probed by viral Kir gene transfer. *J. Mol. Cell. Cardiol*, **32**, 1923-1930.

- Sharma, N., Crane, A., Gonzalez, G., Bryan, J., and Aguilar-Bryan, L. (2000) Familial hyperinsulinism and pancreatic β -cell ATP-sensitive potassium channels *Kidney Int.* **57**, 803-808
- Sheng, M., Liao, Y.J., Jan, Y.N. and Jan, L.Y. (1993) Presynaptic A-current based on heteromultimeric K⁺ channels detected *in vivo*. *Nature* **365**, 72-75
- Shyng, S., Ferrigni, T., and Nichols, C. G. (1997) Regulation of K_{ATP} Channel Activity by Diazoxide and MgADP *J. Gen. Physiol.* **110**, 643-654
- Shyng S.L., Barbieri A., Gumusboga A., Cukras C., Pike L., Davis J.N., Stahl P.D. and Nichols C.G. 2000. Modulation of nucleotide sensitivity of ATP-sensitive potassium channels by phosphatidylinositol-4-phosphate 5-kinase. *PNAS.* **97**: 937-941
- Sommer JR, Johnson EA. Ultrastructure of cardiac muscle. In: Berne RM, ed. *Handbook of Physiology. Section 2. The Cardiovascular System*. Bethesda, MD: American Physiological Society; 1979:113–186.
- Song, D.K., and Ashcroft, M. (2001) ATP Modulation of ATP-sensitive Potassium Channel ATP Sensitivity Varies with the Type of SUR Subunit. *JBC.* **276**, 7143-7149
- Spector, P.S., Curren, M.E., Zou, A., Keating, M.T. and Sanguinetti, M.C. (1996) Fast inactivation causes rectification of the I_{Kr} channel. *Journal of General Physiology* **107**, 611-619.
- Standen, N. B., Quayle, J. M., Davis, N. W., Brayden, J. E., Huang, Y., Nelson, M. T. (1989) Hyperpolarizing vasodilators activate ATP-sensitive K⁺ channels in arterial smooth muscle. *Science* **245**, 177-180
- Sugden, P.H., Bogoyevitch, M.A. (1995). Intracellular signaling through protein kinases in the heart. *Cardiovasc. Res.* **30**, 478-492.

- Suzuki M, Kotake, K., Fujikura, K., Inagaki, N., Suzuki, T., Gono, T., Seino, S. and Takat, K. (1993) Kir6.1: a possible subunit of ATP-sensitive K⁺ channels in mitochondria. *Biochem Biophys Res Commun.* **241**, 693– 697
- Suzuki, M., Sasaki, N., Miki, T., Sakamoto, N., Ohmoto-Sekine, Y., Tamagawa, M., Seino, S., Marbán, E. and Nakaya, H. (2002) Role of sarcolemmal K_{ATP} channels in cardioprotection against ischemia/reperfusion injury in mice. *J.clin. Invest.* **109**, 509-516.
- Szewczyk A, Wojcik G, Lobanov NA, Nalecz MJ. (1997) The mitochondrial sulfonylurea receptor: identification and characterization. *Biochem Biophys Res Commun.* **230**, 611– 615.
- Takahashi, N., Morishige, K., Jahangir, A., Yamada, M., Findlay, I., Koyama, H. and Kurachi, Y. (1994) Molecular cloning and functional expression of cDNA encoding a second class of inward rectifier potassium channels in mouse brain. *Journal of Biological Chemistry* **269**, 23274-23279
- Takano, M., Noma, A. (1993) The ATP-sensitive K⁺ channel *Prog. Neurobiol.* **41**, 21-30
- Takata, K., Kasahara, T., Kasahara, M., Ezaki, O. and Hirano, H. (1990) *Biochem. Biophys. Res. Comm.* **173**, 67-73
- Taylor, S.S. (1989) cAMP-dependent protein kinase. *JBC*, **264**, 8443-8446
- Thorneloe, K.S., Maruyama, Y., Malcolm, A.T., Light, P.E., Walsh, M.P., Cole, W.C. (2002) Protein kinase C modulation of recombinant ATP-sensitive K⁺ channels composed of Kir6.1 and/ or Kir6.2 expressed with SUR2B. *Journal of Physiology*, **541.1**: 65-80.

- Terzic, A., Jahangir, A., Kurachi, Y. (1995) Cardiac ATP-sensitive K⁺ channels: regulation by intracellular nucleotides and K⁺ channel-opening drugs. *Am. J. Physiol.* **269**, C525-C545
- Thornton, J.D., Liu, G.S., Olsson, R.A. and Downey, J.M (1992). Intravenous pre-treatment with A₁-selective adenosine analogous protects the heart against infarction. *Circulation*, **85**, 659-665.
- Tian, G., Yan, H., Jiang, R.T., Kishi, F., Nakazawa, A. and Tsai, M.D. (1990) Mechanisms of adenylate kinase. Are the essential lysines essential? *Biochemistry*, **29**, 4296-4304
- Towbin H, Gordon J (1984) Immunoblotting and dot immunobinding-current status and outlook. *J Immunol Methods* **72**, 313-340.
- Toyoda, Yoshiya, Ingeborg Friehs, Robert A. Parker, Sidney Levitsky, and James D. McCully. Differential role of sarcolemmal and mitochondrial KATP channels in adenosine-enhanced ischemic preconditioning *Am J Physiol Heart Circ Physiol* **279**: H2694–H2703, 2000.
- Trapp, S., Tucker, S. J., Ashcroft, F. M. (1997) Activation and inhibition of K-ATP currents by guanine nucleotides is mediated by different channel subunits. *Proc. Natl. Acad. Sci.* **94**, 8872-8877
- Trapp, S., Proks, P., Tucker, S.J., Ashcroft, F.M. (1998) Molecular analysis of ATP-sensitive K channel gating and implications for channel inhibition by ATP. *J. Gen. Physiol.* **112**, 333-349
- Trudeau, M.C., Warmke, J.W., Ganetzky, B. and Robertson, G.A. (1995) HERG, a human inward rectifier in the voltage-gated potassium channel family. *Science* **269**, 92-95.

- Tsai, T. D., Shuck, M. E., Thompson, D. P., Bienkowski, M. J., and Lee, K. S. (1995) Intracellular H⁺ inhibits a cloned rat kidney outer medulla K⁺ channel expressed in *Xenopus* oocytes. *Am. J. Physiol.* **268**, C1173-C1178
- Tucker SJ, Gribble FM, Zhao C, Trapp S, Ashcroft FM. 1997. Truncation of Kir6.2 produces ATP-sensitive K⁺ channels in the absence of the sulphonylurea receptor. *Nature* **387**:179–83
- Tucker SJ, Fiona M. Gribble, Peter Proks, Stefan Trapp, Timothy J. Ryder, Trude Haug, Frank Reimann, and Frances M. Ashcroft Molecular determinants of K_{ATP} channel inhibition by ATP. *EMBO J.* 1998 **17**: 3290-3296
- Tucker S.J. and Ashcroft F.M. 1999. Mapping of the physical interaction between the intracellular domains of an inwardly rectifying potassium channel, Kir6.2. *JBC.* **274**: 33393-33397.
- Tusnády GE, Bakos E, Varadi A, Sarkadi B. 1997. Membrane topology distinguishes a subfamily of the ATP-binding cassette (ABC) transporters. *FEBS Lett.* **402**:1–3
- Uhde I, Andreas Toman, Insa Gross, Christina Schwanstecher, and Mathias Schwanstecher Identification of the Potassium Channel Opener Site on Sulfonylurea Receptors. *J. Biol. Chem.* 1999 **274**: 28079-28082
- Vahlhaus, C., Schulz, R., Post, H., Onallah, R. and Heusch, G. (1996) No prevention of ischemic preconditioning by the protein kinase C inhibitor staurosporine in swine. *Circ. Res.* **79**, 407-414
- Van Winkle DM, Chien GL., Wolff RA., Soifer BE., Kuzume K., Davis RF. 1994. Cardioprotection provided by adenosine activation is abolished by blockade of the K_{ATP} channel. *Am J Physiol.* **266**: H829-H839

- Vanden Hoek, T.L., Becker, L.B., Shao, Z., Li, C., Schumacker, P.T. (1998) Reactive oxygen species released from mitochondria during brief hypoxia induce preconditioning in cardiomyocytes. *J Biol Chem.* **273**: 18092-18098.
- Vanden Hoek, T.L., Becker, L.B., Shao, Z., Li, C., Schumacker, P.T. (2000) Preconditioning in cardiomyocytes protects by attenuating oxidant stress at reperfusion. *Circ Res.* **86**: 541-548.
- Wada Y, Yamashita T, Imai K, Miura R, Takao K, Nishi M, Takeshima H, Asano T, Morishita R, Nishizawa K, Kokubun S, Nukada T (2000) A region of the sulfonylurea receptor critical for a modulation of ATP-sensitive K⁺ channels by G-protein subunits. *EMBO J* **19**:4915-4925
- Walker, J.E. , Saraste, M.J. , Runswick, M.J. and Gay, N.J. (1982) Distantly related sequences in the alpha and beta subunits of ATP synthetase, myosin, kinases, and other ATP-requiring enzymes and a common nucleotide binding fold. *EMBO J.*, **1**, 945-951
- Wang, Y., Ashraf, M. (1999) Role of protein kinase C in mitochondrial K_{ATP} channel-mediated protection against Ca²⁺ overload injury in rat myocardium. *Circ Res.* **84**: 1156-1165.
- Warmke, J.W. and Ganetzky, B. (1994) A family of potassium channel genes related to eag in *Drosophila* and mammals. *Proceedings of the National Academy of Sciences* **91**, 3438-3442
- Weinbrenner, C., Liu, G-S., Cohen, M.V., Downey, J.M. (1997) Phosphorylation of tyrosine 182 of p38 mitogen-activated protein kinase correlates with the protection of preconditioning in the rabbit heart. *J. Mol. Cell. Cardiol.* **29**, 2383-2391
- Woodward, R., Stevens, E. B., and Murrell-Lagnado, R. D. (1997) *J. Biol. Chem.* **272**, 10823-10830

- Xie, L. H., Takano, M., Kakei, M., Okamura, M., and Noma, A. (1999) Wortmannin, an inhibitor of phosphatidylinositol kinases, blocks the MgATP-dependent recovery of Kir6.2/SUR2A channels. *J. Physiol. (Lond.)* **514**, 655-665
- Xie L.H., Horie M. and Takano M. 1999. Phospholipase C-linked receptors regulate the ATP-sensitive potassium channel by means of phosphatidylinositol 4,5-bisphosphate metabolism. *PNAS*. **96**: 15292-15297
- Xu, H., Cui, N., Yang, Z., Wu, J., Giwa, L.R., Abdulkadir, L., Sharma, P. and Jiang, C. (2001) Direct Activation of Cloned K_{ATP} Channels by Intracellular Acidosis. *J. Biol. Chem.* **276**, 12898-12902
- Yamada M, Isomoto S, Matsumoto S, Kondo C, Shindo T, et al.1997. Sulfonylurea receptor 2B, KIR 6.1 form a sulfonylurea-sensitive but ATP-insensitive K⁺ channel. *J. Physiol.* **499**:715–20
- Yang, Z., and Jiang, C. (1999) Opposite effects of pH on open-state probability and single channel conductance of Kir4.1 channels. *J.Physiol.* **520**, 921-927.
- Yao, Z., Gross, G.J. (1994) Effects of the K_{ATP} channel opener bimakalim on coronary blood flow, monophasic action potential duration, and infarct size in dogs. *Circulation.* **89**, 1769-1775
- Yao, Z., Tong, J., Tan, X., Li, C., Shao, Z., Kim, W.C., vanden Hoek, T.L., Becker, L.B., Head, C.A., Schumacker, P.T. (1999) Role of reactive oxygen species in acetylcholine-induced preconditioning in cardiomyocytes. *Am J Physiol.* **277**: H2504-H2509.

- Yi, C., Giblin, J.P., Clapp, L.H. and Tinker, A. (2000) A mechanism for ATP-sensitive potassium channel diversity: Functional coassembly of two pore-forming subunits. *PNAS*, **98**, 729-734.
- Yokoshiki H, Katsube Y, Sunugawa M, Seki T, Sperelakis N (1997a) Distribution of actin cytoskeleton attenuates sulphonylurea inhibition of cardiac ATP-sensitive K⁺ channels. *Pflugers Arch.* **434**: 203-205
- Yokoshiki H, Katsube Y, Sunugawa M, Sperelakis N. (1997b). Levosimendan, a novel Ca²⁺ sensitizer, activates the glibenclamide-sensitive K⁺ channel in rat arterial myocytes. *Eur. J. Pharmacol.* **333**, 249-259
- Yongge Liu, PhD; Toshiaki Sato, MD, PhD; Brian O'Rourke, PhD; Eduardo Marban, MD, PhD Mitochondrial ATP-Dependent Potassium Channels Novel Effectors of Cardioprotection? *Circulation* 1998; **97**: 2463-2469.
- Zanke, B.W., Rubie, E.A., Winnett, E., Chan, J., Randall, S, et al. (1996). Mammalian mitogen-activated protein kinase pathways are regulated through formation of specific kinase-activator complexes. *J. Biol. Chem.* **271**, 29876-29881.
- Zaritsky, J.J., Redell, J.B., Tempel, B.L. and Schwarz, T.L. (2001). The consequences of disrupting cardiac inwardly rectifying K⁺ current (IK1) as revealed by the targeted deletion of the murine kir2.1 and Kir2.2 genes. *Journal of physiology* **533**, 697-710.
- Zerangue, N., Schwappach, B., Jan, Y.N. and Yan, L.Y. (1999) A new ER trafficking signal regulates the subunit stoichiometry of plasma membrane K_{ATP} channels. *Neuron* **22**, 537-548
- Zhao, T.C., Hines, D.S. and Kukreja, R.C. (2001) Adenosine-induced late preconditioning in mouse hearts: role of p38 MAP kinase and mitochondrial K_{ATP} channels. *A.M.J.Physiol Heart. Circ. Physiol.* **280**, H1278-H1285

- Zhou, H., Tate, S.S. and Palmer, L.G. (1994) Primary structure and functional properties of an epithelial K channel. *American Journal of Physiology* **266**, C809-C824.

